Geological Carbon Sequestration and its Influence on Subsurface Microbial Diversity and Metabolic Carbon Cycling

Mariana Erasmus

Geological Carbon Sequestration and its Influence on Subsurface Microbial Diversity and Metabolic Carbon Cycling

By

Mariana Erasmus

Submitted in fulfillment of the requirements for the degree

PHILOSOPHIAE DOCTOR

In the

Department of Microbial, Biochemical and Food Biotechnology

Faculty of Natural and Agricultural Sciences

University of the Free State

Bloemfontein

Republic of South Africa

August 2015

Promotor: Prof. E. van Heerden

Co-promotors: Prof. D. Litthauer
: Prof. T.C. Onstott
: Prof. T.J. Phelps
: Dr. T. Surridge

I dedicate this thesis to my godchild, Hayley Shardelow.

"Words of wisdom are spoken by children at least as often as scientists."

~ James Newman

"The more I study science, the more I believe in God."

~ Albert Einstein

"If at first, the idea is not absurd, then there is no hope for it."

~ Albert Einstein

"The value of a college education is not the learning of many facts, but the training of the mind to think."

~ Albert Einstein

"It isn't what you learn that makes you successful, but what you use of what you learn."

~ Percy H Whiting

CONTENTS

ACKNOWLEDGEMENTS

This was a very big research project and so many people were involved for whom I wish to express my sincere gratitude and appreciation, in no specific order, because without them, I would not have been able to complete this research.

- My promoter, my supervisor and my mentor, **Prof. Esta van Heerden**, for the immense role she played in making me the scientist I am today, since I started in her laboratory as an undergraduate student twelve years ago, for every opportunity she gave me to help build my career through local and international interactions, for all her guidance and especially her faith in me throughout this study and my career thus far and for her invaluable assistance in finalizing this thesis. I could not have asked for a better mentor and will always be grateful for everything I have learned from her.

- My co-promoters, **Prof. Derek Litthauer**, **Prof. Tullis Onstott**, **Prof. Tommy Phelps** and **Dr. Tony Surridge**, for their valuable support throughout this research, but also for sharing their knowledge with me and for always being willing to help and give advice when needed, not only for this project but every time I turned to them with a question or a problem. I have learned so much from each one of them.

- The teams from the **Star Diamonds Mine, Petra Diamonds** and **Frontier Mining**, for making a study site available for this research and for allowing me access for the duration of this project, but especially **Ben Visser**, for accommodating me every time I went to the mine. They were always welcoming and willing to help in any way they could.

- **My family** - my parents, **Rassie and Ria Erasmus** and my sister and brother-in-law, **Elilyia and Morné Shardelow**, for all the sacrifices they made so that I can have the opportunity to study, for all their long hours that went into finalizing this script. I will always be grateful for their unfailing love, their endless understanding and support

and for financial assistance, not only for the time of this study, but throughout my life. My niece and godchild, **Hayley Shardelow**, and all my four-legged “children” just for being a light in my life.

- **Everyone** in the **Departments of Instrumentation and Electronics**, who contributed to building and designing the high-pressure equipment used in this research, especially **Piet Botes**, whom I feel did a magnificent job and always thought about my safety first.

- **Wally van der Hoven** and **Sarel Marais**, for their tremendous amount of hours and effort that went into the final designs and the construction of the high-pressure bioreactor. So much time, money, struggles and frustrations went into this equipment and they were always willing to help again, each time when we encountered yet another problem. They were always so enthusiastic about solving the problem, which encouraged me to try again until we finally overcame each obstacle.

- **Dr. Fanie Otto** from **SASOL**, for his contribution towards components used in the bioreactor. High-pressure equipment is very expensive and he saved us a lot of money.

- **Annalize Visser** and **WG van der Hoven** for all their effort into drawing the official designs for my high-pressure equipment.

- **Elmarie Prinsloo**, for her endless support and encouragement towards Esta and myself, especially during the final days of writing this thesis.

- **Hanlie Grobler** and **Prof. Pieter van Wyk** from the Centre for Microscopy for all the hours they spent with me in front of the SEM, helping me to obtain some very magnificent images.

- **Prof. Rob Bragg**, for taking the photos of all the high-pressure equipment.

- **All collaborators**, national and international, who helped with specific analyses, but also gave insights into various aspects that facilitated this research project.

- **Everyone** in the **Department of Microbiology, Biochemistry and Food Biotechnology**, who shared ideas, made suggestions, helped where they could and for their guidance and interest shown.

- **All the past and previous members of the Extreme Biochemistry research group** who have been part of my family in the lab, as well as all my other **friends and family** for their friendship, for supporting me through good and bad times, for sharing in my success and failures and for their care and understanding, inside and outside of this department, but especially **Jou-An Chen**, **Elizabeth Ojo**, **Errol Cason**, **Marcele Vermeulen**, **Kay Kuloyo** and **Arista van der Westhuizen** for they were always willing to help me with either sampling and preparation, administrative arrangements, data analyses or any experiment where I needed assistance.

- The **South African Centre for Carbon Capture and Storage** (SACCCS), the **National Research Foundation** (NRF), the **Ernst and Ethel Eriksen Trust**, the **Technology Innovation Agency** (TIA), the **TATA group**, the **Dean** from the **Faculty of Natural and Agricultural Sciences**, the **Office for International Affairs** at the UFS, the **Deep Carbon Observatory** (DCO) and Shimadzu for any means of financial support during this study, whether it was for equipment, for travel, for research or for personal funds.

- Above all to **God**, my Creator, my Friend and my Saviour for every opportunity and giving me the ability to do this work and for all His love, grace and guidance during these years and throughout my life. *In Deo Confidimus*.

LIST OF SYMBOLS AND ABBREVIATIONS

%	Percentage
~	More or less
<	Less than
>	Greater than
≥	Greater than/Equal to
°C	Degrees Celsius
°F	Degrees Fahrenheit
$\mu g.ml^{-1}$	Microgram per millilitre
µl	Microliter
µm	Micrometre
µM	Micromolar
μ_{max}	Maximum specific growth rate
‰	Per mille/Parts per thousand
Acetyl-CoA	Acetyl coenzyme A
Aer	Aerotaxis receptor
AF	Acetate fermentation
AMS	Accelerator mass spectrometry
APSR	Adenylylsulphate reductase
Arc	Archaea
atm	Atmosphere
ATP	Adenosine triphosphate
Bac	Bacteria
BID	Barrier discharge ionization
BLAST	Basic local alignment search tool
bp	Base pairs
BP	Before present
CA	Carbonic anhydrase
CAD	Computer-aided design

CAE	Computer-aided engineering
CAF	Central analytical facilities
CBM	Coal bed methane
CCS	Carbon capture and storage
cDNA	Complementary deoxyribonucleic acid
cm	Centimetre
cm^3	Cubic centimetre
CO2CRC	Carbon dioxide cooperative research centre
CoB-SH	Coenzyme B
CoM-SH	Coenzyme M
CR	CO_2 reduction
CSIR	Council for scientific and industrial research
CTAB	Cetyl trimethylammonium bromide
DCO	Deep carbon observatory
DGGE	Denaturing gradient gel electrophoresis
dH_2O	Distilled water
DIC	Dissolved inorganic carbon
DNA	Deoxyribonucleic acid
dNTPs	Deoxyribonucleotide triphosphates
DO	Dissolved oxygen
DOC	Dissolved organic carbon
DSMZ	Deutsche sammlung von mikroorganismen und zellkulturen
dsrA	Dissimilatory sulphite reductase alpha subunit
dsrC	Dissimilatory sulphite reductase gamma subunit
EC	Electrical conductivity
ECBM	Enhanced coal bed methane
ed.	Edition
EDS	Energy dispersive x-ray
EDTA	Ethylenediaminetetraacetic acid
EGR	Enhanced gas recovery
emPCR	Emulsion polymerase chain reaction
EOR	Enhanced oil recovery
EPA	United States environmental protection agency
EPS	Extracellular polymeric substances
et al.	et alii/and others

EtBr	Ethidium bromide
EtOH	Ethanol
Euk	Eukarya
FE-SEM	Field emission scanning electron microscopy
FFKM	Perfluoro-elastomers
FW	Fissure water
g	Gram
$g.L^{-1}$	Gram per litre
G3P	Glyceraldehyde-3-phosphate
GC	Gas chromatography
gDNA	Genomic deoxyribonucleic acid
GFL®	Gesellschaft für labortechnik
GMWL	Global meteoric water line
h^{-1}	Per hour
HDPE	High-density polyethylene
HDR	Heterodisulphide reductase
HPLC	High performance liquid chromatograph
IC	Ion chromatography
ICP	Inductively coupled plasma
ICP-AES	Inductively coupled plasma atomic emission spectroscopy
IGS	Institute for ground water studies
in silco	Performed on computer/Via computer simulation
in situ	On-site
IPCC	Intergovernmental panel on climate change
IPTG	Isopropyl β-D-1-thiogalactopyranoside
IR	Infrared
ISBN	International standard book number
Ka	Thousand years ago/from the present
km	Kilometre
kPa	Kilopascal
L	Litre
$L.min^{-1}$	Litre per minute
LB	Luria-bertani
LExEn	Life in extreme environments
LOI	Loss on ignition

LTP	Life tree project
M	Molar
m	Metre
Ma	Million years ago/from the present
masl	Metres above sea level
mbs	Metres below surface
MCP	Methyl-accepting chemotaxis protein
mg	Milligram
$mg.L^{-1}$	Milligram per litre
$mg.mL^{-1}$	Milligram per millilitre
MG-RAST	Metagenomics RAST
ml	Millilitre
$ml.L^{-1}$	Millilitre per litre
$ml.min^{-1}$	Millilitre per minute
mm	Millimetre
mM	Millimolar
MM	Minimal medium
mm^2	Square millimetre
MPa	Megapascal
$mS.cm^{-1}$	Millisiemens per centimetre
$mS.m^{-1}$	Millisiemens per meter
mV	Millivolts
$MΩ.cm^{-1}$	Mega-ohm per centimetre
N	Normal/normality
$N.m^{-1}$	Newton metre
NADPH	Nicotinamide adenine dinucleotide phosphate
NASA	National aeronautics and space administration
NCBI	National centre for biotechnology information
NDIR	Non-dispersive infrared sensor
ng	Nanogram
$ng.µl^{-1}$	Nanogram per microlitre
nm	Nanometre
NMR	Nuclear magnetic resonance
NMWC	Nominal molecular weight cut-off
Myr^{-1}	Per million years

NSF	National science foundation
NZ	New Zealand
OD	Optical density
ORP	Oxidation reduction potential
Pc	Critical pressure
PCOR	Plains carbon dioxide reduction partnership
PCR	Polymerase chain reaction
PES	Polyethersulone
PGM^{TM}	Personal genome machine^{TM}
pH	Measure of the acidity or basicity of a solution
pHi	Intracellular pH
Pmol	Picomole
pmol.µl^{-1}	Picomole per microlitre
ppm	Parts per million
PS	Polysulfone
Pt	Platinum
PTFE	Polytetrafluoroethylene
PTP	Pico titer plate
PVC	Polyvinyl chloride
PVDF	Polyvinylidene fluoride
rDNase	Recombinant DNase
Rh	Rhodium
RID	Refractive index detector
RNA	Ribonucleic acid
rpm	Revolutions per minute
rRNA	Ribosomal ribonucleic acid
RSA	Republic of South Africa
RT	Reverse transcription
RuBisCO	Ribulose-1,5-biphosphate carboxylase/oxygenase
SACCCS	South African centre for carbon capture and storage
SANEDI	South African national energy development institute
SANERI	South African national energy research institute
sc-CO_2	Supercritical carbon dioxide
SD	Star Diamonds
SEM	Scanning electron microscopy

SOC	Super optimal broth with catabolite repression (SOB with added glucose)
SRB	Sulphate-reducing bacteria
STP	Standard temperature and pressure
TAE	Tris-acetate-ethylenediaminetetraacetic acid
Taq DNA polymerase	Thermostable deoxyribonucleic acid polymerase named after *Thermus aquaticus*
Tc	Critical temperature
TCA	Tricarboxylic acid
TDS	Total dissolved solids
TE	Tris-ethylenediaminetetraacetic acid
TEEIC	Tribal energy and environmental information clearinghouse
TfbI	Transformation buffer I
TfbII	Transformation buffer II
TFF	Tangential flow filtration
Tm	Melting temperature of primers
TN	Total nitrogen
TOC	Total organic carbon
UFS	University of the Free State
UHP	Ultra-high purity
UPS	Uninterruptible power supply
USA	United States of America
UV	Ultraviolet
UV/Vis	Ultraviolet-visible spectrophotometry
V	Volts
V.	Version
v/v	Volume per volume
v/v/v	Volume per volume per volume
w/v	Weight per volume
WTW	Wissenschaftlich-technische werkstätten
x g	Acceleration due to gravity
X-Gal	5-Bromo-4-chloro-3-indolyl-beta-D-galactopyranosidehosphate
XRF	X-ray fluorescence analyses

LIST OF FIGURES

LIST OF TABLES

CHAPTER 1

LITERATURE REVIEW

1.1 GLOBAL CLIMATE CHANGE AND THE GREENHOUSE EFFECT

The average global temperatures are increasing and have resulted in changes in the weather and climate. Global warming is used to describe the current and on-going increase in the average global temperature of the atmosphere near the surface of the Earth and is caused mostly by increasing concentrations of greenhouse gases, in particular carbon dioxide (CO_2) in the atmosphere (Vitousek, 1994; Pacala & Socolow, 2004; Ramanan *et al*., 2009; Solomon *et al*., 2009; Velea *et al*., 2009; EPA, 2015; IPCC, 2015; NASA, 2015; SACCCS, 2015; TEEIC, 2015). Global warming represents only one aspect of climate change, since climate change refers to any significant change in measures of climate, for instance temperature, precipitation, or wind patterns which continues for an extended period of time such as decades and even longer (Vitousek, 1994; EPA, 2015). Climate change is occurring from natural factors such as respiration and volcanic eruptions, but ultimately, human activities are the biggest contributor to the recent climate changes.

According to the last available global greenhouse gas emission by source, made by the Intergovernmental Panel on Climate Change (IPCC) in 2007, human activities such as deforestation, transportation, industrial processes, and selected agricultural practices have resulted in the release of large amounts of additional CO_2 and other greenhouse gases into the atmosphere, with the leading contributor for these emissions being from the burning of fossil fuels such as coal, natural gas, and oil for power generation and energy supply (Figure 1.1) (Vitousek, 1994; Solomon *et al*., 2009; Velea *et al*., 2009; EPA, 2015; SACCCS, 2015; TEEIC, 2015). These additional emissions are responsible for the greenhouse effect (Figure 1.2). Radiation, primarily from the sun, reaches the surface of the Earth in the form of visible light, ultraviolet (UV), infrared (IR) and other forms of radiation. Around 30% of this radiation that reaches the Earth's atmosphere is immediately reflected back out to space through clouds, ice, snow, sand and other reflective surfaces

(NASA, 2015). The remaining 70% is absorbed by the oceans, land, and atmosphere, thereby, warming up the Earth and heat is released in the form of IR thermal radiation, which is then radiated back into the atmosphere on its way to space (EPA, 2015).

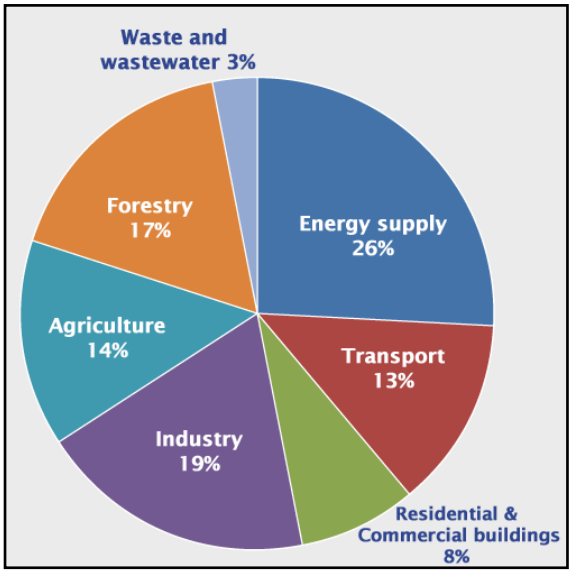

Figure 1.1: Global greenhouse gas emissions by source, based on global emissions from 2004 [Taken from EPA, (2015)].

As the layer of greenhouse gases around the planet grows thicker, more heat is trapped in the atmosphere, less radiates away and the Earth slowly heats up, causing the temperature on the Earth to rise and the climate to change and ultimately results in harmful consequences to human health, the economy, and the ecosystems (Vitousek, 1994; Velea *et al*., 2009; EPA, 2015; IPCC, 2015; TEEIC, 2015).

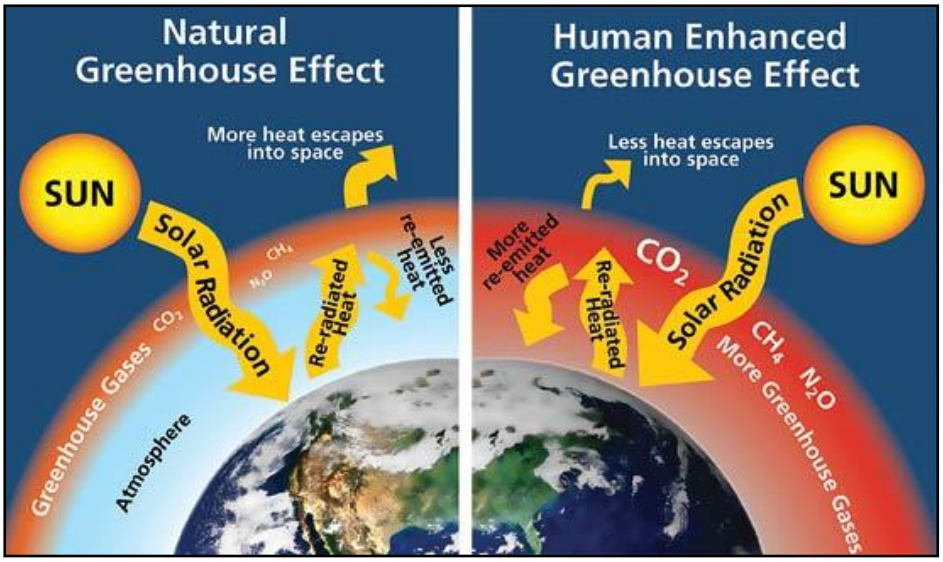

Figure 1.2: Natural and human enhanced greenhouse effects [Taken from livescience.com, (2015)].

According to the last available global greenhouse gas emission by gas, made by the IPCC in 2007, these gases include water vapour, CO_2, methane (CH_4), nitrous oxide (N_2O), and fluorinated gases. Of these emissions, CO_2 is the most important anthropogenic greenhouse gas (Figure 1.3) (EPA, 2015).

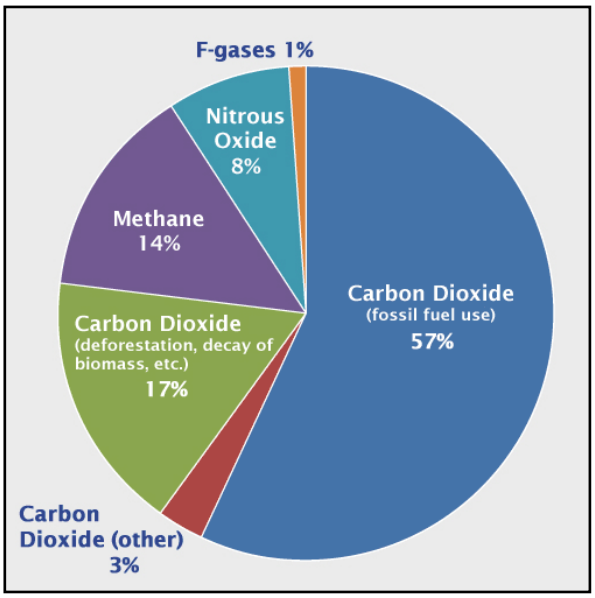

Figure 1.3: Global greenhouse gas emissions by gas, based on global emissions from 2004 [Taken from EPA, (2015)].

Since the beginning of the Industrial Revolution in the early 1800's, the CO_2 levels in the atmosphere have increased by more than 40%, from ~280 parts per million (ppm) in the year 1850 to ~400 ppm today (Figure 1.4), and are at its highest in 650 000 years (Vitousek, 1994; Pacala & Socolow, 2004; Velea *et al*., 2009; NASA, 2015; SACCCS, 2015). The global CO_2 emissions due to the burning of fossil fuels have increased >16 times during 1900 and 2008 (Boden *et al*., 2010). This has resulted in massive impacts on what is considered normal conditions on the Earth such as changes in rainfall, resulting in floods, droughts, or intensive heat-waves. The oceans are warming and becoming more acidic, ice caps are melting, and sea levels are rising (EPA, 2015; IPCC, 2015; NASA, 2015).

The average temperature of the Earth has increased by 1.4°F (~0.8°C) over the last 100 years (Figure 1.5), where nine of the ten warmest years occurred since the year 2000, with 2014 ranked as the warmest year on record.

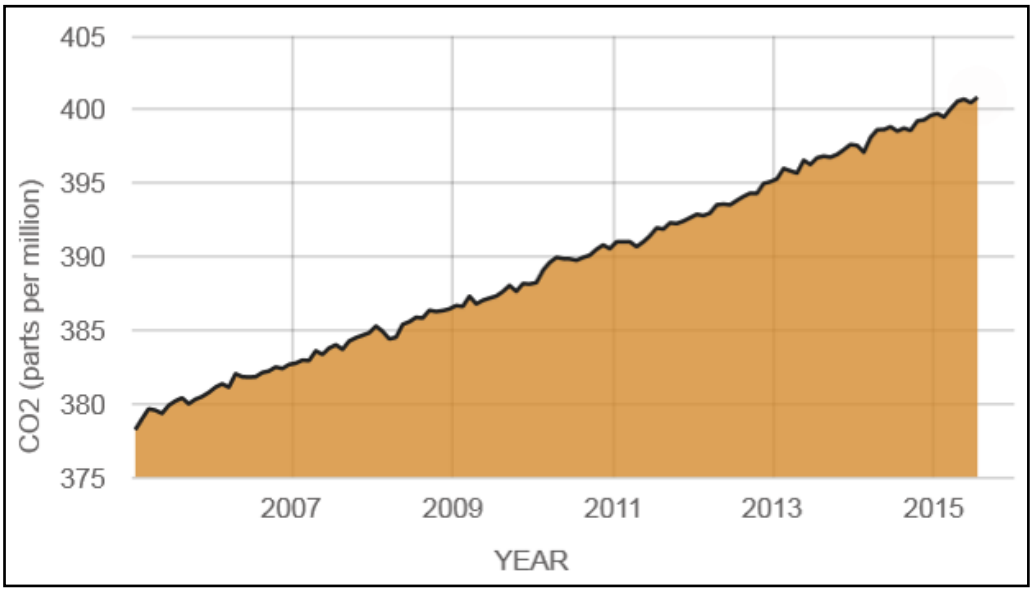

Figure 1.4: Direct measurements for the increase in the atmospheric CO_2 levels during recent years [Taken from NASA, (2015)].

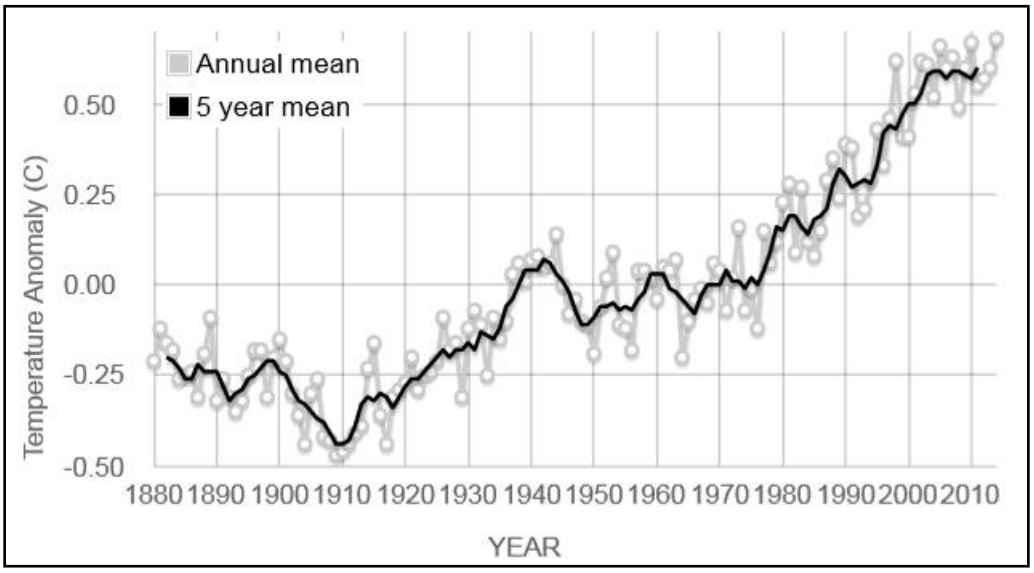

Figure 1.5: The change in global surface temperature relative to 1951-1980 average temperatures [Taken from NASA, (2015)].

Predictions are that the temperatures will increase with another 2 - 11°F over the next century and that these perceived small changes can result potentially dangerous shifts in the climate and weather (NASA, 2015). Each September, the Arctic sea ice reaches its minimum and is now declining at a rate of 13.3% per decade, relative to the 1981 to 2010 average (NASA, 2015).

Since 2002, Antarctica has been losing about 134 billion metric tons of ice per year, while the Greenland ice sheet has been losing an estimated 287 billion metric tons per year (NASA, 2015). The rise in sea levels are mainly caused by two global warming related factors which are the added water from melting land ice and the expansion of sea water as it warms and the global average sea level has risen by ~178 mm during the past century (NASA, 2015).

Carbon dioxide can stay in the atmosphere for almost a century, therefore, the Earth will continue to heat up in future decades (Solomon *et al*., 2009; EPA, 2015). As these and other changes become more prominent, humanity and the environment will be facing more severe challenges. Consequently, active carbon management is essential to control the increase in global CO_2 emissions and thereby mitigate the impact of climate change by enacting policies that essentially reduce the concentration of CO_2 in the atmosphere (Pacala & Socolow, 2004; Surridge & Cloete, 2009; Morozova *et al*., 2010; EPA, 2015). A possible solution is to replace the use of fossil fuels such as oil, coal, and gas with energy sources like solar, wind and possibly nuclear and use them more efficiently, but the first steps are to address the existing fossil fuel base infrastructure and the excessive levels of CO_2 being emitted globally. Therefore, sequestering anthropogenic CO_2 from the atmosphere may allow some time to make the transition to low carbon-emitting technologies (Metz *et al*., 2007; Sherwood Lollar & Ballentine, 2009; Surridge & Cloete, 2009; Cloete, 2010).

1.2 CARBON SEQUESTRATION

Carbon sequestration, also known as carbon capture and storage (CCS) is a process where CO_2 is stored away from the atmosphere, as a means to mitigate global climate change (Metz *et al*., 2007; Holloway, 2007; Cunningham *et al*., 2009; Morozova *et al*., 2010; Glossner, 2013; Mu *et al*., 2014) and has the potential to store millions of tonnes of CO_2. In order to mitigate the CO_2 emissions on a scale that can stabilize the atmospheric greenhouse gases and make an impact on climate change, storage on this scale is necessary. Consequently, CCS has the potential to help meet emission reduction goals (Metz *et al*., 2007; Holloway, 2007; Surridge & Cloete, 2009; Peters *et al*., 2011).

Several possibilities exist for the potential storage of CO_2 (Figure 1.6), and include direct/artificial and indirect/natural sequestration. During direct/artificial sequestration, the CO_2 is captured before being released into the atmosphere, and stored through geological sequestration or ocean sequestration. For indirect/natural sequestration, terrestrial or biological sequestration is used, and involves the removal of the CO_2 from the atmosphere through plants, trees and subsequent storage in soil. CO_2 can also be fixed into inorganic carbonates in the subsurface, through mineral sequestration/carbonation (Metz *et al*., 2007; Cloete, 2010; EPA, 2015; PCOR, 2015; TEEIC, 2015).

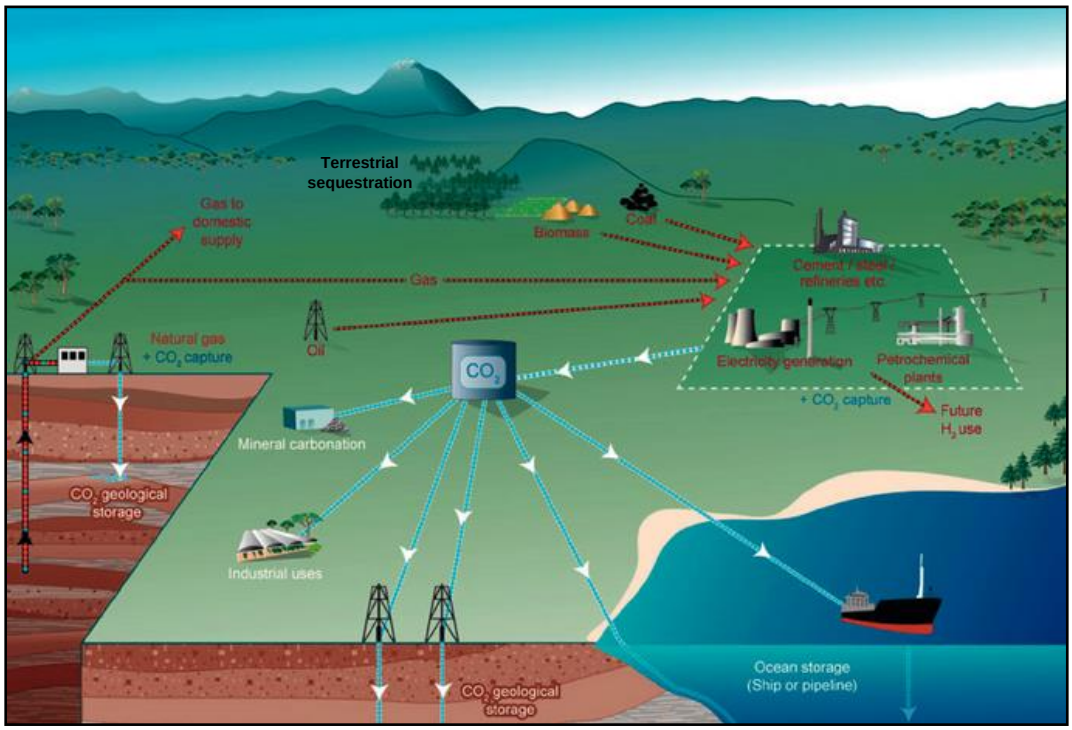

Figure 1.6: Potential storage options for CO_2 [Adapted from Sims *et al*., (2007)].

1.2.1 Geological Sequestration

During geological sequestration (Figure 1.7), anthropogenic CO_2 is injected into underground formations such as depleted oil and gas fields, un-minable coal beds, and deep saline formations, either onshore or offshore (Metz *et al*., 2007; Cloete, 2010; TEEIC, 2015). During storage in depleted oil and gas fields, the CO_2 is trapped in the pore spaces of the sedimentary rock, leading to enhanced oil and gas recovery (EOR and EGR). For the un-minable coal beds, the CO_2 displaces the coal bed methane (CBM) by adsorption onto the coal surfaces, leading to enhanced CBM recovery (ECBM) (Cloete, 2010).

Storage of CO_2 in deep saline formations is generally expected to take place at depths of >800 metres below surface (mbs), or where the ambient pressure and temperature conditions will result in the CO_2 being in a supercritical state, thereby filling the pore spaces of the sedimentary rock (Benson & Cole, 2008; Cunningham *et al*., 2009; Cloete, 2010; Nondorf *et al*., 2011; Glossner, 2013; Gulliver, 2014).

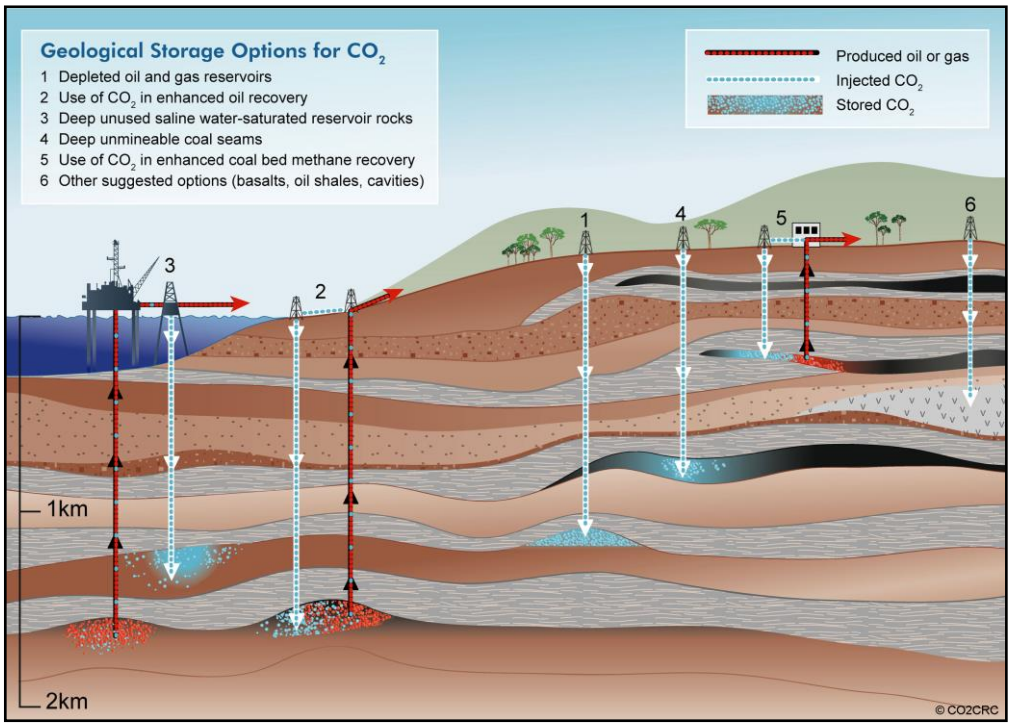

Figure 1.7: Possible geological storage options for CO_2 [Taken from the Carbon dioxide Cooperative Research Centre, (2015) (CO2CRC.com)].

During storage in deep saline formations, the first step is capturing the CO_2, generated from human activity and from large industrial facilities such as power plants, oil refineries or cement plants. The captured CO_2 is separated from other gases and pressurized to a supercritical fluid. This fluid is then transported to its destination, either through the use of pipelines, trucks, or ships, and is injected deep below the surface of the Earth into porous rock such as sandstone, which has the necessary porosity and permeability (Figure 1.8). This rock should be overlaid with an impermeable cap rock such as shale, which acts as a seal to prevent CO_2 from migrating back to the surface of the Earth and ultimately entering the atmosphere (Metz *et al*., 2007; Holloway, 2007; Cunningham *et al*., 2009; Cloete, 2010; Glossner, 2013; Gulliver, 2014; TEEIC, 2015).

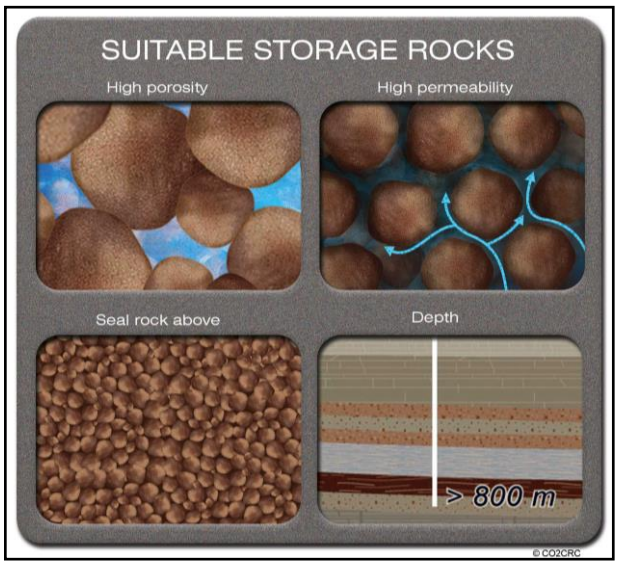

Figure 1.8: Properties for suitable storage rocks [Taken from the Carbon dioxide Cooperative Research Centre, (2015) (CO2CRC.com)].

1.2.2 Ocean Sequestration

During ocean sequestration (Figure 1.9), anthropogenic CO_2 can potentially be injected into the water column, at >1 000 mbs, through the use of a fixed pipeline or a moving ship or by depositing it onto the sea floor, at >3 000 mbs, through the use of a fixed pipeline or an offshore platform (Metz *et al*., 2007).

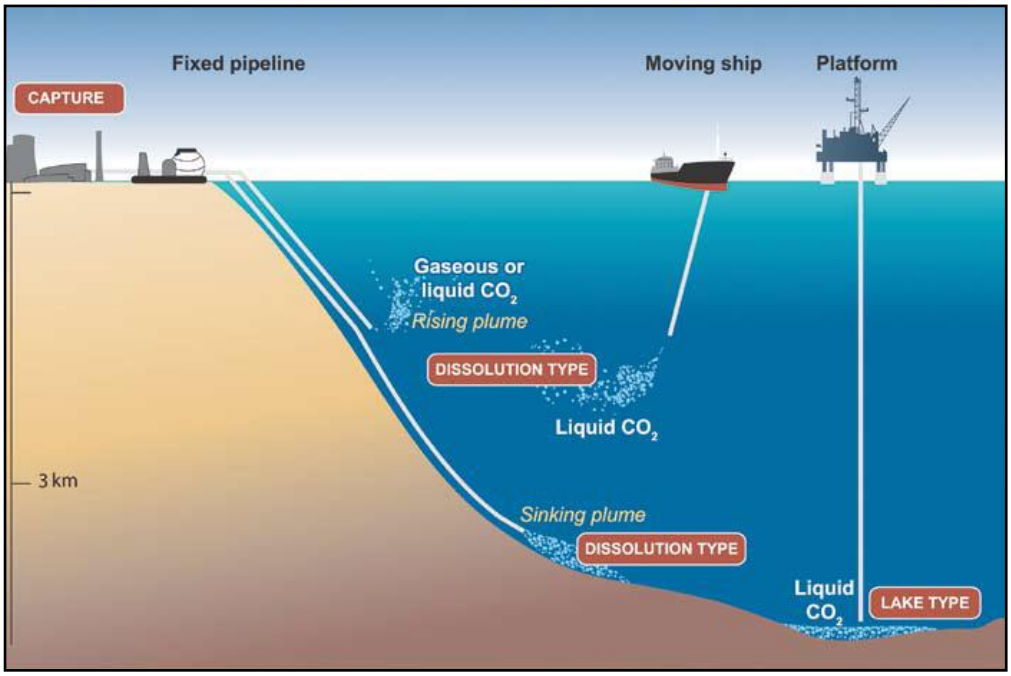

Figure 1.9: Possible ocean storage options for CO_2 [Taken from the Carbon dioxide Cooperative Research Centre, (2015) (CO2CRC.com)].

At >1 000 mbs, the CO_2 will be able to dissolve and disperse to form part of the global carbon cycle where it will eventually equilibrate with the CO_2 in the atmosphere. At >3 000 mbs, the CO_2 is denser than water and should form a lake that would delay the dissolution of the CO_2 into the surrounding environments (Metz *et al*., 2007).

1.2.3 Terrestrial Sequestration

Terrestrial sequestration (Figure 1.10) is the natural process of CO_2 sequestration that occurs with trees, plants, animals, the oceans, and soil (PCOR, 2015; TEEIC, 2015).

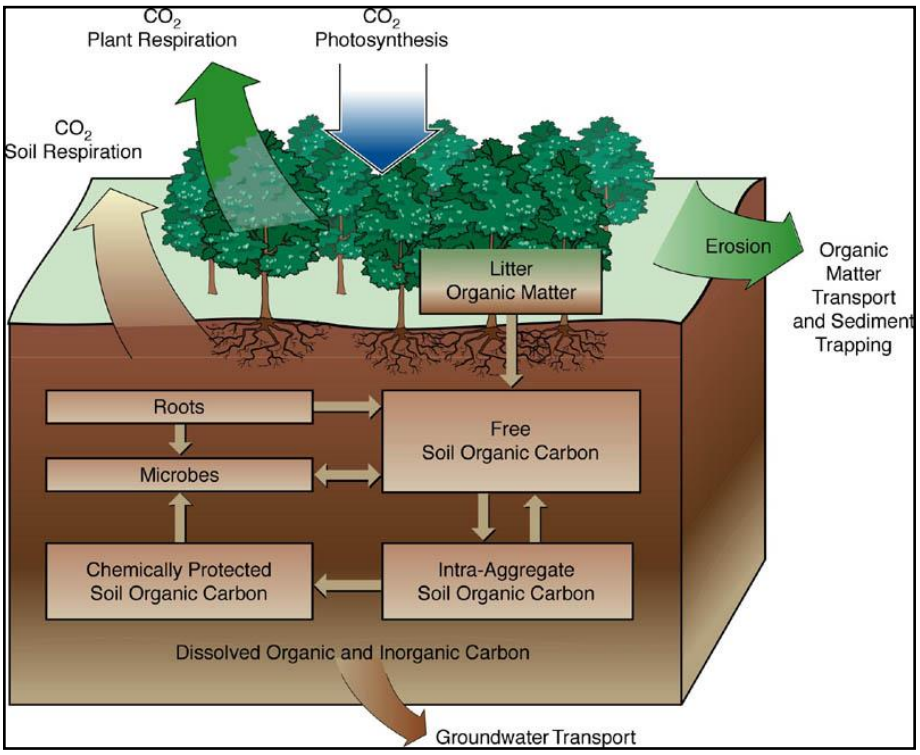

Figure 1.10: The process of terrestrial sequestration [Taken from tececo.com, (2015)].

Trees and plants can use atmospheric CO_2 to live and grow through photosynthesis. During this process, the CO_2 becomes part of the plant and may result in carbon that is sequestered for a long period of time in stems and roots, as well as in the soil. When the plant or tree dies, the plant material decomposes, releasing some of the carbon into the atmosphere and capturing the rest within the soil which increases the soil's organic matter content. Terrestrial sequestration can be increased through forest management, reforestation, and afforestation (PCOR, 2015; TEEIC, 2015).

1.2.4 Mineral Sequestration

Mineral sequestration/carbonation (Figure 1.11) is a chemical process of CO_2 storage wherein the atmospheric CO_2 reacts with metal oxides such as calcium oxide (CaO) or magnesium oxide (MgO) to produce stable carbonate minerals. These oxides are found in silicate minerals or industrial waste streams. This is naturally a very slow process, but can be enhanced through pre-treatment of the minerals (Metz *et al*., 2007; Cloete, 2010).

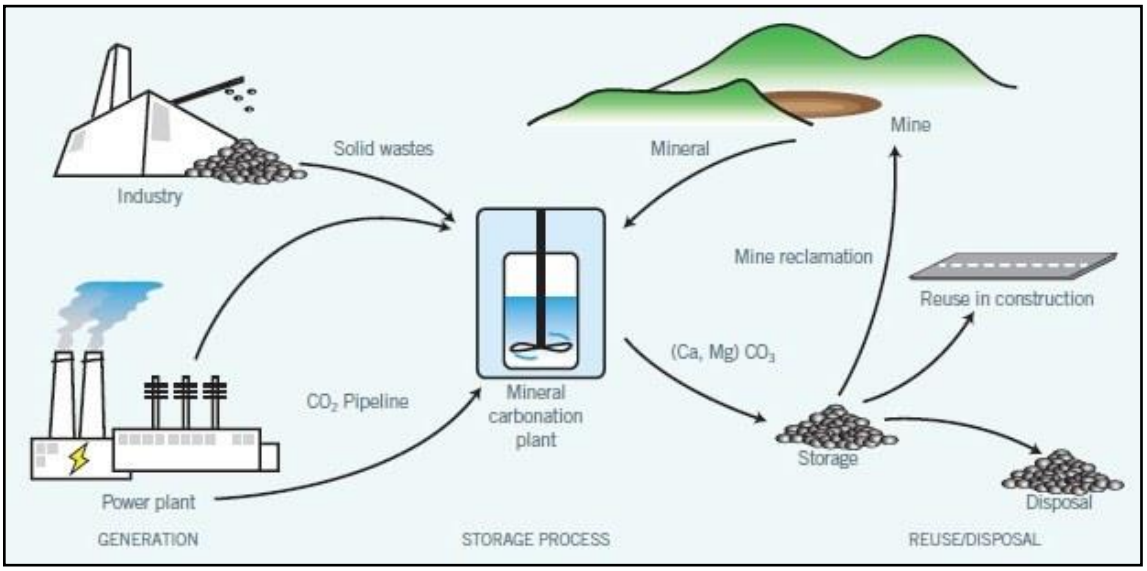

Figure 1.11: The process for mineral carbonation [Taken from decarboni.se, (2015)].

1.3 CARBON SEQUESTRATION IN SOUTH AFRICA

Possible carbon sequestration sites exist worldwide, but these storage formations are not evenly distributed (Figure 1.12), therefore, the potential for underground storage of CO_2 varies for each country. During preliminary investigations by the Council for Scientific and Industrial Research (CSIR) in 2004, it was determined that South Africa has various sites (Figure 1.13) for the storage of CO_2 and that of the more than 400 million tonnes of annual carbon dioxide emissions in South Africa ~60% can be sequestered (Surridge & Cloete, 2009; Cloete, 2010).

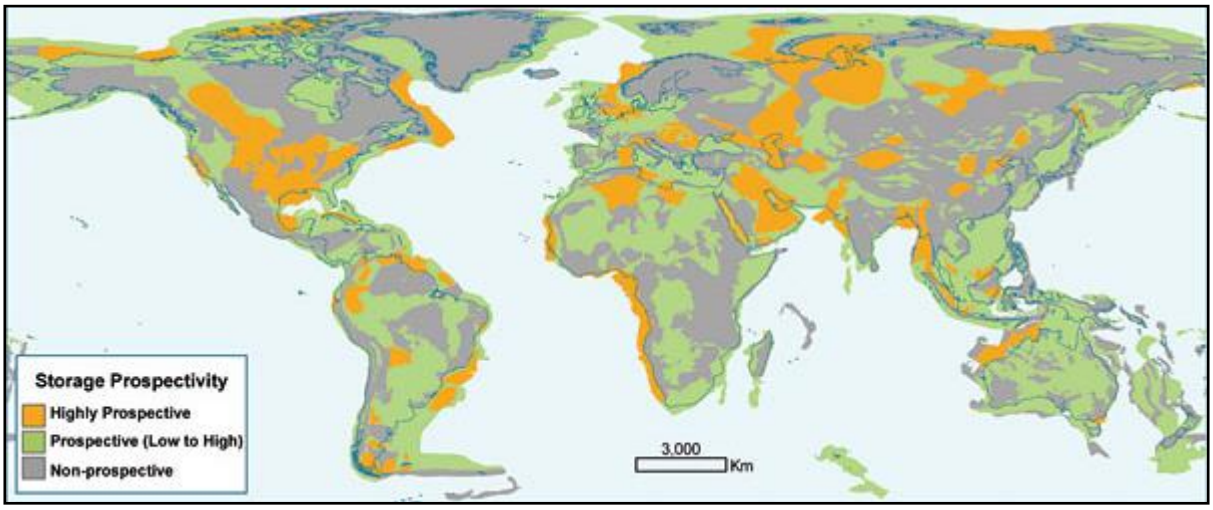

Figure 1.12: Global CO_2 storage potential, with estimate storage capacities of 2 – 10 trillion tons of CO_2 [Taken from stanford.edu, (2015)].

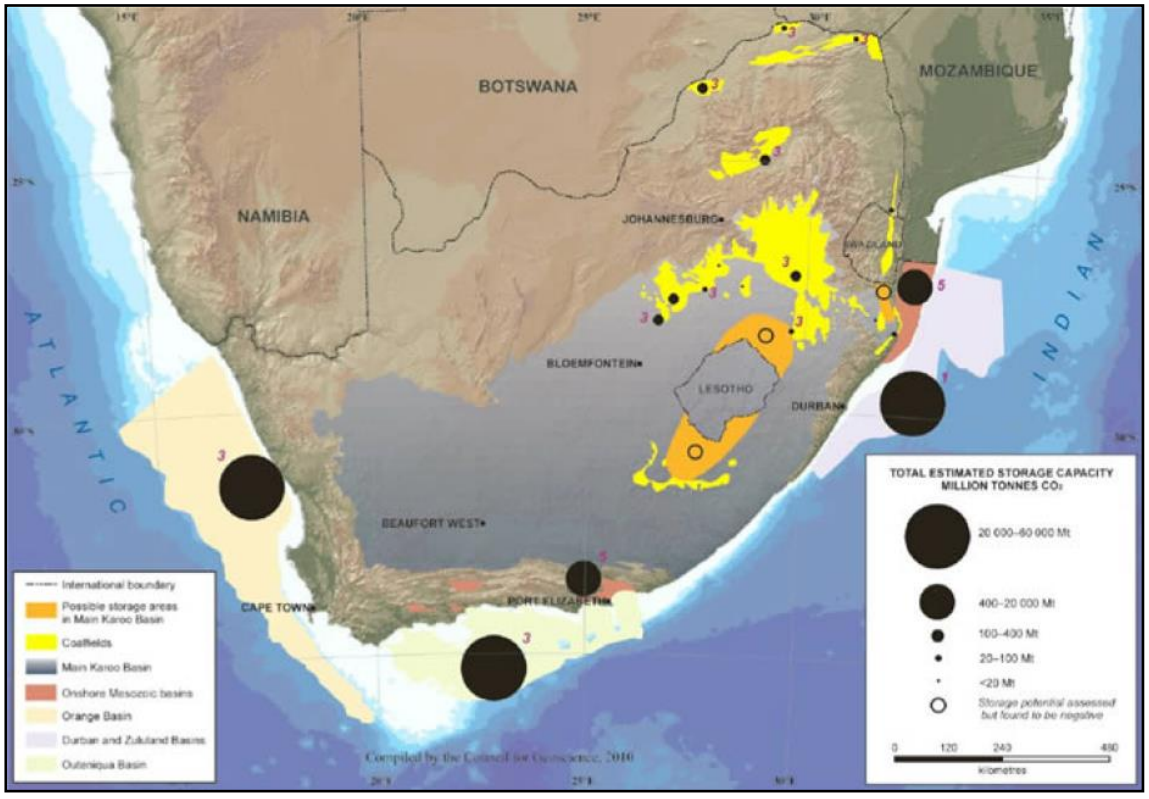

Figure 1.13: Possible CO_2 storage sites for South Africa [Taken from Cloete, (2010)].

During 2007, a long-term mitigation scenario study was conducted to determine all the actions that South Africa could undertake to limit the emissions of greenhouse gases. During 2009, an investigation into the regulation gaps for CCS was initiated by the Department of Energy and in In March 2009, the South African Centre for Carbon Capture

and Storage (SACCCS) was established with the support of South African National Energy Development Institute (SANEDI), previously known as the South African National Energy Research Institute (SANERI) and in 2010, a detailed Atlas on geological storage of CO_2 in South Africa was released (Surridge & Cloete, 2009; Cloete, 2010; SACCCS, 2015). This Atlas indicated that South Africa's CO_2 emissions will increase until 2020 - 2025, stabilize for a decade and then decrease dramatically after 2030 – 2035 (Cloete, 2010).

1.4 THE CARBON CYCLE

The carbon cycle is the circulation and transformation of carbon back and forth between living material and the environment, which includes the terrestrial biosphere, the oceans, the atmosphere, and the geosphere (Detwiler & Hall, 1987; Houghton *et al*., 1995; Sedjo, 2001; Graber, 2011; TEEIC, 2015).

During carbon cycling between the terrestrial biosphere and the atmosphere, terrestrial plants remove carbon from the atmosphere through photosynthesis, where the CO_2 is stored and used for growth. Animals can absorb this carbon through ingestion of plants, where the carbon from nutrients and food is consumed and CO_2 is released as waste back into the atmosphere through respiration. Plants can then again absorb this CO_2 or microorganisms can break down the animal manure into methane and CO_2. This is similar to microorganisms degrading dead plants and animals and converting the carbon into CO_2 and methane that becomes part of the soil. Over long periods of time, this dead organic matter is compacted and will become part of the geosphere through a process called sedimentation, the process responsible for the production of fossil fuels such as oil and coal (Detwiler & Hall, 1987; Houghton *et al*., 1995; Sedjo, 2001; Graber, 2011; TEEIC, 2015).

Carbon cycles between the atmosphere and the ocean through a process called diffusion and aquatic plant life absorbs carbon through photosynthesis. Marine life can absorb this carbon through consumption, which is then returned to the water in air through respiration. When these organisms die, they decay and release carbon into the ocean which can be transferred to the ocean floor through sedimentation. Carbon enters the oceans from the geosphere in the form of bicarbonate. Bicarbonate also forms in the oceans when the atmospheric CO_2 dissolves in the water. Some of the marine life can use this bicarbonate to build their skeletons or it can form limestone. The limestone sinks to the bottom of the

ocean, sequestering the carbon in the geosphere for a long time. As ocean waters flows between the cold poles and the equator, and as it cycles to and from the warm shallow waters and the cold deep water, it absorbs and releases carbon from the atmosphere, typically as CO_2 (Detwiler & Hall, 1987; Houghton *et al*., 1995; Sedjo, 2001; Graber, 2011; TEEIC, 2015).

Several processes are involved in cycling carbon between the geosphere and the atmosphere such as volcanic eruptions and the production of cement. Cement is made from limestone removed from the geosphere, and involves heating this limestone, thus releasing its stored carbon as CO_2. The burning of fossil fuels also releases carbon into the atmosphere (Detwiler & Hall, 1987; Houghton *et al*., 1995; Sedjo, 2001; Graber, 2011; TEEIC, 2015).

1.5 THE DEEP SUBSURFACE AND CARBON CYCLING

The terrestrial subsurface biosphere has been estimated to contain 40–50% of the world's biomass in the form of microorganisms, extending deeper than four kilometres into the Earth's crust, with cell concentrations ranging from $1x10^9$ to 28 cells/gram or cells/ml (Zhang *et al*., 2005; Wang *et al*., 2007; Chivian *et al*., 2008; Borgonie *et al*., 2011; Magnabosco *et al*., 2014; Mu *et al*., 2014; Rajala *et al*., 2015). However, comprehensive studies on the phylogenetic diversity and distribution are geographically limited as a result of the vast capacity of the subsurface ecosystems, but also due to the difficulty in obtaining samples from these extreme and highly reducing environments. Thus, the diversity, abundance and function of these subsurface microorganisms remains largely unknown (Ghiorse & Wilson, 1988; Gold, 1992; Parkes *et al*., 1994; White *et al*., 1998; Whitman *et al*., 1998; Pedersen, 2000; Teske, 2005; Chivian *et al*., 2008; Fry *et al*., 2008; Ragon *et al.*, 2013; Rajala *et al*., 2015).

Even though the terrestrial subsurface includes a substantial fraction of the global biosphere (Pedersen, 1993; Onstott *et al*., 1998; Whitman *et al*., 1998), these microorganisms are likely to be inactive or have exceptionally slow metabolisms, as they are living under extreme energy limiting conditions, especially due to the low nutrient availability in subsurface environments (Jørgensen & D'Hondt, 2006; Jørgensen & Boetius, 2007; Sogin *et al*., 2010; Rajala *et al*., 2015). Geochemical evidence suggests

that these *in situ* microbial metabolisms are estimated to be in the nano- to micromolar range per year, with an average turnover time of decades or centuries (Phelps *et al*., 1994; Onstott *et al*., 2009). Excluded from the presence of sunlight, the deep subsurface provides a natural environment where energy-yielding processes such as radiolytic decomposition of water to yield H_2, O_2, and H_2O_2, with the subsequent oxidation of minerals containing reduced forms of sulphur, iron, manganese, or even arsenic may sustain carbon cycling (Lovley & Chapelle, 1995; Onstott *et al*., 2006; Sogin *et al*., 2010). Thus, an increase in the metabolic activities of the subsurface microorganisms may occur through the accessibility of chemical energy at sedimentary and/or geochemical interfaces, and is usually derived from redox reactions involving organic matter or inorganic electron donors such as iron, hydrogen, methane, and hydrogen sulphide (Chapelle *et al*., 2002; Nealson *et al*., 2005; Onstott *et al*., 2006; Jorgensen & Boetius, 2007; Ragon *et al.*, 2013).

It was found that H_2 might be the most important energy source for these subsurface communities, since subsurface microbial communities make use of substrates, obtained from geochemical processes and not from photosynthetically derived organic carbon (Stevens & McKinley, 1995; Pedersen, 2001; Lin *et al*., 2005; Nealson *et al*., 2005; Onstott *et al*., 2006). Studies conducted on the biogeochemistry of the deep subsurface indicate that, even though all three domains of life (Archaea, Bacteria and Eukarya) have been found to be present in the subsurface, it is generally dominated by the Bacteria, especially the Proteobacteria and the Firmicutes, and that the leading microbial activities in these extreme environments are methanogenesis, sulphate reduction, and fermentation, the terminal steps in the degradation of organic compounds in the carbon cycle (Banfield *et al*., 1999; Takai *et al*., 2001; Kotelnikova, 2002; Baker *et al*., 2003; Newberry *et al*., 2004; Onstott, 2005; Webster *et al*., 2006; Fry *et al*., 2008; Basso *et al*., 2009; Morozova *et al*., 2010; Ragon *et al*., 2013; Lau *et al*., 2014; Magnabosco *et al*., 2014). However, the role of the microbial communities in the carbon cycling occurring in the subsurface, remains poorly understood and are only minimally represented in carbon cycle models (Sogin *et al*., 2010; Rajala *et al*., 2015).

Therefore, an important aspect to consider during carbon sequestration, is the potential response of the subsurface microbial communities towards elevated CO_2 levels, since these microorganisms can play a significant role in the carbon cycling that occurs in the subsurface (Chapelle *et al*., 2002; Morozova *et al*., 2010; Bordenave *et al*., 2012; Mu *et al*., 2014). Most of the prokaryotic microbial communities contain individuals that can grow

autotrophically, thus, contribute to a supply of organic carbon for heterotrophic microorganisms. Even though the Calvin cycle is known to be the most important autotrophic carbon fixation pathway, it is restricted to organisms with high-energy yield from a chemotrophic or phototrophic existence (Hügler *et al*., 2005). Therefore, the subsurface microorganisms could utilize different CO_2 fixation pathways such as the reductive tricarboxylic acid (TCA) cycle, the reductive acetyl-CoA pathway, and the 3-hydroxypropionate cycle (Hügler *et al*., 2005).

Heterotrophic microorganisms cannot fix carbon; thus, they use organic carbon for growth (Hogg, 2013) and obtain their energy from the oxidation of organic compounds such as lipids, proteins, and carbohydrates, especially glucose. Biologic oxidation of these organic compounds results in the synthesis of Adenosine triphosphate (ATP). Heterotrophic metabolism includes respiration and fermentation (Jurtshuk, 1996; Hogg, 2013). During respiration, the organic compounds are completely oxidized to CO_2 and H_2O. For aerobic respiration, molecular O_2 is the terminal electron acceptor, whereas with anaerobic respiration, NO_3^-, SO_4^{2-}, CO_2, or fumarate can serve as the terminal electron acceptors, depending on the microorganism. Fermentation requires an organic compound such as glucose as a terminal electron or hydrogen acceptor and the formation of end products result from anaerobic dissimilation of organic compounds. Energy, in the form of ATP, is generated through dehydrogenation reactions through the enzymatic breakdown of glucose (Jurtshuk, 1996; Hogg, 2013).

Autotrophic microorganisms can make use of CO_2 as their sole carbon source and include the photoautotrophs, which can use light as their energy source and CO_2 as the carbon source, as well as the chemoautotrophs (also known as the chemolitotrophs or the chemolitoautotrophs), which use inorganic chemicals as their energy source and CO_2 as the carbon source (Jurtshuk, 1996; Lim, 2003; Hogg, 2013). Through a process called photophosphorylation, the photoautotrophs can convert light energy to chemical energy (ATP) during photosynthesis. The chemoautotrophs can remove electrons from inorganic compounds and through using the electron transport chain, reduced nicotinamide adenine dinucleotide phosphate (NADPH) is formed as the end product (Jurtshuk, 1996; Lim, 2003; Hogg, 2013). The resulting ATP and NADPH can be used for CO_2 fixation with the Calvin cycle.

Bacterial methanogenesis can take place without the presence of sunlight by a group of microorganisms, called the methanogens. These microorganisms are thought to be responsible for contributing towards greenhouse gas emissions as they produce methane, for example, in cow manure, since they are abundant in these anoxic habitats (Koide, 1999). The methanogens use CO_2 as the carbon source for growth and as a final electron acceptor to produce methane and fix CO_2 using the reductive acetyl-CoA pathway. Thus, if CO_2 is injected into the deep subsurface and dissolves in groundwater, the methanogens can reduce the CO_2 to produce methane, when H_2 is available (Koide, 1999; Ju *et al*., 2008; Glossner, 2013). Methane is less soluble in water than CO_2 and can easily migrate to Earth's surface. Therefore, if no cap rock or seal exists to trap the methane in the subsurface, it will be emitted into the atmosphere and contribute to climate change (Koide, 1999).

1.6 CONCLUSIONS

Climate change is predominantly caused by increasing concentrations of greenhouse gases, more specifically CO_2, in the atmosphere. Human activities, mainly from the burning of fossil fuels, are the biggest contributor to the increase in the average global temperature of the Earth's atmosphere and to limit these CO_2 emissions, carbon resources have to be managed more effectively.

As a possible solution, storage of anthropogenic CO_2 into geological formations, away from the atmosphere, may allow some time for the world to transition to renewable energy. However, CO_2 storage sites require that intensive studies before, during, and after injection should be done since there are several potential risks during carbon sequestration if these activities are not monitored.

South Africa has determined that various potential sites for the storage of CO_2 are available and that of the more than 400 million tonnes of annual carbon dioxide emissions in South Africa, ~60% can be sequestered. However, during the past few years, there has been an increased understanding of the volume and activities of life in the deep subsurface. The coupled hydrological, microbiological and geochemical processes occurring within these extreme environments may result in natural chemical fluxes that could influence water quality. The deep terrestrial biosphere in South Africa is dominated by radiogenic noble gases and crustal-derived carbon sources, with microbial metabolisms dominated by methanogenesis, sulphate reduction, and fermentation.

The terrestrial subsurface biosphere remains an extreme environment where microbial communities evolved various mechanisms in order to survive the high pressures and temperatures, the limited energy and nutrient sources, the extreme acidity and alkalinity, the metal toxicity, as well as radioactive processes encountered in the subsurface. Therefore, these microorganisms not only have the ability to adapt to these conditions, but they can also change their surrounding environment in order to provide the necessary nutrients to sustain them. As a result, their survival depends mainly on their ecological and metabolic capabilities (Pikuta *et al*., 2007; Reith, 2011).

Microbial activity in subsurface environments could potentially play a critical role in the cycling of carbon and other elements between the deep and shallow environments on

Earth (Sogin *et al*., 2010). Consequently, the metabolic activity of these subsurface microbial communities and their response to varying environmental conditions could contribute to substantial changes in the structure and chemical composition of the rock formations by influencing the porosity and permeability of the storage reservoir. These changes can result in possible leakage of the CO_2, or even methane, since the CO_2 may be fixed into organic matter by chemoautotrophs and in addition converted into methane by the methanogens.

1.7 REFERENCES

- **Baker, B.J., Moser, D.P., MacGregor, B.J., Fishbain, S., Wagner, M., Fry, N.K., Jackson, B., Spoelstra, N., Loos, S., Takai, K., Sherwood Lollar, B., Fredrickson, J.K., Balkwill, D., Onstott, T.C., Wimpee, C.F. and Stahl, D.A.** (2003). Related Assemblages of Sulphate Reducing Bacteria Associated with Ultra Deep Gold Mines of South Africa and Deep Basalt Aaquifers of Washington State. *Environ Microbiol*. **5(4)**:267–277.

- **Banfield, J.F., Barker, W.W., Welch, S.A. and Taunton, A.** (1999). Biological Impact on Mineral Dissolution: Application of the Lichen Model to Understanding Mineral Weathering in the Rhizosphere. *Proc. Natl. Acad. Sci*. **96**:3404-3411.

- **Basso, O., Lascourreges, J.F., Le Borgne, F., Le Goff, C. and Margot, M.** (2009). Characterization by Culture and Molecular Analysis of the Microbial Diversity of a Deep Subsurface Gas Storage Aquifer. *Res. Microbiol*. **160**:107–116.

- **Benson, S.M. and Cole, D.R.** (2008). CO_2 Sequestration in Deep Sedimentary Formations. *Elements*. **4**:325-331.

- **Boden, T.A., Marland, G. and Andres, R.J.** (2010). Global, Regional, and National Fossil-Fuel CO_2 Emissions. Carbon Dioxide Information Analysis Centre, Oak Ridge National Laboratory, U.S. Department of Energy, Oak Ridge, Tenn., USA.

- **Bordenave, S., Chatterjee, I. and Voordouw, G.** (2012). Microbial Community Structure and Microbial Activities Related to CO_2 Storage Capacities of a Salt Cavern. *Int. Biodeterior. Biodegrad*. **81**:82-87.

- **Borgonie, G., García-Moyano, A., Litthauer, D., Bert, W., Bester, A., van Heerden, E., Möller, C., Erasmus, M. and Onstott, T.C.** (2011). Nematoda from the Terrestrial Deep Subsurface of South Africa. *Nature*. **474**:79-82.

- **Chapelle, F.H., O'Neill, K., Bradley, P.M., Methé, B.A., Ciufo, S.A., Knobel, L.L. and Lovley, D.R.** (2002). A Hydrogen-Based Subsurface Microbial Community Dominated by Methanogens. *Nature*. **415**:312-315.

- **Chivian, D., Brodie, E.L., Alm, E.J., Culley, D.E., Dehal, P.S., DeSantis, T.Z., Gihring, T.M., Lapidus, A., Lin, L., Lowry, S.R., Moser, D.P., Richardson, P.M., Southam, G., Wanger, G., Pratt, L.M., Andersen, G.L., Hazen, T.C., Brockman, F.J., Arkin, A.P. and Onstott, T.C.** (2008). Environmental Genomics Reveals a Single-Species Ecosystem Deep Within Earth. *Science*. **322**:275-278.

- **Cloete, M.** (2010). Atlas on Geological Storage of Carbon Dioxide in South Africa. Council for Geoscience.

- **Cunningham, A.B., Gerlach, R., Spangler, L. and Mitchell, A.C.** (2009). Microbially Enhanced Geologic Containment of Sequestered Supercritical CO_2. *Energy Procedia*. **1**:3245-3252.

- **Detwiler, R.P. and Hall, C.A.** (1987). Tropical forests and the Global Cycle. *Science*. **23**:42-47.

- **Fry, J.C., Parkes, R.J., Cragg, B.A., Weightman, A.J. and Webster, G.** (2008). Prokaryotic Biodiversity and Activity in the Deep Subseafloor Biosphere. *FEMS Microbiol.Ecol*. **66**:181-196.

- **Ghiorse, W.C. and Wilson, J.T.** (1988). Microbial Ecology of the Terrestrial Subsurface. *Adv. Appl. Microbiol*. **33**:107-172.

- **Glossner, A.** (2013). Terminal Microbial Metabolisms in the Deep Subsurface under Conditions Relevant to CO_2 Sequestration and Enhancing Methanogenesis from Coal. *PhD Thesis, Colorado School of Mines*.

- **Gold, T.** (1992). The Deep, Hot Biosphere. *Proc. Natl. Acad. Sci*. **89**:6045-6049.

- **Graber, J.** (2011). The Genomic Science Program: Microbial Communities and the Carbon Cycle National Academies Report: A New Biology for the 21st Century.

- **Gulliver, D.M.** (2014). Concentration - Dependent Effects of CO_2 on Subsurface Microbial Communities under Conditions of Geologic Carbon Storage and Leakage. *PhD Thesis, Carnegie Mellon University*.

- **Hogg, S.** (2013). Essential Microbiology (2nd ed.). *Wiley-Blackwell Publishers.* ISBN: 9781119978909.

- **Holloway, S.** (2007). Carbon Dioxide Capture and Geological Storage. *Phil. Trans. R. Soc. A*. **365**:1095-1107.

- **Houghton, L.G., Filho, M., Bruce, J., Lee, H., Callander, B.A., Haites, E., Harris, N. and Maskell, K.** (1995). CO_2 and the carbon cycle. In Climate Change 1994: Radiative Forcing of Climate Change and an Evaluation of the IPCC IS92 Emission Scenarios. Cambridge University Press, Cambridge, U.K. 35-71.

- http://climate.nasa.gov/. (2015).

- http://decarboni.se/publications/accelerating-uptake-ccs-industrial-use-captured-carbon-dioxide/appendix-f-co2-feedstock. (2015).

- http://news.stanford.edu/news/2007/june13/carbon-061307.html. (2015).

- http://teeic.indianaffairs.gov/. (2015).

- http://www.co2crc.com.au/. (2015).

- http://www.epa.gov/climatechange/. (2015).

- http://www.ipcc.ch/index.htm. (2015).

- http://www.livescience.com/37743-greenhouse-effect.html. (2015).

- http://www.sacccs.org.za/. (2015).

- http://www.tececo.com/sustainability.role_soil_sequestration.php. (2015).

- http://www.undeerc.org/pcor/. (2015).

- **Hügler, M., Wirsen, C.O., Fuchs, G., Taylor, C.D. and Sievert, S.M.** (2005). Evidence for Autotrophic CO_2 Fixation via the Reductive Tricarboxylic Acid Cycle by Members of the ε Subdivision of Proteobacteria. *Journal of Bacteriology.* **187(9)**:3020-3027.

- **Jørgensen, B.B and Boetius, A.** (2007). Feast and Famine – Microbial Life in the Deep-Sea Bed. *Nature Reviews Microbiology*. **5**:770-781.

- **Jørgensen, B.B. and D'Hondt, S.** (2006). ECOLOGY: A Starving Majority Deep Beneath the Seafloor. *Science*. **314**:932-934.

- **Ju, D., Shin, J., Lee, H., Kong, S., Kim, J. and Sang, B.** (2008). Effects of pH Conditions on the Biological Conversion of Carbon Dioxide to Methane in a Hollow-Fibre Membrane Biofilm Reactor (Hf–MBfR). *Desalination.* **234**:409-415.

- **Jurtshuk, P.** (1996). Bacterial Metabolism. Chapter 4 in Medical Microbiology (4^{th} ed.).

- **Koide, H.** (1999). Geological Sequestration and Microbiological Recycling of CO_2 in Aquifers. *Proc. 4th Int. Conf. on Greenhouse Gas Control Technologies, Pergamon.* 201-205.

- **Kotelnikova, S.** (2002). Microbial Production and Oxidation of Methane in Deep Subsurface. *Earth-Sci. Rev*. **58**:367–395.

- **Lau, M.C.Y., Cameron, C., Magnabosco, C., Brown, C.T., Schilkey, F., Grim, S., Hendrickson, S., Pullin, M., Sherwood Lollar, B., van Heerden, E., Kieft, T.L. and Onstott, T.C.** (2014). Phylogeny and Phylogeography of Functional Genes Shared Among Seven Terrestrial Subsurface Metagenomes Reveal N-Cycling and Microbial Evolutionary Relationships. *Front. Microbiol*. **5**:531.

- **Lim, D.** (2003). Microbiology (3rd ed.). *Kendall/Hunt Publishers.* ISBN: 0787292036.

- **Lin, L., Hall, J., Lippmann-Pipke, J., Ward, J.A., Sherwood Lollar, B., DeFlaun, M., Rothmel, R., Moser, D., Gihring, T.M., Mislowack, B. and Onstott, T. C.** (2005). Radiolytic H_2 in Continental Crust: Nuclear Power for Deep Subsurface Microbial Communities. *Geochem. Geophys. Geosyst*. **6(7)**:Q07003.

- **Lovley, D.R. and Chapelle, F.H.** (1995). Deep Subsurface Microbial Processes. *Review of Geophysics*. **33(3)**:365-381.

- **Magnabosco, C., Tekere, M., Lau, M.C.Y., Linage, B., Kuloyo, O., Erasmus, M., Cason, E., van Heerden, E., Borgonie, G., Kieft, T.L., Olivier, J. and Onstott, T.C.** (2014). Comparisons of the Composition and Biogeographic Distribution of the Bacterial Communities Occupying South African Thermal Springs with those Inhabiting Deep Subsurface Fracture Water. *Frontiers in Microbiology*. **5**:679.

- **Metz, B., Davidson, O.R., Bosch, P.R., Dave, R. and Meyer, L.A.** (2007). IPCC Climate Change: Mitigation of Climate Change. Contribution of Working Group III to the Fourth Assessment Report of the Intergovernmental Panel on Climate Change. Cambridge University Press, Cambridge, United Kingdom and New York, NY, USA.

- **Morozova, D., Wandrey, M., Alawi, M., Zimmer, M., Vieth, A., Zettlitzer, M and Würdemann, H.** (2010). Monitoring of the Microbial Community Composition in Saline Aquifers during CO_2 Storage by Fluorescence *in situ* Hybridisation. *International Journal of Greenhouse Gas Control*. **4**:981-989.

- **Mu, A., Boreham, C., Leong, H.X., Haese, R.R. and Moreau, J.W.** (2014). Changes in the Deep Subsurface Microbial Biosphere Resulting from a Field-Scale CO_2 Geosequestration Experiment. *Frontiers in Microbiology*. **5**:209.

- **Nealson, K.H., Inagaki, F. and Takai, K.** (2005). Hydrogen-Driven Subsurface Lithoauthotrophic Microbial Ecosystem (SLiMEs): Do they exist and Why Should we Care? *Trends in Microbiology*. **13**:405-410.

- **Newberry, C.J., Webster, G., Cragg, B.A., Parkes, R.J., Weightman, A.J. and Fry, J.C.** (2004). Diversity of Prokaryotes and Methanogenesis in Deep Subsurface Sediments from the Nankai Trough, Ocean Drilling Program Leg 190. *Environ.Microbiol*. **6**:274-287.

- **Nondorf, L., Gutierrez, M. and Plymate, T.G.** (2011). Modelling Carbon Sequestration Geochemical Reactions for a Proposed Site in Springfield, Missouri. *Environmental Geosciences*. **18**:91-99.

- **Onstott, T.C.** (2005). Impact of CO_2 Injections on Deep Subsurface Microbial Ecosystems and Potential Ramifications for the Surface Biosphere. Chapter 30 in Carbon Dioxide Capture for Storage in Deep Geologic Formations – Results from the CO_2 Capture Project, Geological Storage of Carbon Dioxide with Monitoring and Verification. *Elsevier Publishing*. **2**:1217-1250. ISBN: 0080445705.

- **Onstott, T.C., Colwell, F.S., Kieft, T.L., Murdoch, L. and Phelps, T.J.** (2009). New Horizons for Deep Subsurface Microbiology. *Microbe Magazine.* **4(11)**:499–505.

- **Onstott, T.C., Lin, L., Davidson, M., Mislowack, B., Borcsik, M., Hall, J., Slater, G., Ward, J., Sherwood Lollar, B., Lippmann-Pipke, J., Boice, E., Pratt, L.M., Pfiffner, S., Moser, D., Gihring, T., Kieft, T.L., Phelps, T.J., van Heerden, E., Litthauer, D., DeFlaun, M., Rothmel, R., Wanger, G. and Southam G.** (2006). The Origin and Age of Biogeochemical Trends in Deep Fracture Water of the Witwatersrand Basin, South Africa. *Geomicrobiol. J*. **23**:369–414.

- **Onstott, T.C., Phelps, T.J., Kieft, T., Colwell, F.S., Balkwill, D.L., Fredrickson, J.K. and Brockman, F.J.** (1998). In: Enigmatic Microorganisms and Life in Extreme Environments. *Springer Science & Business Media Publishers*. ISBN: 9780792354925.

- **Pacala, S. and Socolow, R.** (2004). Stabilization Wedges: Solving the Climate Problem for the Next 50 Years with Current Technologies. *Science*. **305**:968-972.

- **Parkes, R.J., Cragg, B.A., Bale, S.J., Getliff, J.M., Goodman, K., Rochelle, P.A., Fry, J.C., Weightman, A.J. and Harvey, S.M.** (1994). Deep Bacterial Biosphere in Pacific-Ocean Sediments. *Nature.* **371**:410-413.

- **Pedersen, K.** (1993). The Deep Subterranean Biosphere. *Earth Sci. Rev*. **34**:243-260.

- **Pedersen, K.** (2000). Exploration of Deep Intraterrestrial Microbial Life: Current Perspectives. *FEMS Microbiol. Lett*. **185**:9-16.

- **Pedersen, K.** (2001). Diversity and Activity of Microorganisms in Deep Igneous Rock Aquifers of the Fennoscandian Shield. In Subsurface Microbiology and Biogeochemistry. *John Wiley Publishers*. 97–139.

- **Peters, C.A., Dobson, P.F., Oldenburg, C.M., Wang, J.S.Y., Onstott, T.C., Scherer, G.W., Freifeld, B.M., Ramakrishnan, T.S., Stabinski, E.L., Liang, K. and Verma, S.** (2011). LUCI: A Facility at DUSEL for Large-Scale Experimental Study of Geologic Carbon Sequestration. *Energy Procedia*. **4**:5050-5057.

- **Phelps, T.J., Murphy, E.M., Pfiffner, S.M. and White, D.C.** (1994). Comparison between Geochemical and Biological Estimates of Subsurface Microbial Activities. *Microb. Ecol*. **28**:335-349.

- **Pikuta, E.V., Hoover, R.B. and Tang, J.** (2007). Microbial Extremophiles at the Limits of Life. *Critical Reviews in Microbiology.* **33**:183-209.

- **Ragon, M., Van Driessche, A.E.S., García-Ruíz, J.M., Moreira, D. and López-García, P.** (2013). Microbial Diversity in the Deep-Subsurface Hydrothermal Aquifer Feeding the Giant Gypsum Crystal-Bearing Naica Mine, Mexico. *Frontiers in Microbiology*. **4**:37.

- **Rajala, P., Bomberg, M., Kietäväinen, R., Kukkonen, I., Ahonen, L., Nyyssönen, M. and Itävaara, M.** (2015). Rapid Reactivation of Deep Subsurface Microbes in the Presence of C-1 Compounds. *Microorganisms*. **3**:17-33.

- **Ramanan, R., Kannan, K., Sivanesan, S.D., Mudliar, S., Kaur, S., Tripathi, A.K. and Chakrabarti, T.** (2009). Bio-sequestration of Carbon Dioxide using Carbonic Anhydrase Enzyme Purified from *Citrobacter freundii*. *World J Microbiol Biotechnol*. **25**:981-987.

- **Reith, F.** (2011). Life in the Deep Subsurface. *Geology.* **39(3)**:287-288.

- **Sedjo, A.** (2001). Forest Carbon Sequestration: Some Issues for Forest Investments. *Resources for the Future.* 1-34.

- **Sherwood Lollar, B. and Ballentine, C.J.** (2009). Insights Into Deep Carbon Derived from Noble Gases. *Nature Geoscience*. **2**:543-547.

- **Sims, R.E.H., Schock, R.N., Adegbululgbe, A., Fenhann, J., Konstantinaviciute, I., Moomaw, W., Nimir, H.B., Schlamadinger, B., Torres-Martínez, J., Turner, C., Uchiyama, Y., Vuori, S.J.V., Wamukonya, N. and Zhang, X.** (2007). Energy supply. In Climate Change 2007: Mitigation. Contribution of Working Group III to the Fourth Assessment Report of the Intergovernmental Panel on Climate Change. *Cambridge University Press, Cambridge*.

- **Sogin, M., Edwards, K. and D'Hondt, S.** (2010). DCO Deep Life Workshop. Catalina Island, California.

- **Solomon, S., Plattner, G., Knutti, R. and Friedlingstein, P.** (2009). Irreversible Climate Change due to Carbon Dioxide Emissions. *Proc. Natl. Acad. Sci*. **106(6)**:1704-1709.

- **Stevens, T.O. and McKinley, J.P.** (1995). Lithoautotrophic Microbial Ecosystems in Deep Basalt Aquifers. *Science.* **270**:450-454.

- **Surridge, A.D. and Cloete, M.** (2009). Carbon Capture and Storage in South Africa. *Energy Procedia*. **1**:2741-2744.

- **Takai, K., Moser, D., DeFlaun, M., Onstott, T.C. and Fredrickson, J.K.** (2001). Archaeal Diversity in Waters from Deep South African Gold Mines. *Applied and Environmental Biology.* **67(12)**:5750-5760.

- **Teske, A.P.** (2005). The Deep Subsurface Biosphere is Alive and Well. *Trends Microbiol.* **13(9)**:402-404.

- **Velea, S., Dragos, N., Serban, S., Ilie, L., Stalpeanu, D., Nicoara, A. and Stepan, E.** (2009). Biological Sequestration of Carbon Dioxide from Thermal Power Plant Emissions by Absorbtion in Microalgal Culture Media. *Romanian Biotechnological Letters*. **14(4)**:4485-4500.

- **Vitousek, P.M.** (1994). Beyond Global Warming: Ecology and Global Change. *Ecology*. **75(7)**:1861-1876.

- **Wang, P., Lin, L., Yu, H., Cheng, T., Song, S., Kuo, L., Yeh, E., Lin, W. and Wang, C.** (2007). Cultivation-Based Characterization of Microbial Communities Associated with Deep Sedimentary Rocks from Taiwan Chelungpu Drilling Project Cores. *Terr. Atmos. Ocean. Sci*. **18**:395-412.

- **Webster, G., Parkes, R.J., Cragg, B.A., Newberry, C.J., Weightman, A.J. and Fry, J.C.** (2006). Prokaryotic Community Composition and Biogeochemical Processes in Deep Subseafloor Sediments from the Peru Margin. *FEMS Microbiol. Ecol*. **58**:65-85.

- **White, D.C., Phelps, T.J. and Onstott, T.C.** (1998). What's Up Down There? *Current Opinion in Microbiology*. **1**:286-290.

- **Whitman, W.B., Coleman, D.C. and Wiebe, W.J.** (1998). Prokaryotes: the Unseen Majority. *Proc. Natl. Acad. Sci*. **95**:6578-6583.

- **Zhang, G., Dong, H., Zhiqin X., Zhao, D. and Zhang, C.** (2005). Microbial Diversity in Ultra-High-Pressure Rocks and Fluids from the Chinese Continental Scientific Drilling Project in China. *Geomicrobiology Journal*. **23**:499-514.

CHAPTER 2

INTRODUCTION TO PRESENT STUDY

2.1 ABSTRACT

Climate change is taking place world-wide due to the already high levels of greenhouse gases in the atmosphere, specifically CO_2, and this is mainly due to anthropogenic inputs such as the global use of fossil fuels and other human or industrial activities (Vitousek, 1994; Pacala & Socolow, 2004; Ramanan *et al*., 2009; Solomon *et al*., 2009; Velea *et al*., 2009; EPA, 2015; SACCCS, 2015). In the past, little consideration was given to CO_2 as an undesirable emission, but due to an atmospheric increase from 280 ppm in 1850 to 400 ppm currently (NASA, 2015; SACCCS, 2015), it has moved to the top of the list for the most undesirable emission on the international climate change agenda (Surridge & Cloete, 2009). Due to industrialization and the growth in population around the world, the use of fossil fuels is predicted to increase, resulting in a corresponding increase in CO_2 emissions to the atmosphere (Solomon *et al*., 2009; Surridge & Cloete, 2009), and this will result in several long-term, undesirable and unmanageable impacts on the economy, the ecology and human health and therefore, carbon resources have to be managed more effectively. This is especially important for emerging countries with coal based energy such as South Africa where coal is the majority of South Africa's main energy supply and the demand is projected to keep increasing (Surridge & Cloete, 2009; Cloete, 2010).

As a means to reduce anthropogenic CO_2 emissions, South Africa is investigating the possibility of CO_2 storage in geological structures while developing alternative renewable and/or nuclear energies that could replace the use of fossil fuel based energy (Sherwood Lollar & Ballentine, 2009; Surridge & Cloete, 2009; Cloete, 2010). During geological sequestration, the captured CO_2 will be injected several hundreds of metres below the surface of the Earth to porous rocks such as sandstone, where the CO_2 will be in a supercritical state (Cunningham *et al*., 2009; Cloete, 2010; Nondorf *et al*., 2011). The molecular phylogenetic surveys performed by members of the Deep Carbon Observatory (DCO) Deep Life research program and the Life in Extreme Environments (LExEn)

research program, funded by the National Science Foundation (NSF), have demonstrated that the South African and other subsurface biomes, exactly where CO_2 will be stored, harbour highly diverse and novel microbial communities and the metabolic activities of these subsurface biomes is closely tied to the geochemical and mineralogical processes (Stevens *et al*., 1993; Phelps *et al*., 1994; Fredrickson & Onstott, 1996; Colwell *et al*., 1997; Onstott *et al*., 1998; Pedersen *et al*., 2000; Moser *et al*., 2003; Kieft *et al*., 2005; Gihring *et al*., 2006; Onstott *et al*., 2009; Borgonie *et al*., 2011; Ragon *et al*., 2013; Lau *et al*., 2014; Rajala *et al*., 2015). As a result, sequestering CO_2 could influence these microorganisms on a diversity and metabolic level, but to date, studies on subsurface microbial communities have taken a back seat to geological approaches within this research field.

Consequently, predicting the potential impact of long term CO_2 sequestration on the subsurface biome and their contribution to carbon cycling is impossible without an experimental knowledge base. However, the first pilot CO_2 storage project experiment for South Africa is planned for 2017, with a demonstration plant planned for 2020, and then the commercial operations are planned for 2025 (SACCCS, 2015). Thus, in order to understand the microbial interaction with the CO_2, as well as the rock-microbial interactions that might influence the storage process, bench-scale simulations of these interactions was selected for this research, with the use of specifically designed, high pressure equipment. These are essential questions, not only with respect to carbon sequestration but also to study the effect that the storage will have on current subsurface communities and their role in carbon cycling and ultimately subsurface biogeochemistry.

2.2 POSSIBLE OCCURENCES DURING CARBON SEQUESTRATION

As described by Basava-Reddi, (2012), predictions are that if CO_2 is injected into the subsurface where microorganisms are present, it is likely to cause an initial decrease in cell numbers as many microorganisms may not survive the initial conditions. However, once injection is completed, a gradual increase in numbers may occur as some of the microorganisms may adapt to these extreme conditions and utilise the CO_2 to produce the necessary organic compounds as part of biotic cycling.

The injected CO_2 could also affect physicochemical parameters, like the pH, which in turn, will also affect microbial communities. The extent to which this will occur is dependent on

the biome present, the geology of the storage rock, as well as the chemistry of the water (Basava-Reddi, 2012). Microorganisms will interact with the sequestered CO_2 and their activity can potentially cause direct effects, including mineral formation or degradation, changes in the porosity of the storage rock through biofilm formation, and corrosion or indirect effects, including changes in the pH and redox conditions through cycling (Basava-Reddi, 2012). This might result in either positive or negative effects on the storage formations. Potential positive effects include biofilm formation that can help trap the CO_2 in the storage rock, thus increasing storage security, as well as enhanced solubility and mineral trapping. Potential negative effects might include enhancing or selecting for methanogens which can lead to possible enhanced methane generation, changes in the porosity of the rock which will affect the storage capacity, and could result in potential methane leakage to the surface (Morozova *et al*., 2010; Basava-Reddi, 2012; Mu *et al*., 2014).

2.3 REFERENCES

- **Basava-Reddi, L.** (2012). Microbial Effects on CO_2 Storage. IEAGHG Report.

- **Borgonie, G., García-Moyano, A., Litthauer, D., Bert, W., Bester, A., van Heerden, E., Möller, C., Erasmus, M. and Onstott, T.C.** (2011). Nematoda from the Terrestrial Deep Subsurface of South Africa. *Nature*. **474**:79-82.

- **Cloete, M.** (2010). Atlas on Geological Storage of Carbon Dioxide in South Africa. Council for Geoscience.

- **Colwell, F.S., Onstott, T.C., Dilwiche, M.E., Chandler, D., Fredrickson, J.K., Yao, Q., McKinley, J.P., Boone, D.R., Griffiths, R., Phelps, T.J., Ringelberg, D., White, D.C., LaFreniere, L., Balkwill, D., Lehman, R.M., Konisky, J. and Long, P.E.** (1997). Microorganisms from Deep, High Temperature Sandstones: Constraints on Microbial Colonization. *FEMS Microbiol Rev*. **20**:425-435.

- **Cunningham, A.B., Gerlach, R., Spangler, L. and Mitchell, A.C.** (2009). Microbially Enhanced Geologic Containment of Sequestered Supercritical CO_2. *Energy Procedia*. **1**:3245-3252.

- **Fredrickson, J.K. and Onstott, T.C.** (1996). Microbes Deep Inside the Earth. *Sci Am*. **275**:68-73.

- **Gihring, T.M., Moser, D.P., Lin, L., Davidson, M., Onstott, T.C., Morgan, L., Milleson, M., Kieft, T.L., Trimarco, E., Balkwill, D.L. and Dollhopf, M.E.** (2006). The Distribution of Microbial Taxa in the Subsurface Water of the Kalahari Shield, South Africa. *Geomicrobiol. J*. **23**:415–430.

- http://climate.nasa.gov/. (2015).

- http://www.epa.gov/climatechange/. (2015).

- http://www.sacccs.org.za/. (2015).

- **Kieft, T.L., McCuddy, S.M., Onstott, T.C., Davidson, M., Lin, L., Mislowack, B., Pratt, L., Boice, E., Sherwood Lollar, B., Lippmann-Pipke, J., Pfiffner, S.M., Phelps, T.J., Gihring, T., Moser, D. and van Heerden, A.** (2005). Geochemically Generated, Energy-Rich Substrates and Indigenous Microorganisms in Deep, Ancient Groundwater. *Geomicrobiol. J*. **22**:325–335.

- **Lau, M.C.Y., Cameron, C., Magnabosco, C., Brown, C.T., Schilkey, F., Grim, S., Hendrickson, S., Pullin, M., Sherwood Lollar, B., van Heerden, E., Kieft, T.L. and Onstott, T.C.** (2014). Phylogeny and Phylogeography of Functional Genes Shared Among Seven Terrestrial Subsurface Metagenomes Reveal N-Cycling and Microbial Evolutionary Relationships. *Front. Microbiol*. **5**:531.

- **Morozova, D., Wandrey, M., Alawi, M., Zimmer, M., Vieth, A., Zettlitzer, M and Würdemann, H.** (2010). Monitoring of the Microbial Community Composition in Saline Aquifers during CO_2 Storage by Fluorescence *in situ* Hybridisation. *International Journal of Greenhouse Gas Control*. **4**:981-989.

- **Moser, D.P., Onstott, T.C., Fredrickson, J.K., Brockman, F.J., Balkwill, D.L., Drake, G.R., Pfiffner, S.M., White, D.C., Takai, K., Pratt, L.M., Fong, J., Sherwood Lollar, B., Slater, G., Phelps, T.J., Spoelstra, N., DeFlaun, M., Southam, G., Welty, A.T., Baker, B.J. and Hoek, J.** (2003). Temporal Shifts in the Geochemistry and Microbial Community Structure of an Ultradeep Mine Borehole Following Isolation. *Geomicrobiol. J*. **20**:517–548.

- **Mu, A., Boreham, C., Leong, H.X., Haese, R.R. and Moreau, J.W.** (2014). Changes in the Deep Subsurface Microbial Biosphere Resulting from a Field-Scale CO_2 Geosequestration Experiment. *Frontiers in Microbiology*. **5**:209.

- **Nondorf, L., Gutierrez, M. and Plymate, T.G.** (2011). Modelling Carbon Sequestration Geochemical Reactions for a Proposed Site in Springfield, Missouri. *Environmental Geosciences*. **18**:91-99.

- **Onstott, T.C., Colwell, F.S., Kieft, T.L., Murdoch, L. and Phelps, T.J.** (2009). New Horizons for Deep Subsurface Microbiology. *Microbe Magazine.* **4(11)**:499–505.

- **Onstott, T.C., Phelps, T.J., Kieft, T., Colwell, F.S., Balkwill, D.L., Fredrickson, J.K. and Brockman, F.J.** (1998). In: Enigmatic Microorganisms and Life in Extreme Environments. *Springer Science & Business Media Publishers*. ISBN: 9780792354925.

- **Pacala, S. and Socolow, R.** (2004). Stabilization Wedges: Solving the Climate Problem for the Next 50 Years with Current Technologies. *Science*. **305**:968-972.

- **Pedersen, K., Motemedi, M., Karnland, O. and Sandén, T.** (2000). Cultivability of Microorganisms Introduced into a Compacted Bentonite Clay Buffer under High-Level Radioactive Waste Repository Conditions. *Eng Geol*. **58**:149-161.

- **Phelps, T.J., Murphy, E.M., Pfiffner, S.M. and White, D.C.** (1994). Comparison between Geochemical and Biological Estimates of Subsurface Microbial Activities. *Microb. Ecol*. **28**:335-349.

- **Ragon, M., Van Driessche, A.E.S., García-Ruíz, J.M., Moreira, D. and López-García, P.** (2013). Microbial Diversity in the Deep-Subsurface Hydrothermal Aquifer Feeding the Giant Gypsum Crystal-Bearing Naica Mine, Mexico. *Frontiers in Microbiology*. **4**:37.

- **Rajala, P., Bomberg, M., Kietäväinen, R., Kukkonen, I., Ahonen, L., Nyyssönen, M. and Itävaara, M.** (2015). Rapid Reactivation of Deep Subsurface Microbes in the Presence of C-1 Compounds. *Microorganisms*. **3**:17-33.

- **Ramanan, R., Kannan, K., Sivanesan, S.D., Mudliar, S., Kaur, S., Tripathi, A.K. and Chakrabarti, T.** (2009). Bio-sequestration of Carbon Dioxide using Carbonic Anhydrase Enzyme Purified from *Citrobacter freundii*. *World J Microbiol Biotechnol*. **25**:981-987.

- **Sherwood Lollar, B. and Ballentine, C.J.** (2009). Insights Into Deep Carbon Derived from Noble Gases. *Nature Geoscience*. **2**:543-547.

- **Solomon, S., Plattner, G., Knutti, R. and Friedlingstein, P.** (2009). Irreversible Climate Change due to Carbon Dioxide Emissions. *Proc. Natl. Acad. Sci*. **106(6)**:1704-1709.

- **Stevens, T.O., McKinley, J.P. and Fredrickson, J.K.** (1993). Bacteria Associated with Deep, Alkaline, Anaerobic Groundwaters in Southeast Washington. *Microb Ecol*. **25**:35-50.

- **Surridge, A.D. and Cloete, M.** (2009). Carbon Capture and Storage in South Africa. *Energy Procedia*. **1**:2741-2744.

- **Velea, S., Dragos, N., Serban, S., Ilie, L., Stalpeanu, D., Nicoara, A. and Stepan, E.** (2009). Biological Sequestration of Carbon Dioxide from Thermal Power Plant Emissions, by Absorbtion in Microalgal Culture Media. *Romanian Biotechnological Letters*. **14(4)**:4485-4500.

- **Vitousek, P.M.** (1994). Beyond Global Warming: Ecology and Global Change. *Ecology*. **75(7)**:1861-1876.

CHAPTER 3

SAMPLING, CHARACTERIZATION AND MICROBIAL DIVERSITY OF THE SITE DESIGNATED TO MIMIC CARBON SEQUESTRATION CONDITIONS

3.1 INTRODUCTION

The CO_2 captured and compressed during the geological CCS process is sequestered several hundreds of metres below the surface of the Earth in porous rocks such as sandstone (Cunningham *et al*., 2009; Cloete, 2010). However, the subsurface environment is a well-established, diverse and geologically complex domain that comprises a substantial percentage of the Earth's biomass in the form of microorganisms where important biogeochemical cycles work to sustain life (Stevens *et al*., 1993; Phelps *et al*., 1994; Fredrickson & Onstott, 1996; Colwell *et al*., 1997; Onstott *et al*., 1998; Pedersen *et al*., 2000; Moser *et al*., 2003; Kieft *et al*., 2005; Gihring *et al*., 2006; Onstott *et al*., 2009; Borgonie *et al*., 2011; Ragon *et al*., 2013; Lau *et al*., 2014; Rajala *et al*., 2015), therefore, consideration should be given to the interaction between the sequestered CO_2 and the subsurface biome, as well as the geological environments.

Comprehensive studies on the subsurface diversity and geochemistry have revealed that microorganisms from all three domains of life have been found in the South African gold, diamond, and platinum mines (Takai *et al*., 2001; Moser *et al*., 2003; Kieft *et al*., 2005; Gihring *et al*., 2006; Lin *et al*., 2006a; Lin *et al*., 2006b; Onstott *et al*., 2009; Borgonie *et al*., 2011; Lau *et al*., 2014; Magnabosco *et al*., 2014). Therefore, microorganisms are expected to be present at locations considered for geological storage of CO_2. These subsurface researchers have developed extensive sampling techniques to ensure that the microorganisms studied from the deep subsurface are not from contamination through mining or sampling activities, but that they represent the geological setting (Baker *et al*., 2003; Balkwill *et al*., 2004; Takai *et al*., 2001; Borgonie *et al*., 2011). However, it is possible that the diversity of the subsurface communities can be influenced through mixing

of water types and thus can change over time. Some examples include: 1.) when hydrogen-enriched, ultrabasic subsurface fluids mix with oxygenated surface freshwater (Brazelton *et al*., 2013), 2.) when sulphate-rich water, found at depths above 300 mbs, mix with methane-rich water, found at depths below 300 mbs (Bomberg *et al*., 2015), and 3.) when the highly saline hydrothermal fluid mixes with low salinity paleo-meteoric water (Ward *et al*., 2004; Onstott *et al*., 2006).

Overall, the chemoautotrophic nature of the subsurface ecosystem increases with depth (Onstott, 2005). This means that the microorganisms in the deep subsurface will be more likely to use CO_2 to produce compounds needed for survival such as hydrocarbons, but this depends largely on the geochemistry of the rock and formation water, temperature, and availability of electron donors and acceptors (Onstott, 2005). These chemoautotrophic microorganisms gain their energy through the oxidation of hydrogen (H_2), methane (CH_4), hydrogen sulphide (H_2S), ammonia (NH_3), ferrous iron (Fe^{2+}), and manganese (Mn^{2+}). Several groups of microorganisms are capable of producing biomass through chemosynthesis, a process through which these microorganisms use chemical energy to fix CO_2 and are dependent on the availability of CO_2, sulphate (SO_4^{2-}), sulphur (S), ferric iron (Fe^{3+}), oxygen (O_2), or nitrate (NO_3^-) as electron acceptors (Jørgensen & Boetius, 2007). These nutrient and chemical energy sources are usually generated through radiolysis, thermogenesis, water-rock interactions or microbial activity and the availability thereof in the subsurface determines the microbial activity in such environments (Kieft *et al*., 2005; Lin *et al*., 2006b; Onstott *et al*., 2006; Etiope & Sherwood Lollar, 2013; Lau *et al*., 2014). Since these sources are very limited, the activity of the subsurface microorganisms is generally very slow (Phelps *et al*., 1994; Teske, 2005; Jorgensen & D'Hondt, 2006; Jorgensen & Boetius, 2007; Onstott *et al*., 2009), but can have both direct and indirect effects. Direct effects include mineral formation/degradation, corrosion, and changes in the porosity due to biofilm formation. Indirect effects include redox and pH changes (Basava-Reddi, 2012), due to interaction with the geological setting.

Although the microbial communities of the deep subsurface are dominated by four anaerobic physiological types - the methanogens, the sulphate/sulphur-reducing bacteria, the fermentative anaerobes, and the Fe(III)-reducing bacteria (Takai *et al*., 2001; Kotelnikova, 2002; Baker *et al*., 2003; Newberry *et al*., 2004; Onstott, 2005; Webster *et al*., 2006; Fry *et al*., 2008; Basso *et al*., 2009; Morozova *et al*., 2010; Ragon *et al*., 2013), it has been shown that the deep subsurface is an active biosphere that contains a diverse

group of microorganisms with most, if not all, of the physiological types of microorganisms that are thought to be significant in sedimentary environments found in the deep subsurface (Parkes *et al*., 1994; Lovley & Chapelle, 1995; Whitman *et al*., 1998; Sahl *et al*., 2008; Morozova *et al*., 2010).

3.1.1 Geological Sequestration Sedimentary Rock

During geological carbon sequestration, the CO_2 is stored in formations such as sandstone because of the porosity and permeability of the rock (Price & Smith, 2008; Metz *et al*., 2005). Sandstone (Figure 3.1), also known as arenite, is a clastic sedimentary rock which is composed mainly of sand-sized minerals or rock grains (Pettijohn *et al*., 1987; Fichter, 2000; Stow, 2005).

Figure 3.1: Sandstone rock with a clastic texture [Taken from Geology4today, (2015)].

Clastic rock consists of fragments of pre-existing calcite, clays, and silicate minerals or rock fragments that were transported by mechanical and chemical weathering and originated through lithification - a process in which sediments compact under pressure, expel connate fluids, and gradually become solid rock. Connate fluids are liquids that were trapped in the pores of sedimentary rocks as they were formed. Rocks, in which sand-sized grains (1/16 mm to 2 mm) are the majority, are called sandstone (Pettijohn *et al*., 1987; Fichter, 2000; Stow, 2005). The minerals in sandstone, the most common in the Earth's crust, are quartz, feldspars, and lithic fragments. Matrix may also exist in the interstitial spaces between the rock and mineral grains. Sandstone formations allow

filtration of water and other fluids and are porous enough to store large quantities, making them valuable aquifers (Jackson, 1997; Boggs, 2000).

3.2 AIMS OF THIS CHAPTER

The main aims of this chapter were to:

- Obtain a study site with similar geological strata and depth as the proposed sites for CCS in South Africa and to do a comprehensive characterization over time of the biogeochemistry of the study site.
- Analyse the water and gas from the sampling environment for possible changes in the fissure water due to mixing with other water sources, as well as to obtain information regarding the geochemical balance in the borehole's groundwater that will provide insight into the possible electron donor and acceptor options to sustain biological cycling.
- Complete extensive diversity studies on the subsurface biome in order to obtain a profile of the different species present, as well as to investigate if any natural shifts in the microbial community structure occurred over time before the introduction of additional CO_2.

3.3 MATERIALS AND METHODS

Unless otherwise specified, the following were applied throughout this research: 1.) All chemicals were obtained from BDH Chemicals Ltd, B&M Scientific cc., BD Biosciences, Bio-Rad Laboratories, Inc., Sigma-Aldrich®, or Merck Millipore. 2.) For media preparations, uniLAB® quality reagents were used and for buffer preparations and all molecular techniques, univAR® quality reagents were used. 3.) All gases were obtained from Air Liquide (Pty) Ltd. 4.) The Nano-pure water was 18 MΩ.cm^{-1} Barnstead™ Nanopure™ water (Thermo Scientific) that was filtered and UV treated. 5.) The distilled water (dH_2O) used was 15 MΩ.cm^{-1} Barnstead™ TII water (Thermo Scientific) that was filtered and UV treated. 6.) Sterilization involved autoclaving for 20 minutes at 121°C and 103.4 kPa (1.034 bar). 7.) All graphs were made with Microsoft® Excel (Microsoft® Corporation).

Sampling and analyses of the fissure water, gas, and subsurface biome, to characterize the borehole's groundwater, included sampling techniques that were designed to maintain subsurface conditions with preservative addition for reliable analyses. Unless otherwise specified, the methods and equipment used for sampling in the mine are standard operating procedures and previously published methods that were developed and adapted over an extensive period of time by members of the Deep Subsurface sampling team (Takai *et al*., 2001; Lippmann *et al*., 2003; Moser *et al*., 2003; Ward *et al*., 2004; Lin *et al*., 2006a; Sherwood Lollar *et al*., 2008; Onstott *et al*., 2009; Stepanauskas, 2012; Purtschert *et al*., 2013; Magnabosco *et al*., 2014). These researchers are part of the DCO Deep Life research program and they are international collaborators, interacting with the Extreme Biochemistry Research group at the University of the Free State (Bloemfontein, RSA), which has been the focal point for this interaction since the year 2000. Samples were transported back to the University of the Free State (UFS) for the necessary processing, while selected samples were sent to the various collaborators for specific analyses.

3.3.1 Sampling Requirements

To understand the deep carbon cycle and its interaction with the subsurface biome, the major physical, chemical and biological conditions for geologic carbon sequestration had to be considered. Deep carbon sequestration would require storage in porous rock at depths of ~800 mbs, an environment with high pressure and temperature (Benson & Cole,

2008; Cloete, 2010; Nondorf *et al*., 2011). Therefore, this research involved subsurface biomes from geological strata and depth similar to the proposed sites for CCS in South Africa (Cloete, 2010). The ideal site was one where sampling of the microbial community could be conducted >600 mbs in a permeable sandstone region. The Star Diamonds mine made such a site available for at least a 3 year period.

3.3.2 The Study Site

The Star Diamonds mine (Latitude South: 28°19.062', Longitude East: 026°47.083', Elevation: 1464 masl) (Figure 3.2) is located approximately 40 km south of Welkom, in the Theunissen district of the Free State province in South Africa and is currently owned by the Frontier Mining Projects (Previously owned by Petra Diamonds).

Figure 3.2: The Star Diamonds mine with shaft 4 that was used as the study site for this research.

The mine is situated east of a dolerite hill on the Adelaide Subgroup of the Beaufort Group (Vermaak, 2012). The first 15 levels inside the mine form part of the Beaufort Group. The Ecca Group is found between levels 15 and 16 with the Dwyka Group from level 16 downwards. The Beaufort Group is the third of the main subdivisions of the Karoo Supergroup of geological strata in South Africa and consists mainly of sandstones and

shale, deposited in the Karoo Basin from the middle Permian to the early part of the middle Triassic periods (Rubidge, 2005; Selden & Nudds, 2011).

3.3.3 The Borehole

The borehole was drilled approximately 0.6 m into the Karoo sandstone until fissure water was intersected (Figure 3.3) and cased (Figure 3.4) to fit the sampling equipment. A diamond drill and compressed air was used to drill the borehole. By not using service water in the drilling process, chances of additional contamination introduced from the service water, were limited. The borehole was drilled on 19 March 2012 and the first sampling occurred within 48 hours, after safety clearance was granted for the site.

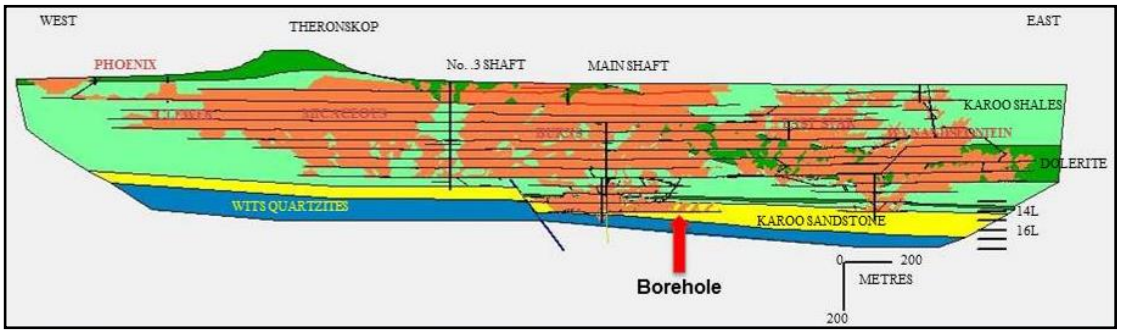

Figure 3.3: An approximate position of the borehole, intersecting the Karoo sandstone fissure of the Star Diamonds mine (Supplied by Petra Diamonds/Frontier Mining).

Figure 3.4: The encased borehole, intersecting the Karoo sandstone fissure water, which was used for sampling in the Star Diamonds mine.

The borehole is situated approximately 640 mbs with a site elevation of 824 metres above sea level (masl) and can be found at shaft 4, level 15 East, cross cut 24. The coordinates of the borehole are: x: -133399.4, y: -19986.8, z: -872.140. This borehole was exclusively used for the research purpose of this project through the courtesy of the team from the Star Diamonds mine (Petra Diamonds/Frontier Mining).

3.3.4 Fissure Water and Gas Sampling and Analyses

Fissure water and gas were sampled through an organic-free manifold (Figure 3.5) that was connected to the casing inside the borehole. This manifold enabled distribution of the water through quick connect clips to the different sampling vials, thus enabling simultaneous sampling of multiple samples, but it also allowed for contamination free sampling by preventing direct contact of the fissure water with the mine air. It also contained a valve for regulation and measurement of the water and gas flow.

Figure 3.5: The organic-free manifold used for sampling, connected to the casing inside the borehole.

Before each sampling event, all manifolds and other sampling equipment were thoroughly cleaned with soapy water and rinsed with Nano-pure water, followed by 70% (v/v) ethanol (EtOH). Equipment was air dried in a laminar flow cabinet (Labotec®), wrapped in autoclave bags and sterilized by autoclaving. Once on-site, the manifold was attached to the borehole and flushed for several minutes with the fissure water by opening all valves before collecting any samples. All samples were collected through sterile Polytetrafluoroethylene (PTFE) tubing (Watson-Marlow) or sterile Masterflex® Norprene

tubing (Cole-Parmer®) that was attached to the quick connect clips of the manifold. All equipment, sampling vials and samples were handled on-site with latex gloves. Unless otherwise specified, fissure water and gas samples were sampled and analysed using previously published methods (Sherwood Lollar *et al*., 2002; Lippmann *et al*., 2003; Moser *et al*., 2003; Ward *et al*., 2004; Lin *et al*., 2006a; Onstott *et al*., 2006; Sherwood-Lollar *et al*., 2008; Purtschert *et al*., 2013; Lau *et al*., 2014).

3.3.4.1 On-Site Physicochemical Analyses

Several on-site analyses were conducted during sampling to monitor the basic geochemistry of the fissure water for indications of any changes or mixing that might occur inside the borehole over time. All these analyses and measurements were done in triplicate according to the procedures of Moser *et al*., (2003); Lin *et al*., (2006a); and Lau *et al*., (2014).

Field parameters (Figure 3.6A) included pH, temperature, salinity, and electrical conductivity (EC), measured with the ExStik®II EC500 handheld probe (EXTECH® Instruments) and oxidation reduction potential (ORP), measured with the ExStik®II RE300 handheld probe (EXTECH® Instruments). All probes were calibrated before sampling using the standard solutions and operating procedures provided by the manufacterer.

Visual colorimetric CHEmets® kits (CHEMetrics Inc.) (Figure 3.6B) were used to measure the amount of dissolved oxygen (DO), hydrogen sulphide (H_2S), dissolved iron (Fe^{2+}), total iron, and hydrogen peroxide (H_2O_2) that is formed from radiolysis of water (H_2O) (Chivian *et al*., 2008). All measurements were conducted according to the manufacturer's instructions. To eliminate contamination from the casing inside the borehole, all dissolved and total iron samples were filtered using a sterile 0.45 µM cellulose acetate membrane syringe filter (GVS Filter Technology Inc., Lasec) prior to the CHEMets® analyses. For the DO, the funnel provided with the kit was connected to the sampling manifold through a syringe-tipped Masterflex® Norprene tube (Cole-Parmer®) and water was allowed to slowly overflow (Figure 3.6C). Before the ampoule was inserted, care was taken that no bubbles could be observed inside the funnel.

To determine the water flow rate, a 1 L measuring cylinder was filled with water flowing from the borehole (Figure 3.6D) and the time for the cylinder to reach the 1 L mark was recorded. For the gas flow rate, a specifically designed gas stripper (Figure 3.6E) was used (Courtesy of B. Sherwood Lollar) according to the procedure of Ward *et al*., (2004). The gas stripper was submerged in a bucket that was half filled with fissure water from the borehole. All the taps were opened and the release valve closed. The graduated Perspex beaker was completely filled with fissure water through the telescopic tube. After all the air was displaced from the gas stripper and the rubber tubing, the taps were closed again. The borehole was connected to the inlet tube and the tap was opened to let gas collect inside the graduated Perspex beaker. The time for the gas to displace a fixed volume of water was recorded (Figure 3.6F).

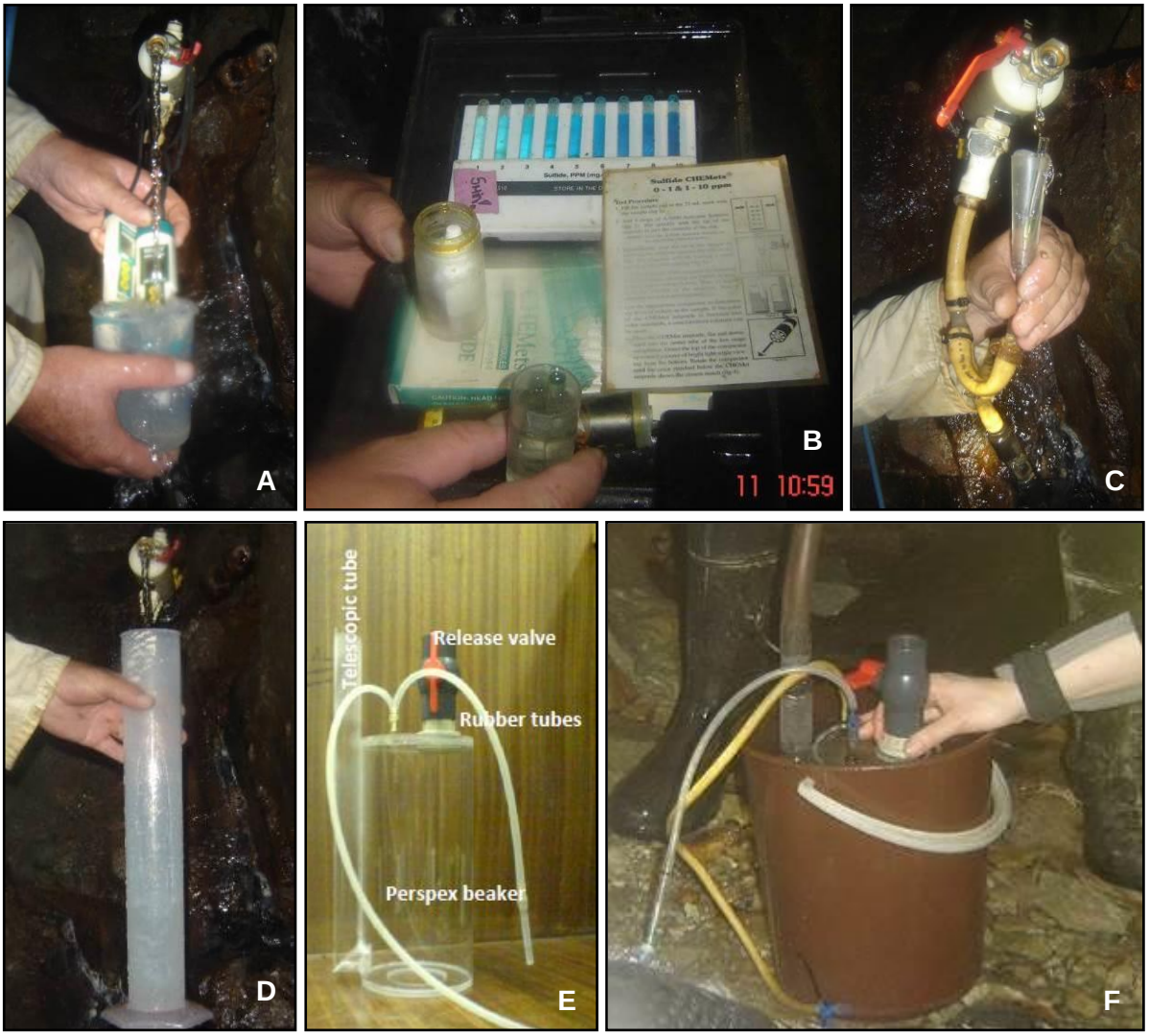

Figure 3.6: On-site equipment used for (A) handheld probe measurements, (B) CHEMets® kits, (C) dissolved oxygen, (D) water flow rate, and (E and F) gas flow rate.

3.3.4.2 Collection of Fissure Water for Geochemical Analyses

For the geochemical analyses, different types of sampling vials were used that had to be prepared before sampling according to the procedures of Moser *et al*., (2003); Ward *et al*., (2004); Lin *et al*., (2006a); and Lau *et al*., (2014). All sample bottles were prewashed overnight with 10% (v/v) hydrochloric acid (HCl) (Rotzsche, 1991), followed by rinsing three times with Nano-pure water. This was necessary to dissolve and remove all carbonates, iron hydroxides and organic compounds and impurities. All serum vials used were, after being washed and rinsed with the Nano-pure water, allowed to dry before being wrapped in foil and baked overnight in an annealing oven at 450°C. Blue chlorobutyl stoppers (Bellco Glass Inc.) and Teflon septa were washed with 1 M sodium hydroxide (NaOH) and rinsed in Nano-pure water before use. Cleaned serum vials were sealed with the rubber stoppers, crimp sealed with an aluminium cap and autoclaved. For the serum vials that were flushed, a needle was inserted through the chlorobutyl rubber stopper and the vial was pressurized for ten seconds at 50 kPa (0.5 bar) by connecting it directly to the nitrogen gas (99.999%) with a sterile Tygon tube (Thermo Fisher Scientific) and a sterile in-line 0.2 µM Isopore™ membrane filter (Merck Millipore) that was inserted into a sterile 25 mm in-line Polyacetal Gelman holder (Pall Life Sciences, Sigma-Aldrich®) (Figure 3.7A). A second needle was inserted as an outlet (Figure 3.7B) and the vial was flushed for one minute with nitrogen. The second needle was slowly removed in two movements and the vial was again pressurized for ten seconds, where after all the vials were autoclaved.

Unless otherwise stated, sample bottles were completely filled. For the filtered samples, water was collected on-site through a sterile 0.2 µM cellulose acetate membrane syringe filter (GVS Filter Technology Inc., Lasec) (Figure 3.7C) to remove particulate matter and to reduce the biological activity in the sample. Serum vials were filled on-site by connecting a sterile syringe-tipped Masterflex® Norprene tube (Cole-Parmer®) to the quick connect clip of the sampling manifold. A needle was added onto the syringe tip and inserted through the blue chlorobutyl rubber stopper. A second needle was inserted as an outlet (Figure 3.7D) and water was allowed to fill the vial until the water came out through the outlet needle.

Several preservatives were added to some of the sample vials before sampling took place. Poisons such as cadmium chloride ($CdCl_2$) and saturated Mercury(II) chloride ($HgCl_2$) were

used to inhibit biological activity after sampling. Acids such as concentrated hydrochloric acid (HCl), sulphuric acid (H_2SO_4), and nitric acid (HNO_3) were used for better preservation of the species being analysed.

The following samples were taken for fissure water chemistry analyses: For anion analyses, a 500 ml Nalgene bottle was filled and measured by ion chromatography (IC) using a DX-120 IC system (Dionex). For formate ($HCOO^-$) and acetate ($C_2H_3O_2^-$), a 60 ml serum vial was, sealed with a blue chlorobutyl rubber stopper (Bellco Glass Inc.), was filled three quarters by filtering the water and measured by IC using a DX-320 IC system (Dionex). For cation analyses, five drops of concentrated HNO_3 was added to a 50 ml falcon tube and the tube was filled with filtered water. Cations were measured using inductively coupled plasma (ICP), Optima 3000 DV (PerkinElmer Inc.). For the ammonia (NH_3) and ammonium (NH_4^+) sample, a 40 ml serum vial was sealed with a blue chlorobutyl rubber stopper (Bellco Glass Inc.), 200 µl concentrated H_2SO_4 was added to decrease the pH of the water sample below five, and autoclaved. The vial was filled with filtered water and the concentrations were measured by the phenol/hypochlorite method (Parsons *et al*., 1984). The sulphur species sample was collected in the same way as described for formate/acetate, except that the serum vial was also flushed with nitrogen (99.999%), before sampling and contained 0.2 g $CdCl_2$. The bisulfide (HS^-) content was measured by filtering and dissolving the zinc sulphide (ZnS) precipitate with 0.1 M HCl, and measuring the zinc (Zn) content through inductively coupled plasma atomic emission spectroscopy (ICP-AES), Optima 4300 DV (PerkinElmer Inc.), while the sulphate (SO_4^{2-}) and thiosulphate ($S_2O_3^{2-}$) content of the filtrate was measured by IC using a DX-320 IC system (Dionex). A 500 ml Nalgene bottle was filled three quarters to obtain a phosphorous (P) sample and phosphate (PO_4^{3-}) concentrations were measured with a DX-320 IC system (Dionex). For the total nitrogen (TN), the dissolved organic carbon (DOC), and the dissolved inorganic carbon (DIC), four 250 ml glass bottles with PTFE lined caps (Thermo Fisher Scientific) and eight 125 ml High-density polyethylene (HDPE) bottles (Lasec) were used. The glass bottles were also baked in an annealing oven as previously discussed and all the bottles were filled with filtered water using a Whatman Polycap 36TC, 0.2 µM capsule filter (Thermo Fisher Scientific). The TN was measured simultaneously with the DOC using a TOC-VCSH carbon analyser (Shimadzu) with a TNM-L nitrogen analyser (Shimadzu). The DIC was eliminated through acidification and sparging and the DOC was combusted and measured using a non-dispersive infrared sensor (NDIR). The TN was measured by a chemi-luminescence detector connected in

series with the NDIR. DIC was measured on an Aurora 1030W TOC Analyser (Moser *et al*., 2003; Lin *et al*., 2006a; Onstott *et al*., 2006; Lau *et al*., 2014).

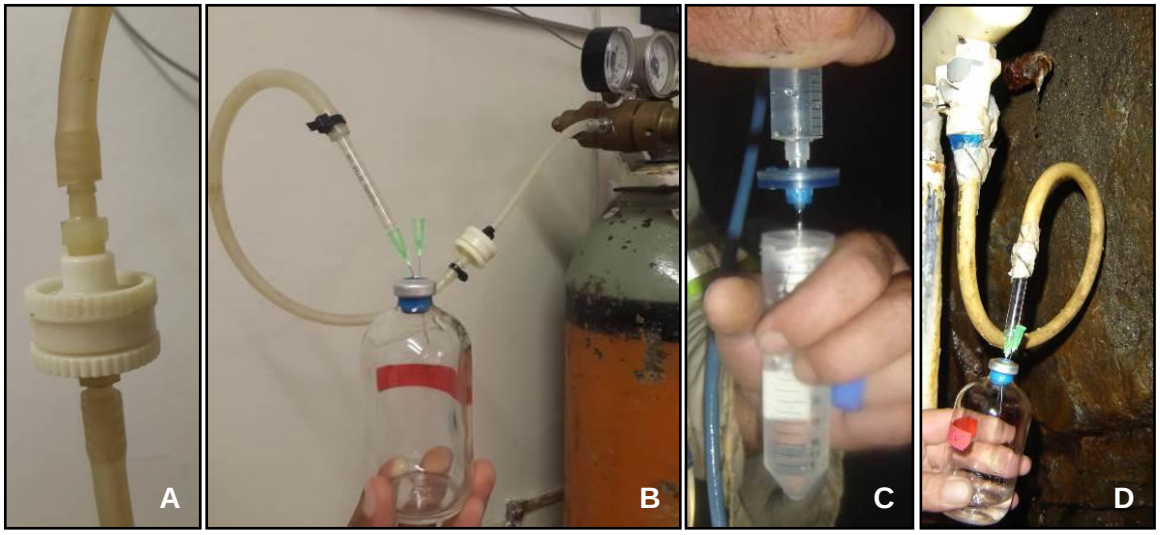

Figure 3.7: Methods used for (A) the sterile 0.2 µM Isopore™ membrane filter that was inserted into a sterile 25 mm in-line Polyacetal Gelman holder, (B) flushing serum vials with nitrogen gas, (C) filtering water through a sterile 0.2 µM syringe filter, and (D) on-site sampling of serum vials.

3.3.4.3 Collection of Gas and Fissure Water for Gas Chemistry and Isotope Analyses

For gas composition, 150 ml serum vials were acid washed, baked and prepared as discussed in Section 3.3.4.2. Saturated $HgCl_2$ (100 µl) was added and the vials were sealed with rubber stoppers and crimp sealed with an aluminium cap. The vials were evacuated by connecting them directly to a vacuum pump (Edwards) with a rubber tube, ending in a syringe tip and a needle that was inserted through the rubber stopper (Figure 3.8A). The pump was switched on until the gauge was at approximately 0.3 mbar and the reading started to slowly drop. When the gauge reached 0.02 mbar, the needle was removed. Once on-site, eight evacuated 150 ml serum vials were filled with gas according to the procedures of Sherwood Lollar *et al*., (2002) and Ward *et al*., (2004). Gas samples were obtained by closing the inlet tap from the gas stripper. A needle was connected to the outlet valve and with the tap still open, the needle was inserted into the serum vial for at least two minutes (Figure 3.8B). After the vial was filled, the outlet tap was closed and the needle removed. A 50 ml syringe was connected to the inlet tube and the tap was opened

to fill the syringe with gas. A needle was connected to the syringe and the gas was injected into the serum vial until the plunger pushed out when released. This indicated that the vial was over pressurized. When the gas flow rate was too slow, evacuated 150 ml serum vials were simply filled with fissure water as discussed in Section 3.3.4.2 and again over pressurized by adding additional 20 ml fissure water. While the vials were filled, they were submerged inside a bucket with fissure water (Figure 3.8C). The headspace that formed inside the serum vial was then used as the sample.

Gas compositions that were tested for by gas chromatography (GC) included iso/n-C1-C5, oxygen (O_2), and nitrogen (N_2) using a thermal conductivity detector, hydrogen (H_2) and carbon monoxide (CO) using a reduced gas detector, carbon dioxide (CO_2) and methane (CH_4) using a flame ionization detector. Other gases tested for included helium (He), argon (Ar), nitrous oxide (N_2O), and methanethiolate (CH_3S). Ultra-high purity (UHP) argon (Ar) was used as the carrier gas, but when measuring Ar, UHP He was used. Sample dilution to instrumental linear response range was conducted using UHP Ar/He.

Additional gas samples that could include noble gas analyses were taken according to the procedure of Lippmann *et al*., (2003), with modifications from the laboratory of B. Sherwood Lollar. Copper tubes with a 7 mm outer diameter were cut to approximately 70 cm in length. This was done just before sampling to limit the amount of oxidation inside them. The tubes were flushed by connecting them directly to the nitrogen gas (99.999%) with a sterile Tygon tube (Thermo Fisher Scientific) and a sterile in-line 0.2 µM Isopore™ membrane filter (Merck Millipore) that was inserted into a sterile 25 mm in-line Polyacetal Gelman holder (Pall Life Sciences, Sigma-Aldrich®) (Figure 3.8D). After flushing, the ends were sealed with parafilm (Lasec). Once on-site, four copper tubes were connected in sequence using Tygon tubing. The tubes were pushed at least one centimetre into the Tygon tubing to ensure a tight fitting. At the end of the last copper tube (furthest from the borehole), a longer piece of Tygon tubing was attached and submerged into a beaker of fissure water (Figure 3.8E). The other end of the copper tubes (closest to the borehole), was attached to the outlet valve of the gas stripper discussed in Section 3.3.4.1. The outlet tap was opened and the four tubes were flushed by allowing the gas to flow through for approximately 15 minutes. Flow of gas could be established by ensuring that bubbles were formed at the end that was submerged into the bucket with fissure water. After sampling, each of the four copper tubes was sealed with a crimper at both ends (Figure 3.8F and G) and submerged into a beaker of fissure water to ensure no leaks. Tubes were sealed one

at a time, starting with the copper tube furthest from the borehole and allowing one minute of purging before sealing the next tube.

Figure 3.8: Methods used for (A) evacuating serum vials, (B) collecting gas samples on-site, (C) collecting water samples for gas when the gas flow was too slow, (D) flushing of the copper tubes with nitrogen gas (99.999%), (E) preventing air from flowing back into the copper tubes, and (F and G) crimp sealing of the copper tubes.

The concentrations of the dissolved gases were derived from the gas volume abundance, the ratio of water to gas flow rates, and Henry's law constants according to the procedure of Andrews & Wilson, (1987) and are considered to be minimum estimates due to the potential degassing of fluid internally within a partially depressurized fracture zone (Lippmann *et al*., 2003).

Isotope analyses of the gas included $\delta^{2}H$ and $\delta^{13}C$ for methane (CH_4). For the fissure water isotope analyses of $\delta^{18}O_{CH4}$ and $\delta D/\delta^{2}H_{CH4}$ (deuterium), the sample was collected in a 60 ml narrow mouth Nalgene bottle (Moser *et al*., 2003; Lin *et al*., 2006a; Onstott *et al*., 2006; Lau *et al*., 2014). For the $\delta^{14}C_{DIC}$, a 500 ml Nalgene bottle, containing 1 ml of a saturated $HgCl_2$ solution, were filled. Immediately after sampling, the bottle was sealed to prevent contamination by the CO_2 in air. The conventional Radiocarbon Age and $\delta^{14}C$ are reported according to the procedures of Stuiver & Polach, (1977). The fraction modern (F)

is the blank corrected fraction modern normalized to $\delta^{13}C$ of -25 $g.L^{-1}$ (Donahue *et al*., 1990). The $\delta^{13}C$ normalization was performed using $\delta^{13}C$ measured by accelerator mass spectrometry (AMS), thus accounting for AMS fractionation. The reported errors comprise statistical errors in sample and standard determinations, combined in quadrature with a system error based on the analyses of an on-going series of measurements on an oxalic acid standard.

3.3.5 Sandstone Sampling and Analyses

Karoo sandstone (Figure 3.9) was obtained from the Star Diamonds mine to be used in several different experiments. The sandstone was collected from the same area where the borehole is located.

Figure 3.9: The Karoo sandstone obtained from the Star Diamonds mine.

3.3.5.1 Crushing and Sterilizing

The sandstone was crushed using a jaw crusher and separated according to size using a 2.8 mm and a 4.7 mm strainer (4.7 mm < X > 2.8 mm) (Figure 3.10).

Figure 3.10: Separation of the crushed rock using a 2.8 mm and a 4.7 mm strainer.

The crushed rock was sterilized through either autoclaving, acid washing, or both. Acid washing was conducted by an overnight wash step in 10% (v/v) HCl (Rotzsche, 1991), followed by rinsing three times with sterile Nano-pure water. This was all done under sterile conditions in a laminar flow cabinet (Labotec®). When both methods were used, the rock was first washed and rinsed before being autoclaved.

3.3.5.2 X-Ray Fluorescence Analyses

The composition of the sandstone was analysed by X-Ray fluorescence analyses (XRF) (Rollinson, 1993; Von Eynatten *et al*., 2003) for any possible changes that might have occurred during processing. XRF analyses were conducted at the Department of Geology at the UFS (Bloemfontein, RSA).

The crushed sandstone was milled to powder using a tungsten mill, where after 8 g of the powder was added to 3 g of Hoechst wax ($C_6H_8O_3N_2$). This was mixed for 20 minutes in a Turbula mixer to ensure that the sample was mixed homogeneously and pressed to pressures greater than 395 $N.m^{-1}$ to make a pellet for measuring the trace-elements and sodium. The total loss on ignition (LOI) was calculated by heating the powdered sample to 110°C (dehydration) for 2 hours and then over night at 1050°C. A flux of 0.2445 g lanthanum oxide (La_2O_3), 0.705 g lithium tetraborate ($Li_2B_4O_7$), 0.5505 g lithium carbonate (Li_2CO_3), and 0.02 g sodium nitrate ($NaNO_3$) was added to 0.28 g of the powdered sample. This mixture was then heated in a platinum (Pt) crucible to 1000°C for approximately 5 minutes until a consistent fluid formed. The fluid was poured into a mould and pressed to create a fusion disc for measuring the major-elements. Analyses were conducted by Xray fluorescence spectrometry using an Axios XRF spectrometer (PANalytical) with a rhodium (Rh) tube. Major-element oxides were recalculated to 100% with the LOI included.

3.3.6 Diversity Analyses of the Deep Subsurface Microbial Biome

The number of species (the species richness) and the sizes of the species populations (the species evenness) within a community are both important parameters to consider when describing the diversity within a community (Liu *et al*., 1997). However, the portion of microbial species that can be cultured and identified based on their physiological and biochemical properties through the use of traditional culture-dependant methods only

represent a small fraction of the existing diversity (Amann *et al*., 1995; Liu *et al*., 1997). It is also likely that the diversity within a community will change if the culture conditions differ even slightly from the conditions of their original environment. This will introduce essential biases in the diversity of the community due to the methods used for isolation (Dunbar *et al*., 1997; Liu *et al*., 1997).

Therefore, for a more comprehensive characterization of the subsurface biome, samples were collected for genomic deoxyribonucleic acid (gDNA) and total ribonucleic acid (RNA) isolations by using various types of filters and larger quantities of fissure water. Unless otherwise specified, subsurface microbial biomes were sampled and analysed according to the procedures of Takai *et al*., (2001); Moser *et al*., (2003); Lin *et al*., (2006a); Lau *et al*., (2014); and Magnabosco *et al*., (2014).

3.3.6.1 Cornelius® Canister Sampling

For continual monitoring of the diversity over time, fissure water was collected anaerobically in a 12.6 L stainless steel Cornelius® canister (Cornelius® Inc.) (Figure 3.11) according to the procedures of Takai *et al*., (2001); Moser *et al*., (2003); and Lin *et al*., (2006a). Before each sampling, the canister was thoroughly cleaned with soapy water and rinsed with Nano-pure water, followed by 70% (v/v) EtOH. The canister was air dried in a laminar flow cabinet (Labotec®) and sterilized together with all tubing and fittings needed to connect the canister to the sampling manifold attached to the borehole. The outlet valve on the cap was opened before autoclaving (Figure 3.11A). After sterilization, the outlet valve was closed and the canister was allowed to cool to room temperature. The canister was flushed for 10 minutes at 50 kPa (0.5 bar) by connecting it directly to the nitrogen gas (99.999%) with an autoclaved inlet adaptor fitted to sterile Tygon tubing (Thermo Fisher Scientific) and a sterile in-line 0.2 µM Isopore™ membrane filter (Merck Millipore) that was inserted into a sterile 25 mm in-line Polyacetal Gelman holder (Pall Life Sciences, Sigma-Aldrich®) (Figure 3.11B). During flushing the outlet valve was opened. Before canisters were used, the outlet valve was quickly opened to ensure that the canister maintained positive pressure.

On-site, the inlet of the canister was directly connected to a quick connect clip of the sampling manifold by using sterile PTFE tubing (Watson-Marlow) (Figure 3.11C). As water

flowed into the canister, the outlet valve was opened until the canister was overflowing (Figure 3.11D). In the laboratory, the fissure water was displaced from the canister through the addition of nitrogen gas (99.999%) at 50 kPa by connecting the inlet of the canister directly to the nitrogen with an autoclaved inlet adaptor fitted to sterile Tygon tubing (Thermo Fisher Scientific) and an in-line 0.2 µM Isopore™ membrane filter (Merck Millipore) (Figure 3.11E). The fissure water is displaced using positive pressure (Figure 3.11F) and the cells were collected on sterile Supor® 200 membrane disc filters (Pall Life Sciences) that were inserted into sterile 47 mm in-line Polycarbonate Gelman holders (Pall Life Sciences, Sigma-Aldrich®) (Figure 3.11G). After filtration, the filters were stored in cryogenic vials (Thermo Fisher Scientific) at -20°C until further processing.

Figure 3.11: Methods used for (A) sterilizing the canister with the outlet valve opened, (B) flushing the canister, (C and D) collecting fissure water on-site, and (E-G) filtering water from the canister.

3.3.6.2 Sterivex™ Filter Sampling

As an alternative means to the Cornelius® canisters, sterile Sterivex™ - GP 0.22 µM, polyethersulone (PES) filters (Millipore Corporation) (Figure 3.12A) were connected to the borehole to collect biomass according to the procedure of Brazelton *et al*., (2012). The filter caps were removed and the filters were attached to the quick connect clips of the sampling manifold by using a sterile syringe-tipped Masterflex® Norprene tube (Cole-Parmer®) (Figure 3.12B). The filters had to stay connected inside the mine for at least one month to obtain larger quantities of biomass. Filters were stored at -20°C until further processing.

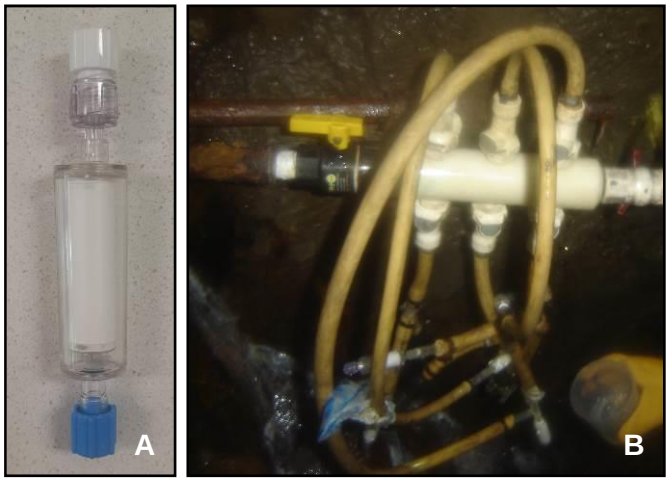

Figure 3.12: (A) The Sterivex™ filters used to (B) collect biofilm on-site through direct connection to a quick connect clip of the sampling manifold.

3.3.6.3 Tangential Flow Filtration

In order to obtain a concentrated sample of the subsurface biome, large volumes of fissure water were filtered and concentrated using tangential flow filtration (TFF) according to the procedure of Kuwabara and Harvey, (1990). Fissure water was collected in the mine with sterile 50 L Nalgene Carboy bottles. The water was transported back to the laboratory where TFF was carried out under sterile conditions inside a laminar flow cabinet (Labotec®) (Figure 3.13A). The water was filtered using a sterile 100 000 NMWC pore size, polysulfone (PS), ultrafiltration hollow fibre cartridge [63.5 cm (length) x 5.1 cm (outer diameter)] (GE Healthcare).

This process was repeated on-site to obtain sufficient biome quantities (Figure 3.13B). A 50 L sterile Nalgene Carboy bottle was also filled with un-concentrated fissure water, and together with the concentrated water, transported back to the laboratory where it was stored at 4°C to be used in different experiments as needed.

Figure 3.13: Tangential flow filtration of the fissure water (A) inside the laboratory and (B) inside the mine.

3.3.6.4 Massive Filter Sampling

For collecting biomass from larger quantities of fissure water, a massive filter (Figure 3.14A) was used according to the procedures of Lau *et al*., (2014) and Magnabosco *et al*., (2014). Before each sampling, the filter holder was thoroughly cleaned with soapy water and rinsed with Nano-pure water, followed by 70% (v/v) EtOH and air dried in a laminar flow cabinet (Labotec®). A 0.1 µM Osmonics Nylon filter cartridge (GE Healthcare) was inserted into the filter holder and the lid was closed. The massive filter, together with all tubing and fittings used, were placed in an autoclave bag and sterilized before use.

On-site, the inlet of the massive filter was directly connected to a quick connect clip of the sampling manifold using sterile PTFE tubing (Watson-Marlow) (Figure 3.14B) and the outlet of the massive filter was directly connected to a flow meter (Figure 3.14C). The filter had to stay connected inside the mine for at least one month to obtain large quantities of biomass.

Figure 3.14: (A) A massive filter used for collecting biofilm from fissure water in larger quantities through (B) direct connection to a quick connect clip of the sampling manifold to the inlet side of the filter and (C) the flow accumulator connected to the outlet side of the filter.

Unfortunately the pressure from the borehole was not enough to obtain a flow of water through the filters and the filters had to be removed after three days. A new massive filter was prepared as discussed previously, but this time connected to a peristaltic pump (Millipore Corporation) and a Nalgene Carboy bottle that served as a reservoir once the bottle was filled (Figure 3.15). The cap of the Carboy bottle had three connections – one inlet and two outlets (Figure 3.15A). The inlet of the cap was directly connected to a quick connect clip of the sampling manifold using sterile PTFE tubing (Watson-Marlow), as shown before in Figure 3.14B. The first outlet was connected to the peristaltic pump that was set to operate at maximum speed (600 rpm) with sterile Masterflex® Norprene tubing (Cole-Parmer®) (Figure 3.15B) and the second outlet was left open as an overflow (Figure 3.15C). A sterile 0.2 µM nylon filter cloth was placed underneath the cap to cover the opening of the Carboy bottle. Both the inlet of the cap and the outlet that was connected to the peristaltic pump had a tube connected on the inside of the cap (Figure 3.15D) that went through the filter all the way to the bottom of the Carboy. This was done so that the biofilm was collected inside the carboy and not on the filter. The filter was replaced every second day. The peristaltic pump was connected to the inlet of the massive filter (Figure 3.15E) and the outlet of the massive filter was directly connected to a flow accumulator, as shown before in Figure 3.14C. The numbers on the flow accumulator were recorded before being attached to the filter. This time enough pressure was created for the water to keep on flowing through the filter which was left connected to the borehole for one month.

Upon retrieval of the massive filter, immediately after disconnecting the filter from the borehole, the water inside the filter holder was discarded through the inlet/outlet and the filter holder was filled with a sterile, salt-saturated RNA preservative solution [20 mM ethylenediaminetetraacetic acid (EDTA), 0.3 M sodium citrate, 4.3 M ammonium sulphate, pH 5.2, adjusted with concentrated sulphuric acid (H_2SO_4)] (Lau *et al*., 2014). The filter holder was sealed with sterile threaded plugs, transported back to the laboratory at the UFS (Bloemfontein, RSA), and stored overnight at 4°C to ensure saturation of all the membrane layers of the filter. The filter was then removed from the filter holder under sterile conditions, wrapped in aluminium foil and stored at -80°C until further processing.

The Nalgene Carboy that contained large amounts of cells, was closed with a sterile cap and the water was transported back to the laboratory at the UFS (Bloemfontein, RSA) and stored at 4°C to be used in different experiments as needed.

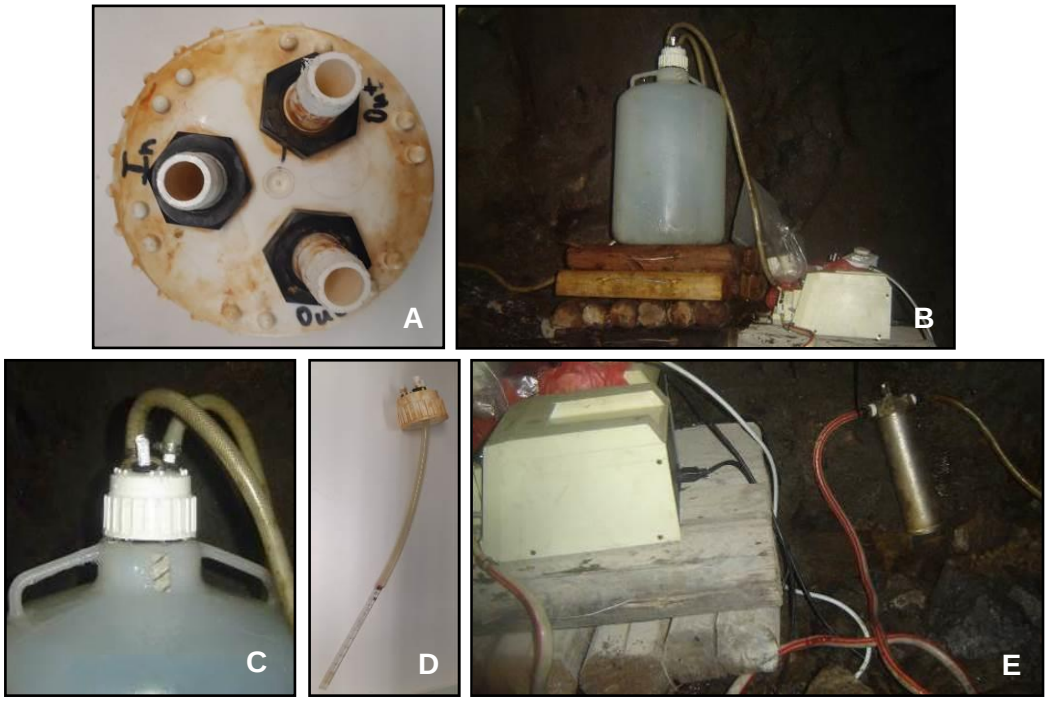

Figure 3.15: (A) The cap of the Carboy bottle with one inlet and two outlets with (B) one of the outlets connected to the pump, and (C) the other outlet left open as an overflow, (D) the tube connected on the inside of the cap, and (E) the pump connected to the inlet of the massive filter.

3.3.6.5 Polyvinyl Chloride Cartridge Sampling

As an alternative to the massive filters, sterile Polyvinyl chloride (PVC) cartridges, filled with crushed sandstone (Figure 3.16) were connected to the borehole (Moser *et al*., 2003). These cartridges were custom-made by the Department of Instrumentation at the UFS (Bloemfontein, RSA). The cartridge consisted of a hollow PVC casing that was fitted on the one side with a quick connect clip and a reducer on the other side. Each cartridge also had two screw caps for proper sealing during storage (Figure 3.16A). The sandstone was added to provide surfaces for microbial attachment and colonization. A quick connect clip and reducer was attached to the cartridge and together with the screw caps, wrapped in aluminium foil and sterilized.

On-site the cartridges were directly connected to the sampling manifold (Figure 3.16B) and the cartridges stayed connected to the borehole for one month. Once the cartridges were removed, they were sealed with the sterile caps, wrapped in aluminium foil and transported back to the laboratory at the UFS (Bloemfontein, RSA) where they were stored at -80°C until further processing.

Figure 3.16: (A) The custom made PVC cartridges with its fitting and caps and (B) the cartridges directly connected to the sampling manifold on the borehole.

3.3.6.6 Microbial Diversity Assessments using Denaturing Gradient Gel Electrophoresis

Denaturing gradient gel electrophoresis (DGGE) was used to determine the genetic diversity of the microbial communities from the subsurface biome.

3.3.6.6.1 Genomic DNA Isolation

Genomic DNA was isolated from all the filters of the Cornelius® canisters, the Sterivex™ filters, as well as from the biome that was concentrated using TFF. The filters were allowed to thaw and cut into small pieces under sterile conditions. The filter pieces, as well as the concentrated TFF water were added to the tubes containing the beads and the gDNA was isolated using the NucleoSpin® Soil kit (Macherey-Nagel) according to the manufacturer's instructions. The integrity of the gDNA was evaluated using agarose gel electrophoresis. All of the agarose gels used throughout this research consisted of 1% (w/v) agarose in Tris-Acetate-EDTA (TAE) buffer (40 mM Tris, 40 mM acetic acid, 1 mM EDTA, pH 7.4) with 0.6 $\mu g.ml^{-1}$ ethidium bromide (EtBr) (Merck Millipore). Genomic DNA (10 µl) was added to 2 µl loading dye (Fermentas) before being separated in the gel at 90 V for 60 minutes. Either MassRuler™ DNA Ladder Mix or O'GeneRuler™ DNA Ladder Mix (Both from Thermo Scientific) was used to determine the size of the amplicons and the gel was visualized using the ChemiDoc XRS UV/Vis Gel Documentation system with Quantity One V.4.5 software (Bio-Rad Laboratories, Inc.). The concentration and purity of the gDNA was measured using the NanoDrop® ND-1000 UV/Vis Spectrophotometer (Inqaba Biotech™).

3.3.6.6.2 Polymerase Chain Reaction

A polymerase chain reaction (PCR) was conducted on the gDNA to amplify the Archaeal 16S (~600 bp), Bacterial 16S (~1500 bp) and Eukaryal 18S (~1700 bp) rRNA gene fragments using the universal oligonucleotide primers for each gene as indicated in Table 3.1. Control reactions were prepared for each of the different groups using sterile water as the negative control and gDNA from *Halobacterium salinarum, Escherichia coli* and *Saccharomyces cerevisiae* as the templates for the positive controls for Archaea, Bacteria and Eukarya, respectively.

Table 3.1: The universal oligonucleotide primers used for amplification of the Archaeal 16S, Bacterial 16S and Eukaryal 18S rRNA gene fragments.

Primer	Nucleotide sequence	Tm (°C)	rRNA gene	Reference
Arc333F	5'-TCC AGG CCC TAC GGG-3'	56.9	Archaea 16S	Lepp *et al*., 2004
Arc958R	5'-YCC GGC GTT GAM TCC AAT T-3'	56.6	Archaea 16S	De Long, 1992
Bac27F	5'-AGA GTT TGA TCM TGG CTC AG-3'	53.2	Bacteria 16S	Turner *et al*., 1999
Bac1492R	5'-GGT TAC CTT GTT ACG ACT T-3'	49.4	Bacteria 16S	Turner *et al*., 1999
EukA	5'-AAC CTG GTT GAT CCT GCC AGT-3'	58.9	Eukarya 18S	Diez *et al*., 2001
EukB	5'-TGA TCC TTC TGC AGG TTC ACC TAC-3'	58.4	Eukarya 18S	Diez *et al*., 2001

The PCR was performed in a total reaction volume of 25 µl using a 2720 Thermal Cycler (Applied Biosystems®). The reaction mixture consisted of 12.5 µl GoTaq® Green master mix (2X) [a premixed ready-to-use solution that contains the Taq DNA polymerase, dNTPs (400 µM), magnesium chloride ($MgCl_2$) (3 mM) and reaction buffers (pH 8.5)], 1 µl each of both the forward and reverse primers (10 µM), 50 ng.μl^{-1} template and sterile Nano-pure water filled to the reaction volume.

Optimized reaction conditions for Archaeal 16S consisted of an initial denaturing step at 94°C for 2 minutes, followed by 30 cycles of denaturing at 95°C (30 seconds), annealing at 61°C (30 seconds) and elongation at 72°C (1.5 minutes). A final elongation step of 1 minute at 72°C was added to ensure complete elongation of the amplified product. For Bacterial 16S, optimized reaction conditions consisted of an initial denaturing step at 95°C for 5 minutes, followed by 30 cycles of denaturing at 95°C (30 seconds), annealing at 49°C (45 seconds) and elongation at 72°C (1 minute), with a final elongation step of 10 minutes at 72°C. For Eukaryal 18S, optimized reaction conditions consisted of an initial denaturing step at 94°C for 1.5 minutes, followed by 30 cycles of denaturing at 94°C (30 seconds), annealing at 60°C (1 minute) and elongation at 72°C (45 seconds), with a final elongation step of 5 minutes at 72°C.

The PCR products were visualized on a 1% (w/v) agarose gel. Purification of the PCR products was achieved by excising the desired band from the agarose gel using a non-UV Dark Reader™ DR-45M transilluminator (Clare Chemical Research) and extracted using the BioFlux BioSpin Gel Extraction Kit (Bioer Technology Co., Ltd) according to the manufacturer's instructions. The concentration and purity of the purified products were

measured using the NanoDrop® ND-1000 UV/Vis Spectrophotometer (Inqaba Biotech™). All PCR reactions were done in triplicate and combined into one tube to increase concentrations before purifications were done.

3.3.6.6.3 Nested Polymerase Chain Reaction

A nested DGGE PCR was conducted on all the purified samples to amplify the V3/V4 hypervariable regions for Archaea (~600 bp), Bacteria (~600 bp) and Eukarya (~600 bp) using the DGGE oligonucleotide primers for each gene as indicated in Table 3.2. A GC-clamp was added to the forward primers.

Table 3.2: The DGGE oligonucleotide primers used for amplification of the V3/V4 hypervariable regions for Archaea, Bacteria and Eukarya, respectively. Underlined sequences indicate the GC-clamp.

Primer	Nucleotide sequence	Tm (°C)	V3/V4	Reference
Arc344F-GC	5'-CGC CCG CCG CGC GCG GCG GGC GGG GCG GGG GCA CGG GGG GAC GGG GYG CAG CAG GCG CGA-3'	86.2	Archaea	Casamayor *et al*., 2002
Arc934R	5'-GTG CTC CCC CGC CAA TTC CT-3'	62.9	Archaea	Casamayor *et al*., 2002
Bac341F-GC	5'-CGC CCG CCG CGC GCG GCG GGC GGG GCG GGG GCA CGG GGG GCC TAC GGG AGG CAG CAG-3'	85.1	Bacteria	Muyzer *et al*., 1993
Bac908R	5'-CCG TCA ATT CMT TTG AGT TT-3'	49.9	Bacteria	Turner *et al*., 1999
Euk1AF-GC	5'-CGC CCG CCG CGC GCG GCG GGC GGG GCG GGG GCA CGG GGG GCT GGT TGA TCC TGC CAG-3'	84.1	Eukarya	Diez *et al*., 2001
Euk516R	5'-ACC AGA CTT GCC CTC C-3'	54.3	Eukarya	Diez *et al*., 2001

The DGGE PCR was performed in a total reaction volume of 25 µl using a 2720 Thermal Cycler (Applied Biosystems®) as discussed in Section 3.3.6.6.2. Optimized reaction conditions for the Archaeal V3/V4 region consisted of an initial denaturing step at 94°C for 2 minutes, followed by 30 cycles of denaturing at 95°C (30 seconds), annealing at 61°C (30 seconds) and elongation at 72°C (1.5 minutes). A final elongation step of 1 minute at 72°C was added to ensure complete elongation of the amplified product. For the Bacterial V3/V4 region, optimized reaction conditions consisted of an initial denaturing step at 95°C for 4 minutes, followed by 30 cycles of denaturing at 95°C (1 minute), annealing at 55°C (1

minute) and elongation at 72°C (1.5 minutes), with a final elongation step of 10 minutes at 72°C. For the Eukaryal V3/V4 region, optimized reaction conditions consisted of an initial denaturing step at 95°C for 4 minutes, followed by 30 cycles of denaturing at 95°C (1 minute), annealing at 56°C (1 minute) and elongation at 72°C (1.5 minutes), with a final elongation step of 10 minutes at 72°C. The DGGE PCR products were visualized on a 1% (w/v) agarose gel.

3.3.6.6.4 Denaturing Gradient Gel Electrophoresis

The products from the nested DGGE PCR were used to construct preliminary diversity profiles using the DGGE Dcode™ universal mutation detection system (Bio-Rad Laboratories, Inc.) as described by Diez *et al*., (2001). The gradient of urea/formamide denaturants for Archaea and Bacteria ranged from 40% - 60% and for Eukarya ranged from 40% - 65%. Electrophoresis was performed with a 7% (w/v) polyacrylamide gel (acrylamide/bisacrylamide 40%, 37.5:1 ratio, Merck Millipore) in Tris-Acetate-EDTA (TAE) buffer (40 mM Tris, 40 mM acetic acid, 1 mM EDTA, pH 7.4) at 60°C. The entire nested DGGE PCR product was used and separated in the gel at 100 V for 16 hours. The gel was stained with 0.6 $\mu g.ml^{-1}$ ethidium bromide (EtBr) (Merck Millipore) for 30 minutes in TAE buffer and visualized using the ChemiDoc XRS UV/Vis Gel Documentation system with Quantity One V.4.5 software (Bio-Rad Laboratories, Inc.).

3.3.6.6.5 Gel Extraction, Re-amplification and Purification

Selected DGGE bands were excised from the gel using the ChemiDoc XRS UV/Vis Gel Documentation system with Quantity One V.4.5 software (Bio-Rad Laboratories, Inc.) and eluted overnight at 50°C in 50 µl sterile Nano-pure water. The concentration and purity of the eluted DGGE products were measured using the NanoDrop® ND-1000 UV/Vis Spectrophotometer (Inqaba Biotech™).

The concentrations of the recovered DNA were increased through re-amplification of the V3/V4 hypervariable regions from the eluted DGGE products for Archaea (~600 bp), Bacteria (~600 bp) and Eukarya (~500 bp) using the oligonucleotide primers for each gene as indicated in Table 3.3.

Table 3.3: The oligonucleotide primers used for the re-amplification of the V3/V4 hypervariable regions for Archaea, Bacteria and Eukarya, respectively.

Primer	Nucleotide sequence	Tm (°C)	V3/V4	Reference
Arc344F	5'-ACG GGG YGC AGC AGG CGC GA-3'	72.9	Archaea	Casamayor *et al*., 2002
Arc934R	5'-GTG CTC CCC CGC CAA TTC CT-3'	62.9	Archaea	Casamayor *et al*., 2002
Bac341F	5'-CCT ACG GGA GGC AGC AG-3'	58.9	Bacteria	Muyzer *et al*., 1993
Bac908R	5'-CCG TCA ATT CMT TTG AGT TT-3'	49.9	Bacteria	Turner *et al*., 1999
Euk1AF	5'-CTG GTT GAT CCT GCC AG-3'	52.8	Eukarya	Diez *et al*., 2001
Euk516R	5'-ACC AGA CTT GCC CTC C-3'	54.3	Eukarya	Diez *et al*., 2001

The PCR was performed in a total reaction volume of 25 µl using a 2720 Thermal Cycler (Applied Biosystems®) as discussed in Section 3.3.6.6.2.

Optimized reaction conditions for the Archaeal V3/V4 region consisted of an initial denaturing step at 94°C for 2 minutes, followed by 30 cycles of denaturing at 95°C (30 seconds), annealing at 59°C (30 seconds) and elongation at 72°C (1.5 minutes). A final elongation step of 1 minute at 72°C was added to ensure complete elongation of the amplified product. For the Bacterial V3/V4 region, optimized reaction conditions consisted of an initial denaturing step at 95°C for 4 minutes, followed by 30 cycles of denaturing at 95°C (1 minute), annealing at 53°C (1 minute) and elongation at 72°C (1.5 minutes), with a final elongation step of 10 minutes at 72°C. For the Eukaryal V3/V4 region, optimized reaction conditions consisted of an initial denaturing step at 95°C for 4 minutes, followed by 30 cycles of denaturing at 95°C (1 minute), annealing at 54°C (1 minute) and elongation at 72°C (1.5 minutes), with a final elongation step of 10 minutes at 72°C. The re-amplified PCR products were visualized on a 1% (w/v) agarose gel and purified (Section 3.3.6.6.2).

3.3.6.6.6 Sanger Sequencing and Analyses

The purified DGGE products were sequenced to determine the genetic diversity of the subsurface microbial community. Sanger sequencing was conducted using the ABI Prism® Big Dye™ Terminator Cycle Sequencing Ready Reaction Kit V.3.1 (Applied Biosystems) according to the manufacturer's instructions.

The reaction was performed in a total volume of 10 µl and consisted of 0.5 µl premix, 2 µl dilution buffer, 1 µl primer (3.2 pmol.µl^{-1}), template (200-500 ng.µl^{-1}) and sterile Nano-pure water filled to the reaction volume. Reaction conditions consisted of an initial denaturing step at 96°C for 1 minute, followed by 25 cycles of denaturing at 96°C (10 seconds), annealing at 50°C (5 seconds) and elongation at 60°C (4 minutes). The primers in Section 3.3.6.6.5, Table 3.3 were used, and separate reactions were made for the forward and reverse primers.

The PCR products were purified using an EDTA/EtOH precipitation protocol for sequencing clean-up. The sequencing reaction volume was adjusted to 20 µl, transferred to a 1.5 ml eppendorf tube containing 5 µl EDTA and 60 µl absolute EtOH (Merck Millipore), mixed for 5 seconds and allowed to precipitate for 15 minutes at room temperature. The mixture was centrifuged (20 000 *x g*, 10 minutes, 4°C) using an Allegra^{TM} 25R centrifuge (Beckman Coulter^{TM}) and the supernatant was removed through aspiration, without disturbing the pellet. 70% (v/v) EtOH (60 µl) was added to the pellet and centrifuged once more (20 000 *x g*, 5 minutes, 4°C). The supernatant was removed through aspiration and the pellet was dried for 5 minutes using a Concentrator 5301 (Eppendorf). The samples were covered in foil and stored in the dark at 4°C until sequenced. Sequencing reactions were conducted with a 3130*xl* Genetic Analyzer, HITACHI (Applied Biosystems) at the UFS (Bloemfontein, RSA).

For the 16S and 18S rRNA gene sequences, the sequence data was analysed and assembled to create contigs using the Geneious software (V.7.1.7). Analysed sequences for 16S were aligned against the life tree project (LTP) 119 rRNA database from SILVA (Pruesse *et al*., 2007) using a variant (BLASTN) algorithm (Zhang *et al*., 2000) of the basic local alignment search tool (BLAST). Analysed sequences for 18S were aligned against the Nucleotide collection (nr/nt) database from the National Centre for Biotechnology Information (NCBI) using the BLASTN algorithm (Altschul *et al*., 1997), by excluding uncultured and environmental samples in order to obtain the closest family. The first fifteen hits were used to assign higher order classification and were filtered based on 50% identity.

3.3.6.7 Microbial Diversity Assessments using Targeted 16S and 18S rRNA Gene Sequencing

3.3.6.7.1 Genomic DNA Isolation

Genomic DNA was isolated from the massive filters as well as the PVC cartridges. The massive filters were prepared by removing the filters from the -80°C freezer and allowed to thaw. The filter was cut into ~2 cm sections and the different layers of the filter were separated into the inner fibrous membrane, the massive filter, and the outer fibrous membrane. The different layers were each cut into smaller pieces and used for gDNA isolations by adding the filter pieces to the tubes containing the beads. For the PVC cartridges, the cartridges were removed from the -80°C freezer and allowed to thaw. The rock was removed from the cartridge and added to a tube without beads. The rock was used to break the cells in this case.

The gDNA was isolated using two different methods. The first method used was the NucleoSpin® Soil kit (Macherey-Nagel) according to the manufacturer's instructions. The second method used was according to the procedures of Lau *et al*., (2014). The reaction tubes were kept on ice throughout the extraction process to limit nucleic acid degradation. The cells were lysed by adding sterile cetyl trimethylammonium bromide (CTAB) lysis buffer (2X) [8.18 $g.L^{-1}$ NaCl, 0.5 M EDTA (4 ml), 1 M Tris, pH 8.0 (10 ml), 2 $g.L^{-1}$ CTAB in dH_2O] containing lysozyme (5 $mg.mL^{-1}$) and proteinase K (0.2 $mg.mL^{-1}$) to the tubes containing the material from the filters. The tubes were vortexed for one minute, incubated in a water bath at 60°C for 30 minutes and rinsed with sterile Tris-EDTA (TE) buffer (1X) [1 M Tris, pH 8.0 (10 ml), 0.5 M EDTA (2 ml) in dH_2O]. A phenol/chloroform/isoamyl alcohol (25:24:1 v/v/v) extraction was conducted by adding 4 ml of the phenol/chloroform/isoamyl alcohol to each 5 ml of the lysate. The mixture was incubated in a water bath at 60°C for one minute, added to an ice-bath for 5 minutes and centrifuged (4 300 *x g,* 10 minutes, room temperature) using an Allegra™ 25R centrifuge (Beckman Coulter™). The gDNA was precipitated by adding isopropanol (1:1 v/v) to the mixture and gently inverted to mix. The tubes were incubated in an ice-bath for 30 minutes and centrifuged (4 300 *x g,* 15 minutes, room temperature) using an Allegra™ 25R centrifuge (Beckman Coulter™). The supernatant was discarded and the pellets were rinsed with ice-cold 75% EtOH and allowed to air dry. Once dried, the pellets were re-suspended in 300 µl sterile TE buffer (1X), containing RNase A (10 $\mu g.ml^{-1}$) (Fermentas) and incubated in a water bath at 37°C

for 30 minutes. NaCl (0.1 M) and two volumes of absolute EtOH were added to the mixture, incubated at -20°C for 30 minutes and centrifuged (11 500 *x g,* 30 minutes, room temperature) using an Allegra™ 25R centrifuge (Beckman Coulter™) to collect the gDNA. The gDNA was subjected to quality control as discussed in Section 3.3.6.6.1.

3.3.6.7.2 MiSeq Illumina® Sequencing and Analyses

16S rRNA metagenome sequence analyses were conducted on the gDNA using the MiSeq Illumina® platform. The main steps included performing a standard 16S rRNA gene PCR using 16S forward and reverse primers which contained Illumina® adaptors and target specific sequences. Amplicons were quantified using the NanoDrop ND-3300 UV/Vis Spectrophotometer (Inqaba Biotech™) to determine the amount needed for the library preparation. An Index PCR-limited cycle PCR was conducted using the Nextera XT DNA Sample Preparation and the Nextera XT Index Kits (Illumina®). Barcodes/indices were added to the 5' and 3' ends of the amplicons to enable demultiplexing of the forward and reverse reads. Sequencing reactions were conducted using the Miseq Reagents Cartridge and Incorporation buffer on the Illumina® MiSeq instrument at Inqaba BiotechTM (Hatfield, RSA). The primers and standards used were as recommended by the manufacturer. The data was analysed with the automated analysis platform Metagenomics RAST (MG-RAST) using the default settings (Meyer *et al*., 2008).

3.3.6.7.3 Roche GS Junior Sequencing and Analyses

18S rRNA metagenome sequence analyses were conducted on the gDNA using the Roche GS Junior platform. The main steps included performing a standard 18S rRNA gene PCR using 18S barcoded forward primers, containing 454 adaptor-tag/barcode-target specific sequences and an 18S reverse primer, containing 454 adaptor-target specific sequences. Amplicons were quantified using the NanoDrop ND-3300 UV/Vis Spectrophotometer (Inqaba BiotechTM) to determine the number of copies (amplicons) per bead for emulsion PCR (emPCR). For the emPCR, the GS Junior Titanium emPCR Reagent Kit (Roche Life Science) was used according to the manufacturer's instructions. The emPCR product recovery was followed by enrichment of DNA carrying beads and counting thereof to load the PicoTiterPlate (PTP) using the GS Junior Titanium PicoTiterPlate Kit (Roche Life Science). These were sequenced using the GS Junior

Titanium Sequencing Kit (Roche Life Science) according to the manufacturer's instructions. Sequencing reactions were conducted with the Roche 454 GS Junior (Roche Life Science) at Inqaba BiotechTM (Hatfield, RSA). The primers and standards used were as recommended by the manufacturer. The data was analysed with MG-RAST using the default settings (Meyer *et al*., 2008).

3.3.6.7.4 Ion Torrent PGM™ Sequencing and Analyses

Both 16S and 18S rRNA metagenome sequence analyses were conducted on the gDNA using the Ion Torrent Personal Genome Machine™ (Ion PGM™) platform (Life Technologies™). The 18S library was constructed from the gDNA for up to 400 base-read sequencing using the Ion Xpress™ Plus Fragment Library Kit (Life Technologies™) according to the manufacturer's instructions for enzyme shearing. The 16S library was constructed from the gDNA for a 200 – 400 base-read sequencing using the Ion 16S™ Metagenomics Kit (Thermo Fisher Scientific) according to the manufacturer's instructions. The template was prepared from the 16S library using the Ion PGM™ Template OT2 400 Kit (Life Technologies™) according to the manufacturer's instructions and sequenced using the Ion PGM™ Hi-Q™ Sequencing Kit (Life Technologies™) according to the manufacturer's instructions. All assessments of the DNA were done using a 2100 Bioanalyzer® (Agilent® Technologies Inc.). The entire 18S region was sequenced and assembled as contigs. For the 16S, the V2-V4, and V6-V9 regions were sequenced. Sequencing reactions were conducted with the Ion Torrent PGM™ (Life Technologies™) at the Central Analytical Facilities (CAF), Stellenbosch University (Stellenbosch, RSA). The primers and standards used were as recommended by the manufacturer. The data was analysed with MG-RAST using the default settings (Meyer *et al*., 2008).

3.3.6.8 Microbial Diversity Assessments of the Fissure Water using Visual Methods

Each time fissure water was collected, different staining and microscopy techniques were conducted in order to visualize the microorganisms in the water and to determine whether the cells were alive or dead.

3.3.6.8.1 Negative Stain

Negative staining involved the addition of a small drop of the Nigrosin dye (1% w/v) to a clean, dry microscope slide. A drop of the fissure water was added to the Nigrosin, spread over the entire slide using a second microscope slide, and allowed to air dry. The stained cells were viewed with an Axioskop light microscope (Zeiss) under the 100x oil immersion magnification and images were captured using a DS-Fi1 (Nikon) camera with NIS Elements imaging software (V.3.22.00).

This stain can be used to indicate if a microorganism contains distinctive structures such as endospores, a flagellum, or a capsule (Clark, 1981; Green, 1990). The Nigrosin dye is negatively charged and therefore repelled by the negative charge of the microorganisms. This prevents the stain from entering the cell and staining the cytoplasm and as a result, the shapes and sizes of the microorganisms are seen as colourless shapes against the stained background. This stain can also be used to assess viability since the living cells will exclude the dye but it will enter the dead cells (Sanderson, 1994). Another advantage of using this stain is that fixation by heat or alcohol is not needed and therefore the microorganisms are seen in more life-like shapes.

3.3.6.8.2 Live/Dead Stain

A live/dead stain was conducted using the LIVE/DEAD® BacLight™ Bacterial Viability Kit (Molecular Probes, Inc., Invitrogen, Promega) according to the manufacturer's instructions. The stained cells were viewed with an Axioskop light microscope (Zeiss) under the 100x oil immersion magnification and images were captured using a DS-Fi1 (Nikon) camera with NIS Elements imaging software (V.3.22.00).

This kit uses SYTO® 9 as the green-fluorescent nucleic acid stain and propidium iodide as the red-fluorescent nucleic acid stain. The SYTO® 9 stain enters all bacteria in the sample – the microorganisms with intact cell membranes and those with damaged cell membranes, whereas the propidium iodide enters only into the microorganisms with damaged cell membranes, causing a reduction in the SYTO® 9 stain fluorescence when both dyes are present. Therefore, microorganisms that are alive with intact cell membranes will stain green, while microorganisms that are dead or have damaged cell

membranes will stain red when viewed under fluorescence. The excitation/emission for the dyes are 480/500 nm for the SYTO® 9 stain and 490/635 nm for the propidium iodide (Molecular Probes, Inc.).

3.3.6.8.3 Gram Stain

For the Gram-staining properties of the microorganisms, a Gram stain (Bartholomew & Mittwer, 1952) was conducted by heat fixing a drop of the fissure water onto a microscope slide. This was followed by flooding the entire slide with crystal violet for one minute and rinsing with dH_2O. An iodine solution was then used to flood the slide for one minute and rinsed with dH_2O. The decolourizer, ethanol (95% v/v) was added drop wise onto the slide, until the violet colour was no longer present and the slide was rinsed with dH_2O. The counter stain, safranin red, was used by flooding the slide for one minute and rinsed with dH_2O to remove any excess dye. Slides were air dried and the stained cells were viewed with an Axioskop light microscope (Zeiss) under the 100x oil immersion magnification and images were captured using a DS-Fi1 (Nikon) camera with NIS Elements imaging software (V.3.22.00).

The Gram stain differentiates microorganisms based on the chemical and physical properties of their cell walls through the detection of peptidoglycan – the basic component of the bacterial cell wall (Bartholomew & Mittwer, 1952).

3.3.6.8.4 Scanning Electron Microscopy

Scanning electron microscopy (SEM) and energy dispersive X-ray (EDS) analyses were conducted on the biome that was concentrated using TFF, as well as on the biomass that was attached to the sandstone in the PVC cartridges. For the fissure water samples, 100 ml of the water was filtered by collecting the biomass on a 0.2 µM Isopore Polycarbonate membrane filter (Merck Millipore). For the sandstone samples, a small piece of the crushed rock with attached biofilm was used.

The samples were fixed in 0.1 M sodium phosphate-buffered glutaraldehyde (3%, pH 7.0) for at least 3 hours, followed by a 1 hour fixation in similarly buffered osmium tetroxide (1%). The samples were dehydrated in a graded ethanol series (50%, 70% and 95%) for

20 minutes in each phase. This was followed by two changes of 1 hour each, in 100% ethanol. The samples were dried using a critical point dryer (Tousimis), mounted onto 10 mm Cambridge aluminium stubs (Ted Pella Inc.) with epoxy glue and gold coated (60 nm) with a sputter coater (Bio-Rad). The specimens were examined with a JSM-7800F Extreme-resolution Analytical Field Emission SEM (FE-SEM) equipped with a 80 mm^2 X-Max energy dispersive X-ray analyses system (Oxford Instruments) and analysed using Aztec Software. SEM and EDS analyses were done at the Centre for Microscopy at the UFS (Bloemfontein, RSA).

3.3.7 Summary of all Samplings and Collaborators

Table 3.4: A summary of the sampling conducted at the Star Diamonds mine.

Sampling:	1	2	3	4	5	6	7	8	9	10	11	12	13	14	15	16	17	18
Day:	21	24	24	06	29	18	19	20	31	28	23	06	11	26	28	16	15	20
Month:	03	03	04	06	06	07	07	07	08	01	04	06	03	06	07	10	12	01
Year:	2012	2012	2012	2012	2012	2012	2012	2012	2012	2013	2013	2013	2014	2014	2014	2014	2014	2015
On-site Physicochemical Analyses:																		
pH	Y	Y	N	Y	Y	Y	Y	Y	Y	Y	Y	Y	Y	Y	N	N	N	N
Temperature	Y	Y	N	Y	Y	Y	Y	Y	Y	Y	Y	Y	Y	Y	N	N	N	N
Salinity	Y	Y	N	Y	Y	Y	Y	Y	Y	Y	Y	Y	Y	Y	N	N	N	N
EC	Y	Y	N	Y	Y	Y	Y	Y	Y	Y	Y	Y	Y	Y	N	N	N	N
ORP	Y	Y	N	Y	Y	Y	Y	Y	Y	Y	Y	Y	Y	Y	N	N	N	N
DO	Y	Y	N	Y	Y	Y	Y	Y	Y	Y	Y	Y	Y	Y	N	N	N	N
H_2S	Y	Y	N	Y	Y	Y	Y	Y	Y	Y	Y	Y	Y	Y	N	N	N	N
PO_4^{3-}	Y	Y	N	Y	Y	Y	Y	Y	Y	Y	Y	Y	Y	Y	N	N	N	N
Fe^{2+}	Y	Y	N	Y	Y	Y	Y	Y	Y	Y	Y	Y	Y	Y	N	N	N	N
Total Fe	Y	Y	N	Y	Y	Y	Y	Y	Y	Y	Y	Y	Y	Y	N	N	N	N
H_2O_2	Y	Y	N	Y	Y	Y	Y	Y	Y	Y	Y	Y	Y	Y	N	N	N	N
Water Flow Rate	Y	Y	N	Y	Y	Y	Y	Y	Y	Y	Y	Y	Y	Y	N	Y	Y	N
Gas Flow Rate	N	Y	N	Y	N	N	N	N	N	N	N	Y	N	N	N	N	N	N
Water Chemistry Analyses:																		
Anion/Cation	Y	N	N	N	N	N	N	N	N	N	Y	Y	Y	Y	N	N	N	N
Formate/Acetate	Y	N	N	N	N	N	N	N	N	N	N	N	N	N	N	N	N	N
Sulphur Species/Phosphorous	Y	N	N	N	N	N	N	N	N	N	N	N	N	N	N	N	N	N
NH_3/NH_4^+	Y	N	N	N	N	N	N	N	N	N	N	N	N	N	N	N	N	N
TN/DOC/DIC	Y	N	N	N	N	N	N	N	N	N	N	N	N	N	N	N	N	N
Water Isotope Analyses:																		
$\delta^{14}C_{DIC}$	Y	N	N	N	N	N	N	N	N	N	N	N	N	Y	N	N	N	N
$\delta^{18}O$ and $\delta D/\delta^2H$	Y	N	N	N	N	N	N	N	N	N	N	N	N	N	N	N	N	N
Gas Chemistry and Isotope Analyses:																		
Serum Vials with Gas/Water	N	Y	N	N	N	N	N	N	N	N	N	Y	N	N	N	N	N	N
Copper Tubes	N	Y	N	N	N	N	N	N	Y	N	N	Y	N	N	N	N	N	N
Diversity:																		
Cornelius® Canister	Y	N	N	Y	Y	Y	Y	Y	Y	Y	Y	Y	Y	Y	Y	N	N	N
Sterivex™ Filter	N	N	N	N	I&R	N	N	N	N	N	N	I&R	N	N	N	N	N	N
Tangential Flow Filtration	Y	N	Y	N	N	N	N	N	N	Y	Y	N	N	N	N	N	N	N
Massive Filter	I	R	N	N	N	N	N	N	N	N	N	N	N	I	R	N	N	N
PVC Cartridges	N	N	N	N	N	N	N	N	N	N	N	N	N	N	N	N	I	R

Legend: Y = Sample was taken, N = Sample was not taken, I = Filter was installed, R = Filter was retrieved.

Table 3.5: The collaborators and institutions responsible for the analyses of selected samples.

Water Chemistry Analyses:	
Anion	Institute for Ground Water Studies, University of the Free State, Bloemfontein, RSA
Cation	Institute for Ground Water Studies, University of the Free State, Bloemfontein, RSA
Formate/Acetate	Princeton University, Princeton, New Jersey, USA
Sulphur Species	Princeton University, Princeton, New Jersey, USA
Phosphorous	Princeton University, Princeton, New Jersey, USA
NH_3/NH_4^+	Princeton University, Princeton, New Jersey, USA
TN/DOC/DIC	Princeton University, Princeton, New Jersey, USA / University of Toronto, Ontario, Canada
Water Isotope Analyses:	
$\delta^{14}C_{DIC}$	Rafter Radiocarbon, National Isotope Centre, GNS Science, NZ
$\delta^{18}O$ and $\delta D/\delta^2H$	University of Toronto, Ontario, Canada
Gas Chemistry and Isotope Analyses:	
Serum Vials with Gas/Water	Princeton University, Princeton, New Jersey, USA / University of Toronto, Ontario, Canada
Copper Tubes	University of Bern, Bern, Switzerland

3.4 RESULTS AND DISCUSSIONS

3.4.1 Fissure Water and Gas Analyses

3.4.1.1 On-Site Physicochemical Analyses

On-site analyses were conducted during sampling as discussed in Section 3.3.4.1, to monitor the basic geochemistry of the fissure water. These analyses were done over a period of 27 months, at random samplings, and are shown in Table 3.6.

Table 3.6: The basic on-site analyses of the fissure water measured over time.

Sampling:	1	2	4	5	6	7	8	9
Day:	21	24	06	29	18	19	20	31
Month:	03	03	06	06	07	07	07	08
Year:	2012	2012	2012	2012	2012	2012	2012	2012
Analyses:								
pH	8.45	8.65	8.27	8.21	8.18	8.41	8.41	8.7
Temperature (°C)	31.2	31.3	31.1	30.7	31.0	30.9	30.9	30.4
Salinity ($g.L^{-1}$)	3	3	3	3	2	3	3	3
EC ($mS.cm^{-1}$)	3.84	3.84	4.30	3.82	3.86	3.96	4.01	4.60
ORP (mV)	-112	-131	-146	-226	-221	-210	-215	-168
DO ($mg.L^{-1}$)	0.2	0.1	0.05	0.8	0.4	0.1	0.1	0.05
H_2S ($mg.L^{-1}$)	0	0.1	0.1	0.15	0.1	0.2	0.2	0.4
Fe^{2+} ($mg.L^{-1}$)	0.1	0	<0.1	0	0	<0.1	0.1	<0.1
Total Fe ($mg.L^{-1}$)	<0.1	0	<0.1	0.4	0.1	<0.1	0.1	0.1
H_2O_2 ($mg.L^{-1}$)	0	0	0	0	0	0	0	0
Water Flow Rate ($L.min^{-1}$)	7.50	7.50	7.14	4.88	6.67	6.67	6.67	6.21
Gas Flow Rate ($ml.min^{-1}$)	-	207	167	-	-	-	-	-

Sampling:	10	11	12	13	14	16	17
Day:	28	23	06	11	26	16	15
Month:	01	04	06	03	06	10	12
Year:	2013	2013	2013	2014	2014	2014	2014
Analyses:							
pH	8.66	8.4	8.48	8.33	8.32	-	-
Temperature (°C)	28.3	30.5	30.3	30.3	30.5	-	-
Salinity ($g.L^{-1}$)	2.00	2.00	2.29	2.21	2.26	-	-
EC ($mS.cm^{-1}$)	4.63	4.17	4.63	4.63	4.51	-	-
ORP (mV)	-127	-94	-77	-104	-184	-	-
DO ($mg.L^{-1}$)	0.05	0.1	0.1	0.8	0.8	-	-
H_2S ($mg.L^{-1}$)	0.4	0.4	0.4	0.2	0.5	-	-
Fe^{2+} ($mg.L^{-1}$)	<0.1	<0.1	<0.1	<0.1	<0.1	-	-
Total Fe ($mg.L^{-1}$)	<0.1	<0.1	0.2	<0.1	<0.1	-	-
H_2O_2 ($mg.L^{-1}$)	0	0	0	0	0	-	-
Water Flow Rate ($L.min^{-1}$)	4.39	5.46	4.5	3.33	2.73	3.33	3.53
Gas Flow Rate ($ml.min^{-1}$)	-	-	-	-	-	-	-

Legend: EC = electrical conductivity, ORP = oxidation reduction potential, DO = dissolved oxygen, "-" = Not measured.

Throughout the time during which the borehole was monitored, the fissure water maintained a consistent moderate temperature and an alkaline pH, with an average of 30.6°C and 8.4, respectively. This is fairly similar for results obtained by Lin *et al*., (2006a)

and Magnabosco *et al*., (2014), for the shallower fracture water samples. Although differences were observed in the ORP over time, the fissure water had a sustained reducing environment, with an average of -155 mV, even though the presence of dissolved oxygen (0.3 $mg.L^{-1}$) was observed. The detection of H_2S (0.24 $mg.L^{-1}$) was expected, due to the reducing environment. The EC was measured to estimate the total dissolved solids (TDS) in the fissure water, indicating a calculated average of 2.7 $g.L^{-1}$, with moderate salinity of 2.6 $g.L^{-1}$. Very low concentrations of Fe^{2+} (0.08 $mg.L^{-1}$) and total Fe (0.12 $mg.L^{-1}$) were observed and no H_2O_2 was detected, indicating that radiolysis of water could not be observed. The borehole had an average water flow rate of 5.6 $L.min^{-1}$ and gas flow rate of 187 $ml.min^{-1}$.

3.4.1.2 Geochemical Analyses

Geochemical analyses of the fissure water were conducted as discussed in Section 3.3.4.2, to also provide insight into the possible electron donor and acceptor conditions for biological cycling, and are shown in Table 3.7 and Figure 3.17. Determinands with values always below the detection limits are not shown.

Table 3.7: Geochemical analyses of the fissure water.

Sampling:	1	11	12	13	14
Day:	21	23	06	11	26
Month:	03	04	06	03	06
Year:	2012	2013	2013	2014	2014
Analyses:					
pH	8.46	8.16	7.71	7.35	7.87
EC ($mS.m^{-1}$)	430	432	424	431	434
DOC ($mg.L^{-1}$)	0.25	-	-	0.69	0.64
DIC ($mg.L^{-1}$)	5.3	-	-	-	-
TN ($mg.L^{-1}$)	0.415	-	-	-	-
TOC ($mg.L^{-1}$)	-	1.00	1.07	0.97	1.53
TDS ($mg.L^{-1}$)	2062	2301	2497	2223	2440
Lactate ($mg.L^{-1}$)	0.025	-	-	-	-
HS^- ($mg.L^{-1}$)	2.87	-	-	-	-
NO_3^- ($mg.L^{-1}$)	0.049	-	-	-	-
NH_4^+ ($mg.L^{-1}$	0.27	-	-	-	-
P-Alkalinity ($mg.L^{-1}$)	0	0	0	0	0
M-Alkalinity ($mg.L^{-1}$	25	24.1	24.3	22	26.2
Calcium Hardness ($mg.L^{-1}$)	-	141.8	157.6	10	-
Magnesium Hardness ($mg.L^{-1}$)	-	7.1	7.1	783	-
Total Hardness ($mg.L^{-1}$)	-	148.9	164.7	793	-
Aluminium as Al ($mg.L^{-1}$)	0.18	0.014	0.022	0.037	0.024
Ammonia as N ($mg.L^{-1}$)	-	-	0.562	0.84	0.617
Barium as Ba ($mg.L^{-1}$)	0.035	-	-	-	0.718
Boron as B ($mg.L^{-1}$)	-	-	-	2.87	-
Bromide as Br ($mg.L^{-1}$)	5.06	6.8	6.54	6.47	9.11
Cadmium as Cd ($mg.L^{-1}$)	-	-	-	-	<0.001
Calcium as Ca ($mg.L^{-1}$)	43	56.7	63.05	3.9	64.7
Chloride as Cl ($mg.L^{-1}$)	963	1326	1467	1405	1497
Cobalt as Co ($mg.L^{-1}$)	0.0013	-	-	-	-

Copper as Cu (mg.L^{-1})	<d.l.	-	0.005	0.019	0.002
Fluoride as F (mg.L^{-1})	4.89	4.16	4.09	5.14	4.91
Iron as Fe (mg.L^{-1})	-	0.031	0.047	0.013	0.017
Lead as Pb (mg.L^{-1})	-	-	<0.010	<0.010	<0.010
Magnesium as Mg (mg.L^{-1})	15.9	1.72	1.74	190.9	3.4
Manganese as Mn (mg.L^{-1})	0.720	0.030	0.023	0.032	0.022
Potassium as K (mg.L^{-1})	2.7	8.13	9.37	25.3	9.6
Sodium as Na (mg.L^{-1})	954	871	920	585.9	827
Strontium as Sr (mg.L^{-1})	0.32	-	-	-	-
Sulphate as SO_4 (mg.L^{-1})	0.94	2.3	<10	<5	5.53
Sulphur as S (mg.L^{-1})	64	-	-	-	-
Zinc as Zn (mg.L^{-1})	0.018	-	0.025	0.031	0.017

Legend: EC = electrical conductivity, DOC = dissolved organic carbon, DIC = dissolved inorganic carbon, TN = total nitrogen, TOC = total organic carbon, TDS = total dissolved solids, P-Alkalinity = phenolphthalein alkalinity, M-Alkalinity = total alkalinity, "-" = Not measured.

Results remained relatively constant over time and were fairly similar to data obtained from the shallower samples as discussed in Lin *et al*., (2006a). The fissure water had a high mineral content, was moderately saline and contained low sulphate, ammonium, and nitrate concentrations, having average values of 1332 mg.L^{-1} chloride, ~2.92 mg.L^{-1} sulphate, 0.27 mg.L^{-1} ammonium, and ~0.049 mg.L^{-1} nitrate. The DIC (5.3 mg.L^{-1}) was significantly higher than the DOC (0.25 mg.L^{-1}). The high DIC concentrations suggest high bicarbonate and CO_2 levels in the fissure water, whereas the low DOC concentrations suggest low organic matter content. Very low concentrations of the trace elements were present in the fissure water. When the parameters were compared with a Durov diagram, created with The Geochemist's Workbench® (V.10 Professional) software (Figure 3.17), it can be seen that the fissure water stayed geochemically very similar over time, indicating that influx from other water sources due to mixing was negligible for this period.

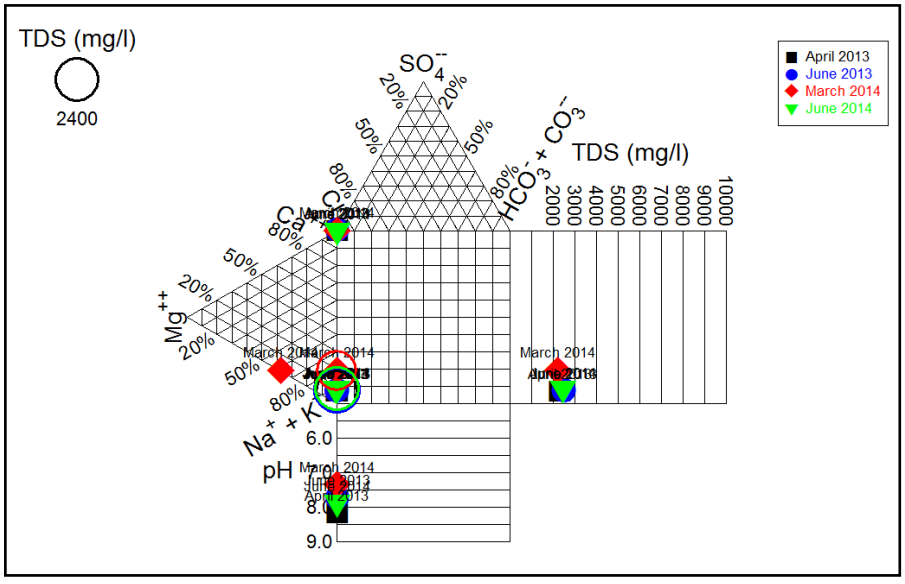

Figure 3.17: A Durov diagram for the geochemical analyses of the fissure water.

3.4.1.3 Gas Chemistry and Isotope Analyses

Analyses of the dissolved gas compositions in the fissure water were conducted as discussed in Section 3.3.4.3. Results obtained showed high concentrations of CH_4 (82.7%), with trace amounts of O_2 (0.01%), H_2 (0.0004%), CO (0.0035%), CO_2 (0.01%), and He (0.82%). The amount of N_2 obtained was 15.79% and 1.44% for Ar. As for the C_2H_6, C_3H_8, iso- & n-C_4H_{10}, and iso- & n-C_5H_{12} samples, the amounts obtained were all <0.01%. Onstott *et al*., (2006) indicated that the H_2 is sustaining the subsurface microbial communities such as the H_2-utilizing sulphate-reducing bacteria (SRB) and methanogens, and is produced by water radiolysis at a rate of ~1 XRS Myr^{-1}. Therefore the importance of the detection of H_2 in the fissure water is that it appears to be the most important energy source available to deep subsurface communities (Lin *et al*., 2005; Nealson *et al*., 2005).

Isotope analyses of the gas and the fissure water were tested as discussed in Section 3.3.4.3 and results were added to the graphs from Ward *et al*., (2004) (Figure 3.18). The δ^2H_{CH4} and $\delta^{13}C_{CH4}$ analyses yielded values of -190‰ and -51.3‰, respectively (Figure 3.18A). The $\delta^{14}C_{DIC}$ yielded a value of -952‰ (~0.8), resulting in the fissure water having a calculated conventional radiocarbon age of 24 320 (~131) years, before present (BP) and the $\delta^{18}O$ and $\delta D/\delta^2H$ analyses yielded values of -6.27‰ and -38.64‰, respectively, falling on the global meteoric water line (GMWL) (Figure 3.18B), as described in Craig, (1961). According to Onstott *et al*., (2006), paleo-meteoric water ranges in age from ~10 Ka to >1.5 Ma, is of low salinity, falls along the GMWL and is rich in CO_2 and atmospheric noble gas, therefore, the fissure water from the Star Diamonds mine represents a subsurface residence time consistent with the isotopic signatures that indicate fissure water of paleo-meteoric origin. These results are consistent with mixing between thermogenic and microbial gases, with positional and isotopic characteristics that are consistent with production by methanogens utilizing the CO_2 reduction pathway (Sherwood Lollar *et al*., 2008), and indicates methane with a biogenic origin. All these isotopic analyses corresponded with results obtained by Ward *et al*., (2004); Onstott *et al*., (2006); Sherwood Lollar *et al*., (2008); Lau *et al*., (2014); and Magnabosco *et al*., (2014), for the samples collected at approximately the same depth as the borehole used in this research (Section 3.3.3).

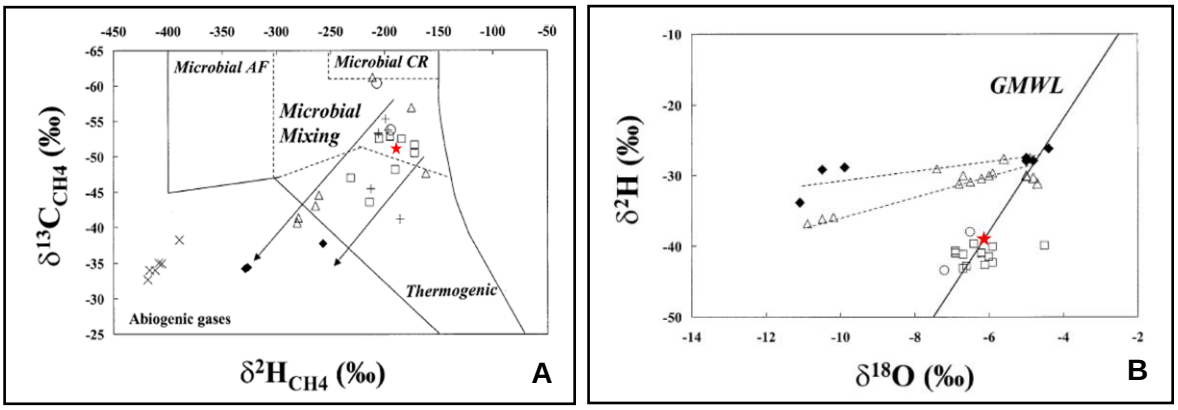

Figure 3.18: (A) $\delta^{13}C_{CH4}$ and $\delta^{2}H_{CH4}$ values for all samples compared to empirically determined fields for thermogenic gas and microbial gas produced by CO_2 reduction (CR) and acetate fermentation (AF) as described in Whiticar, (1999) and (B) $\delta^{2}H_{H2O}$ and $\delta^{18}O_{H2O}$ for fissure water samples. The global meteoric waterline (GMWL) is from Craig, (1961). In both graphs, samples from the Karoo formation (Middelbult mine) are indicated by (+). All samples from the Witwatersrand Supergroup are open symbols, and all samples from the Ventersdorp Supergroup are solid symbols. Symbols from individual mines are as follows: Merriespruit and Masimong (circles), Beatrix (squares), Evander (triangles), Kloof (diamonds). Kidd Creek data (X) are for abiogenic methane (Sherwood Lollar *et al*., 2002). (Obtained from Ward *et al*., 2004). Samples from the Star Diamonds mine are indicated by a red star.

3.4.2 Sandstone X-Ray Fluorescence Analyses

Major-element XRF analyses were conducted as discussed in Section 3.3.5.2 on the sandstone from the Star Diamonds mine, before and after sterilization thereof. Results of the analyses are shown in in Table 3.8.

Table 3.8: Major-element XRF analyses of the sandstone, before and after sterilization.

	Sandstone	Sandstone Autoclaved	Sandstone Acid Washed	Sandstone Autoclaved & Acid Washed
Analyses:				
Al_2O_3 (%)	20.81	20.131	20.123	20.142
Fe_2O_3 (%)	1.065	1.247	1.198	1.28
CaO (%)	0.064	0.051	0.031	0.035
MgO (%)	0.17	0.197	0.202	0.261
MnO (%)	0.012	0.06	0.055	0.061
Na_2O (%)	0	0	0	0
K_2O (%)	2.64	2.518	2.5	2.512
P_2O_5 (%)	0.039	0.045	0.045	0.043
TiO_2 (%)	1.103	1.131	1.119	1.125
SiO_2 (%)	74.01	74.304	74.363	74.316
LOI (%)	0.087	0.316	0.364	0.225
Total (%)	100	100	100	100

All sandstone consists of the same general minerals that form the basis of the sandstones. These minerals are generally quartz and feldspars and consist mainly of silicon (Jackson, 1997; Boggs, 2000). From the XRF results obtained, it can be seen that the major components of the sandstone are silicon (74%) and aluminium (20%). The rest of the components are in the minority.

Thus, the sterilization through autoclaving and acid washing did not appear to influence the percentages of the minerals that were tested for during the experiments.

3.4.3 Characterization and Diversity of the Deep Subsurface Microbial Biome

3.4.3.1 Microbial Diversity Assessments using Denaturing Gradient Gel Electrophoresis

Although microbial diversity assessments were carried out on all the canisters, the Sterivex™ filters and the TFF concentrated fissure water that were sampled over time (Table 3.4), only one agarose gel of each domain of life for the PCR, the nested DGGE PCR, and the DGGE are shown in the results as a representative of all the samples.

3.4.3.1.1 Genomic DNA Isolation and Polymerase Chain Reaction

Genomic DNA was isolated from all the filters of the Cornelius® canisters, the Sterivex™ filters, as well as the TFF concentrated fissure water as discussed in Section 3.3.6.6.1. Amplification of the Archaeal 16S (~600 bp) (Figure 3.19B), the Bacterial 16S (~1500 bp) (Figure 3.19C), and the Eukaryal 18S (~1700 bp) (Figure 3.19D) rRNA gene fragments were done as discussed in Section 3.3.6.6.2.

Amplicons, of expected size for each primer set, were obtained for the rRNA gene fragments from all the samples. The bands of interest were excised from the agarose gel and purified (Section 3.3.6.6.2).

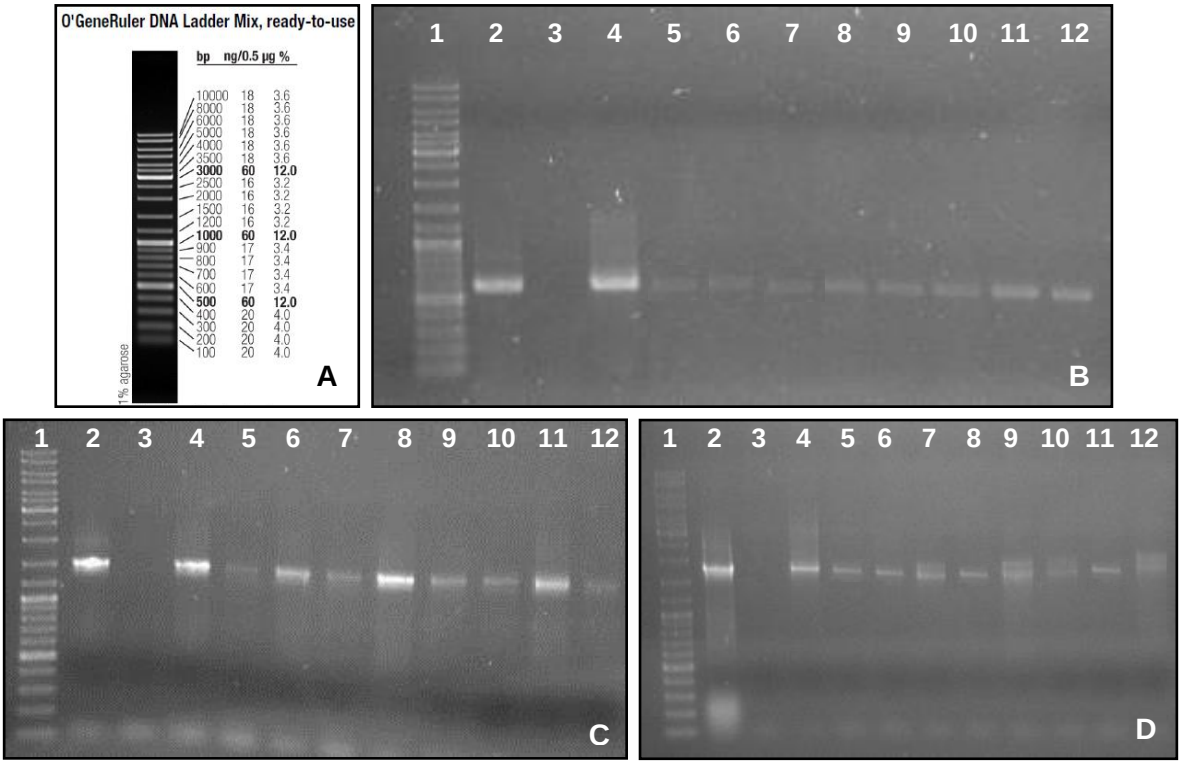

Figure 3.19: (A) The O'GeneRuler™ DNA Ladder Mix (Thermo Scientific), used to determine the size of the amplicons, with the amplified rRNA gene fragments for (B) Archaea, (C) Bacteria, and (D) Eukarya. In lane 1, the O'GeneRuler™ DNA Ladder Mix is shown. Lanes 2 and 3 contain the positive and negative controls, respectively. The samples are shown in lanes 4 – 12.

3.4.3.1.2 Nested Polymerase Chain Reaction

The purified PCR products were used to amplify the V3/V4 hypervariable regions for Archaea (~600 bp) (Figure 3.20B), Bacteria (~600 bp) (Figure 3.20C), and Eukarya (~600 bp) (Figure 3.20D) using a nested DGGE PCR as discussed in Section 3.3.6.6.3. Amplicons were obtained for the V3/V4 hypervariable regions from all the samples.

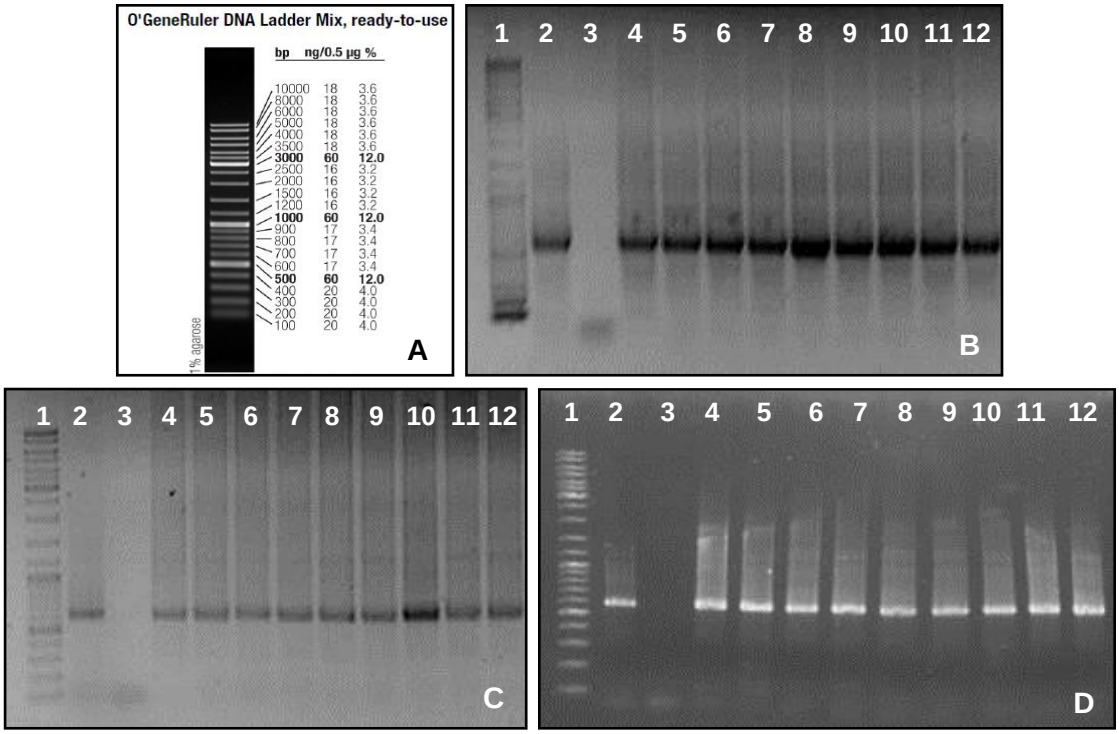

Figure 3.20: (A) The O'GeneRuler™ DNA Ladder Mix (Thermo Scientific), used to determine the size of the amplicons, with the amplified V3/V4 hypervariable regions for (B) Archaea, (C) Bacteria, and (D) Eukarya. In lane 1, the O'GeneRuler™ DNA Ladder Mix is shown. Lanes 2 and 3 contain the positive and negative controls, respectively. The samples are shown in lanes 4 – 12.

3.4.3.1.3 Denaturing Gradient Gel Electrophoresis, Sanger Sequencing and Analyses

The DGGE PCR products were used to construct a preliminary diversity profile for Archaea (Figure 3.21A), Bacteria (Figure 3.21B), and Eukarya (Figure 3.21C), through the use of DGGE (Section 3.3.6.6.4).

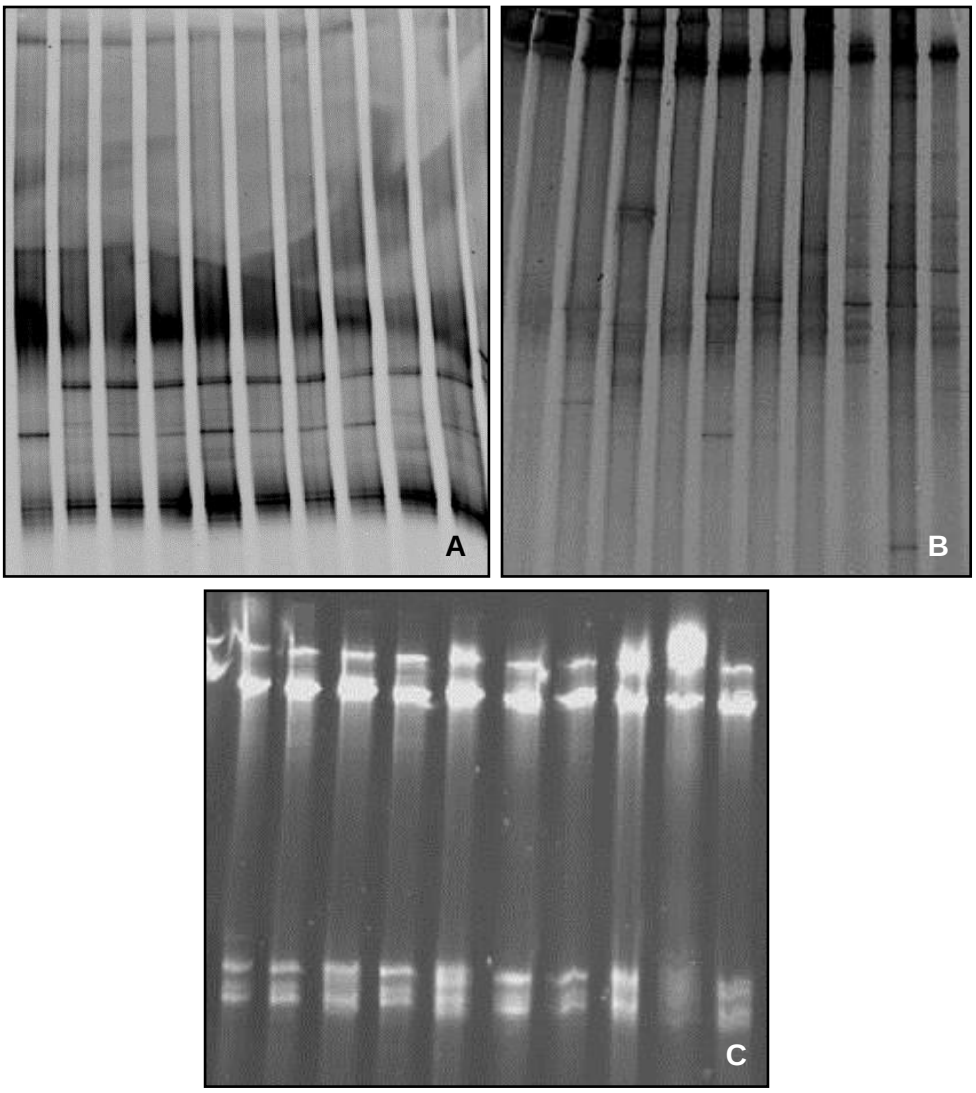

Figure 3.21: DGGE diversity profiles for (A) Archaea, (B) Bacteria, and (C) Eukarya.

From the DGGE assessments, it can be seen that all three domains of life (Archaea, Bacteria, and Eukarya) were present in the subsurface biome. This corresponded with results obtained by numerous researchers for various subsurface samplings at different locations, with some of them as described in Phelps *et al*., (1994); Takai *et al*., (2001); Moser *et al*., (2003); Kieft *et al*., (2005); Gihring *et al*., (2006); Lin *et al*., (2006a); Lin *et al*., (2006b); Onstott *et al*., (2009); Borgonie *et al*., (2011); Ragon *et al*., (2013); Lau *et al*., (2014); Magnabosco *et al*., (2014); and Mu *et al*., (2014).

The DGGE results indicate that the Archaea and Eukarya profiles were consistent between the various sampling events, but differences were obtained within the Bacterial profiles. However, there are some drawbacks in using the DGGE technique, with one of

them being that only small fragments are separated through electrophoresis and may therefore limit the information obtained through sequencing and as a result, minor populations can be below the detection limit (Duarte *et al*., 2012). Another drawback is that different DNA sequences may have similar mobilities due to their identical GC content. Therefore, one band on a gel can represent more than one species. Also possible intra-specific or intra-isolate heterogeneity of the rRNA genes, as well as multiple copy numbers of the 16S rRNA operons of microorganisms can result in one species representing more than one band on a gel, giving an underestimation of the microbial diversity (Nakatsu *et al*., 2000; Muyzer *et al*., 2004; Michaelsen *et al*., 2006; Duarte *et al*., 2012). As a result, final conclusions about diversity cannot be made by just evaluating a DGGE gel alone, since results obtained can be misleading, but this technique can be used as a quick indication to show if there are any possible variations in the microbial community present in the sample, if it is kept in mind that there are shortcomings. Therefore, sequencing and analyses were done on selected DGGE bands as discussed in Sections 3.3.6.6.5 and 3.3.6.6.6.

The analysed sequences indicated that the Bacteria were dominated by the Proteobacteria phylum, mainly consisting of the Alpha-, Beta-, and Gammaproteobacteria classes. This was followed by the Firmicutes phylum, consisting of the Bacilli and Clostridia classes and the Actinobacteria class of the Bacteriodetes phylum. For the Eukarya, the main phyla present were the Ascomycota, the Annelida, and the Basidiomycota. The Archaea were dominated by the Euryarchaeota phylum, which included the Methanococci, the Thermococci, the Methanobacteria, and the Methanomicrobia classes, followed by the Crenarchaeota containing the Thermoprotei class. These results corresponded with subsurface diversity results obtained by numerous researchers (Banfield *et al*., 1999; Takai *et al*., 2001; Kotelnikova, 2002; Baker *et al*., 2003; Moser *et al*., 2003; Newberry *et al*., 2004; Onstott, 2005; Webster *et al*., 2006; Fry *et al*., 2008; Basso *et al*., 2009; Morozova *et al*., 2010; Ragon *et al*., 2013; Lau *et al*., 2014; Magnabosco *et al*., 2014).

3.4.3.2 Microbial Diversity Assessments using Targeted 16S and 18S rRNA Gene Sequencing

The microbial diversity results discussed in this Section, are only a representation of the diversity that has been found using the different next generation sequencing techniques

and even though the rarefaction curve, indicating the annotated species richness (Figure 3.22E), did not reach a plateau, the reduced slope of the curve towards the end suggested that the sequences are representative of the microbial community. These results confirmed what has been shown with the DGGE analyses that microorganisms from all three domains of life (Archaea, Bacteria, and Eukarya) were found to be present within the biome of the fissure water (Figure 3.22). The biome was dominated by the Bacteria (>90%), but also contained a small fraction of Eukarya and Archaea. Various studies on subsurface biomes have concluded that the subsurface is generally dominated by the Bacteria and the microbial activities that dominate these extreme environments are fermentation, methanogenesis, and sulphate-reduction (Banfield *et al*., 1999; Takai *et al*., 2001; Kotelnikova, 2002; Baker *et al*., 2003; Newberry *et al*., 2004; Onstott, 2005; Webster *et al*., 2006; Fry *et al*., 2008; Basso *et al*., 2009; Morozova *et al*., 2010; Ragon *et al*., 2013).

Extending the DGGE results, the Bacterial domain (Figure 3.23), was found to be dominated by the Proteobacteria phylum, followed by the Firmicutes and the Bacteroidetes. The Proteobacteria mainly consisted of Beta- and Gammaproteobacteria classes, followed by smaller fractions of the Delta- and Alphaproteobacteria. The majority of the Firmicutes were from the Bacilli and Clostridia classes. This is similar to what has been found by Moser *et al*., 2003; Lau *et al*., 2014; and Magnabosco *et al*., 2014; that the Proteobacteria is the most abundant phylum in the subsurface. For the Eukaryal domain (Figure 3.24), the main phyla present were Arthropoda, Streptophyta, Nematoda, Apicomplexa, and Chlorophyta. The majority of the Arthropoda consisted of the Insecta class and most of the Nematoda were of the Chromadorea class. The Archaeal domain (Figure 3.25) was dominated by the Euryarchaeota phylum, which include the methanogens and halobacteria, followed by the Thermoprotei which is a class of the Crenarchaeota.

Other than the methanogens which can fix CO_2, several sulphate-reducing bacteria were found amongst the Deltaproteobacteria such as the Desulfobacterales, Desulfovibrionales, and Syntrophobacterales orders (Muyzer & Stams, 2008). Amongst the microorganisms known to fix nitrogen, the Cyanobacteria and Chlorobi phyla, as well as the Pseudomonadales, Rhizobiales, and Actinomycetales orders were found to be present. This confirmed that microorganisms with various metabolisms were present in the subsurface biome (Figure 3.22).

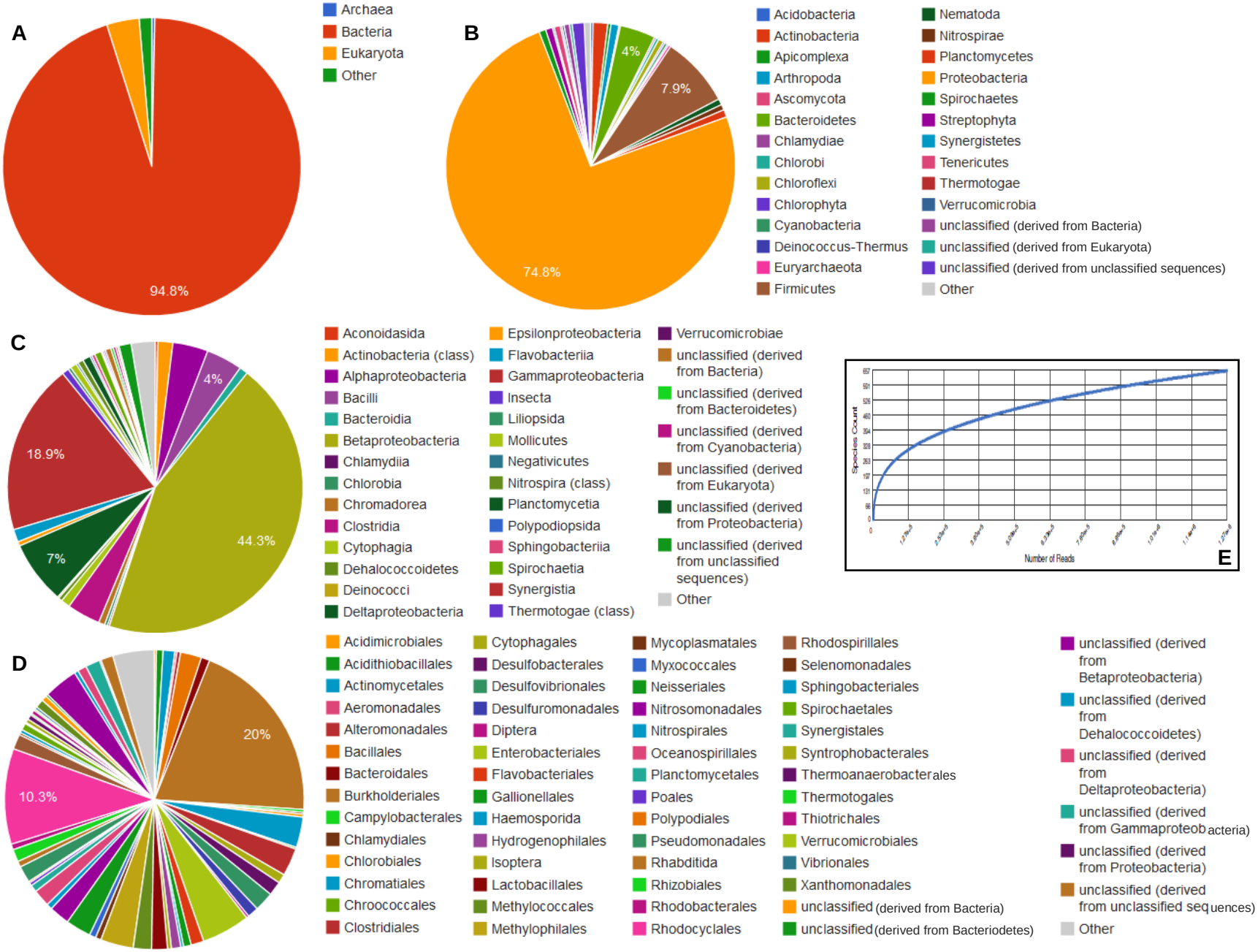

Figure 3.22: MG-RAST taxonomic hit distribution of the diversity in the subsurface biome for (A) domain, (B) phylum, (C) class, and (D) order, with (E) a rarefaction curve indicating the annotated species richness.

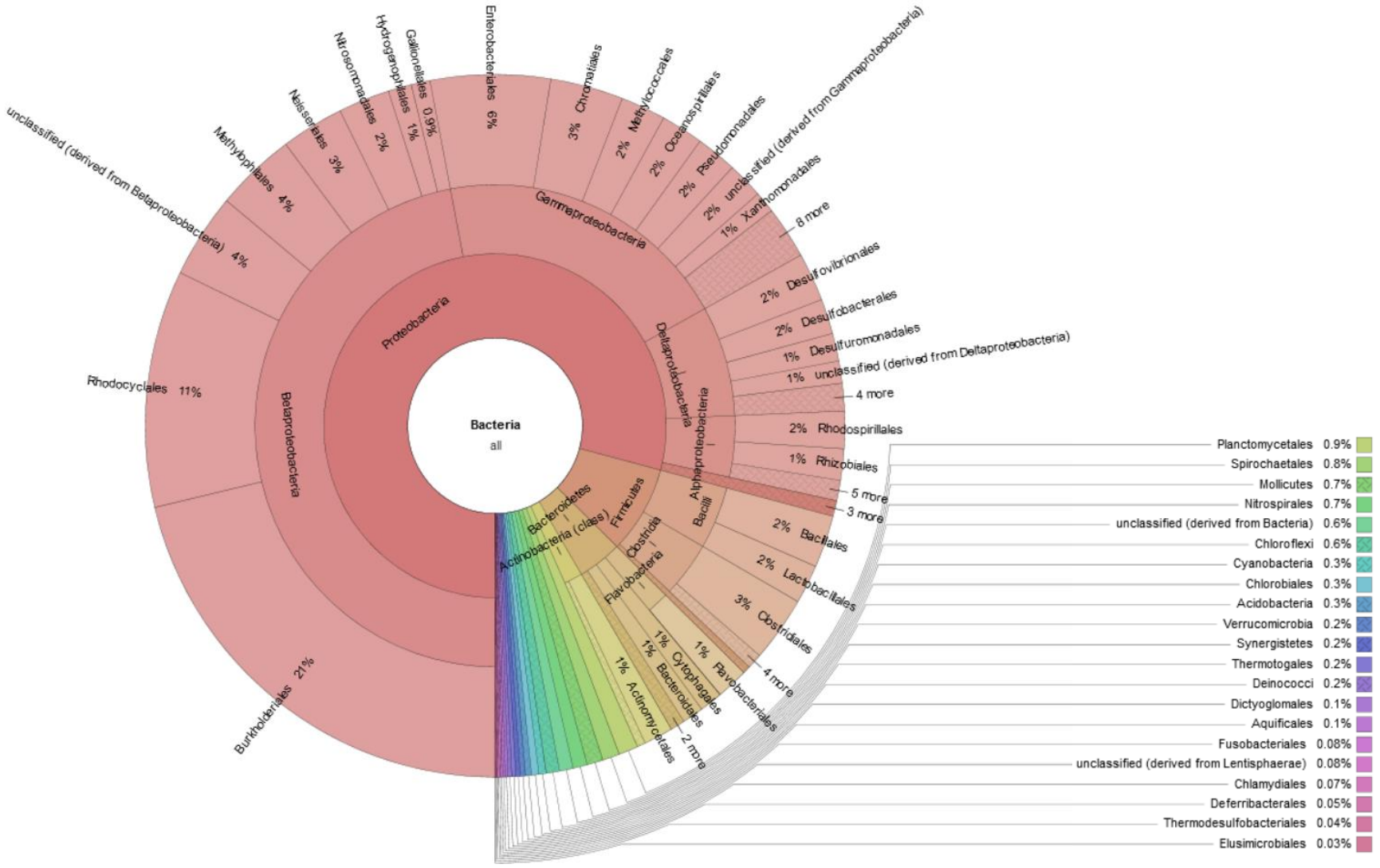

Figure 3.23: MG-RAST Krona diagram for the Bacteria at order level.

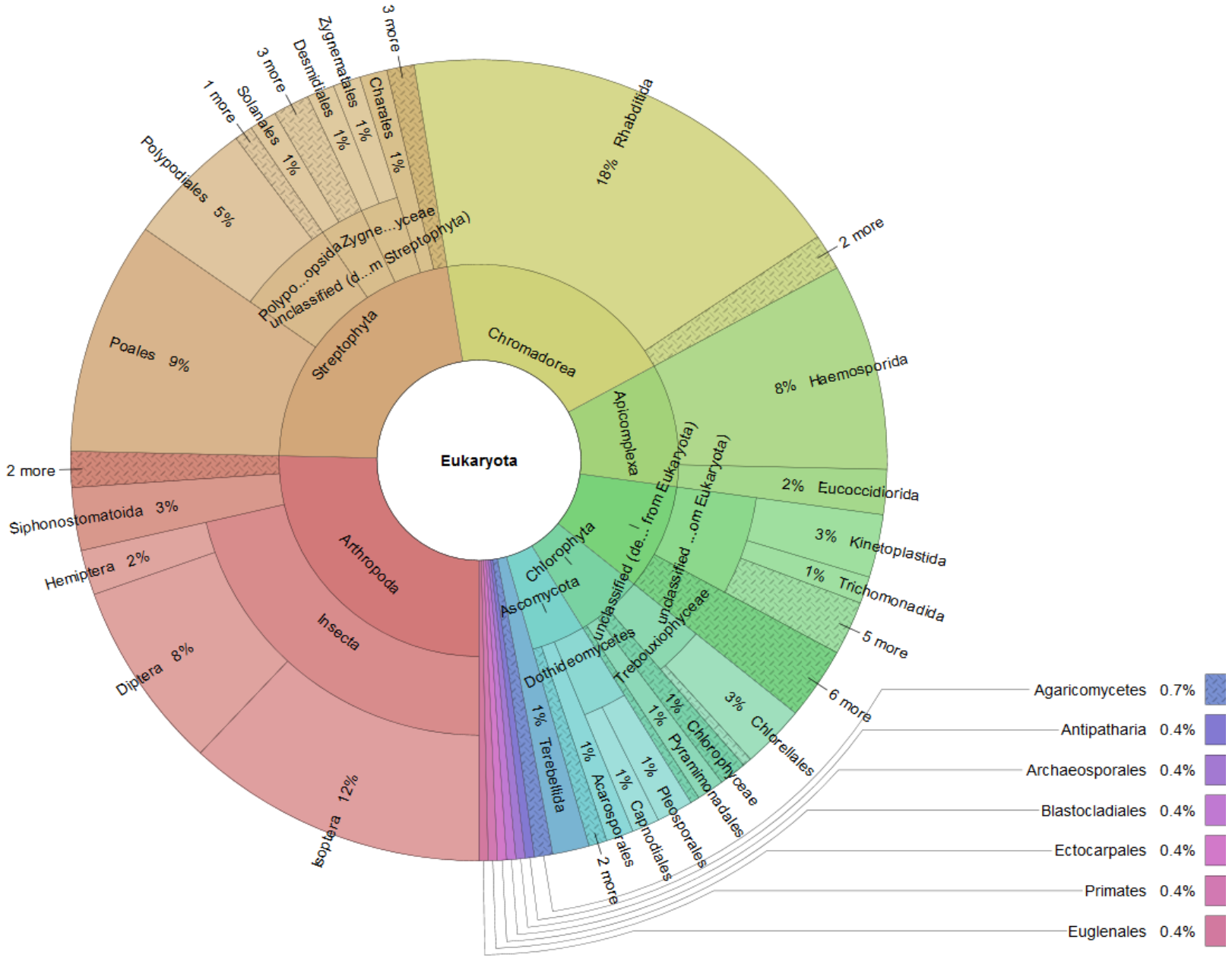

Figure 3.24: MG-RAST Krona diagram for the Eukarya at order level.

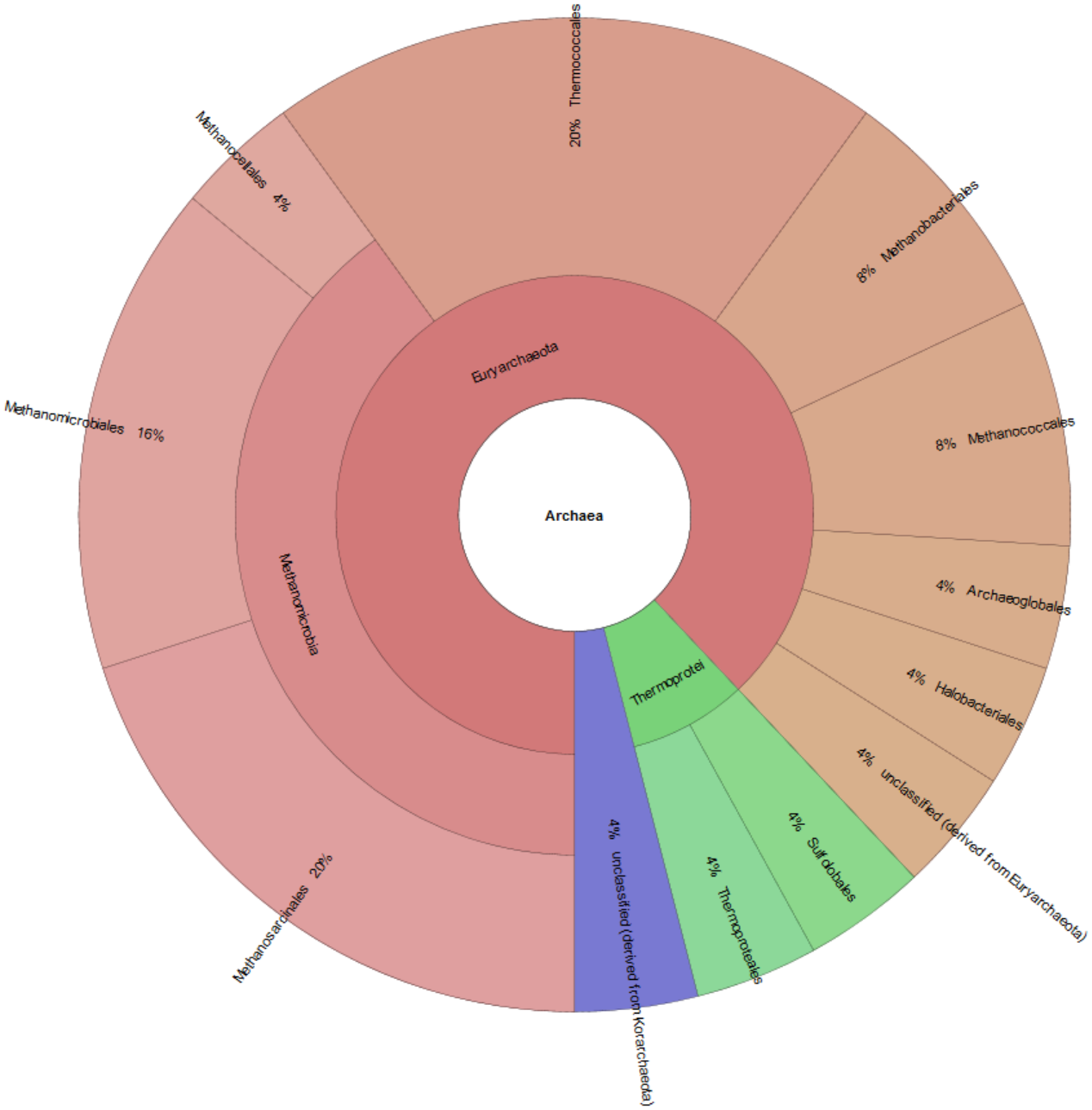

Figure 3.25: MG-RAST Krona diagram for the Archaea at order level.

3.4.3.3 Microbial Diversity Assessments of the Fissure Water using Visual Methods

Microscopy images shown throughout this document are a representation of some of the diversity that has been found. Images were only used to indicate the various morphologies present, whether the microorganisms were alive or dead and what their Gram-staining properties are. These images should not be used as a quantification method for the amount of biomass obtained or to determine the ration of live and dead cells. The camera used to capture the images had a defect on its lens which is reflected on all the images. The defect can be seen in the bottom left corner of each image and should not be seen as a biological structure.

3.4.3.3.1 Staining

The negative stain images (Figure 3.26) and the live/dead stain images (Figure 3.27) indicated that several diverse microorganisms with varying morphology and distinctive structures were present in the subsurface biome. It can also be seen that several macrostructures, as well as biofilm-like structures through the accumulation of cells were found and even though these structures were not identified, they are indicative of the complex nature of the biofilms found in the subsurface (Borgonie *et al*., 2011; Blanco *et al*., 2014).

Biofilms are described as complex aggregations of microorganisms, strongly attached to a surface and encased within a self-produced extracellular matrix of polymeric substances (EPS). Biofilms are thought to be the major form of microbial life in natural environments, due to the biofilm offering structural support and protection from physical, chemical and biological stresses. Biofilms can also provide the optimal location relative to substrates required for metabolic function, as well as symbiotic benefits in multi-species communities (Watnick & Kolter, 2000; Costerton & Stewart, 2001; Stoodley *et al*., 2002; Mitchell *et al*., 2009; Lewandowski & Beyenal, 2013). Biofilms are characterized by structural heterogeneity, genetic diversity, and complex community interactions (Mitchell *et al*., 2009), and were likely formed by the microorganisms in the

subsurface to protect themselves from stresses created by the extreme conditions which the biomes encounter in the subsurface.

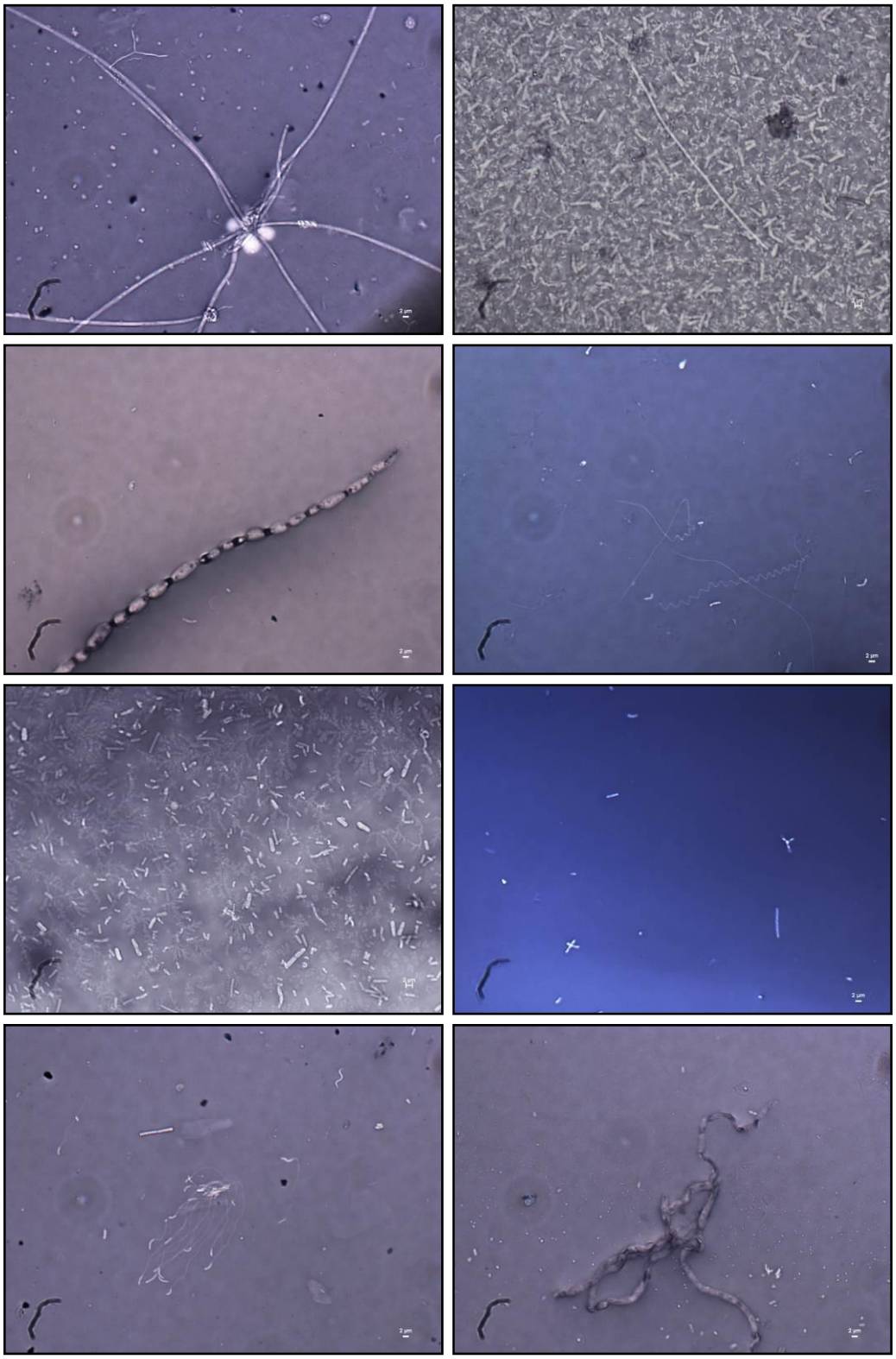

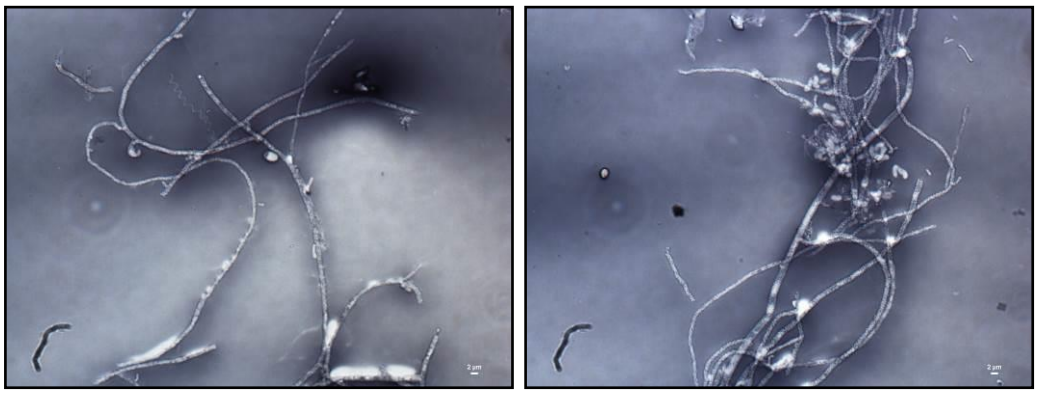

Figure 3.26: Negative stain images of the fissure water from the Star Diamonds mine. All scale bars are equal to 2 µm.

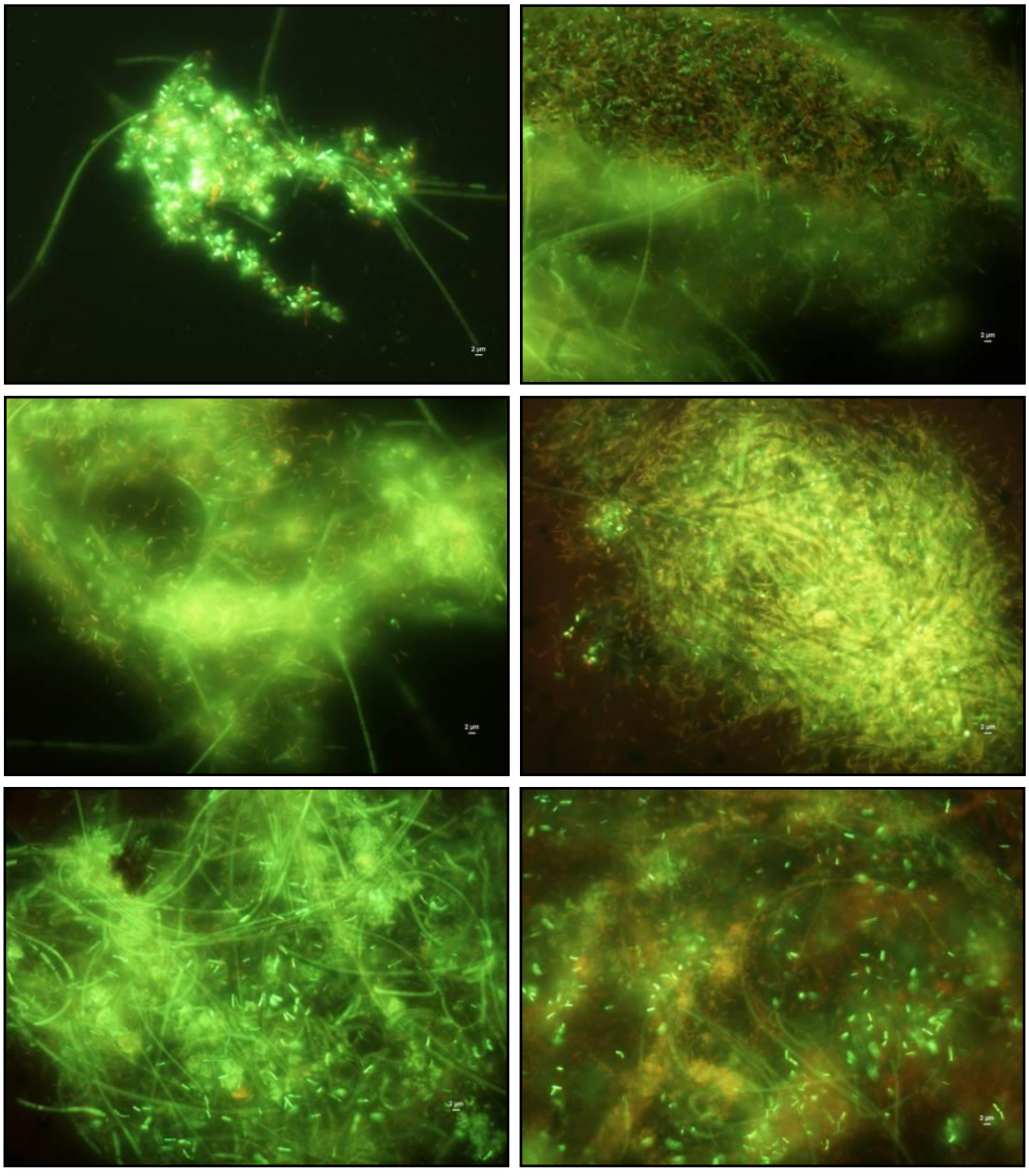

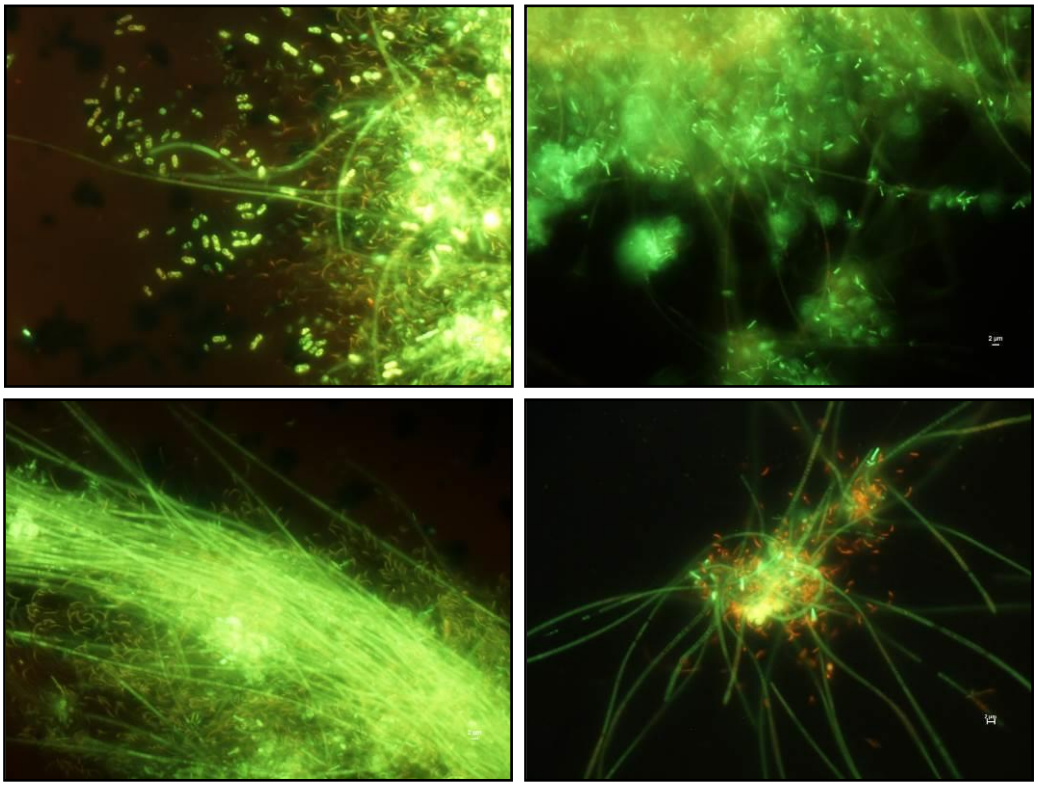

Figure 3.27: Live/dead stain images of the fissure water from the Star Diamonds mine. All scale bars are equal to 2 µm.

Subsurface biomes in general are dominated by the Gram-negative Proteobacteria and the Firmicutes, which are mainly Gram-positive (Moser *et al*., 2003; Lin *et al*., 2006a; Lau *et al*., 2014; Magnabosco *et al*., 2014). This was confirmed for the subsurface biome from the Star Diamonds mine through the diversity results (Section 3.4.3.2), therefore, it was expected that microorganisms from both the Gram-positive and the Gram-negative groups should be present in the subsurface biome. This was confirmed by the Gram stain images (Figure 3.28).

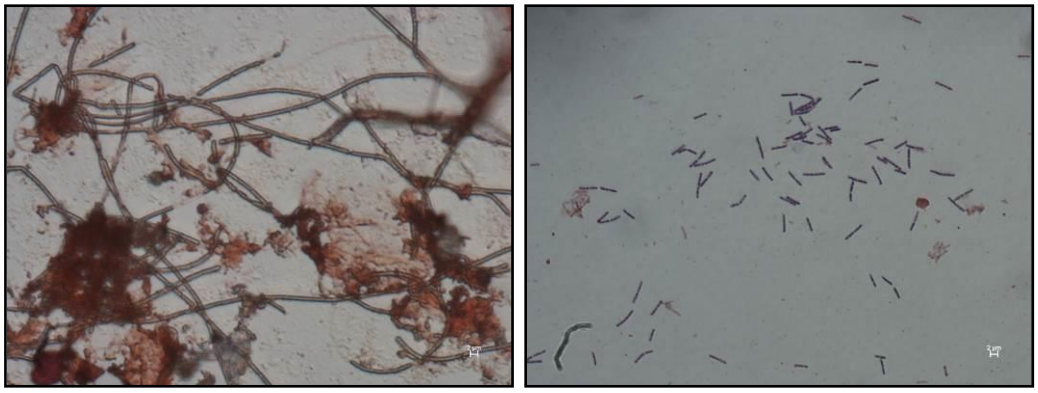

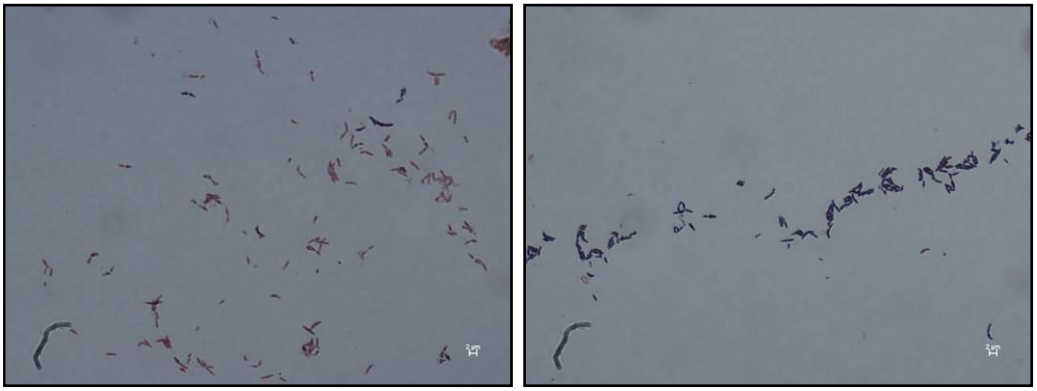

Figure 3.28: Gram stain images of the fissure water from the Star Diamonds mine. All scale bars are equal to 2 µm.

3.4.3.3.2 Scanning Electron Microscopy

Scanning electron microscopy (Figure 3.29) was conducted as discussed in Section 3.3.6.8.4. Images were falsely coloured using Adobe® Photoshop (V.CS5). EDS analyses confirmed that the biofilm consisted of biological material.

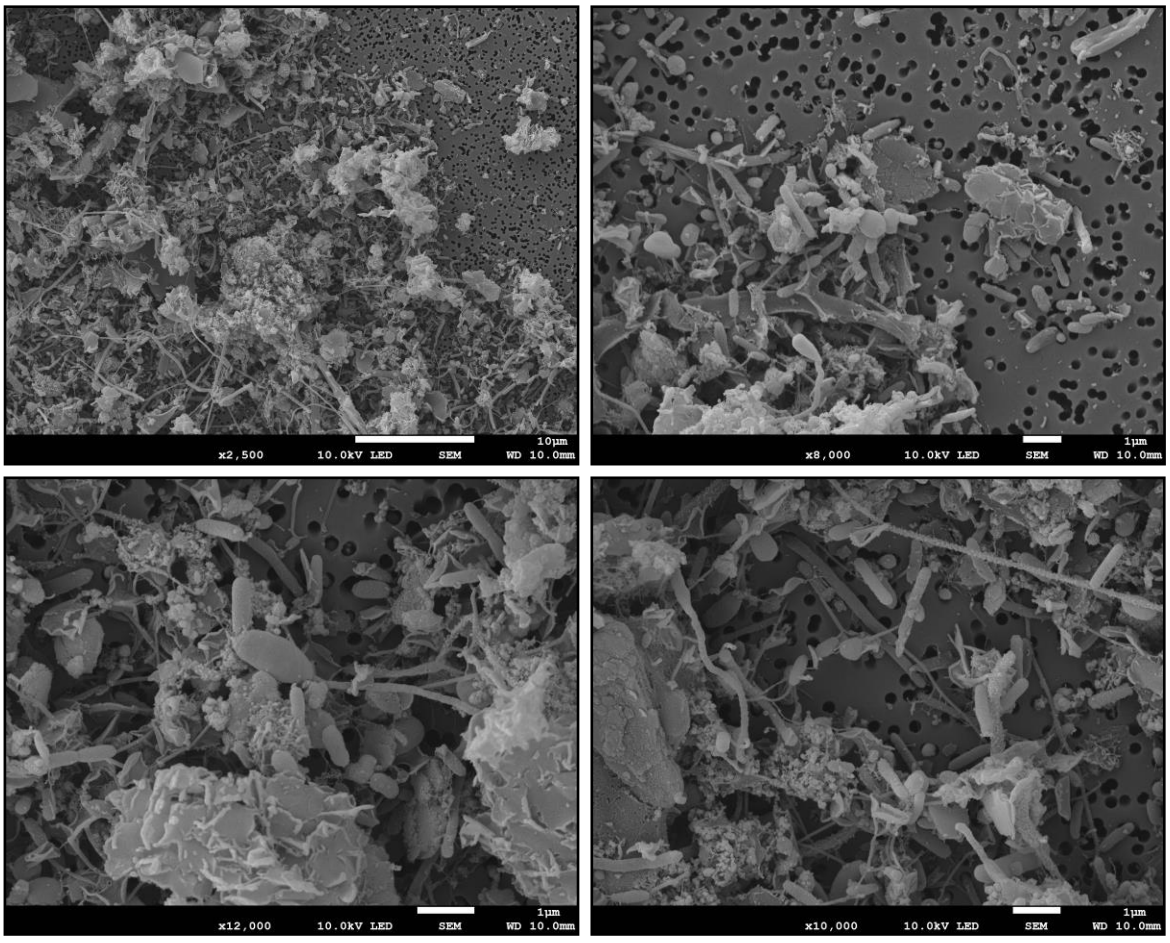

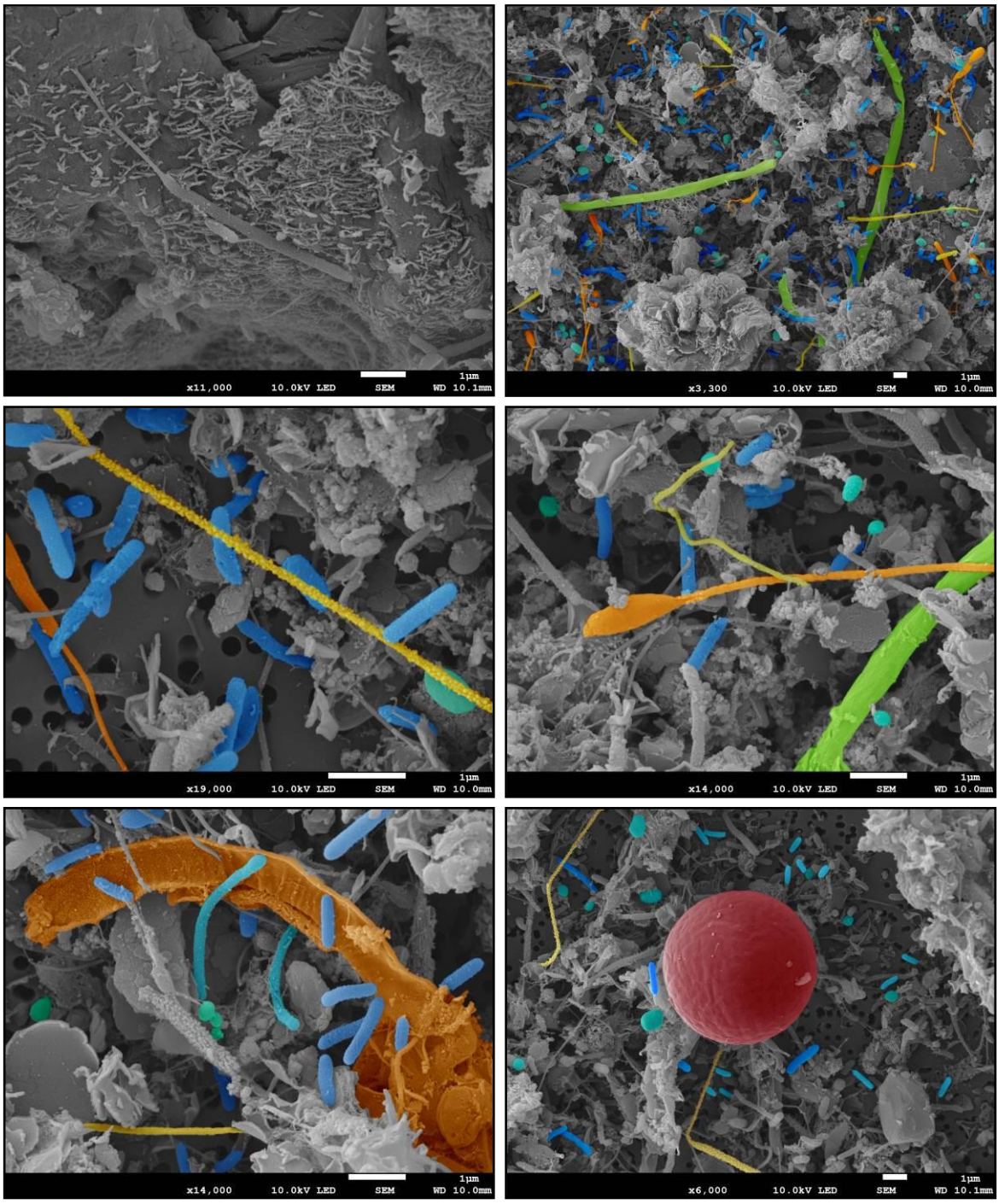

Figure 3.29: Scanning electron microscopy images of the fissure water and biofilm from the Star Diamonds mine. Scale bars are equal to either 10 µm or 1 µm.

3.5 CONCLUSIONS

A study site was obtained in the Karoo sandstone within the Star Diamonds mine and comprehensive sampling was conducted of the fissure water to characterize the biogeochemistry of the study site over time. On-site analyses revealed that fissure water maintained a consistent moderate temperature and a slightly alkaline pH and even though differences were observed in the ORP over time, the fissure water had a sustained reducing environment. No H_2O_2 was detected, thus indicating no radiolysis in the water. Geochemical analyses of the fissure water were conducted to provide insight into the possible electron donor and acceptor conditions for biological cycling and also confirmed that the water chemistry remained fairly constant, possibly an indication that influx from older water sources are not relevant during this period. The fissure water had a high mineral content, was moderately saline and contained low sulphate, ammonium, and nitrate concentrations.

The fissure water represented a subsurface residence time consistent with the isotopic signatures of paleo-meteoric origin and analyses of the conventional radiocarbon age for the fissure water was calculated at 24 320 (~131) years BP, with values falling on the global meteoric water line, again an indication that mixing with older water was negligible. The water also contained dissolved gases, including CH_4, H_2, and He. Their isotopic signatures were analysed and the results indicated a mixing of thermogenic and biogenic gases, with positional and isotopic characteristics that could be consistent with production by methanogens utilizing the CO_2 reduction pathway.

Over the past 20 years, comprehensive studies of subsurface diversity and geochemistry have revealed a wide diversity of microorganisms from all three domains of life in deep subsurface environments. These studies have shown that their metabolic activities can significantly contribute to the geochemistry of the deep subsurface, even though it happens orders of magnitude slower than for the microorganisms observed in surface environments (Phelps *et al*., 1994; Fredrickson & Onstott, 1996; Colwell *et al*., 1997; Onstott *et al*., 1998; Pedersen *et al*., 2000; Moser *et al*., 2003; Kieft *et al*., 2005; Gihring *et al*., 2006; Onstott *et al*., 2009; Borgonie *et al*., 2011; Ragon *et al*., 2013). The microbial diversity assessments of the fissure water from the Star Diamonds mine indicated that all three domains of life were present in the subsurface biome. The

Bacterial domain was found to be dominated by the Proteobacteria phylum, followed by the Firmicutes. The Proteobacteria mainly consisted of Alpha-, Beta-, and Gammaproteobacteria classes and the majority of the Firmicutes were from the Bacilli and Clostridia classes. The Archaeal domain was dominated by the Euryarchaeota phylum, which includes the methanogens and halobacteria, followed by the Thermoprotei, which is a class of the Crenarchaeota. For the Eukaryal domain, the main phyla present were Arthropoda, Streptophyta, Nematoda, Apicomplexa, and Chlorophyta. This confirmed that microorganisms which grow optimally under chemolithoautotrophic conditions, in the presence of H_2 and CO_2 (as many biomes, from different subsurface environments encounter), as well as microorganisms with heterotrophic metabolisms were present in the subsurface biome and included methanogens, which can fix CO_2, sulphate-reducing bacteria, and microorganisms known to fix nitrogen. Several macrostructures, as well as biofilm-like structures, were found in the subsurface biome, and even though these structures were not identified, it is indicative of the complex nature of the biofilms found in the subsurface.

3.6 REFERENCES

- **Altschul, S.F., Madden, T.L., Schaffer, A.A., Zhang, J., Zhang, Z., Miller, W. and Lipman, D.J.** (1997). Gapped BLAST and PSI-BLAST: a New Generation of Protein Database Search Programs. *Nucleic Acids Res*. **25**:3389-3402.

- **Amann, R.I., Ludwig, W. and Schleifer, K.** (1995). Phylogenetic Identification and *In Situ* Detection of Individual Microbial Cells without Cultivation. *Microbiological Reviews*. **59(1)**:143-169.

- **Andrews, J.N. and Wilson, G.B.** (1987). The Composition of Dissolved Gases in deep Groundwaters and Groundwater Degassing. *Geol. Assoc. Can. Spec. Pap*. **33**:245–252.

- **Baker, B.J., Moser, D.P., MacGregor, B.J., Fishbain, S., Wagner, M., Fry, N.K., Jackson, B., Spoelstra, N., Loos, S., Takai, K., Sherwood Lollar, B., Fredrickson, J.K., Balkwill, D., Onstott, T.C., Wimpee, C.F. and Stahl, D.A.** (2003). Related Assemblages of Sulphate Reducing Bacteria Associated with Ultra Deep Gold Mines of South Africa and Deep Basalt Aaquifers of Washington State. *Environ Microbiol*. **5(4)**:267–277.

- **Balkwill, D.L., Kieft, T.L., Tsukuda, T., Kostandarithes, H.M., Onstott, T.C., Macnaughton, S., Bownas, J. and Fredrickson, J.K.** (2004). Identification of Iron Reducing *Thermus* Strains as *T. scotoductus*. *Extremophiles*. **8**:37–44.

- **Banfield, J.F., Barker, W.W., Welch, S.A. and Taunton, A.** (1999). Biological Impact on Mineral Dissolution: Application of the Lichen Model to Understanding Mineral Weathering in the Rhizosphere. *Proc. Natl. Acad. Sci*. **96**:3404-3411.

- **Bartholomew, W. and Mittwer, T.** (1952). The Gram stain. *Microbiology and Molecular Biology Reviews.* **16(1)**:1–29.

- **Basava-Reddi, L.** (2012). Microbial Effects on CO_2 Storage. IEAGHG Report.

- **Basso, O., Lascourreges, J.F., Le Borgne, F., Le Goff, C. and Margot, M.** (2009). Characterization by Culture and Molecular Analysis of the Microbial Diversity of a Deep Subsurface Gas Storage Aquifer. *Res. Microbiol*. **160**:107–116.

- **Benson, S.M. and Cole, D.R.** (2008). CO_2 Sequestration in Deep Sedimentary Formations. *Elements*. **4**:325-331.

- **Blanco, Y., Rivas, L.A., García-Moyano, A., Aquirre, J., Cruz-Gil, P., Palacín, A., Van Heerden, E. and Parro, V.** (2014). Deciphering the Prokaryotic Community and Metabolisms in South African Deep-Mine Biofilms through Antibody Microarrays and Graph Theory. *PLoS One*. **9(12)**:e114180.

- **Boggs, J.R.** (2000). Principles of sedimentology and stratigraphy (3rd ed.). *Pearson Prentice Hall Publishing*. ISBN: 9780131547285.

- **Bomberg, M., Nyyssönen, M., Pitkänen, P., Lehtinen, A. and Itävaara, M.** (2015). Active Microbial Communities Inhabit Sulphate-Methane Interphase in Deep Bedrock Fracture Fluids in Olkiluoto, Finland. *BioMed Research International*. 979530.

- **Borgonie, G., García-Moyano, A., Litthauer, D., Bert, W., Bester, A., van Heerden, E., Möller, C., Erasmus, M. and Onstott, T.C.** (2011). Nematoda from the Terrestrial Deep Subsurface of South Africa. *Nature*. **474**:79-82.

- **Brazelton, W.J., Morrill, P.L., Szponar, N. and Schrenk, M.O.** (2013). Bacterial Communities Associated with Subsurface Geochemical Processes in Continental Serpentinite Springs. *Applied and Environmental Microbiology*. **79(13)**:3906-3916.

- **Brazelton, W.J., Nelson, B. and Schrenk, M.O.** (2012). Metagenomic Evidence for H_2 Oxidation and H_2 Production by Serpentinite-Hosted Subsurface Microbial Communities. *Frontiers in Microbiology*. **2**:268.

- **Casamayor, E.O., Massana, R., Benlloch, S., ØvreåS, L., Díez, B., Goddard, V.J., Gasol, J.M., Joint, I., Rodríguez-Valera, F. and Pedrós-Alió, C.** (2002).

Changes in Archaeal, Bacterial and Eukaryal Assemblages along a Salinity Gradient by Comparison of Genetic Fingerprinting Methods in a Multipond Solar System. *Environmental Microbiology*. **4(6)**:338-348.

- **Chivian, D., Brodie, E.L., Alm, E.J., Culley, D.E., Dehal, P.S., DeSantis, T.Z., Gihring, T.M., Lapidus, A., Lin, L., Lowry, S.R., Moser, D.P., Richardson, P.M., Southam, G., Wanger, G., Pratt, L.M., Andersen, G.L., Hazen, T.C., Brockman, F.J., Arkin, A.P. and Onstott, T.C.** (2008). Environmental Genomics Reveals a Single-Species Ecosystem Deep Within Earth. *Science*. **322**:275-278.

- **Clark, G.** (1981). Staining Procedures Used by the Biological Stain Commission (4th ed.). *Williams & Wilkins Publishing*. (4th ed.). ISBN: 9780683017076.

- **Cloete, M.** (2010). Atlas on Geological Storage of Carbon Dioxide in South Africa. Council for Geoscience.

- **Colwell, F.S., Onstott, T.C., Dilwiche, M.E., Chandler, D., Fredrickson, J.K., Yao, Q., McKinley, J.P., Boone, D.R., Griffiths, R., Phelps, T.J., Ringelberg, D., White, D.C., LaFreniere, L., Balkwill, D., Lehman, R.M., Konisky, J. and Long, P.E.** (1997). Microorganisms from Deep, High Temperature Sandstones: Constraints on Microbial Colonization. *FEMS Microbiol Rev*. **20**:425-435.

- **Costerton, J.W. and Stewart, P.S.** (2001). Battling Biofilms - the War is Against Bacterial Colonies that Cause some of the most Tenacious Infections known. The Weapon is Knowledge of the Enemy's Communication System. *Scientific American.* **285**:74-81.

- **Craig H.** (1961). Isotopic Variations in Meteoric Waters. *Scienc*e. **133**:1702–1703.

- **Cunningham, A.B., Gerlach, R., Spangler, L. and Mitchell, A.C.** (2009). Microbially Enhanced Geologic Containment of Sequestered Supercritical CO_2. *Energy Procedia*. **1**:3245-3252.

- **Díez, B., Pedrós-Alió, C., Marsh, T.L. and Massana, R.** (2001). Application of Denaturing Gradient Gel Electrophoresis (DGGE) to Study the Diversity of Marine Picoeukaryotic Assemblages and Comparison of DGGE with Other Molecular Techniques. *Applied and Environmental Microbiology*. **67(7)**:2942-2951.

- **Donahue, D.J., Linick, T.W. and Jull, J.T.** (1990). Isotope-Ratio and Background Corrections for Accelerator Mass Spectrometry Radiocarbon Measurements. *Radiocarbon*. 32(2):135-142.

- **Duarte, S., Cássio, F and Pascoal, C.** (2012). Denaturing Gradient Gel Electrophoresis (DGGE) in Microbial Ecology – Insights from Freshwaters. Chapter 3 in Gel Electrophoresis – Principles and Basics. ISBN: 9789535104582.

- **Dunbar, J., White, S. and Forney, L.** (1997). Genetic Diversity through the Looking Glass: Effect of Enrichment Bias. *Applied and Environmental Microbiology*. **63(4)**:1326-1331.

- **Etiope, G. and Sherwood Lollar, B.** (2013). Abiotic Methane on Earth. *Rev. Geophys*. **51**:276-299.

- **Fichter, L.S.** (2000). A Basic Sedimentary Rock Classification. Department of Geology/Environmental Science, James Madison University (JMU), Harrisonburg, Virginia.

- **Fredrickson, J.K. and Onstott, T.C.** (1996). Microbes Deep Inside the Earth. *Sci Am*. **275**:68-73.

- **Fry, J.C., Parkes, R.J., Cragg, B.A., Weightman, A.J. and Webster, G.** (2008). Prokaryotic Biodiversity and Activity in the Deep Subseafloor Biosphere. *FEMS Microbiol.Ecol*. **66**:181-196.

- **Gihring, T.M., Moser, D.P., Lin, L., Davidson, M., Onstott, T.C., Morgan, L., Milleson, M., Kieft, T.L., Trimarco, E., Balkwill, D.L. and Dollhopf, M.E.** (2006).

The Distribution of Microbial Taxa in the Subsurface Water of the Kalahari Shield, South Africa. *Geomicrobiol. J*. **23**:415–430.

- **Green, F.J.** (1990). The Sigma-Aldrich® Handbook of Dyes, Stains and Indicators. 513-515. ISBN: 9780941633222.

- http://www.geology4today.com/rock-textures.html. (2015).

- **Jackson, J.** (1997). Glossary of Geology (4th ed.). *Amer Geological Inst. Publishing*. ISBN: 9780922152346.

- **Jørgensen, B.B and Boetius, A.** (2007). Feast and Famine – Microbial Life in the Deep-Sea Bed. *Nature Reviews Microbiology*. **5**:770-781.

- **Jørgensen, B.B. and D'Hondt, S.** (2006). ECOLOGY: A Starving Majority Deep Beneath the Seafloor. *Science*. **314**:932-934.

- **Kieft, T.L., McCuddy, S.M., Onstott, T.C., Davidson, M., Lin, L., Mislowack, B., Pratt, L., Boice, E., Sherwood Lollar, B., Lippmann-Pipke, J., Pfiffner, S.M., Phelps, T.J., Gihring, T., Moser, D. and van Heerden, A.** (2005). Geochemically Generated, Energy-Rich Substrates and Indigenous Microorganisms in Deep, Ancient Groundwater. *Geomicrobiol. J*. **22**:325–335.

- **Kotelnikova, S.** (2002). Microbial Production and Oxidation of Methane in Deep Subsurface. *Earth-Sci. Rev*. **58**:367–395.

- **Kuwabara, J.S and Harvey, R.W.** (1990). Application of a Hollow-Fiber, Tangential-Flow Device for Sampling Suspended Bacteria and Particles from Natural Waters. *Journal of Environmental Quality*. **19(3)**:625 – 629.

- **Lau, M.C.Y., Cameron, C., Magnabosco, C., Brown, C.T., Schilkey, F., Grim, S., Hendrickson, S., Pullin, M., Sherwood Lollar, B., van Heerden, E., Kieft, T.L. and Onstott, T.C.** (2014). Phylogeny and Phylogeography of Functional Genes

Shared Among Seven Terrestrial Subsurface Metagenomes Reveal N-Cycling and Microbial Evolutionary Relationships. *Front. Microbiol*. **5**:531.

- **Lepp, P.W., Brinig, M.M., Ouverney, C.C, Palm, K., Armitage, G.C and Relman, D.A.** (2004). Methanogenic Archaea and Human Periodontal Disease. *Proc. Natl. Acad. Sci*. **101(16)**:6176-6181.

- **Lewandowski, Z. and Beyenal, H.** (2013). Fundamentals of Biofilm Research. (2nd ed.). *CRC Press*. ISBN: 9781466559592.

- **Lin, L., Hall, J., Lippmann-Pipke, J., Ward, J.A., Sherwood Lollar, B., DeFlaun, M., Rothmel, R., Moser, D., Gihring, T.M., Mislowack, B. and Onstott, T. C.** (2005). Radiolytic H_2 in Continental Crust: Nuclear Power for Deep Subsurface Microbial Communities. *Geochem. Geophys. Geosyst*. **6(7)**:Q07003.

- **Lin, L., Hall, J., Onstott, T. C., Gihring, T., Sherwood Lollar, B., Boice, E., Pratt, L., Lippmann-Pipke, J. and Bellamy, R.E.S.** (2006a). Planktonic Microbial Communities Associated with Fracture-Derived Groundwater in a Deep Gold Mine of South Africa. *Geomicrobiol. J*. **23**:475–497.

- **Lin, L., Wang, P., Rumble, D., Lippmann-Pipke, J., Boice, E., Pratt, L.M., Sherwood Lollar, B., Brodie, E.L., Hazen, T.C., Andersen, G.L., DeSantis, T.Z., Moser, D.P., Kershaw, D. and Onstott, T.C.** (2006b). Long-Term Sustainability of a High-Energy, Low-Diversity Crustal Biome. *Science*. **314**:479–482.

- **Lippmann, J., Stute, M., Torgersen, T., Moser, D.P., Hall, J., Lin, L., Borcsik, M., Bellamy, R.E.S. and Onstott, T.C.** (2003). Dating Ultra-Deep Mine Waters with Noble Gases and ^{36}Cl, Witwatersrand Basin, South Africa. *Geochim Cosmochim Acta*. **67**:4597–4619.

- **Liu, W., Marsh, T.L., Cheng, H. and Forney, L.J.** (1997). Characterization of Microbial Diversity by Determining Terminal Restriction Fragment Length Polymorphism of Genes Encoding 16S rRNA. *Applied and Environmental Microbiology*. **63(11)**:4516-4522.

- **Lovley, D.R. and Chapelle, F.H.** (1995). Deep Subsurface Microbial Processes. *Review of Geophysics*. **33(3)**:365-381.

- **Magnabosco, C., Tekere, M., Lau, M.C.Y., Linage, B., Kuloyo, O., Erasmus, M., Cason, E., van Heerden, E., Borgonie, G., Kieft, T.L., Olivier, J. and Onstott, T.C.** (2014). Comparisons of the Composition and Biogeographic Distribution of the Bacterial Communities Occupying South African Thermal Springs with those Inhabiting Deep Subsurface Fracture Water. *Frontiers in Microbiology*. **5**:679.

- **Metz, B., Davidson, O., De Coninck, H., Loos, M and Meyer, L.** (2005). Carbon Dioxide Capture and Storage - Intergovernmental Panel on Climate Change (IPCC) Special Report. *Cambridge University Press*. ISBN: 9780521866439.

- **Meyer, F., Paarmann, D., D'Souza, M., Olson, R., Glass, E.M., Kubal, M., Paczian, T., Rodriguez, A., Stevens, R., Wilke, A., Wilkening, J. and Edwards, R.A.** (2008). The Metagenomics RAST Server – A Public Resource for the Automatic Phylogenetic and Functional Analysis of Metagenomes. *BMC Bioinformatics*. **9**:386.

- **Michaelsen, A., Pinzari, F., Ripka, K., Lubitz, W. and Piñar, G.** (2006). Application of Molecular Techniques for Identification of Fungal Communities Colonising Paper Material. *International Biodeterioration and Biodegradation*. **58**:133-141.

- **Mitchell, A.C., Phillips, A.J., Hiebert, R., Gerlach, R., Spangler, L.H. and Cunningham, A.B.** (2009). Biofilm Enhanced Geologic Sequestration of Supercritical CO_2. *International Journal of Greenhouse Gas Control*. **3**:90-99.

- **Morozova, D., Wandrey, M., Alawi, M., Zimmer, M., Vieth, A., Zettlitzer, M and Würdemann, H.** (2010). Monitoring of the Microbial Community Composition in Saline Aquifers during CO_2 Storage by Fluorescence *in situ* Hybridisation. *International Journal of Greenhouse Gas Control*. **4**:981-989.

- **Moser, D.P., Onstott, T.C., Fredrickson, J.K., Brockman, F.J., Balkwill, D.L., Drake, G.R., Pfiffner, S.M., White, D.C., Takai, K., Pratt, L.M., Fong, J., Sherwood Lollar, B., Slater, G., Phelps, T.J., Spoelstra, N., DeFlaun, M., Southam, G., Welty, A.T., Baker, B.J. and Hoek, J.** (2003). Temporal Shifts in the Geochemistry and Microbial Community Structure of an Ultradeep Mine Borehole Following Isolation. *Geomicrobiol. J*. **20**:517–548.

- **Mu, A., Boreham, C., Leong, H.X., Haese, R.R. and Moreau, J.W.** (2014). Changes in the Deep Subsurface Microbial Biosphere Resulting from a Field-Scale CO_2 Geosequestration Experiment. *Frontiers in Microbiology*. **5**:209.

- **Muyzer, G. and Stams, A.J.** (2008). "The ecology and biotechnology of sulphate-reducing bacteria. *Nature Reviews Microbiology*. **6**:441-454.

- **Muyzer, G., Brinkoff, T., Nübel, U., Santegoeds, C., Schäfer, H and Wawer, C.** (2004). Denaturing Gradient Gel Electrophoresis (DGGE) in Microbial Ecology. In: Molecular Microbial Ecology Manual (2nd ed.) *Kluwer academic publishers*. ISBN: 9781402048609.

- **Muyzer, G., De Waal, E.C., Uitterlinden, A.G.** (1993). Profiling of Complex Microbial Populations by Denaturing Gradient Gel Electrophoresis Analysis of Polymerase Chain Reaction-Amplified Genes Coding for 16S rRNA. *Applied and Environmental Microbiology*. **59(3)**:695-700.

- **Nakatsu, C.H., Torsvik, V. and Øvreas, L.** (2000). Soil Community Analysis using DGGE of 16S rDNA Polymerase Chain Reaction Products. *Soil Science Society of America Journal*. **64**:1382-1388.

- **Newberry, C.J., Webster, G., Cragg, B.A., Parkes, R.J., Weightman, A.J. and Fry, J.C.** (2004). Diversity of Prokaryotes and Methanogenesis in Deep Subsurface Sediments from the Nankai Trough, Ocean Drilling Program Leg 190. *Environ.Microbiol*. **6**:274-287.

- **Nondorf, L., Gutierrez, M. and Plymate, T.G.** (2011). Modelling Carbon Sequestration Geochemical Reactions for a Proposed Site in Springfield, Missouri. *Environmental Geosciences*. **18**:91-99.

- **Onstott, T.C.** (2005). Impact of CO_2 Injections on Deep Subsurface Microbial Ecosystems and Potential Ramifications for the Surface Biosphere. Chapter 30 in Carbon Dioxide Capture for Storage in Deep Geologic Formations – Results from the CO_2 Capture Project, Geological Storage of Carbon Dioxide with Monitoring and Verification. *Elsevier Publishing*. **2**:1217-1250. ISBN: 0080445705.

- **Onstott, T.C., Colwell, F.S., Kieft, T.L., Murdoch, L. and Phelps, T.J.** (2009). New Horizons for Deep Subsurface Microbiology. *Microbe Magazine.* **4(11)**:499–505.

- **Onstott, T.C., Lin, L., Davidson, M., Mislowack, B., Borcsik, M., Hall, J., Slater, G., Ward, J., Sherwood Lollar, B., Lippmann-Pipke, J., Boice, E., Pratt, L.M., Pfiffner, S., Moser, D., Gihring, T., Kieft, T.L., Phelps, T.J., van Heerder, E., Litthauer, D., DeFlaun, M., Rothmel, R., Wanger, G. and Southam G.** (2006). The Origin and Age of Biogeochemical Trends in Deep Fracture Water of the Witwatersrand Basin, South Africa. *Geomicrobiol. J*. **23**:369–414.

- **Onstott, T.C., Phelps, T.J., Kieft, T., Colwell, F.S., Balkwill, D.L., Fredrickson, J.K. and Brockman, F.J.** (1998). In: Enigmatic Microorganisms and Life in Extreme Environments. *Springer Science & Business Media Publishers*. ISBN: 9780792354925.

- **Parkes, R.J., Cragg, B.A., Bale, S.J., Getliff, J.M., Goodman, K., Rochelle, P.A., Fry, J.C., Weightman, A.J. and Harvey, S.M.** (1994). Deep Bacterial Biosphere in Pacific Ocean Sediments. *Nature.* **371**:410–413.

- **Parsons, T.R., Maita, Y. and Lalli, C.M.** (1984). A Manual of Chemical and Biological Methods for Seawater Analysis (1st ed.). Pergamon Press. ISBN: 0080302882.

- **Pedersen, K., Motemedi, M., Karnland, O. and Sandén, T.** (2000). Cultivability of Microorganisms Introduced into a Compacted Bentonite Clay Buffer under High-Level Radioactive Waste Repository Conditions. *Eng Geol*. **58**:149-161.

- **Pettijohn, F.J., Potter, P.E. and Siever, R.** (1987). Sand and Sandstone (2nd ed.). *Springer-Verlag Publishing*. ISBN: 9780387963501.

- **Phelps, T.J., Murphy, E.M., Pfiffner, S.M. and White, D.C.** (1994). Comparison between Geochemical and Biological Estimates of Subsurface Microbial Activities. *Microb. Ecol*. **28**:335-349.

- **Price, J and Smith, B.** (2008). Geologic Storage of Carbon Dioxide: Staying Safely Underground. *International Energy Agency (IEA)*.

- **Pruesse, E., Quast, C., Knittel, K., Fuchs B.M., Ludwig, W., Peplies, J. and Glöckner, F.O.** (2007). SILVA: A Comprehensive Online Resource for Quality Checked and Aligned Ribosomal RNA Sequence Data Compatible with ARB. *Nucl. Acids Res*. **35(21)**:7188-7196.

- **Purtschert, R., Sturchio, N.C. and Yokochi, R.** (2013). "Krypton-81 Dating of Old Groundwater. Chapter 5 in Isotope Methods for Dating Old Groundwater. *IAEA Publishing.* 91–124. ISBN: 9789201372109.

- **Ragon, M., Van Driessche, A.E.S., García-Ruíz, J.M., Moreira, D. and López-García, P.** (2013). Microbial Diversity in the Deep-Subsurface Hydrothermal Aquifer Feeding the Giant Gypsum Crystal-Bearing Naica Mine, Mexico. *Frontiers in Microbiology*. **4**:37.

- **Rajala, P., Bomberg, M., Kietäväinen, R., Kukkonen, I., Ahonen, L., Nyyssönen, M. and Itävaara, M.** (2015). Rapid Reactivation of Deep Subsurface Microbes in the Presence of C-1 Compounds. *Microorganisms*. **3**:17-33.

- **Rollinson, H.,** (1993). Using Geochemical Data: Evaluation, Presentation, Interpretation (Longman Geochemistry Series) (1st ed.). *Routledge Publishing.* ISBN: 9780582067011.

- **Rotzsche, H.** (1991). Acid Washing. In Stationary Phases in Gas Chromatography, Vol. 48. *Elsevier Publishers.* 171. ISBN: 0444987339.

- **Rubidge, B.S.** (2005). Re-uniting Lost Continents – Fossil Reptiles from the Ancient Karoo and their Wanderlust. *South African Journal of Geology.* **108(1)**:135–172.

- **Sahl, J.W., Schmidt, R., Swanner, E.D., Mandernack, K.W., Templeton, A.S., Kieft, T.L., Smith, R.L., Sanford, W.E., Callighan, R.L., Mitton, J.B. and Spear, J.R.** (2008). Subsurface Microbial Diversity in Deep-Granitic-Fracture Water in Colorado. *Appl. Environ. Microbiol*. **74**:143–152.

- **Sanderson, J.B.** (1994) Biological Microtechnique (Microscopy Handbook 28 of Royal Microscopial Society). ISBN: 1872748422.

- **Selden, P. and Nudds, J.** (2011). Karoo. Chapter 9 in Evolution of Fossil Ecosystems (2nd ed.). *Manson Publishing.* 104–122. ISBN: 9781840761603.

- **Sherwood Lollar, B., Lacrampe-Couloume, G., Voglesonger, K., Onstott, T. C., Pratt, L.M. and Slater, G.F.** (2008). Isotopic Signatures of CH_4 and Higher Hydrocarbon Gases from Precambrian Shield Sites: A Model for Abiogenic Polymerization of Hydrocarbons. *Geochim. Cosmochim. Acta*. **72**:4778–4795.

- **Sherwood Lollar, B., Westgate, T.D., Ward, J.A., Slater, G.F. and Lacrampe-Couloume, G.** (2002). Abiogenic Formation of Gaseous Alkanes in the Earth's Crust as a Minor Source of Global Hydrocarbon Reservoirs. *Nature*. **416b**:522–524.

- **Stepanauskas, R.** (2012). Single Cell Genomics: An Individual Look at Microbes. *Current Opinion in Microbiology*. **15**:613-620.

- **Stevens, T.O., McKinley, J.P. and Fredrickson, J.K.** (1993). Bacteria Associated with Deep, Alkaline, Anaerobic Groundwaters in Southeast Washington. *Microb Ecol*. **25**:35-50.

- **Stoodley, P., Sauer, K., Davies, D.G. and Costerton, J.W.** (2002). Biofilms as Complex Differentiated Communities. *Annual Review of Microbiology*. **56**:187-209.

- **Stow, D.A.V.** (2005). Sedimentary Rocks in the Field: A Colour Guide. *Manson Publishing*. ISBN: 9781874545682.

- **Stuiver, M. and Polach, H.A.** (1977). Discussion, Reporting of ^{14}C Data. *Radiocarbon*. **19(3)**:355-363.

- **Takai, K., Moser, D., DeFlaun, M., Onstott, T.C. and Fredrickson, J.K.** (2001). Archaeal Diversity in Waters from Deep South African Gold Mines. *Applied and Environmental Biology.* **67(12)**:5750-5760.

- **Teske, A.P.** (2005). The Deep Subsurface Biosphere is Alive and Well. *Trends Microbiol.* **13(9)**:402-404.

- **Turner, S., Pryer, K.M., Miao, V.P.W. and Palmer, J.D.** (1999). Investigating Deep Phylogenetic Relationships among Cyanobacteria and Plastids by Small Subunit rRNA Sequence Analysis. *J. Eukaryot. Microbiol*. **46(4)**:327-338.

- **Vermaak, C.** (2012). Water Monitoring Report for Star Diamonds (Theunissen).

- **Von Eynatten, H., Barceló-Vidal, C. and Pawlowsky-Glahn, V.** (2003). Composition and Discrimination of Sandstones: A Statistical Evaluation of Different Analytical Methods. *Journal of Sedimentary Research*. **72(1)**:47-57.

- **Ward, J.A., Slater, G.F., Moser, D.P., Lin, L., Lacrampe-Couloume, G., Bonin, A. S., Davidson, M., Hall, J.A., Mislowack, B., Bellamy, R.E.S., Onstott, T.C. and Sherwood Lollar, B.** (2004). Microbial Hydrocarbon Gases in the

Witwatersrand Basin, South Africa: Implications for the Deep Biosphere. *Geochim. Cosmochim. Acta*. **68**:3239–3250.

- **Watnick, P and Kolter, R.** (2000). Biofilm, City of Microbes. *Journal of Bacteriology*. **182**:2675-2679.

- **Webster, G., Parkes, R.J., Cragg, B.A., Newberry, C.J., Weightman, A.J. and Fry, J.C.** (2006). Prokaryotic Community Composition and Biogeochemical Processes in Deep Subseafloor Sediments from the Peru Margin. *FEMS Microbiol.Ecol*. **58**:65-85.

- **Whiticar, M.J.** (1999). Carbon and Hydrogen Isotope Systematics of Bacterial Formation and Oxidation of Methane. *Chem. Geol*. **161**:291–314.

- **Whitman, W.B., Coleman, D.C. and Wiebe, W.J.** (1998). Prokaryotes: the Unseen Majority. *Proc. Natl. Acad. Sci*. **95**:6578–6583.

- **Zhang, Z., Schwartz, S., Wagner, L. and Miller, W.** (2000). A Greedy Algorithm for Aligning DNA Sequences. *J Comput Biol*. **7(1-2)**:203-214.

CHAPTER 4

MONITORING OF GROWTH AND LOW PRESSURE STUDIES

4.1 INTRODUCTION

The diversity studies of the subsurface biome from the Star Diamonds mine (Chapter 3) displayed an extensive variety in the microbial community and included species from all three domains of life. However, limited, detailed reports of subsurface biome survival, community shifts, or metabolic cycling under low pressures are available (Morozova *et al*., 2010; Glossner, 2013), since previous research studies under pressure usually focussed on the characterization of single microorganisms (Miller *et al*., 1988; Nelson *et al*., 1992; Bothun *et al*., 2004; Boonyaratanakornkit *et al.,* 2007; Takai *et al*., 2008; Hiraki *et al*., 2012). According to Fakruddin & Mannan (2013), two important questions to address when studying a microbial community are how do the microorganisms function and how does the composition of the community adjust due to stress conditions from environmental changes? These changes are usually harmful to the microorganisms and may lead to an overall decrease in metabolic activity, turnover times, and cell density (Phelps *et al*., 1994; Teske, 2005; Onstott *et al*., 2009). Therefore, knowledge regarding the survival of microorganisms within a subsurface biome that are subjected to environmental changes such as different physiological growth conditions with differences in nutrition and the addition of lower pressures, are required to enhance the current literature. As a result, studies of viable cultures that can maintain subsurface cycling are required to investigate how CCS conditions will introduce additional impacts on the biome.

4.1.1 *Eubacterium limosum*

E. limosum is an obligate anaerobic, non-sporulating, acetogenic bacterium from the family, Eubacteriaceae (Song & Cho, 2015). It belongs to the Clostridiales order under the Clostridia class, the Firmicutes phylum, and the Bacteria kingdom. They are Gram-

positive rods that contain a thick peptidoglycan layer in their cell wall (Song & Cho, 2015), and are generally isolated from anaerobic digesters (Roh *et al*., 2011), rumen fluid of sheep (Genthner *et al*., 1981), sewage (Genthner *et al*., 1981), or human faeces (Finegold *et al*., 1983). Due to the anaerobic metabolism of *E. limosum* and the fact that it grows optimally under chemolithoautotrophic conditions in the presence of H_2 and CO_2 [as many biomes from different subsurface environments encounter (Lovley & Chapelle, 1995; Stevens, 1997; White *et al*., 1998; Lin *et al*., 2005; Onstott *et al*., 2006; Porter *et al*., 2009; Woycheese *et al*., 2015)], and even under two bar pressure (Genthner *et al*., 1981; Genthner & Bryant, 1982; Drake, 1994; Lelait & Grivet. 1996), it was used as the positive control organism for this research to benchmark growth under pressure.

E. limosum is able to grow on a variety of substrates, including hydrogen (H_2), carbon monoxide (CO), carbon dioxide (CO_2), glucose, and methanol (Genthner *et al*., 1981; Loubière & Lindley, 1991; Lelait & Grivet, 1996; Roh *et al*., 2011). This microorganism has been considered a microbial syngas catalyst due to its high growth rate under pressures above 1 atm (1.01325 bar), when using CO as the sole carbon or energy source (Roh *et al*., 2011). Through the use of the Wood–Ljungdahl pathway [also known as the reductive acetyl coenzyme A (Acetyl-CoA) pathway], *E. limosum* can fix CO and CO_2 to produce Acetyl-CoA which is then converted into acetate, butyrate, or ethanol as fermentation products and has therefore been considered a model strain for bio-energy production from syngas (Loubière & Lindley, 1991; Roh *et al*., 2011).

4.2 AIMS OF THIS CHAPTER

The main aims of this chapter were to:

- Study the potential growth of the subsurface biome from the Star Diamonds mine under different physiological growth environments while assessing diversity changes.
- Introduce lower pressure to the microorganisms in order to determine if they can survive these conditions.

4.3 MATERIALS AND METHODS

Unless otherwise specified, the anaerobic techniques used throughout this research were according to the procedures of Bryant, (1972); Hungate & Macy, (1973); Balch & Wolfe, (1976); and Boone & Bryant, (1980); and all incubations for cultivation purposes of the subsurface biome and *E. limosum* were conducted at 35°C in a temperature controlled incubator. Even though this temperature was slightly higher than the fissure water (Section 3.4.1.1), it was to accommodate the optimum growth temperature for *E. limosum*. This was also selected to ensure that the CO_2 would be in a supercritical state during CCS conditions. All growth curves were constructed using GraphPad Prism® (V.5.03) (GraphPad Software, Inc.), by plotting the mean and error values from three replicates of independent growth studies on a logarithmic scale.

The rate of growth per unit amount of biomass [also known as the maximum specific growth rate (μ_{max})], was calculated using (Equation 4.1) (Pirt, 1975). This was determined by linear regression analyses with Microsoft® Excel (Microsoft® Corporation) of the exponential phase of the growth curve. The period of time required for the population to double [also known as the doubling time (t_d)], was calculated using (Equation 4.2) (Pirt, 1975). The μ_{max} and t_d was calculated for each individual growth curve, followed by obtaining the average of three replicates. The average values with standard deviations (SD) were given in the results.

(Equation 4.1)

(μ_{max}) = maximum specific growth rate
(x_0) = initial biomass concentration
(x_t) = biomass concentration at the time given
(t) = time in hours

(Equation 4.2)

$t_d = \ln(2)/\mu_{max}$
(t_d) = doubling time
(μ_{max}) = maximum specific growth rate

4.3.1 Medium Preparation for the Positive Control Microorganism

Eubacterium limosum (DSM-20543) was obtained from the Deutsche Sammlung von Mikroorganismen und Zellkulturen (DSMZ) culture collection as a lyophilized pellet. The culture was revived using the anaerobic PYG medium (medium 104) from the DSMZ (5 $g.L^{-1}$ trypticase peptone, 5 $g.L^{-1}$ peptone, 10 $g.L^{-1}$ yeast extract, 5 $g.L^{-1}$ beef extract, 5 $g.L^{-1}$ glucose, 2 $g.L^{-1}$ K_2HPO_4, 1 $ml.L^{-1}$ Tween 80, 0.5 $g.L^{-1}$ cysteine-$HCl.H_2O$, 1 $mg.L^{-1}$ resazurin, 40 $ml.L^{-1}$ salt solution, 10 $ml.L^{-1}$ haemin solution, 0.20 $ml.L^{-1}$ vitamin K_1 solution, pH 7.2). The salt solution was prepared by dissolving 0.25 $g.L^{-1}$ $CaCl_2.2H_2O$, 0.5 $g.L^{-1}$ $MgSO_4.7H_2O$, 1 $g.L^{-1}$ K_2HPO_4, 1 $g.L^{-1}$ KH_2PO_4, 10 $g.L^{-1}$ $NaHCO_3$, and 2 $g.L^{-1}$ NaCl in dH_2O. For the haemin solution, 50 mg haemin was dissolved in 1 N NaOH (40 $g.L^{-1}$) and made up to 100 ml with dH_2O. For the vitamin K_1 solution, 0.1 ml of vitamin K_1 was dissolved in 20 ml EtOH (95%) and filter-sterilized. The vitamin K_1 solution, the haemin solution, and the cysteine-$HCl.H_2O$ were only added after the medium has been boiled for 5 minutes and cooled for 10 minutes, while flushing with CO_2 to decrease the oxygen solubility. The pH was adjusted to 7.2 using 8 N NaOH (320 $g.L^{-1}$) and the medium was dispensed into serum vials that were closed with blue chlorobutyl rubber stoppers (Bellco Glass Inc.) and sealed with aluminium crimp caps (Lasec). The medium was degassed for one hour using nitrogen (N_2) gas (99.999%) and subsequently sterilized. The resazurin was added as an oxidation-reduction indicator and the cysteine-$HCl.H_2O$ was added to remove the remaining oxygen (Sambrook *et al*., 1989).

To revive the culture, the ampoule containing the lyophilized pellet, was opened under sterile conditions inside a laminar flow cabinet (Labotec®) and the pellet was transferred in a sterile 1.5 ml eppendorf tube and added, under anaerobic conditions, to a 150 ml serum vial containing 80 ml of the PYG medium. This was done in an anaerobic glove box (Coy Laboratories) that was flushed three times at 200 kPa (2 bar) with nitrogen gas (99.999%), followed by two times with a combination of N_2, CO_2 and H_2 (80:10:10 v/v/v).

4.3.2 Identification of the Positive Control Microorganism

Molecular identification was conducted on *E. limosum* (DSM-20543).

4.3.2.1 Genomic DNA Isolation and Polymerase Chain Reaction

Genomic DNA was isolated from *E. limosum* using the NucleoSpin® Soil kit (Macherey-Nagel) as discussed in Section 3.3.6.6.1. A PCR was conducted to amplify the Bacterial 16S rRNA gene (~1500 bp) (Section 3.3.6.6.2) using the universal oligonucleotide primers for Bacteria (Section 3.3.6.6.2, Table 3.1). The PCR products were visualized on a 1% (w/v) agarose gel and purified (Section 3.3.6.6.2).

4.3.2.2 Ligation of the 16S rRNA Gene

The purified PCR product was ligated into the pGEM®-T Easy Vector system (Promega) (Figure 4.1), as per manufacturer's instructions. The ligation reaction was performed in a total reaction volume of 10 µl and consisted of 2x Rapid Ligation Buffer (5 µl), pGEM®-T Easy Vector (2.5 ng), PCR product (3 µl), and T4 DNA Ligase (0.3 Weiss units). The ligation reaction was incubated overnight at 4°C.

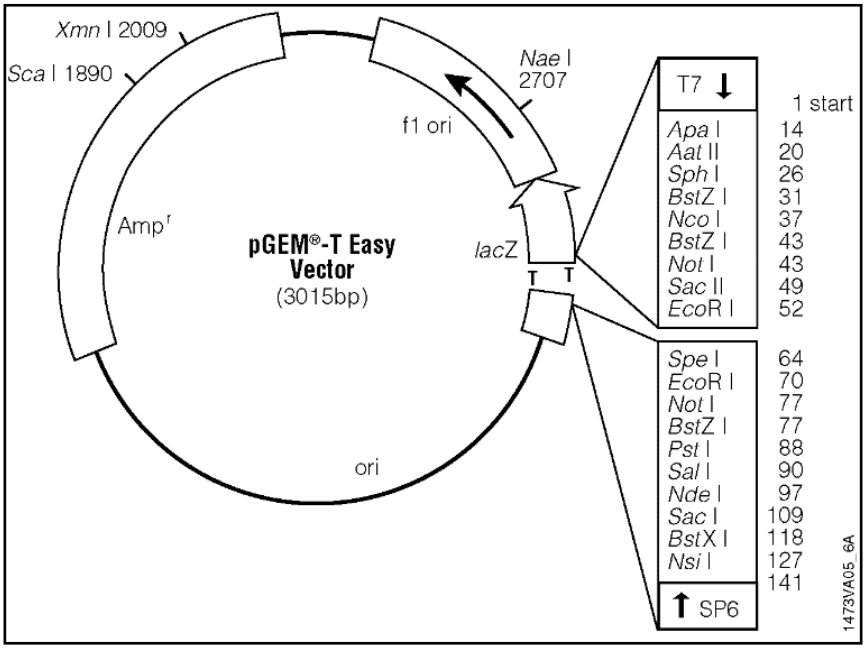

Figure 4.1: The pGEM®-T Easy Vector map and sequence reference points (Promega).

4.3.2.3 Transformation of the 16S rRNA Gene

Competent *Escherichia coli* (*E. coli*) One Shot TOP10 (Invitrogen) cells were prepared according to the procedure of Hanahan, (1983), with modifications. Erlenmeyer flasks containing 100 ml PSI broth (5 $g.L^{-1}$ yeast extract, 20 $g.L^{-1}$ tryptone, 5 $g.L^{-1}$ $MgSO_4.7H_2O$, pH 7.6 with KOH) were inoculated with 1 ml of an overnight culture and grown at 37°C on a rotary shaker (200 rpm), until an optical density (OD) of 0.6 at 600 nm was reached. This was then placed on ice for 30 minutes and centrifuged (3 000 *x g*, 10 minutes, 4°C), to collect cells. The cells were resuspended in 40 ml transformation buffer I (TfbI) (30 mM potassium acetate, 100 mM rubidium chloride, 10 mM $CaCl_2$, 15% glycerol, pH 5.8) and incubated on ice for 15 minutes. Cells were collected through centrifugation (3 000 *x g*, 10 minutes, 4°C) and resuspended in 4 ml transformation buffer II (TfbII) (10 mM MOPS-NaOH, 75 mM $CaCl_2$, 10 mM rubidium chloride, 15% glycerol, pH 6.5). The cell suspension was incubated on ice for 10 minutes and aliquots were made that were snap frozen in liquid nitrogen followed by storage at -80°C until used.

Aliquots (50 µl) of the competent cells were removed and allowed to thaw on ice. The ligated plasmid reactions (5 µl) were added to the cells and incubated on ice for 30 minutes. The cell suspension was heat shocked for 40 seconds at 42°C and immediately placed back in ice-water for 2 minutes. SOC medium (250 µl) (20 $g.L^{-1}$ tryptone, 5 $g.L^{-1}$ yeast extract, 0.01 M NaCl, 0.0025 M KCl, 0.01 M $MgCl_2$, 0.01 M $MgSO_4$, 0.02 M glucose) was added to the transformation reactions and incubated for 60 minutes at 37°C, with gentle shaking. Different volumes were plated on separate Lysogeny broth (LB) plates (10 $g.L^{-1}$ peptone, 5 $g.L^{-1}$ yeast extract, 10 $g.L^{-1}$ NaCl, 18 $g.L^{-1}$ agar, pH 7.0), containing 100 $\mu g.ml^{-1}$ ampicillin, 0.2 mM isopropyl β-D-1-thiogalactopyranoside (IPTG), and 40 $\mu g.ml^{-1}$ 5-bromo-4-chloro-3-indolyl-beta-D-galactopyranosidehosphate (X-Gal) and incubated overnight at 37°C to verify DNA ligation using blue/white selection. Single white colonies were selected from the LB-AIX plates and separately inoculated into 5 ml LB medium containing 60 $\mu g.ml^{-1}$ ampicillin and incubated overnight on a rotary shaker (200 rpm), at 37°C. Plasmids were isolated using the BioFlux BioSpin Plasmid DNA Extraction Kit (Bioer Technology Co., Ltd) according to the manufacturer's instructions.

4.3.2.4 Analyses of the 16S rRNA Gene

Double digestion was conducted on the plasmids using the restriction enzymes *Eco*RI and *Nde*I (Fermentas). Before the digestion was done, the 16S rRNA gene sequence of *E. limosum* ZL2, with accession number JQ085755.1 was retrieved from the Genbank Database (NCBI, 2012) and *in silco* analyses were conducted using the Restriction Mapper (V.3.0) tool, to confirm that the chosen restriction enzymes do not digest the 16S rRNA gene. The digestion reactions were performed in a total reaction volume of 50 µl and consisted of 10 µl purified plasmid, 5 µl buffer Tango (2x), 2.5 µl of each restriction enzyme, and sterile dH_2O. The reaction mixture was incubated at 37°C for 3 hours, where after the enzymes were thermally deactivated at 65°C for 20 minutes. The restriction digestions were visualized on a 1% (w/v) agarose gel and purified (Section 3.3.6.6.2).

Sequencing and analyses of the purified fragments were done as discussed in Section 3.3.6.6.6 using the primer set indicated in Table 4.1.

Table 4.1: The RNA polymerase promoter primers used for sequencing.

Primer	Nucleotide sequence	Tm (°C)
T7 Promoter	5'- TAA TAC GAC TCA CTA TAG GG -3'	47
SP6 Promoter	5'- TAC GAT TTA GGT GAC ACT ATA G -3	42

4.3.3 Cultivation Conditions for *Eubacterium limosum*

Since *E. limosum* is described in the literature to be an obligate anaerobe (Song & Cho, 2015), cultivation under aerobic conditions was not done. To study the growth of *E. limosum* under anaerobic conditions, the nutritionally rich, non-selective PYG medium was prepared as discussed in Section 4.3.1. An additional evaluation was conducted to test the ability of *E. limosum* to grow in the fissure water (FW), from the Star Diamonds mine. This was done with and without the addition of sandstone. The fissure water was used as a minimal medium, containing no additional nutrients and the sandstone was added as a potential nutrient source, since the rock and fissure water will be the

available nutrient source for the microorganisms in the subsurface. Both the PYG and FW contained 0.5 $g.L^{-1}$ cysteine-$HCl.H_2O$ and 1 $mg.L^{-1}$ resazurin and the PYG was prepared using fissure water.

Hungate tubes (20 ml), containing 4 ml of either PYG or FW, were prepared, sealed with a blue chlorobutyl rubber stopper (Bellco Glass Inc.) and degassed for one hour using nitrogen gas (99.999%). The media were sterilized where after inoculums (10% v/v) were made with *E. limosum* under anaerobic conditions (Section 4.3.1). For the FW tubes that contained sandstone, 0.5 g crushed sandstone (Section 3.3.5) was added to the media before being sterilized. Negative controls were prepared for each inoculum.

The tubes were incubated on a rotary shaker (200 rpm), at 35°C. For the time zero reading, a tube was immediately inserted into a photoLab S6 photometer [Wissenschaftlich-Technische Werkstätten (WTW), Labotec®] and the OD was measured at a set 605 nm. This was repeated at each time interval. Before the Hungate tubes were prepared, an OD_{605} of the tube alone was taken using the photometer and this value was subtracted. Growth studies continued for 48 hours and were done in triplicate for each media type. The OD values were plotted against the time intervals to obtain the various growth curves. Visual assessments were conducted on each completed growth study.

In order to study the growth of *E. limosum* under pressure, low pressure were introduced. In the literature, when microorganisms are grown under pressure, several different gas compositions are used, some of them being H_2:CO_2 (80%:20% v/v) (Genthner *et al*., 1981; Girbal *et al*., 1997); H_2:CO_2 (60%:40% v/v) (Leclerc *et al*., 1997); N_2:CO_2 (90:10% v/v) (Men *et al*., 2014); N_2:CO_2 (85%:15% v/v) (Loubière & Lindley, 1991); N_2:CO_2 (80%:20% v/v) (Krumholz *et al*., 1996; Girbal *et al*., 1997; Bainotti *et al*., 1998); N_2:CO_2 (60%:40% v/v) (Genthner & Bryant, 1982) and N_2:CO_2:H_2 (80%:10%:10% v/v/v) (Girbal *et al*., 1997). For the purpose of this research Section, the H_2:CO_2 combination was used. This also mimics conditions where the methanogens, and other anaerobic physiological types dominate the deep subsurface, survive (Takai *et al*., 2001; Kotelnikova, 2002; Baker *et al*., 2003; Onstott, 2005; Basso *et al*., 2009; Morozova *et al*., 2010).

Hungate tubes were again prepared as discussed previously for PYG and for the FW, with and without the addition of sandstone, for the inoculums, as well as for the negative controls. Each tube was pressurized to 2 bar (Figure 4.2A) with a gas ratio of 80% H_2 and 20% CO_2 (v/v) (Genthner *et al*., 1981), while using protective gear. Within the 2 bar, 20% (0.2 fraction of the total) had to be CO_2. This meant that the tubes were pressurized, without releasing gas, to 0.4 bar using CO_2 gas (99.99%) (2 bar x 0.2 fraction = 0.4 bar). To obtain this pressure, the CO_2 regulator was set to 40 kPa (0.4 bar). The other 80% (0.8 fraction of the total) had to be H_2, which meant that the tubes were further pressurized, without releasing gas, to 1.6 bar using H_2 gas (99.999%) (2 bar x 0.8 fraction = 1.6 bar). To obtain this pressure, the H_2 regulator was set to 200 kPa (2 bar).

To pressurize the tubes, sterile syringe-tipped, high pressure Masterflex® Norprene hoses (Cole-Parmer®) were connected to the regulators (Figure 4.2B and C). A sterile 0.2 µM syringe filter and a sterile needle were connected to the syringe (Figure 4.2D). To insert the CO_2, the gas tank was opened with the regulator set on 40 kPa (0.4 bar) and the hose was flushed for 30 seconds. The needle was inserted into the tube while the gas was flowing. The CO_2 was allowed to enter into the tube for five seconds, where after the tube was inverted for six seconds to allow the gas to equilibrate between the hose and the tube. The presence of bubbles was an indication that gas was entering the media. The tube was turned back and the needle was removed with the gas still flowing. The hose was flushed again for ten seconds before the next tube was pressurized with CO_2. To insert the H_2, the gas tank was opened with the regulator set on 200 kPa (2 bar) and the hose was flushed for 30 seconds. The needle was inserted into the tube, while the gas was flowing. The H_2 was allowed to enter into the tube for six seconds, where after the tube was inverted to ensure that gas was no longer entering and the needle was removed with the gas still flowing. The hose was flushed again before the next tube was pressurized with H_2. Before a needle was inserted into the tube, the blue chlorobutyl rubber stopper was first sterilized, by flaming it with 70% ethanol (EtOH).

The pressurized tubes were incubated on a rotary shaker (200 rpm), at 35°C and the OD_{605} was measured as discussed previously using a photoLab S6 photometer [Wissenschaftlich-Technische Werkstätten (WTW), Labotec®]. Growth studies continued for 48 hours and were done in triplicate for each media type. The OD values were plotted

against the time intervals to obtain the various growth curves and visual assessments were conducted on each completed growth study.

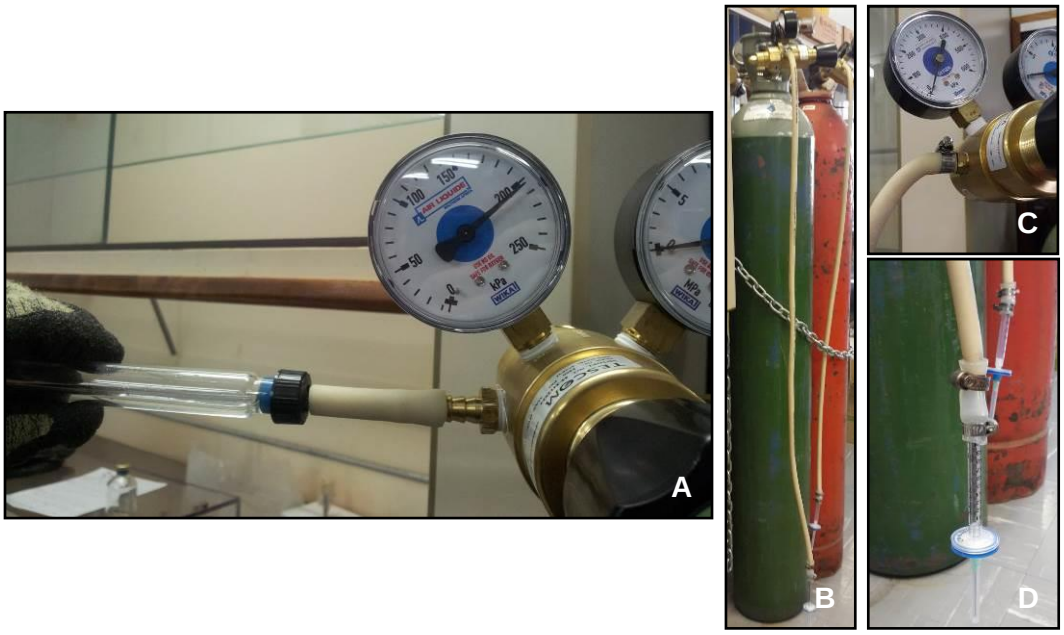

Figure 4.2: (A) A Hungate tube pressurized to 2 bar and (B-D) the syringe-tipped, high pressure hoses used to pressurize the tubes.

E. limosum cultures were stored at mid exponential phase (~18 hours), by preparing Hungate tubes (10 ml) with 2.5 ml glycerol (50% w/v), 7.5 µl resazurin (0.1% w/v), and 20 µl cysteine-HCl.H_2O (2.5% w/v) to each tube. The glycerol was degassed for one hour using nitrogen (N_2) gas (99.999%) and subsequently sterilized. The culture (2.5 ml) was added into each Hungate tube under anaerobic conditions (Section 4.3.1), and stored at -80°C.

4.3.4 Cultivation Conditions for the Subsurface Biome

To study the growth of the subsurface biome from the Star Diamonds mine under aerobic conditions, the nutritionally rich, non-selective LB medium (10 $g.L^{-1}$ peptone, 5 $g.L^{-1}$ yeast extract, 10 $g.L^{-1}$ NaCl, pH 7.0) (Sambrook *et al.*, 1989) was prepared aerobically using fissure water. The additional evaluation of the ability of the subsurface biome to grow in the fissure water alone was again done, with and without the addition of sandstone. Erlenmeyer flasks (1 L) containing 180 ml of the LB medium were prepared

and sterilized. Inoculums (10% v/v) were made under aerobic conditions using the fissure water containing the TFF concentrated subsurface biome (Section 3.3.6.3). When the fissure water alone was used as the growth medium, 200 ml of the concentrated subsurface biome was used directly. For the FW flasks that contained sandstone, 20 g crushed sandstone (Section 3.3.5) was added to the media before sterilization. Negative controls were prepared for each inoculum.

The flasks were incubated on a rotary shaker (200 rpm), at 35°C. For the time zero reading, 1 ml was immediately withdrawn and the OD was measured at 600 nm using a Spectronic® Genesys™ 5 spectrophotometer (Spectronic Instruments). This was repeated at each time interval. Growth studies continued for 32 hours and were done in triplicate for each media type. The OD values were plotted against the time intervals to obtain the various growth curves and microbial diversity assessments were conducted on each completed growth study using visual methods and molecular techniques.

To study the growth of the subsurface biome from the Star Diamonds mine under anaerobic conditions, as well as under low pressures, LB medium and FW, with and without the addition of sandstone, were prepared anaerobically in 20 ml Hungate tubes as discussed in Section 4.3.3 and the inoculums (10% v/v) were made with the TFF concentrated subsurface biome (Section 3.3.6.3). When the fissure water alone was used as the growth medium, 5 ml of the concentrated subsurface biome was used directly. For the pressure studies, the tubes were pressurized to 2 bar using a gas ratio of 80% H_2 and 20% CO_2 (v/v) (Section 4.3.3). The tubes were incubated and measured at OD_{605} as discussed in Section 4.3.3. Growth studies continued for 48 hours and were done in triplicate for each media type. Microbial diversity assessments were again conducted on each completed growth study using visual methods and molecular techniques.

4.3.5 Microbial Diversity Assessments of *Eubacterium limosum* and the Subsurface Biome using Visual Methods

Different staining and microscopy techniques were conducted on all the completed growth studies in order to assess whether any changes in diversity occurred, as well as

whether the cells were alive or dead. This included a negative stain using the Nigrosin dye as discussed in Section 3.3.6.8.1, a live/dead stain using the LIVE/DEAD® BacLight™ Bacterial Viability Kit (Molecular Probes, Inc., Invitrogen, Promega) as discussed in Section 3.3.6.8.2, and a Gram Stain as discussed in Section 3.3.6.8.3.

4.3.6 Microbial Diversity Assessments of the Subsurface Biome using Denaturing Gradient Gel Electrophoresis

DGGE analyses were conducted on the completed growth studies with the subsurface biome to assess whether any changes in diversity occurred under the various conditions.

4.3.6.1 Genomic DNA Isolation and Polymerase Chain Reaction

Genomic DNA was isolated using the NucleoSpin® Soil kit (Macherey-Nagel) as discussed in Section 3.3.6.6.1. A PCR was conducted to amplify the Archaeal 16S (~600 bp), Bacterial 16S (~1500 bp), and Eukaryal 18S (~1700 bp) rRNA gene fragments as discussed in Section 3.3.6.6.2 using the universal oligonucleotide primers for each gene (Section 3.3.6.6.2, Table 3.1). The PCR products were visualized on a 1% (w/v) agarose gel and purified (Section 3.3.6.6.2).

4.3.6.2 Nested Polymerase Chain Reaction

A nested DGGE PCR was conducted on all the purified samples to amplify the V3/V4 hypervariable regions for Archaea (~600 bp), Bacteria (~600 bp), and Eukarya (~600 bp) as discussed in Section 3.3.6.6.3 using the DGGE oligonucleotide primers for each gene (Section 3.3.6.6.3, Table 3.2). The PCR products were visualized on a 1% (w/v) agarose gel.

4.3.6.3 Denaturing Gradient Gel Electrophoresis, Sanger Sequencing and Analyses

The products from the nested DGGE PCR were used to construct preliminary diversity profiles using the DGGE Dcode™ universal mutation detection system (Bio-Rad Laboratories, Inc.) as discussed in Section 3.3.6.6.4. Selected bands were excised from the gel and the concentrations of the recovered DNA were increased through re-amplification of the V3/V4 hypervariable regions from the eluted DGGE products using the oligonucleotide primers as indicated in Section 3.3.6.6.5, Table 3.3. The re-amplified PCR products were visualized on a 1% (w/v) agarose gel and purified (Section 3.3.6.6.2).

Sequencing and analyses of the purified fragments were done as discussed in Section 3.3.6.6.6.

4.4 RESULTS AND DISCUSSIONS

4.4.1 Molecular Identification of the Positive Control Microorganism

4.4.1.1 Genomic DNA Isolation, Polymerase Chain Reaction and Transformation of the 16S rRNA Gene

The gDNA isolated from *E. limosum* (Section 3.3.6.6.1), was used to amplify the Bacterial 16S (~1500 bp) rRNA gene fragment (Figure 4.3) as discussed in Section 3.3.6.6.2.

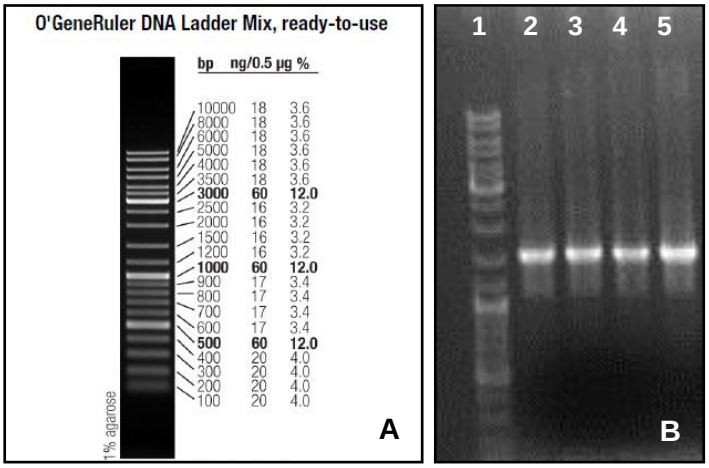

Figure 4.3: (A) The O'GeneRuler™ DNA Ladder Mix (Thermo Scientific) used to determine the size of the amplicons, and (B) the amplified 16S rRNA gene fragment from *E. limosum*. In lane 1, the O'GeneRuler™ DNA Ladder Mix is shown and in lanes 2 – 5, the 16S rRNA gene fragment.

Amplicons were obtained and the bands of interest were excised from the agarose gel and purified as discussed in Section 3.3.6.6.2. The purified PCR products were ligated into the pGEM®-T Easy Vector system (Promega) as discussed in Section 4.3.2.2, and transformed into *E. coli* One Shot TOP10 (Invitrogen) competent cells (Section 4.3.2.3).

4.4.1.2 Analyses of the 16S rRNA Gene

The insert was excised with a double digestion reaction (Figure 4.4B) using the restriction enzymes *Eco*RI and *Nde*I (Fermentas) as discussed in Section 4.3.2.4.

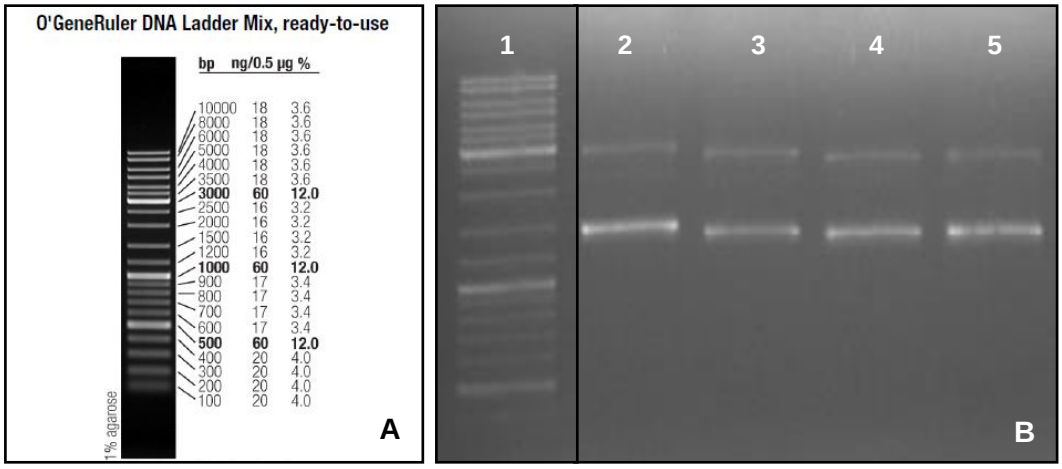

Figure 4.4: (A) The O'GeneRuler™ DNA Ladder Mix (Thermo Scientific) used to determine the size of the inserts, and (B) the double digestion profile for *E. limosum*. In lane 1, the O'GeneRuler™ DNA Ladder Mix are shown and in lanes 2 – 5, the ~3000 bp plasmid backbone and the ~1500 bp insert.

Positive ligation of the insert into the plasmid was obtained with the presence of the ~3000 bp plasmid backbone and the ~1500 bp insert. The inserts were purified (Section 3.3.6.6.2) and analyses were done as discussed in Section 4.3.2.4. Using the first five BLAST results, it was confirmed that the positive control microorganism were *E. limosum* (Table 4.2).

Table 4.2: BLAST results for the 16S rRNA gene sequence of *E. limosum*.

Accession	Description	Identity	E-Value
LC019782.1	*Eubacterium limosum* gene for 16S ribosomal RNA, partial sequence, strain: JCM 9978	99%	0.0
JQ085755.1	*Eubacterium limosum* strain ZL2 16S ribosomal RNA, partial sequence	99%	0.0
NR_113248.1	*Eubacterium limosum* strain JCM 6421 16S ribosomal RNA gene, partial sequence	99%	0.0
HM590802.1	*Eubacterium limosum* strain Tr5 16S ribosomal RNA gene, partial sequence	99%	0.0
NR_074533.1	*Eubacterium limosum* KIST612 strain KIST612 16S ribosomal RNA, complete sequence	99%	0.0

4.4.2 Experimental Layout for the Cultivation of *Eubacterium limosum* and the Subsurface Biome

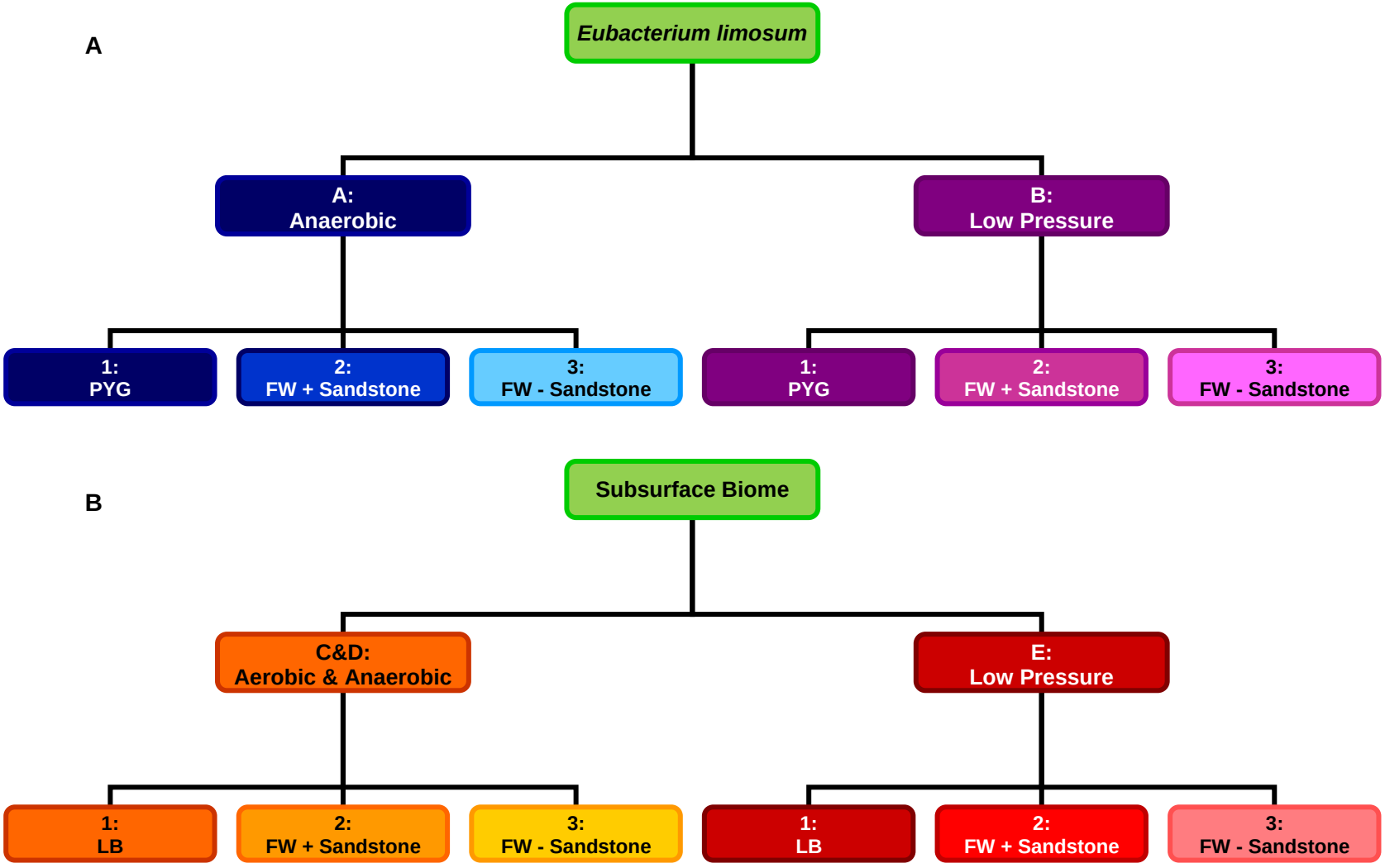

Figure 4.5: A summary of the experimental layout for the cultivation of (A) *E. limosum* and (B) the subsurface biome.

4.4.3 Cultivation and Assessments of *Eubacterium limosum*

Growth curves were obtained for *E. limosum* by analysing the various growth studies under anaerobic conditions and low pressure for 48 hours (Figure 4.6) as discussed in Section 4.3.3. The μ_{max} and t_d were calculated for growth in the PYG medium.

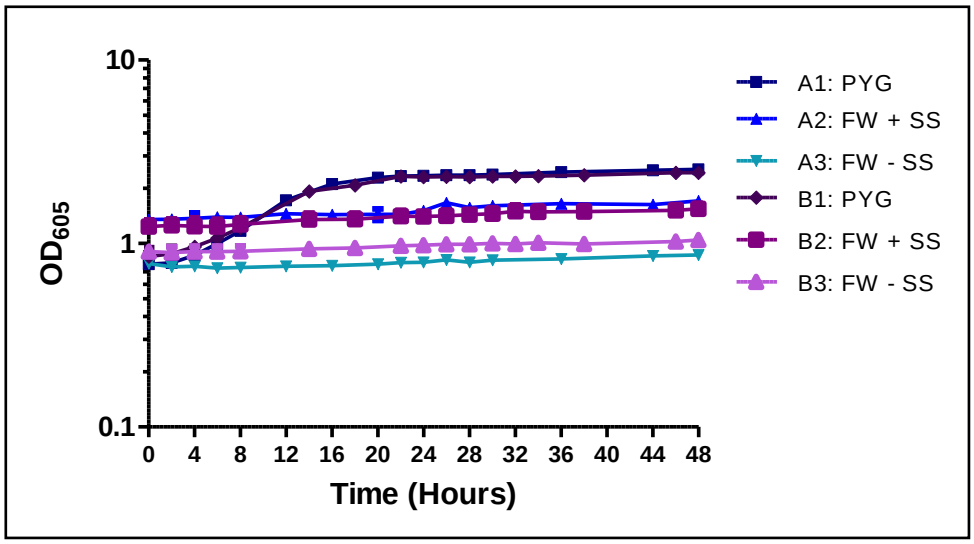

Figure 4.6: Growth curves for *E. limosum* under anaerobic conditions (A) in blue and low pressure (B) in purple (FW = fissure water, +SS = with sandstone, -SS = without sandstone).

From the results obtained, it can be seen that the pressure did not influence the growth of *E. limosum*, since growth curves were similar for the same type of medium used when anaerobic conditions were compared with low pressure. It can also be seen that exponential growth did not occur when the fissure water was used, indicating that the fissure water on its own did not provide all the necessary nutrients for *E. limosum* to grow optimally. The slight increase in the starting OD_{605} for the fissure water with sandstone (occurring for all the growth curves that contained sandstone throughout this chapter) was due to the weathering of the sandstone when in contact with the liquid. These sandstone particles are then detected when measuring the OD, but cannot be seen as growth and therefore it can be concluded that the presence of sandstone also had no effect on the growth, as the trends of the growth curves were similar for the fissure water, with and without the addition of sandstone.

As expected, the best biomass yields were obtained when *E. limosum* was grown in the PYG medium. A μ_{max} of 0.090 h^{-1} and a t_d of 7.68 hours were calculated for growth under anaerobic conditions, with a μ_{max} of 0.071 h^{-1} and a t_d of 9.81 hours for growth under low pressure. This indicated that growth under anaerobic conditions was slightly faster than growth under low pressure. In the literature, several different maximum growth rates are available for *E. limosum*, depending on which substrate was used for studying its growth under specific conditions (Mariotto *et al*., 1989; Le Bloas *et al*., 1993). However, the values for the maximum growth rates obtained in this study are similar to what Loubière & Lindley, (1991) described when studying the use of acetate as an additional co-substrate to improve the growth of *E. limosum* when CO_2 fixation is rate-limiting. They found that when *E. limosum* was grown as a batch culture on methanol/CO_2 in a medium supplemented with acetate, a short exponential growth phase was observed with a μ_{max} of 0.12 h^{-1}, followed by an extended period of decelerating growth. However, when *E. limosum* was grown in the absence of acetate (similar to growth in the PYG medium), growth proceeded at a lower maximum growth rate, having a μ_{max} of 0.075 h^{-1}.

Additional assessments were conducted on all the growth studies using different staining and microscopy techniques as discussed in Section 3.3.6.8. The negative controls remained sterile.

From the negative stain images (Figure 4.7), it can be seen that biomass was obtained for all the parameters tested and that the cells were alive.

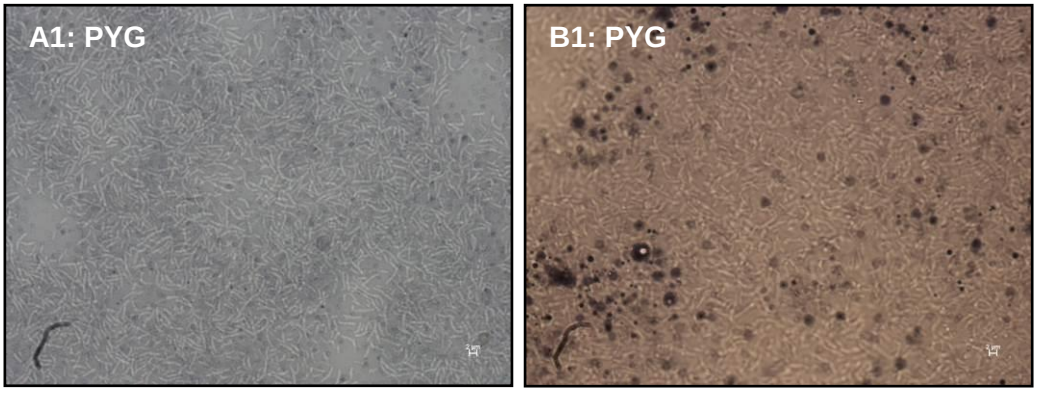

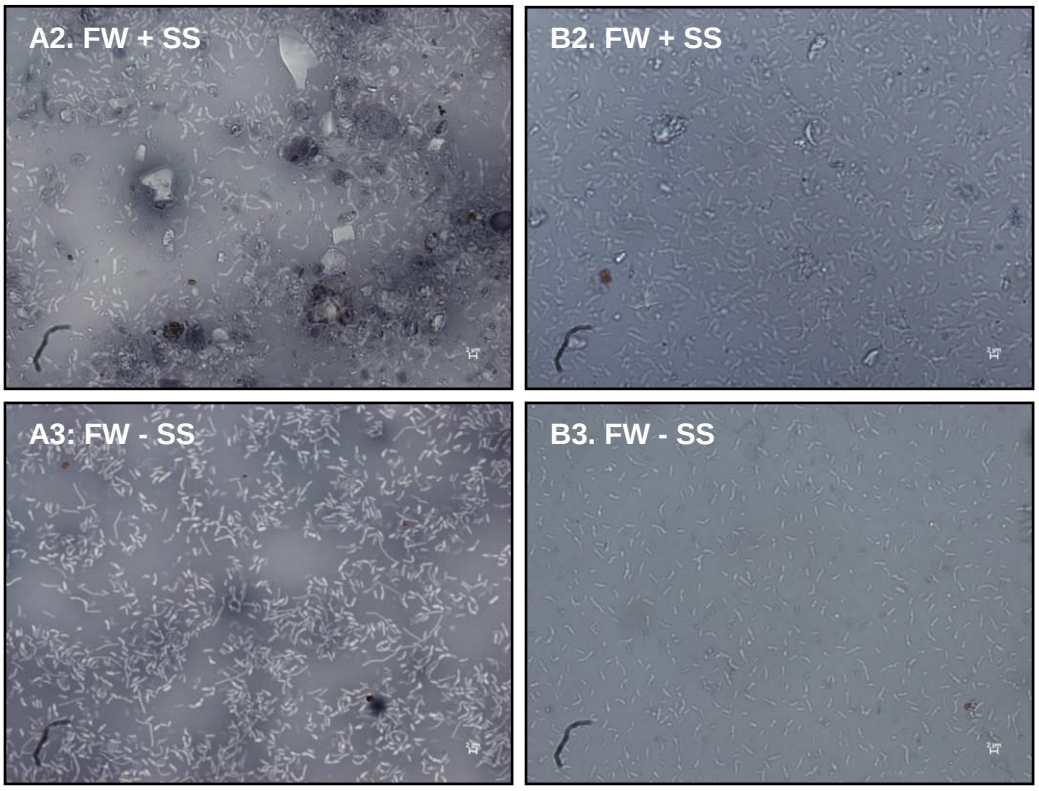

Figure 4.7: Negative stain images of *E. limosum* under anaerobic conditions (A) and low pressure (B). All scale bars are equal to 2 µm.

The live/dead stain images (Figure 4.8) confirmed the previous observations and that most cells stayed alive under all the parameters tested.

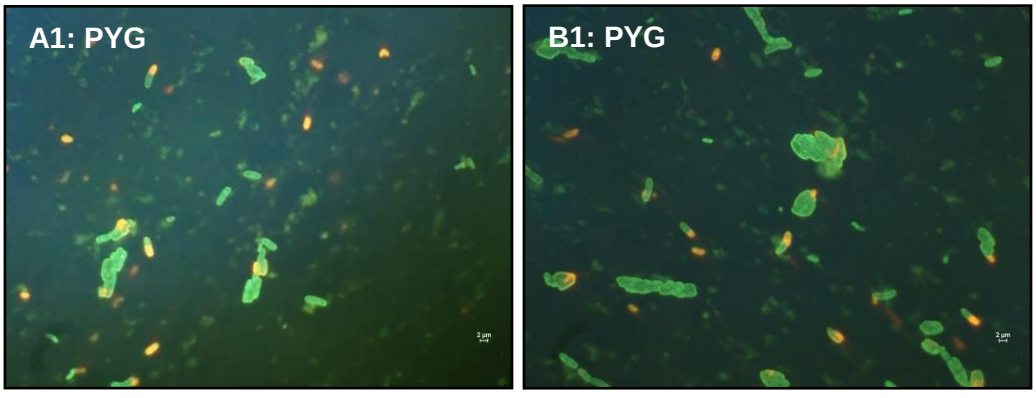

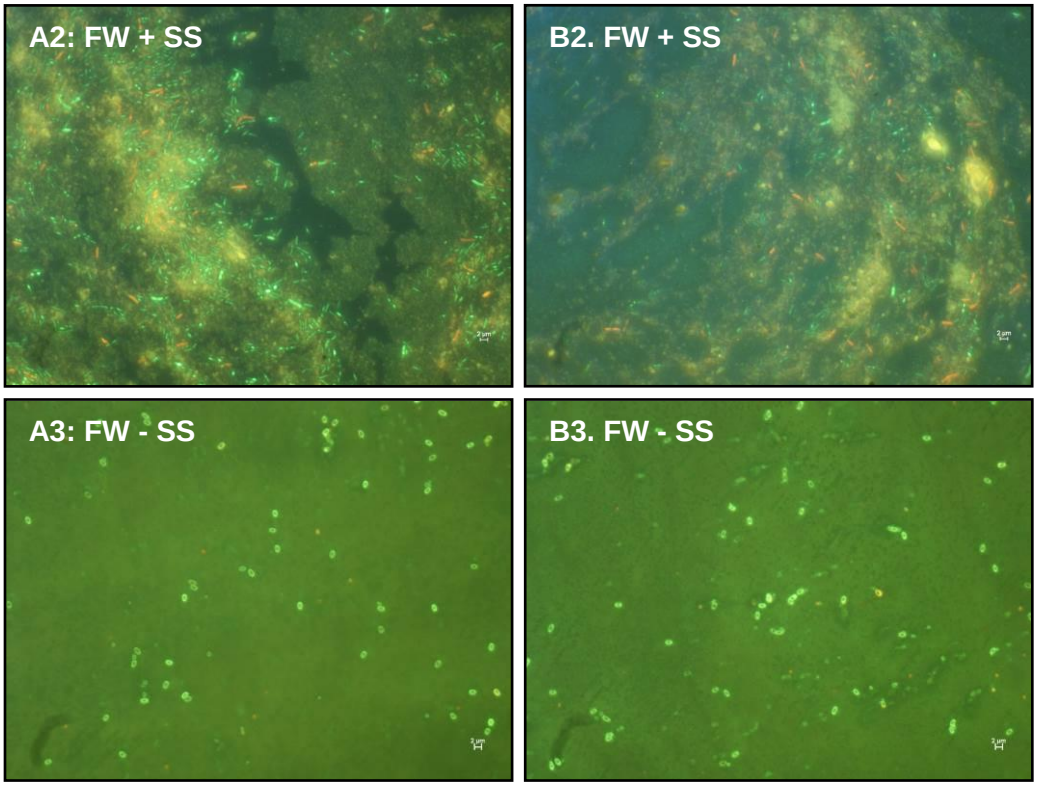

Figure 4.8: Live/dead stain images of *E. limosum* under anaerobic conditions (A) and low pressure (B). All scale bars are equal to 2 µm.

The Gram stain images (Figure 4.9) confirmed that *E. limosum* are, as described in the literature, a pure culture of Gram-positive rods (Song & Cho, 2015).

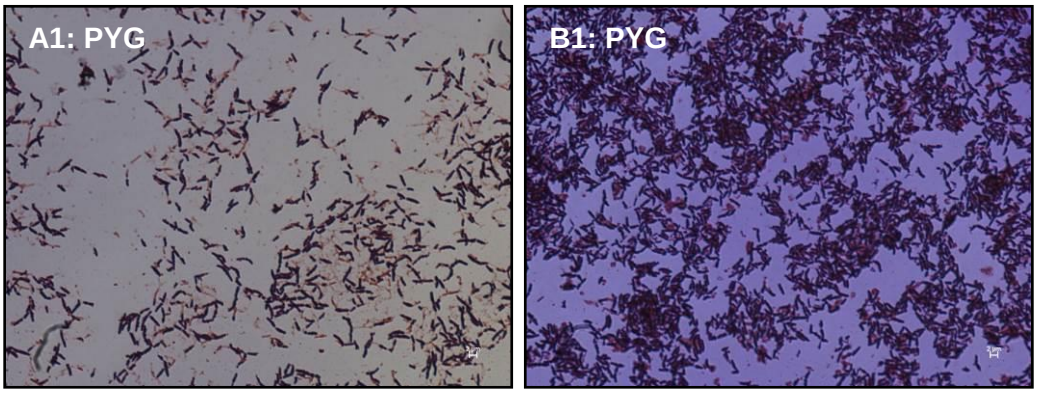

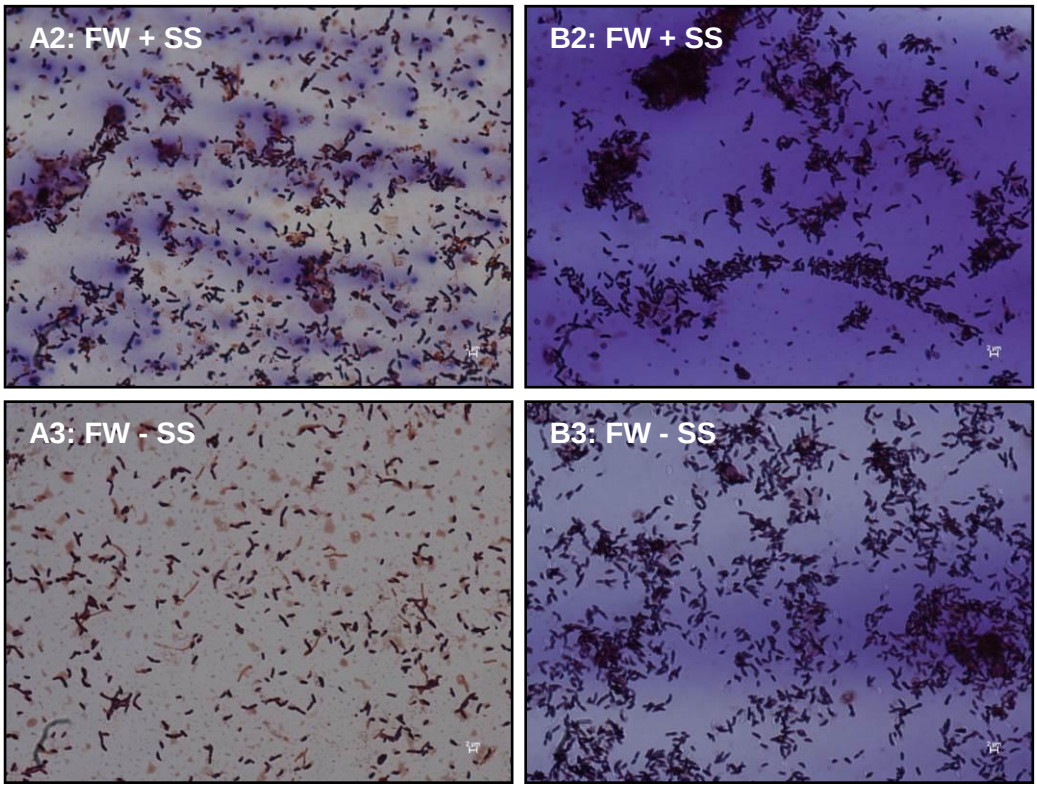

Figure 4.9: Gram stain images of *E. limosum* under anaerobic conditions (A) and low pressure (B). All scale bars are equal to 2 µm.

4.4.4 Cultivation and Assessments of the Subsurface Biome

Growth curves were obtained of the subsurface biome by analysing the various growth studies under aerobic conditions for 32 hours (Figure 4.10), as well as under anaerobic conditions and low pressure for 48 hours (Figure 4.11) as discussed in Section 4.3.4.

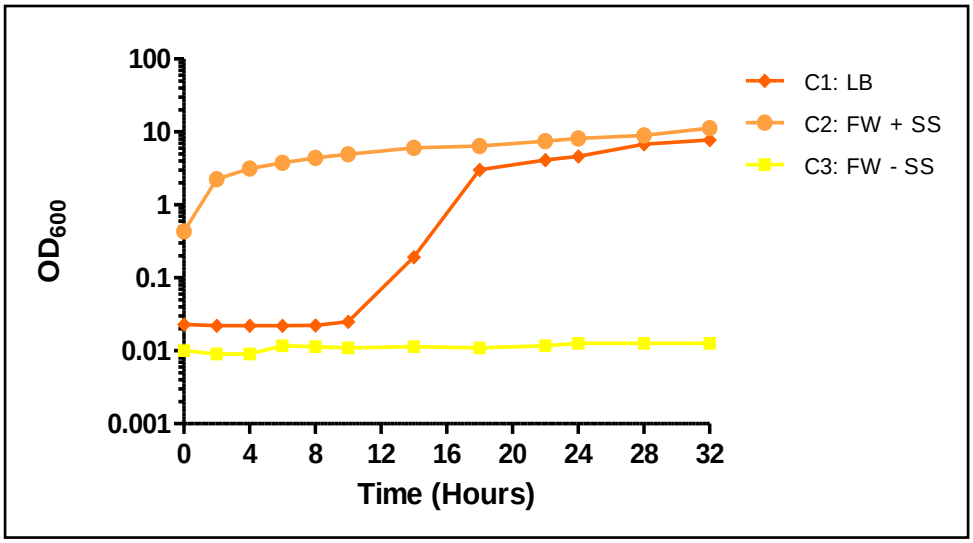

Figure 4.10: Growth curves of the subsurface biome under aerobic conditions (C) in orange/yellow (FW = fissure water, +SS = with sandstone, -SS = without sandstone).

Very high biomass yields were obtained when the subsurface biome was grown in LB medium, but in the fissure water alone, exponential growth did not occur. When sandstone was added to the fissure water, an initial increase in the biomass can be seen, where after it immediately started to reach a plateau. This indicated that the fissure water on its own did not provide the necessary nutrients for the subsurface biome to grow optimally and that the sandstone most likely contributed some of the nutrients initially needed for growth under aerobic conditions, but could not sustain the microorganisms for exponential growth.

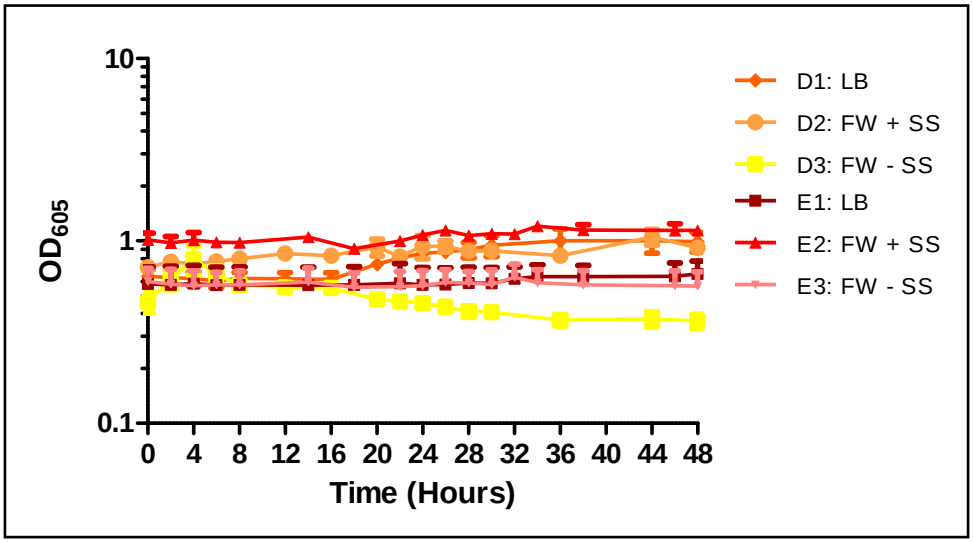

Figure 4.11: Growth curves of the subsurface biome under anaerobic conditions (D) in orange/yellow and low pressure (E) in red/pink (FW = fissure water, +SS = with sandstone, -SS = without sandstone).

From the results of the anaerobic and low pressure growth studies, the best biomass yields were obtained when the subsurface biome was grown in the LB medium, without pressure. As for the rest of the growth studies, exponential growth did not occur under any of the conditions the biome was subjected to. As described in the literature, most of the deep subsurface microorganisms are living under extreme energy limiting conditions where they are likely to be inactive or to display exceptionally low metabolic activity (Jørgensen & D'Hondt, 2006; Jørgensen & Boetius, 2007). Geochemical evidence suggested that the *in situ* microbial metabolism in porous subsurface environments was estimated to be in the nano- to micromolar range per year, with an average turnover time for a subsurface microbial cell estimated to be decades or centuries (Phelps *et al*., 1994; Onstott *et al*., 2009). It was also found that even though subsurface microorganisms are dormant or living at extremely low metabolic rates, their diversity and persistence could offer valuable insights into life in the extremis (Phelps *et al*., 1994; Teske, 2005; Onstott *et al*., 2009). Therefore, it was not expected to obtain high biomass yields with the subsurface biome, especially when grown in the fissure water without any additional nutrients, but it was important to have a biome that could survive the various conditions and stay metabolically active to continue to contribute to carbon cycling.

Additional assessments were conducted on all the growth studies using different staining and microscopy techniques (Section 3.3.6.8) and DGGE analyses (Section 4.3.6). The negative controls remained sterile.

From the negative stain images (Figure 4.12), it can be seen that biomass was obtained for all the parameters tested, even though it was extremely low and that the cells were alive. The biomass from the growth studies with the fissure water contained microorganisms with varying morphology and distinctive structures, but the morphology was less diverse and more uniform for the LB medium. This suggests that when the biome was grown in the nutritionally rich LB medium, the conditions encouraged the growth or domination of selected species. As discussed in Section 3.3.6, it is very likely that the diversity within a community will change if the parameters from the culture conditions differ even slightly from the conditions of their original environment. This will introduce biases in the diversity of the community due to the methods used for isolation (Dunbar *et al*., 1997; Liu *et al*., 1997). Therefore, changes in the diversity could occur when the biome is exposed to different nutritional environments.

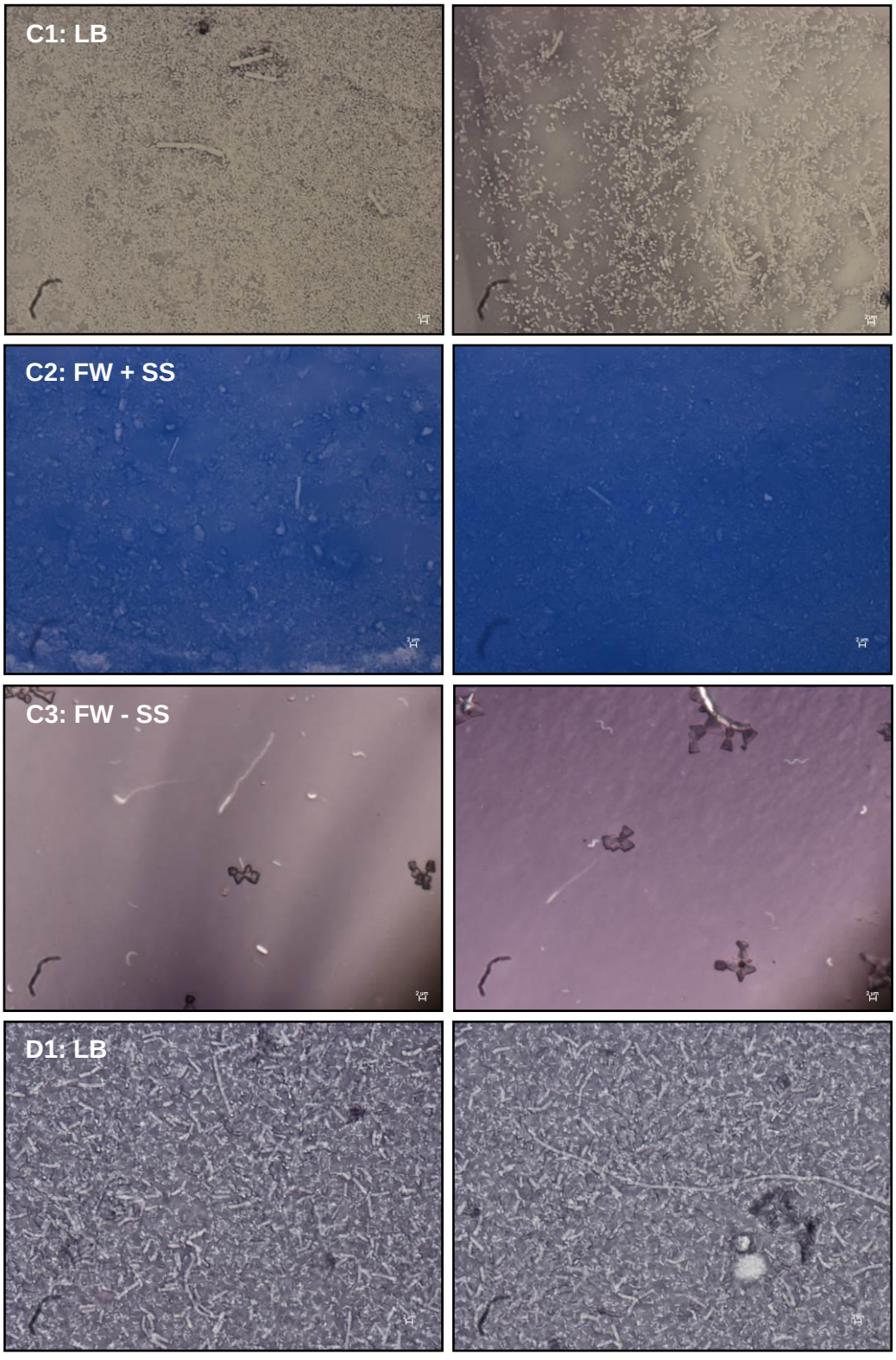
C1: LB
C2: FW + SS
C3: FW - SS
D1: LB

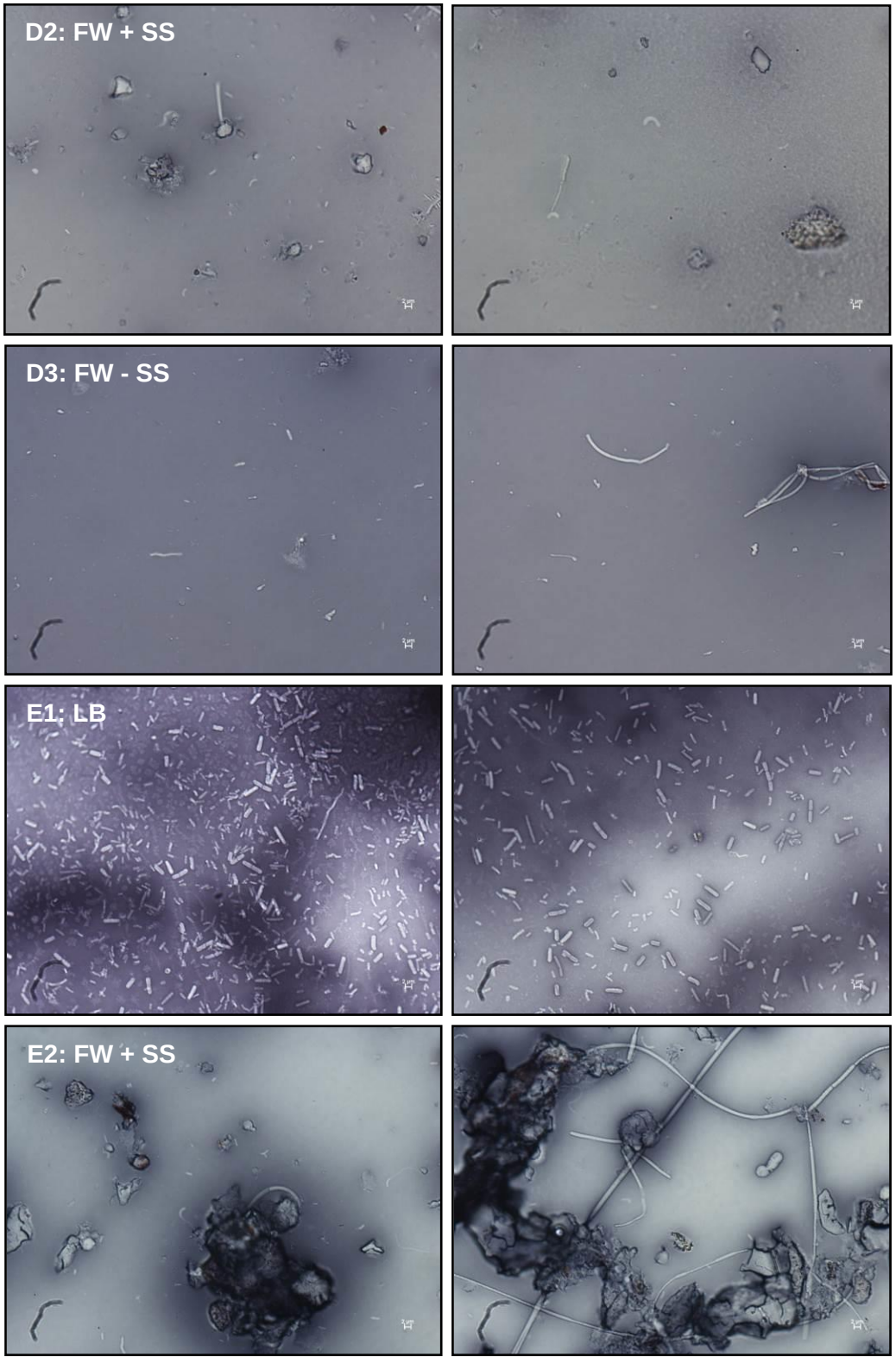
D2: FW + SS
D3: FW - SS
E1: LB
E2: FW + SS

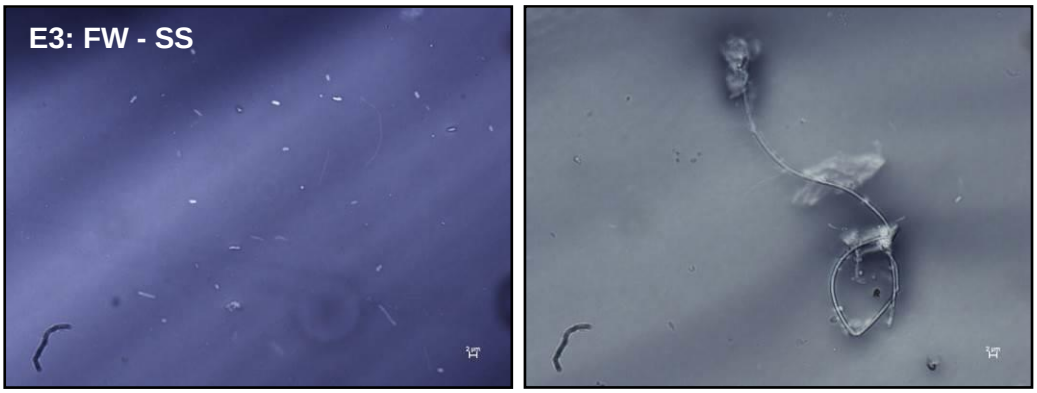

Figure 4.12: Negative stain images of the subsurface biome under aerobic conditions (C), anaerobic conditions (D), and low pressure (E). All scale bars are equal to 2 µm.

The live/dead stain images (Figure 4.13) indicated that the subsurface biome stayed alive under all the parameters tested.

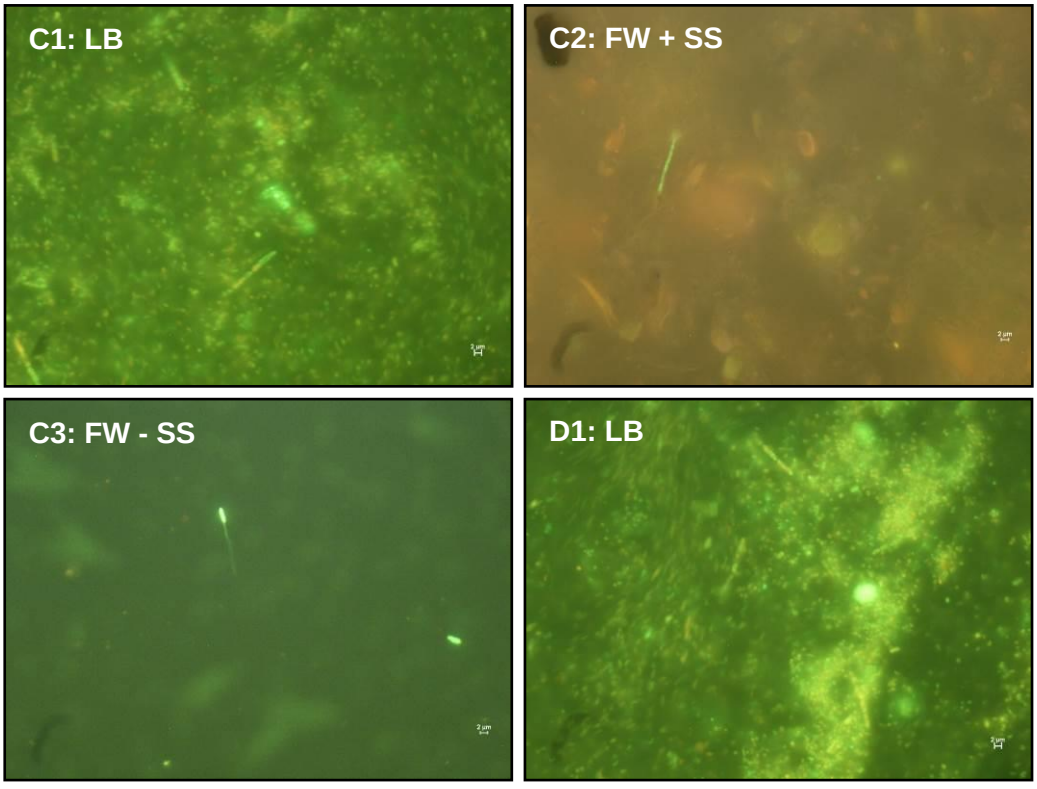

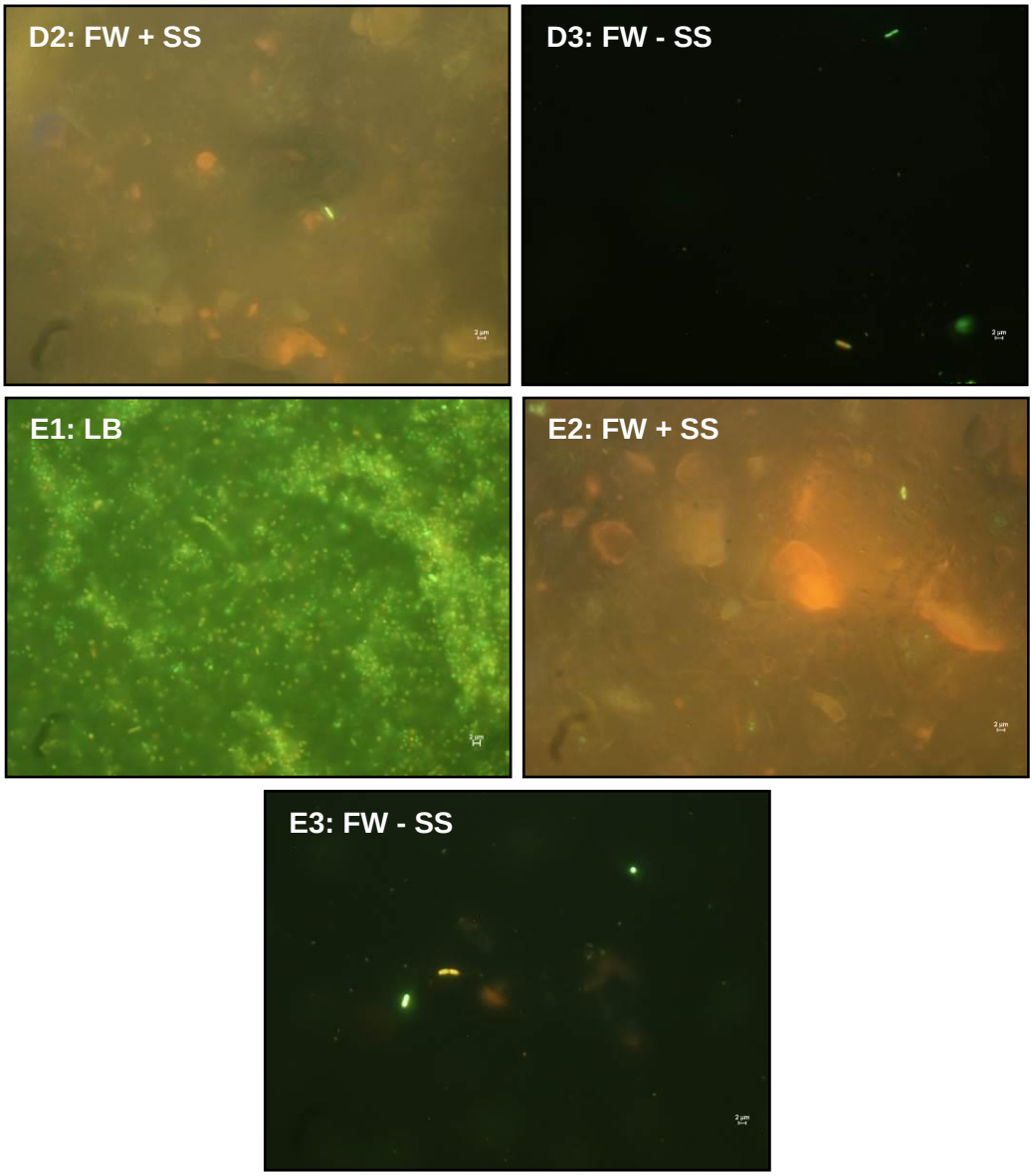

Figure 4.13: Live/dead stain images of the subsurface biome under aerobic conditions (C), anaerobic conditions (D), and low pressure (E). All scale bars are equal to 2 µm.

The Gram stain images (Figure 4.14) indicated that both Gram-positive and Gram-negative microorganisms were present, again confirming the various morphological structures.

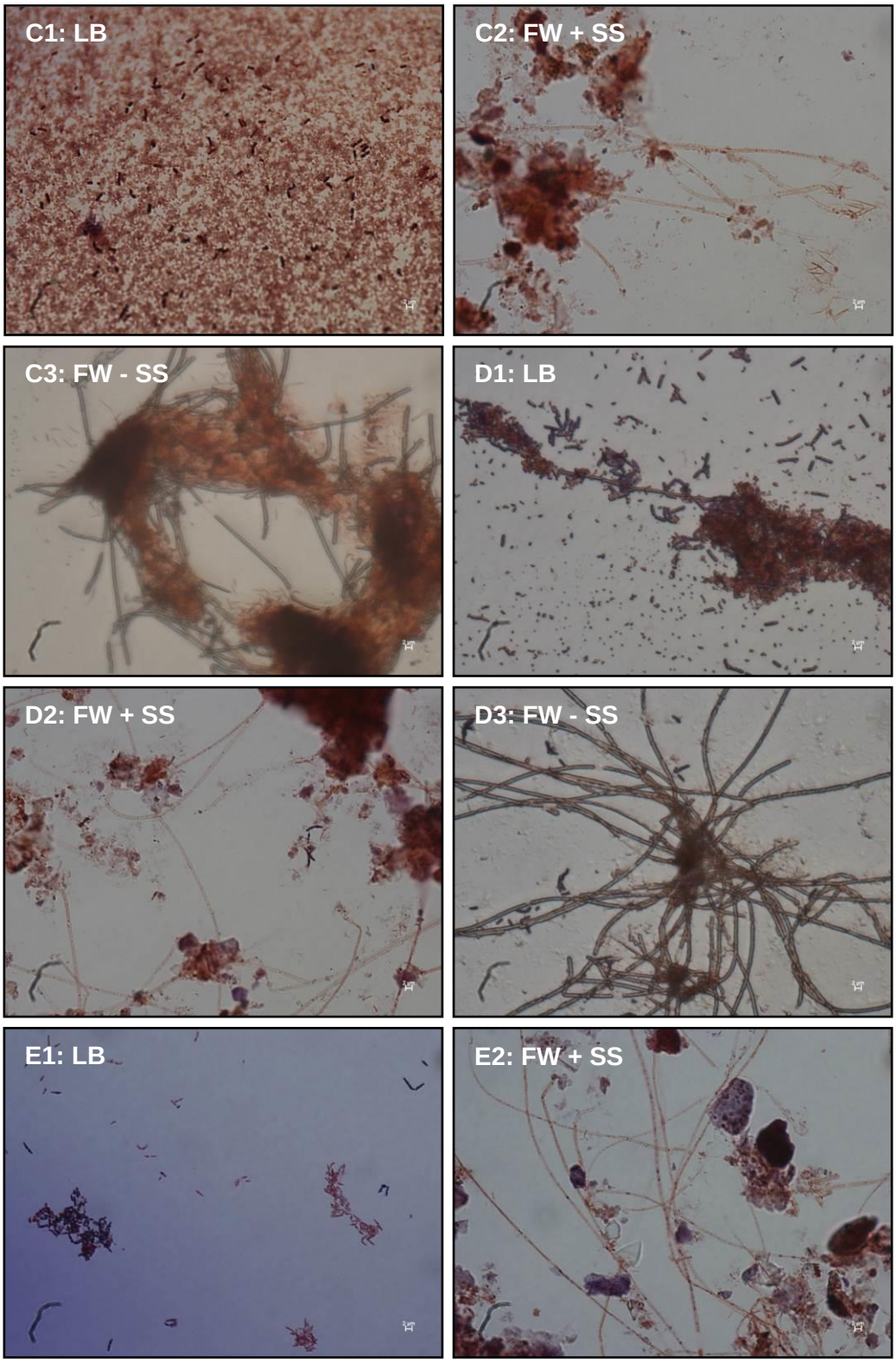
C1: LB
C2: FW + SS
C3: FW - SS
D1: LB
D2: FW + SS
D3: FW - SS
E1: LB
E2: FW + SS

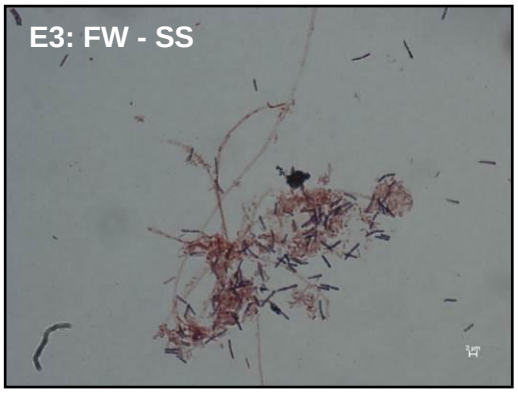

Figure 4.14: Gram stain images of the subsurface biome under aerobic conditions (C), anaerobic conditions (D), and low pressure (E). All scale bars are equal to 2 µm.

4.4.5 Microbial Diversity Assessments of the Subsurface Biome using Denaturing Gradient Gel Electrophoresis

4.4.5.1 Genomic DNA Isolation and Polymerase Chain Reaction

Genomic DNA was isolated from all the growth studies with the subsurface biome (Section 3.3.6.6.1) and used to amplify the Archaeal 16S (~600 bp) (Figure 4.15B), Bacterial 16S (~1500 bp) (Figure 4.15C), and Eukaryal 18S (~1700 bp) (Figure 4.15D) rRNA gene fragments as discussed in Section 3.3.6.6.2. These experiments were done over a period of time and the agarose gels were not visualized simultaneously.

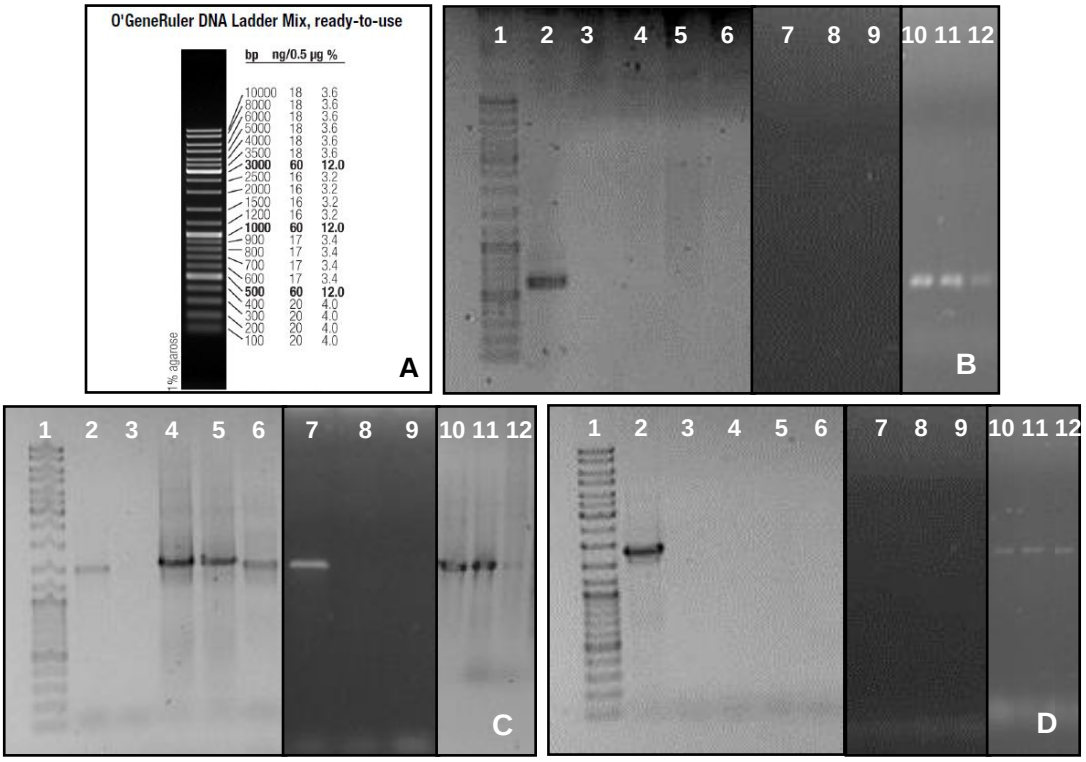

Figure 4.15: (A) The O'GeneRuler™ DNA Ladder Mix (Thermo Scientific) used to determine the size of the amplicons, with the amplified rRNA gene fragments for (B) Archaea, (C) Bacteria, and (D) Eukarya. In lane 1, the O'GeneRuler™ DNA Ladder Mix is shown. Lanes 2 and 3 contain the positive and negative controls, respectively. Lanes 4 – 6 contain the LB, FW + SS, and FW - SS from the aerobic growth studies. Lanes 7 – 9 contain the LB, FW + SS, and FW - SS from the anaerobic growth studies. Lanes 10 – 12 contain the LB, FW + SS, and FW - SS from the low pressure growth studies.

For the aerobic growth studies, amplicons were obtained for LB, FW + SS, and FW – SS, but only for the Bacteria domain. For the anaerobic growth studies only one amplicon was obtained, which was with LB for the Bacteria domain. For the low pressure growth studies, amplicons were obtained for LB, FW + SS, and FW – SS for all three domains. This suggests that changes in the diversity could occur when the biome is exposed to different physiological growth environments. As discussed in Chapter 1, several kinds of microbial metabolism have been described, which includes the obligate aerobes that need oxygen to grow, the obligate anaerobes that are inactivated in the presence of normal atmospheric levels of oxygen, the facultative anaerobes that can grow with or without oxygen, the microaerophiles that need oxygen to survive, but only at levels that are lower than the concentration of oxygen in the atmosphere, and the

aerotolerant microorganisms that do not need oxygen to grow, but are not inactivated in the presence thereof (Prescott *et al*., 1996). The diversity studies of the subsurface biome (Chapter 3) indicated that microorganisms with chemolithoautotrophic, as well as heterotrophic metabolisms are present in the fissure water, and therefore it was expected that changes in the diversity would occur in the different physiological growth environments the subsurface biome was subjected to. The bands of interest were excised from the agarose gel and purified as discussed in Section 3.3.6.6.2.

4.4.5.2 Nested Polymerase Chain Reaction

The purified PCR products were used to amplify the V3/V4 hypervariable regions for Archaea (~600 bp) (Figure 4.16B), Bacteria (~600 bp) (Figure 4.16C), and Eukarya (~600 bp) (Figure 4.16D) using a nested DGGE PCR as discussed in Section 3.3.6.6.3. Amplicons were obtained for the V3/V4 hypervariable regions from all the samples.

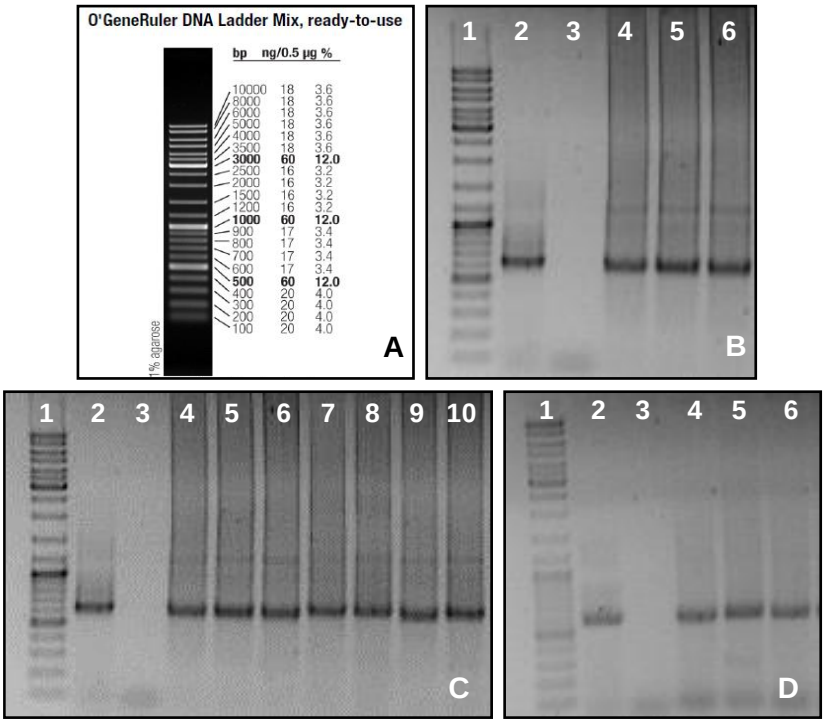

Figure 4.16: (A) The O'GeneRuler™ DNA Ladder Mix (Thermo Scientific) used to determine the size of the amplicons with the amplified V3/V4 hypervariable regions for (B) Archaea, (C) Bacteria, and (D) Eukarya. In lane 1, the O'GeneRuler™ DNA Ladder Mix is shown. Lanes 2 and 3 contain the positive and negative controls, respectively. The DGGE PCR amplicons are shown in the rest of the lanes.

4.4.5.3 Denaturing Gradient Gel Electrophoresis, Sanger Sequencing and Analyses

The DGGE PCR products were used to construct a preliminary diversity profile for Archaea (Figure 4.17A), Bacteria (Figure 4.17B), and Eukarya (Figure 4.17C) through the use of DGGE as discussed in Section 3.3.6.6.4.

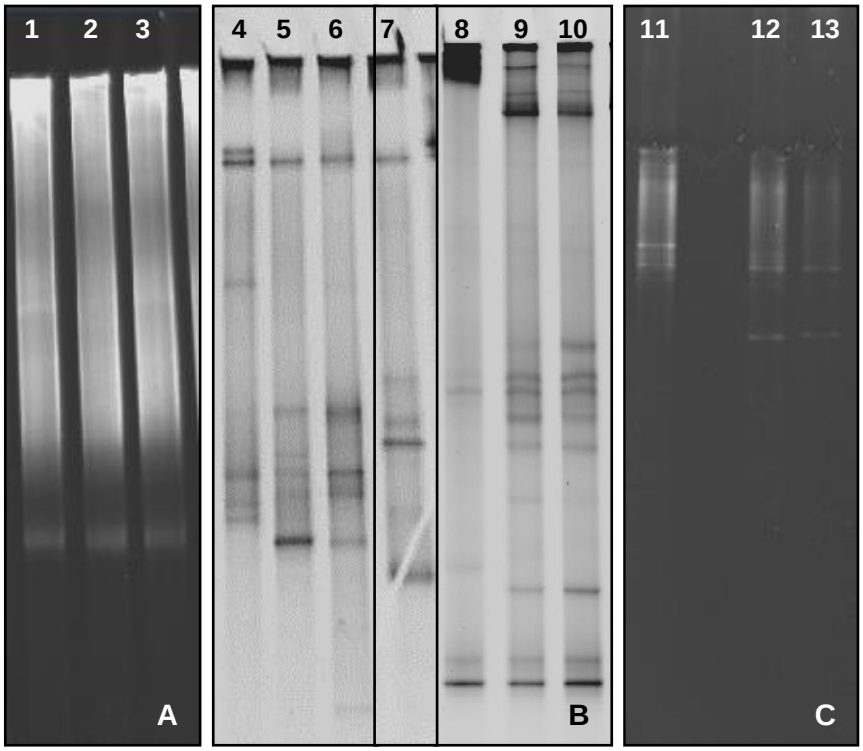

Figure 4.17: DGGE diversity profiles for (A) Archaea, (B) Bacteria, and (C) Eukarya. Lanes 1 – 3, 8 – 10, and 11 – 13 contain the low pressure growth studies, each time in the order of LB, FW + SS, and FW – SS. Lanes 4 – 6 contain the aerobic growth studies in the order of LB, FW + SS, and FW – SS. Lane 7 contain the anaerobic growth study for LB.

The DGGE profiles for the Bacteria and the Eukarya stayed mostly consistent for the fissure water, with and without the addition of the sandstone, indicating that the sandstone did not greatly influence the diversity. Growth in the fissure water with an inadequate nutrient supply has to happen under extreme energy limiting conditions and therefore, as discussed in Section 4.4.4, the microorganisms were most likely to be inactive or to display exceptionally low metabolic activity. Thus, microbial mineral dissolution from the sandstone could not have happened within the limited amount of

time the microorganisms were exposed to the sandstone during the growth studies and therefore, the potential to use the sandstone as a possible nutrient source could not occur and as a result, no profile changes in the diversity was observed. However, except for the Archaea, the profiles changed completely when grown in the LB medium. This confirmed the suggestions from the different staining images (Section 4.4.4), that the nutritional differences could influence the diversity.

Even though the Bacteria were the dominant domain throughout all the parameters tested, the Archaea was the least affected by the nutritional differences in the media, as their profiles stayed fairly consistent. As discussed in Chapter 3, Bacteria is the domain that generally dominate the subsurface, with the microbial activities that dominate these extreme environments being fermentation, methanogenesis, and sulphate-reduction - the more important steps in the degradation of organics in the biogeochemical carbon cycle (Banfield *et al*., 1999; Takai *et al*., 2001; Kotelnikova, 2002; Baker *et al*., 2003; Newberry *et al*., 2004; Onstott, 2005; Webster *et al*., 2006; Fry *et al*., 2008; Basso *et al*., 2009; Morozova *et al*., 2010; Ragon *et al*., 2013). However, studies conducted by Morozova *et al*., (2010), on the composition and activity of the microbial community of a saline CO_2 storage aquifer, revealed temporal out-competition of the sulphate-reducing Bacteria by the methanogenic Archaea, but the Bacteria was ultimately able to adapt to the extreme conditions of the deep subsurface and the changes under unusual conditions. This indicates that the Eukarya will most likely not be able to survive and adapt to CCS conditions, and therefore will probably not play a major role, if any, in carbon cycling in the subsurface.

Sequencing and analyses were conducted on selected DGGE bands as discussed in Sections 3.3.6.6.5 and 3.3.6.6.6. After the aerobic growth studies were completed, only the Bacterial domain was found to be present, which was dominated by the Proteobacteria phylum, mainly consisting of the Alpha- and Gammaproteobacteria classes. This was followed by the Firmicutes phylum, consisting of the Bacilli class and the Actinobacteria class of the Bacteriodetes phylum. For the anaerobic growth studies in these conditions, again only the Bacterial domain was present and was dominated by the Gammaproteobacteria and the Clostridia class from the Firmicutes phylum. For the low pressure growth studies, all three domains of life were found to be present. For the Bacterial domain, the Proteobacteria prevailed as the dominating phylum, consisting of

the Alpha-, Beta-, and Gammaproteobacteria classes. This was followed by the Firmicutes phylum, consisting of the Bacilli class. Within the Archaeal domain, the main class was the Thermoprotei from the Crenarchaeota phylum. The Eukaryal domain contained the Ascomycota, the Basidiomycota, the Ochrophyta, the Alveolata, the Glomeromycota, and the Heterokontophyta. This confirmed that changes in the diversity did occur when the biome was exposed to different physiological conditions and that microorganisms with chemolithoautotrophic, as well as heterotrophic metabolisms were able to survive the various conditions.

4.5 CONCLUSIONS

The positive control microorganism, *E. limosum*, was able to grow and produce high biomass yields in a nutritionally rich medium, under both anaerobic and low pressure conditions, with a μ_{max} similar to that which has been reported in the literature. It was found that the introduction of low pressure did not affect the growth of *E. limosum*, which was expected, since this microorganism is described in the literature to be able to grow under pressures of >1 atm. High biomass yields were obtained when the subsurface biome was grown in a rich medium under aerobic conditions. However, when both *E. limosum* and the subsurface biome was grown in the fissure water, exponential growth did not occur, indicating that the fissure water on its own did not provide all the necessary nutrients for optimum growth. The addition of sandstone also had no effect on growth. Although exponential growth did not occur for all the parameters tested, biomass was obtained and it was confirmed that the microorganisms were still viable and metabolically active.

In Chapter 3, characterization of the fissure water showed a sustained reducing environment with the presence of iron, nitrate, sulphate, and hydrogen with low levels of dissolved oxygen. Accordingly, the diversity studies of the subsurface biome indicated that microorganisms with chemolithoautotrophic and heterotrophic metabolisms are present. From this it was expected that selected species within the subsurface biome should be able to grow under aerobic and anaerobic conditions and that changes in the diversity would occur when the biome was exposed to different nutritional environments, as well as different physiological growth conditions. These changes were observed after the subsurface biome was grown under the various growth conditions and confirmed that microorganisms with chemolithoautotrophic, as well as heterotrophic metabolisms were able to survive. Care has to be taken when growth studies with subsurface biomes are done, as these biomes contain complex physiological individuals. Analyses may not always reveal the true minor community composition and often, this excludes knowledge of their specific contributions. As described in the literature, most of the deep subsurface microorganisms are living under extreme energy limiting conditions where they are likely to be inactive or to display exceptionally low metabolic activities (Phelps *et al*., 1994; Onstott *et al*., 2009), thus, viability may ultimately prove to be more important than specific diversity changes or biomass yields for carbon cycling studies.

4.6 REFERENCES

- **Bainotti, A.E., Yamaguchi, K., Nakashimada, Y. and Nishio, N.** (1998). Kinetics and Energetics of *Acetobacterium* sp. in Chemostat Culture on Methanol-CO_2. *Journal of Fermentation and Bioengineering*. **85(2)**:223-229.

- **Baker, B.J., Moser, D.P., MacGregor, B.J., Fishbain, S., Wagner, M., Fry, N.K., Jackson, B., Speolstra, N., Loos, S., Takai, K., Sherwood Lollar, B., Fredrickson, J.K., Balkwill, D., Onstott, T.C., Wimpee, C.F. and Stahl, D.A.** (2003). Related Assemblages of Sulphate Reducing Bacteria Associated with Ultra Deep Gold Mines of South Africa and Deep Basalt Aaquifers of Washington State. *Environ Microbiol*. **5(4)**:267–277.

- **Balch, W.E. and Wolfe, R.S.** (1976). New Approach to the Cultivation of Methanogenic Bacteria: 2-Mercaptoethanesulfonic Acid (HS-CoM)-Dependent Growth of *Methanobacterium ruminantium* in a Pressurized Atmosphere. *Applied and Environmental Microbiology*. **23(6)**:781-791.

- **Banfield, J.F., Barker, W.W., Welch, S.A. and Taunton, A.** (1999). Biological Impact on Mineral Dissolution: Application of the Lichen Model to Understanding Mineral Weathering in the Rhizosphere. *Proc. Natl. Acad. Sci*. **96**:3404-3411.

- **Basso, O., Lascourreges, J.F., Le Borgne, F., Le Goff, C. and Margot, M.** (2009). Characterization by Culture and Molecular Analysis of the Microbial Diversity of a Deep Subsurface Gas Storage Aquifer. *Res. Microbiol*. **160**:107–116.

- **Boone, D.R. and Bryant, M.P.** (1980). Propionate-Degrading Bacterium, *Syntrophobacter wolinii* sp. nov. gen. nov., from Methanogenic Ecosystems. *Applied and Environmental Microbiology*. **40(3)**:626-632.

- **Boonyaratanakornkit, B.B., Miao, L.Y. and Clark, D.S.** (2007). Transcriptional Responses of the Deep-Sea Hyperthermophile *Methanocaldococcus jannaschii* under Shifting Extremes of Temperature and Pressure. *Extremophiles*. **11**:495-503.

- **Bothun, G.D., Knutson, B.L., Berberich, J.A., Strobel, H.J. and Nokes, S.E.** (2004). Metabolic Selectivity and Growth of *Clostridium thermocellum* in Continuous Culture under Elevated Hydrostatic Pressure. *Appl Microbiol Biotechnol*. **65**:149-157.

- **Bryant, M.P.** (1972). Commentary on the Hungate Technique for Culture of Anaerobic Bacteria. *The American Journal of Clinical Nutrition*. 1324-1328.

- **Drake, H.L.** (1994). Acetogenesis, Acetogenetic Bacteria, and the Acetyl-CoA "Wood/Ljungdahl" Pathway: Past and Current Perspectives. In Acetogenesis. *Chapman and Hall Publishers*. (Drake H.L. ed.).

- **Dunbar, J., White, S. and Forney, L.** (1997). Genetic Diversity through the Looking Glass: Effect of Enrichment Bias. *Applied and Environmental Microbiology*. **63(4)**:1326-1331.

- **Fakruddin, M. and Mannan, K.S.B.** (2013). Methods for Analyzing Diversity of Microbial Communities in Natural Environments. *Ceylon Journal of Science (Bio. Sci.)*. **42(1)**:19-33.

- **Finegold, S.M., Sutter, V.L. and Mathisen, G.E.** (1983). Normal Indigenous Intestinal Flora. Chapter 1 in Human Intestinal Microflora in Health and Disease. *Academic Press*. (Hentges D.J. ed.).

- **Fry, J.C., Parkes, R.J., Cragg, B.A., Weightman, A.J. and Webster, G.** (2008). Prokaryotic Biodiversity and Activity in the Deep Subseafloor Biosphere. *FEMS Microbiol.Ecol*. **66**:181-196.

- **Genthner, B.R. and Bryant, M.P.** (1982). Growth of *Eubacterium limosum* with Carbon Monoxide as the Energy Source. *Applied and Environmental Microbiology*. **43(1)**:70-74.

- **Genthner, B.R., Davis, C.L. and Bryant, M.P.** (1981). Features of Rumen and Sewage Sludge Strains of Eubacterium limosum, a Methanol- and H_2-CO_2-Utilizing Species. *Applied and Environmental Microbiology*. **42(1)**:12-19.

- **Girbal, L., Örlygsson, J., Reinders, B.J. and Gottschal, J.C.** (1997). Why Does *Clostridium acetireducens* not use Interspecies Hydrogen Transfer for Growth on Leucine? *Current Microbiology*. **35**:155-160.

- **Glossner, A.** (2013). Terminal Microbial Metabolisms in the Deep Subsurface under Conditions Relevant to CO2 Sequestration and Enhancing Methanogenesis from Coal. *PhD Thesis, Colorado School of Mines*.

- **Hanahan, D.** (1983) Studies on Transformation of *E. coli* with Plasmid. *Journal of Molecular Biology.* **166**:557-580.

- **Hiraki, T., Sekiguchi, T., Kato, C., Hatada, Y., Maruyama, T., Abe, F. and Konishi, M.** (2012). New Type of Pressurized Cultivation Method Providing Oxygen for Piezotolerant Yeast. *Journal of Bioscience and Bioengineering*. **113(2)**:220-223.

- **Hungate, R.E. and Macy, J.** (1973). The Roll-Tube Method for Cultivation of Strict Anaerobes. *Bull. Ecol. Comm. (Stockholm)*. **17**:123-125.

- **Jørgensen, B.B and Boetius, A.** (2007). Feast and Famine – Microbial Life in the Deep-Sea Bed. *Nature Reviews Microbiology*. **5**:770-781.

- **Jørgensen, B.B. and D'Hondt, S.** (2006). ECOLOGY: A Starving Majority Deep Beneath the Seafloor. *Science*. **314**:932-934.

- **Kotelnikova, S.** (2002). Microbial Production and Oxidation of Methane in Deep Subsurface. *Earth-Sci. Rev*. **58**:367–395.

- **Krumholz, L.R., Sharp, R. and Fishbain, S.S.** (1996). A Freshwater Anaerobe Coupling Acetate Oxidation to Tetrachloroethylene Dehalogenation. *Applied and Environmental Microbiology*. **62(11)**:4108-4113.

- **Le Bloas, P., Guilbert, N., Loubière, P. and Lindley, N.D.** (1993). Growth Inhibition and Pyruvate Overflow during Glucose Metabolism of *Eubacterium limosum* are related to a Limited Capacity to Reassimilate CO_2 by the Acetyl-CoA Pathway. *Journal of General Microbiology*. **139**:1861-1868.

- **Leclerc, M., Bernalier, A., Donadille, G. and Lelait, M.** (1997). H_2/CO_2 Metabolism in Acetogenic Bacteria Isolated from the Human Colon. *Anaerobe*. **3**:307-315.

- **Lelait, M. and Grivet, J.P.** (1996). Carbon Metabolism in *Eubacterium limosum*: a ^{13}C NMR Study. *Anaerobe*. **2**:181-189.

- **Lin, L., Hall, J., Lippmann-Pipke, J., Ward, J.A., Sherwood Lollar, B., DeFlaun, M., Rothmel, R., Moser, D., Gihring, T.M., Mislowack, B. and Onstott, T. C.** (2005). Radiolytic H_2 in Continental Crust: Nuclear Power for Deep Subsurface Microbial Communities. *Geochem. Geophys. Geosyst*. **6(7)**:Q07003.

- **Liu, W., Marsh, T.L., Cheng, H. and Forney, L.J.** (1997). Characterization of Microbial Diversity by Determining Terminal Restriction Fragment Length Polymorphism of Genes Encoding 16S rRNA. *Applied and Environmental Microbiology*. **63(11)**:4516-4522.

- **Loubière, P. and Lindley, N.D.** (1991). The use of Acetate as an Additional Co-Substrate Improves Methylotrophic Growth of the Acetogenic Anaerobe *Eubacterium limosum* when CO_2 Fixation is Rate-Limiting. *Journal of General Microbiology*. **137**:2247-2251.

- **Lovley, D.R. and Chapelle, F.H.** (1995). Deep Subsurface Microbial Processes. *Review of Geophysics*. **33(3)**:365-381.

- **Mariotto, C., Loubière, P., Goma, G. and Lindley, N.D.** (1989). Influence of Various Reducing Agents on Methylotrophic Growth and Organic Acid Production of *Eubacterium limosum*. *Appl Microbiol Biotechnol*. **32**:193-198.

- **Men, Y., Seth, E.C., Yi, S., Allen, R.H., Taga, M.E. and Alvarez-Cohen, L.** (2014). Sustainable Growth of *Dehalococcoides mccartyi* 195 by Corrinoid Salvaging and Remodeling in Defined Lactate-Fermenting Consortia. *Applied and Environmental Microbiology*. **80(7)**:2133-2141.

- **Miller, J.F., Almond, E.L., Shah, N.N., Ludlow, J.M., Zollweg, J.A., Streett, W.B., Zinder, S.H. and Clark, D.S.** (1988). High-Pressure-Temperature Bioreactor for Studying Pressure-Temperature Relationships in Bacterial Growth and Productivity. *Biotechnology and Bioengineering*. **31**:407-413.

- **Morozova, D., Wandrey, M., Alawi, M., Zimmer, M., Vieth, A., Zettlitzer, M and Würdemann, H.** (2010). Monitoring of the Microbial Community Composition in Saline Aquifers during CO_2 Storage by Fluorescence *in situ* Hybridisation. *International Journal of Greenhouse Gas Control*. **4**:981-989.

- **Nelson, C.M., Schuppenhauer, M.R. and Clark, D.S.** (1992). High-Pressure, High-Temperature Bioreactor for Comparing Effects of Hyperbaric and Hydrostatic Pressure on Bacterial Growth. *Applied and Environmental Microbiology*. **58(5)**:1789-1793.

- **Newberry, C.J., Webster, G., Cragg, B.A., Parkes, R.J., Weightman, A.J. and Fry, J.C.** (2004). Diversity of Prokaryotes and Methanogenesis in Deep Subsurface Sediments from the Nankai Trough, Ocean Drilling Program Leg 190. *Environ.Microbiol*. **6**:274-287.

- **Onstott, T.C.** (2005). Impact of CO_2 Injections on Deep Subsurface Microbial Ecosystems and Potential Ramifications for the Surface Biosphere. Chapter 30 in Carbon Dioxide Capture for Storage in Deep Geologic Formations – Results from the CO_2 Capture Project, Geological Storage of Carbon Dioxide with Monitoring and Verification. *Elsevier Publishing*. **2**:1217-1250. ISBN: 0080445705.

- **Onstott, T.C., Colwell, F.S., Kieft, T.L., Murdoch, L. and Phelps, T.J.** (2009). New Horizons for Deep Subsurface Microbiology. *Microbe Magazine.* **4(11)**:499–505.

- **Onstott, T.C., Lin, L., Davidson, M., Mislowack, B., Borcsik, M., Hall, J., Slater, G., Ward, J., Sherwood Lollar, B., Lippmann-Pipke, J., Boice, E., Pratt, L.M., Pfiffner, S., Moser, D., Gihring, T., Kieft, T.L., Phelps, T.J., van Heerden, E., Litthauer, D., DeFlaun, M., Rothmel, R., Wanger, G. and Southam G.** (2006). The Origin and Age of Biogeochemical Trends in Deep Fracture Water of the Witwatersrand Basin, South Africa. *Geomicrobiol. J*. **23**:369–414.

- **Phelps, T.J., Murphy, E.M., Pfiffner, S.M. and White, D.C.** (1994). Comparison between Geochemical and Biological Estimates of Subsurface Microbial Activities. *Microb. Ecol*. **28**:335-349.

- **Pirt, S.J.** (1975). Parameters of growth and analysis of growth data. Chapter 2 in Principles of microbe and cell cultivation. *Wiley Publishers*. ISBN: 9780470690383.

- **Porter, M.L., Engel, A.S., Kane, T.C. and Kinkle, B.K.** (2009). Productivity-Diversity Relationships from Chemolithoautotrophically Based Sulfidic Karst Systems. *International Journal of Speleology*. **38(1)**:27-40.

- **Prescott, L.M., Harley, J.P. and Klein, D.A.** (1996). Microbiology. *Wm. C. Brown Publishers*. ISBN: 9780697293909.

- **Ragon, M., Van Driessche, A.E.S., García-Ruíz, J.M., Moreira, D. and López-García, P.** (2013). Microbial Diversity in the Deep-Subsurface Hydrothermal Aquifer Feeding the Giant Gypsum Crystal-Bearing Naica Mine, Mexico. *Frontiers in Microbiology*. **4**:37.

- **Roh, H., Ko, H., Kim, D., Choi, D.G., Park, S., Kim, S., Chang, I.S. and Choi, I.** (2011). Complete Genome Sequence of a Carbon Monoxide-Utilizing Acetogen, *Eubacterium limosum* KIST612. *Journal of Bacteriology*. **193(1)**:307-308.

- **Sambrook, J., Fritsch, E. F., & Maniatis, T.** (1989). Molecular Cloning: A Laboratory Manual. *Cold Spring Harbor Laboratory Press*. (2nd ed.).

- **Song, Y. and Cho, B.** (2015). Draft Genome Sequence of Chemolithoautotrophic Acetogenic Butanol-Producing *Eubacterium limosum* ATCC 8486. *Genome Announcements*. **3(1)**:e01564-14.

- **Stevens, T.** (1997). Lithoautotrophy in the Subsurface. *FEMS Microbiology Reviews*. **20**:327-337.

- **Takai, K., Moser, D., DeFlaun, M., Onstott, T.C. and Fredrickson, J.K.** (2001). Archaeal Diversity in Waters from Deep South African Gold Mines. *Applied and Environmental Biology.* **67(12)**:5750-5760.

- **Takai, K., Nakamura, K., Toki, T., Tsunogai, U., Miyazaki, M., Miyazaki, J., Hirayama, H., Nakagawa, S., Nunoura, T. and Horikoshi, K.** (2008). Cell Proliferation at 122°C and Isotopically Heavy CH_4 Production by a Hyperthermophilic Methanogen under High-Pressure Cultivation. *Proc. Natl. Acad. Sci*. **105(31)**:10949-10954.

- **Teske, A.P.** (2005). The Deep Subsurface Biosphere is Alive and Well. *Trends Microbiol.* **13(9)**:402-404.

- **Webster, G., Parkes, R.J., Cragg, B.A., Newberry, C.J., Weightman, A.J. and Fry, J.C.** (2006). Prokaryotic Community Composition and Biogeochemical Processes in Deep Subseafloor Sediments from the Peru Margin. *FEMS Microbiol.Ecol*. **58**:65-85.

- **White, D.C., Phelps, T.J. and Onstott, T.C.** (1998). What's Up Down There? *Current Opinion in Microbiology*. **1**:286-290.

- **Woycheese, K.M., Meyer-Dombard, D.R., Cardace, D., Argayosa, A.M. and Arcilla, C.A.** (2015). Out of the Dark: Transitional Subsurface-to-Surface Microbial Diversity in a Terrestrial Serpentinizing Seep (Manleluag, Pangasinan, the Philippines). *Frontiers in Microbiology*. **6**:44.

CHAPTER 5

DESIGN AND CONSTRUCTION OF THE SYRINGE INCUBATORS AND THE BIOREACTOR

5.1 INTRODUCTION

It has been observed in the literature that when deep subsurface microorganisms are grown under lower or normal atmospheric pressures, their response differ from when they are grown under higher pressures, especially their metabolic activity and viability are negatively influence, since these deep subsurface biomes have adapted to their *in situ* high hydrostatic pressures (Yayanos & Dietz, 1983; Fang *et al*., 2010). Prieur, (1997), found that the optimal growth pressures for deep-sea hyperthermophiles are higher than their *in situ* environmental pressure. This was confirmed by Miller *et al*., (1988), that *Methanocaldococcus jannaschii*, which was isolated at 2 600 mbs (corresponding to ~260 atm, Jones *et al*., 1983), grew optimally at 750 atm. In contrast, Prieur, (1997), reported that deep-sea psychrophiles have optimal growth pressures below their *in situ* environmental pressure. It was also found that the addition of pressure, increased the maximum viable temperature of several deep-sea thermophilic Archaea (Holden & Baross, 1995; Canganella *et al*., 1997; Marteinsson *et al*., 1999a) and Boonyaratanakornkit *et al*., (2007), showed that under 500 atm, the optimal growth temperature for *M. jannaschii* was increased by 5°C, with a threefold increase in its specific growth rate. In addition, the gene and protein expression responses for thermophilic and psychrophilic piezophiles are different when grown under higher pressures. Marteinsson *et al*., (1999b), showed that when *Thermococcus barophilus* was grown at 400 atm, an unidentifiable protein was induced, while a stress protein was induced when grown under atmospheric pressure. Vezzi *et al*., (2005), reported that when *Photobacterium profundum*, isolated at 2 500 mbs, was grown under 0.1 MPa (~1 atm), genes involved in protein folding, DNA repair, and amino acid transport were activated, while at 280 atm, genes involved in respiration, fermentation and in regulating polymer degradation were activated. Furthermore, partial pressures of CO_2 and H_2

above 0.01 MPa (~0.1 atm) adjusted the metabolism of several bacteria, fungi, and yeasts (Chicoye *et al*., 1978; Jones & Greenfield, 1982; Eklund, 1984; Lamad *et al*., 1988; Dixon & Kell, 1989; McIntyre & McNeil, 1998). Therefore, in order to possibly understand how these subsurface biomes will operate *in situ*, temperatures and pressures that characterize the deep subsurface must be mimicked using higher pressure equipment.

Several experiments under various high pressures has been carried out to study the effects of high pressures on the genetic, metabolic, biochemical, and physiological aspects of microorganisms, some of which includes biohydrogenations (Schieche *et al*., 1997), enhanced oil and gas recovery (Bubela *et al*., 1987; Cloete, 2010), metabolic activities (Jannasch *et al*., 1996; Abe *et al*., 1999; Abe & Horikoshi, 2001; Bothun *et al*., 2004), the sterilization of microorganisms (Lin *et al*., 1994; Hong *et al*., 1997; Hauben *et al*., 1997; Smelt, 1998; Dillow *et al*., 1999; Lee *et al*., 2001; Zhang *et al*., 2006; Parton *et al*., 2007; Oulé *et al*., 2010), *in situ* recovery of fermentation products (Knutson *et al*., 1999; Berberich *et al*., 2000; Berberich, 2001), transcriptional responses (Boonyaratanakornkit *et al*., 2007), growth and survival of microorganisms under pressure (Yayanos, 1986; Nelson *et al*., 1991; Kato *et al*., 1996; Miller *et al*., 1988; Yanagibayashi *et al*., 1999; Arakawa *et al*., 2006; Takai *et al*., 2008; Hiraki *et al*., 2012; Sauer *et al*., 2012), the dissociation of ribosomes (Schulz *et al*., 1976), gene regulation (Bartlett *et al*., 1989), stabilization of proteins (Hei & Clark, 1994; Sun & Clark, 2001), and the composition of membrane lipids (Delong & Yayanos, 1985; Kaneshiro & Clark, 1995).

These high pressure experiments and numerous others have all been carried out in high pressure reactors or vessels, specifically designed to fit the conditions and requirements of each experiment, some of which includes culture tubes with neoprene stoppers working as piston to pressurize the samples (Orcutt *et al*., 2008), glass syringes or a flexible Teflon container in a reaction chamber (Schmid *et al*., 1978; Hutton *et al*., 2001; Takai *et al*., 2008), flexible nickel tubes (Bernhardt *et al*., 1987), flexible cells made of gold (Seyfried, 1979) or titanium (Seyfried & Janecky, 1985), flexible polyvinylidene fluoride (PVDF) incubator sleeve (Sauer *et al.,* 2012), and several types of bioreactors (Miller *et al*., 1988; Nelson *et al*., 1991; Vance & Brink, 1994; Dillow *et al*., 1999; Park & Clark, 2002; Bothun *et al*., 2004; Parton *et al*., 2007; Zhang *et al*., 2011; Hiraki *et al*.,

2012; Sauer *et al.,* 2012). Methods used for the addition of pressure are usually hydrostatically (Liquid only) (Zobell & Oppenheimer, 1950; Paul & Morita, 1971; Yayanos *et al*., 1982), hyperbarically (Both liquid and gas phases) (Sturm *et al*., 1987; Bernhardt *et al*., 1988; Miller *et al*., 1988; Nelson *et al*., 1991), or directly to solid medium (Yayanos *et al*., 1984).

However, laboratory scale imitations of the deep subsurface conditions do have their limitations in that they may not reflect the true *in situ* environmental activity of the deep subsurface biomes, since the rates of microbial activity can differ orders of magnitude from what actually takes place in the subsurface (Chapelle & Lovley, 1990). Thus the equipment used in the laboratory to mimic the subsurface conditions can only be used to demonstrate the potential for the *in situ* microbial activity but do not give quantitative information on the processes actually taking place (Lovley & Chapelle, 1995). Therefore, *in situ* experiments on the reaction of the subsurface biome under CCS conditions are preferred. But, since the first pilot CO_2 storage project experiment for South Africa are planned for 2017 (SACCCS, 2015), *in situ* environmental conditions that represents the proposed sites for CCS in South Africa (Cloete, 2010) had to be mimicked for this research, through the use of specifically designed, high pressure equipment.

5.2 AIMS OF THIS CHAPTER

The main aims of this chapter were to:

- Design and construct a reactor(s) that can operate under higher pressures, to mimic CCS conditions within the laboratory.

5.3 MATERIALS AND METHODS

Unless otherwise specified, the material used for the construction of all the syringe incubators as well as the bioreactor was 316 stainless steel. The tubing used was ¼ inch and all valves, gauges, nuts, and ferrules were from Swagelok® and designed to operate under high pressures and temperatures (maximum of ≥172 bar and 148°C). Safety precautions were used at all times while operating any of the high pressure reactors.

5.3.1 The Syringe Incubators

Takai *et al*., (2008), have developed a technique for the cultivation and characterization of several native deep-sea chemolithoautotrophs in a gas-rich fluid under high hydrostatic pressures, corresponding to its potential *in situ* environments. This system is based on a liquid medium with a gas mixture inside a gas-tight glass syringe with a butyl rubber piston and sealed with a metallic needle that is closed with a butyl rubber (Figure 5.1). The syringe is then transferred to a pressure vessel, compressed with a hydraulic pump to the desired pressure and incubated (Figure 5.2). By using this system, Takai *et al*., (2008), were able to successfully study the growth, survival, and methane production of *Methanopyrus kandleri* strain 116, under high temperatures and hydrostatic pressures.

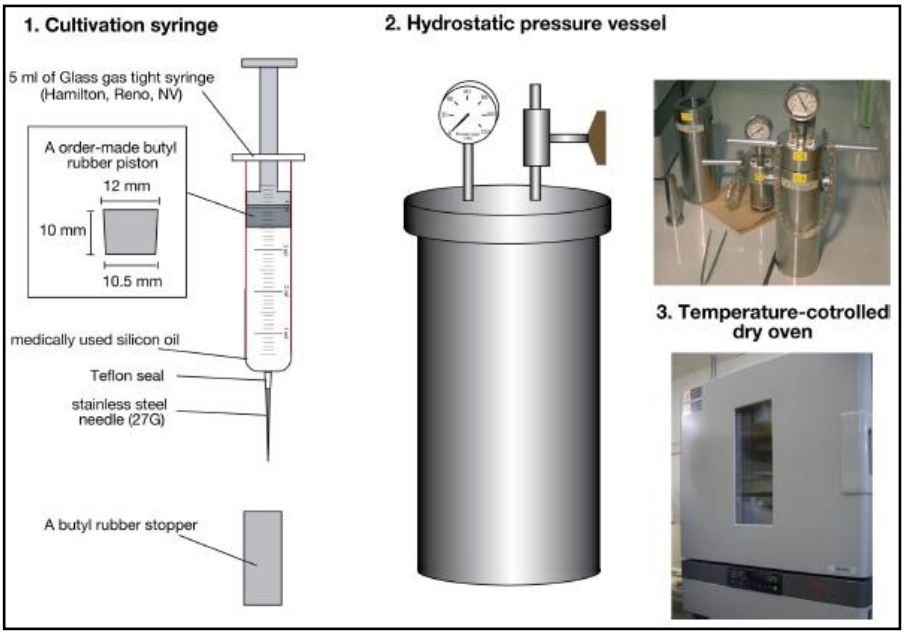

Figure 5.1: Schematic illustration of the microbiological cultivation and incubation technique (Taken from Takai *et al*., 2008).

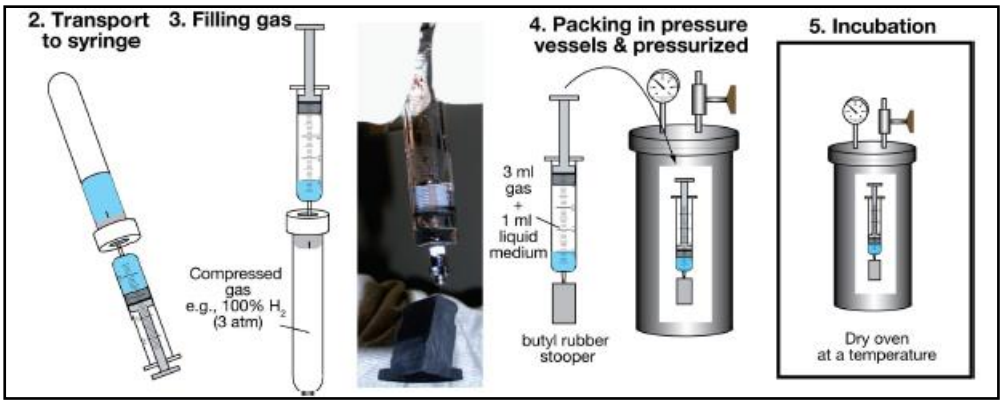

Figure 5.2: Procedure for cultivation in a gas-rich fluid under high hydrostatic pressures (Taken from Takai *et al*., 2008).

Hutton *et al*., (2001), have used a similar system where sealed syringes were incubated inside a pressurized vessel (Figure 5.3) to test the effect of hydrostatic pressure on disc cells.

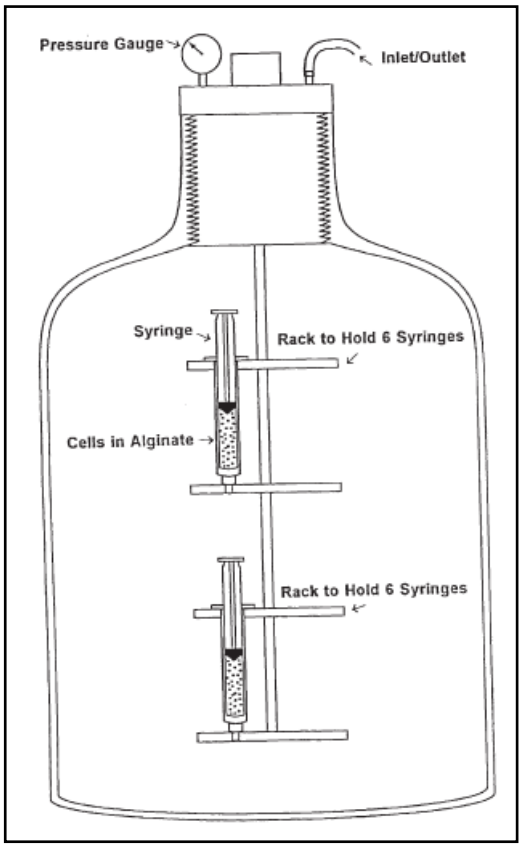

Figure 5.3: Schematic illustration of the syringes inside the pressure vessel (Taken from Hutton *et al*., 2001).

Cultivation of microorganisms in this manner has the advantage that the numerically predominant or the functionally significant microbial populations in the *in situ* environments can be characterized because the *in situ* hydrostatic pressures is a potential key physical parameter which directly affects the growth of the microorganisms (Abe *et al*., 1999; Kato, 2006; Takai *et al*., 2009). But more importantly, the pressures and temperatures are the main physicochemical factors preparing the thermodynamic states of energy and carbon metabolisms for microbial growth. This means that the available gaseous substrates that are dissolved in the liquid phase of the growth medium and much less abundant under lower or normal atmospheric pressures than when compared with the pressures in their *in situ* environments (Charlou *et al*., 2002; Person *et al*., 2005; Lupton *et al*., 2008; Takai *et al*., 2009).

If these *in situ* environmental parameters are ignored in laboratory experiments, metabolic biases can be introduced, due to the enrichment of certain populations that are less dominant in the *in situ* environments but are energetically favourable in laboratory experiments (Takai *et al*., 2009). Therefore, the same cultivation technique [mainly from Takai *et al*., (2008)] was used to study the potential growth and survival of the subsurface biome under high pressures and in a gas-rich environment.

5.3.1.1 Design and Construction

All schematic illustrations for the syringe incubators (Figure 5.4) were created with the solid modelling, computer-aided design (CAD) and computer-aided engineering (CAE) software program, SolidWorks®. The schematic illustrations are not according to scale. Each incubator consisted of a hollowed stainless steel vessel that was fitted with a Teflon syringe ring (Figure 5.4B and E). A syringe was inserted through the hole in the middle of the ring and the holes on the outside of the ring allowed circulation of the water inside the vessels. The lid of the incubator (Figure 5.4C) was made to fit tightly into the vessel and therefore pressure was needed to insert the lid into the vessel. Thus, a handle bar was fitted through the lid which was used to apply the pressure. To ensure a completely sealed-off incubator, a double seal was added, consisting of two high-pressure Neoprene O-rings with Teflon spacers. As a safeguard mechanism to ensure that the lid remained in place while under pressure, a safety pin (Figure 5.4D) was

inserted all the way through the vessel and the lid (Figure 5.4A). An opening was made through the lid (Figure 5.4B) for pressurization of the incubator.

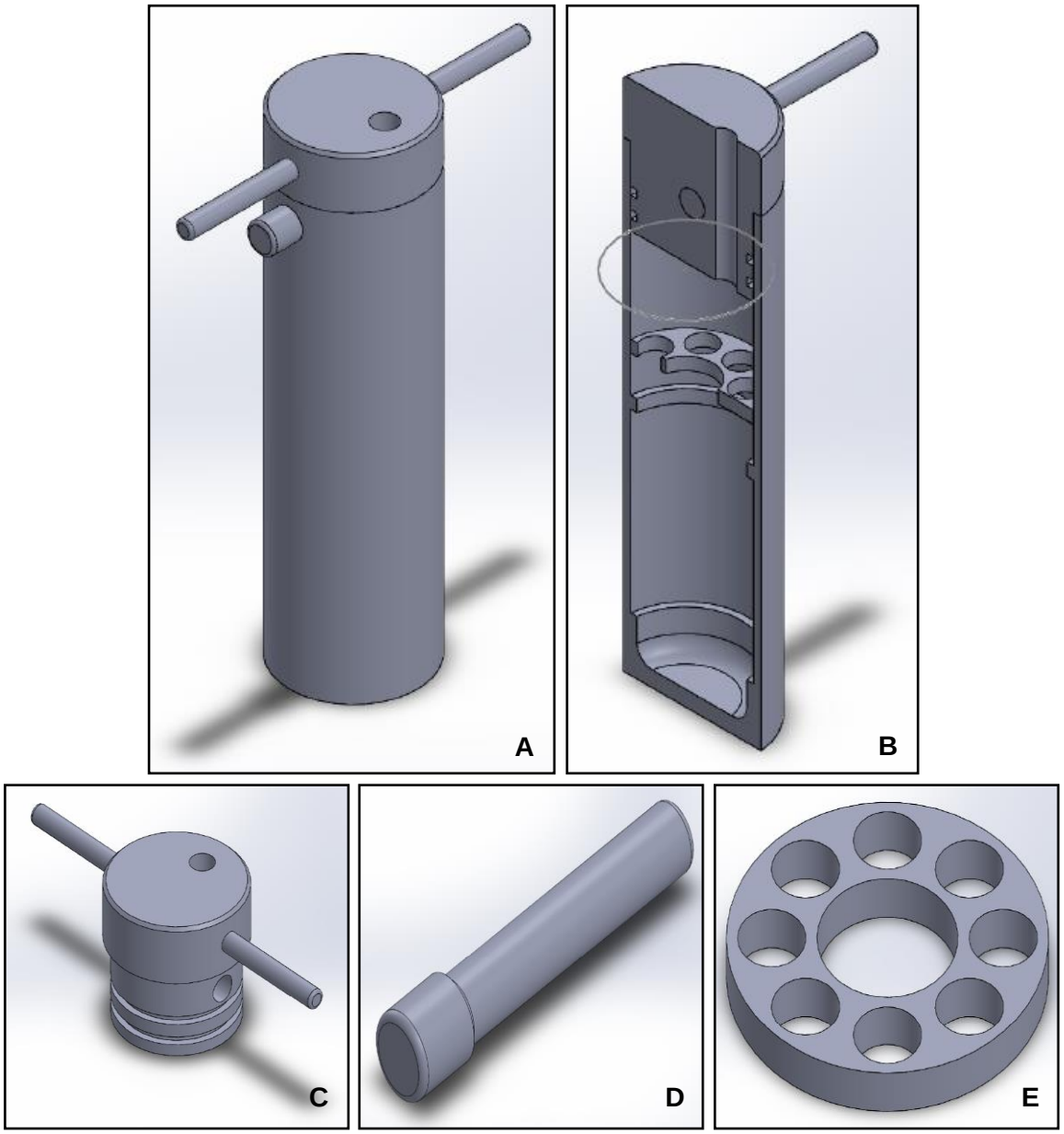

Figure 5.4: Schematic illustrations of (A) the complete syringe incubator, (B) a cut view of the syringe incubator, (C) the lid, (D) the safety pin, and (E) the syringe ring.

A needle valve and pressure gauge (Figure 5.5) was attached to the lid. In this way the syringe incubators could be pressurized to the desired pressure using either gas or a hydraulic pump. These incubators were designed for either 5 ml or 25 ml syringes.

Except for the Swagelok® components, everything on the syringe incubators was custom-made by the Department of Instrumentation at the UFS (Bloemfontein, RSA).

Figure 5.5: Images of (A) all the constructed syringe incubators, (B) the individual components of a syringe incubator, (C) the lid, (D) the 5 ml syringe ring, (E) the 25 ml syringe ring, and (F) the safety pin.

5.3.1.2 Syringe Preparation

All syringe preparations were conducted under sterile conditions in a laminar flow cabinet (Labotec®). The syringes used are non-autoclavable, gas-tight, glass syringes (Hamilton), fitted with 22 gauge stainless steel needles (Hamilton) and sealed with blue chlorobutyl rubber stoppers (Bellco Glass Inc.). Before and after each usage, the syringes, needles and rubber stoppers were sterilized with 70% EtOH, followed by rinsing three times with sterile dH_2O. The desired amount of inoculated medium was added to each syringe, followed by the insertion of the specific gas mixture. The gas mixture was prepared as discussed in Section 4.3.3, but in empty, sterile, serum vials that were crimp sealed with a blue chlorobutyl rubber stopper and an aluminium cap. The gas was transferred to the syringes by inserting the needle that is attached to the syringe, into the serum vial. The syringe was sealed with a blue chlorobutyl rubber stopper, immediately after the gas was added.

5.3.1.3 Operational Procedure

The syringe incubators were filled with water and heated to the operating temperature, 24 hours before use, through incubation in a temperature-controlled dry oven (Therm-O-Mat). This ensured that the stainless steel was already at the desired temperature and therefore the pressure stayed relatively consistent when incubated after pressurization. The water inside the reactors ensured that the internal syringe pressure is in equilibrium with the external pressure. The prepared syringes were transferred into the heated incubators and the incubators were sealed and secured with the safety pin. A hydraulic pump (Jackco®) was connected to the incubators and pressurized to the desired pressure (Figure 5.6). While the pressure was added, the incubators were submerged in a thermostatic water bath [Gesellschaft für Labortechnik (GFL®)], pre-heated to the operating temperature. The needle valve was closed and the incubators were transferred to the temperature-controlled dry oven for incubation. The hydraulic pump was modified so that water was used to pressurize the incubators instead of oil. This was done by connecting the hydraulic pump to a cylinder which was divided in the middle with a piston system. The one side of the cylinder was filled with oil and the other side with water. The hydraulic pump was connected to the oil cylinder and the incubators to the water cylinder. The pump releases oil into the oil cylinder which allows the piston to push

down on the water cylinder. Water is then expelled from the cylinder to pressurize the incubators. When the water cylinder was empty, it was connected to a tap and filled with water. Temperature regulation of the incubators was very important throughout the pressurization and operation steps to ensure that the desired pressure was maintained as closely as possible.

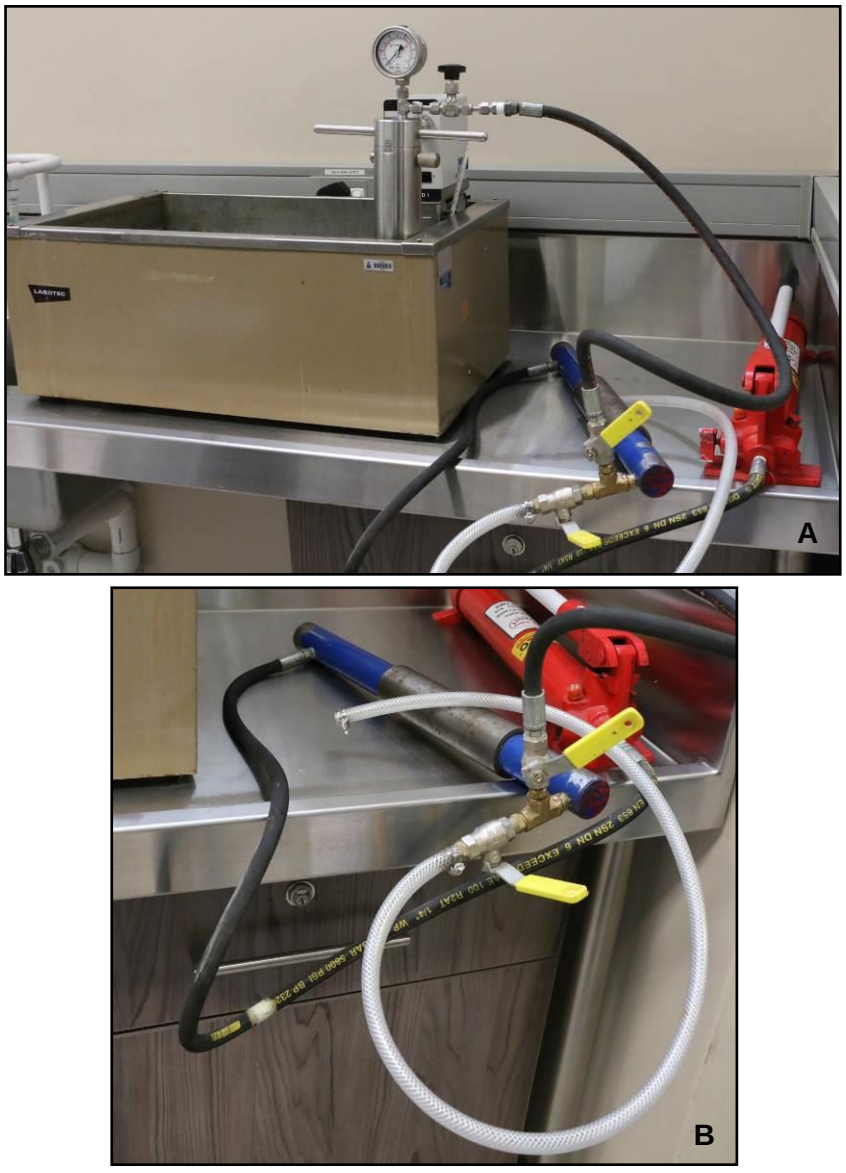

Figure 5.6: (A) Pressurizing the syringe incubators using a hydraulic pump and (B) the modified cylinder connected to the hydraulic pump. The white tubing is used for filling the water cylinder.

To depressurize the syringe incubators, the needle valves were simply opened slowly and the culture from the syringes was added to sterile falcon tubes to be used for analyses in further experiments.

5.3.2 The Bioreactor

With the syringe incubators, the experiments were considered as batch studies. These experiments were done without the addition of sandstone and each syringe was sacrificed at certain time intervals displaying the reactivity of the biome for this period. Care was taken that all syringes in a set of batch experiments contained the same amount of cells. Consequently, no circulation or continuous monitoring was possible. It was also difficult to accurately control the pressures, since the smallest change in temperature during either the pressurization or the incubation resulted in a substantial change in the pressure. In order to study the subsurface biome as a continuous culturing experiment, a novel bioreactor was designed to operate under high pressures in the presence of the supercritical fluid. Even though it was not needed for this research project, the bioreactor is also able to operate at high temperatures.

5.3.2.1 Designs and Constructions

All schematic illustrations for the bioreactor were created using the software program, AutoCAD. This bioreactor was adapted several times to improve its safety and operation and only when major differences were made, it has been indicated through schematic illustrations. In all designs, the CO_2 was used to saturate the reactor and to create the initial pressure. The desired operating pressure and temperature was always ≥80 bar and 35°C, respectively. The schematic illustrations are not according to scale.

The first bioreactor (Figure 5.7) was designed to be a flow-through system, with a constant supply of fresh medium via a high-performance liquid chromatography (HPLC) pump (Shimadzu), but the reactor could be isolated from the medium supply, when needed. The reactor itself consisted of a 316 stainless steel pipe and has an inner diameter of 2.1 cm and 24.5 cm in length (Volume of 84.86 cm^3). Both ends of the pipe body are fitted with high pressure nuts and ferrules.

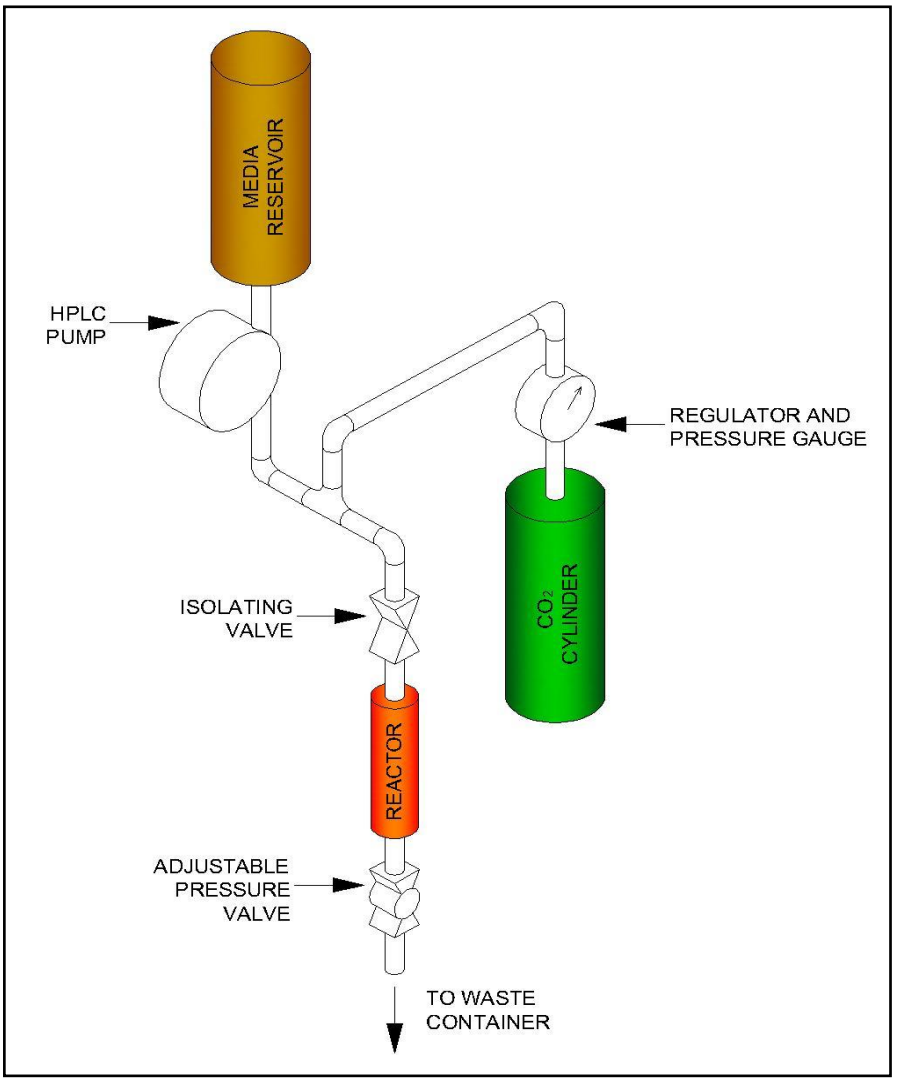

Figure 5.7: Schematic illustration of the first design of the bioreactor.

Over time, small adjustments were made to this design, which included adding a port in the media reservoir for the insertion of additional medium or electron donors when needed. A non-return valve was added before the reactor, to ensure that the gas and medium can only flow through the reactor in one direction and a pressure release valve was added to the system as a safety measurement to prevent pressure build-up. A pressure gauge was added before the reactor to measure the pressure inside the reactor and a liquid sampling port was added at the outlet of the reactor, with a gas sampling port before the reactor. With this bioreactor, the kinetics and continuous measurements could not be done, since fresh medium would have been supplied at all times, therefore no circulation of the liquid would take place. Contact time with the biome was also limited and if the reactor would have been isolated from the media supply, the system would

again be a batch experiment as with the syringe incubators. Therefore, no usable data could be obtained.

For the second design (Figure 5.8), the system was changed to allow circulation of the liquid using the HPLC pump and the CO_2 gas was used to introduce the medium into the reactor. A sieve was inserted into the reactor that served as a filter to prevent blockage of the HPLC pump. Isolating valves were added at strategic points to ensure that the reactor could be closed off without losing pressure.

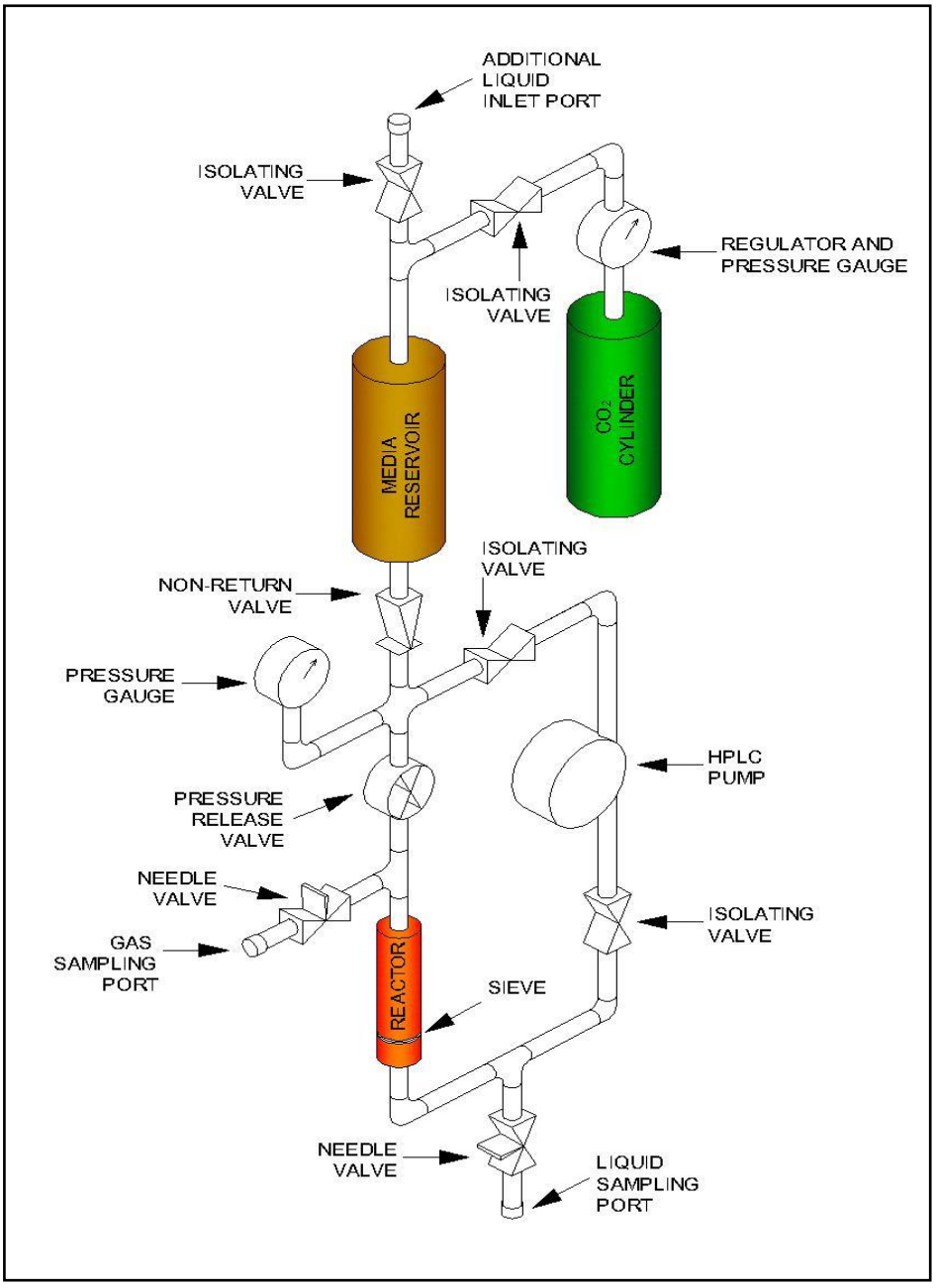

Figure 5.8: Schematic illustration of the second design of the bioreactor.

Final adjustments to this design included to regulate the pressure more effectively and were added to the next design (Figure 5.9) only had a few practical changes which included the addition of a pressure gauge before the media reservoir to ensure that the pressure created with the gas was higher than the pressure inside the reactor for the media supply. An additional pressure release valve was added before the media reservoir and the sieve was removed from the reactor and replaced with an in-line pre-filter after the reactor to ensure that the filter can be removed or changed, if needed, without having to open or disturb the reactor.

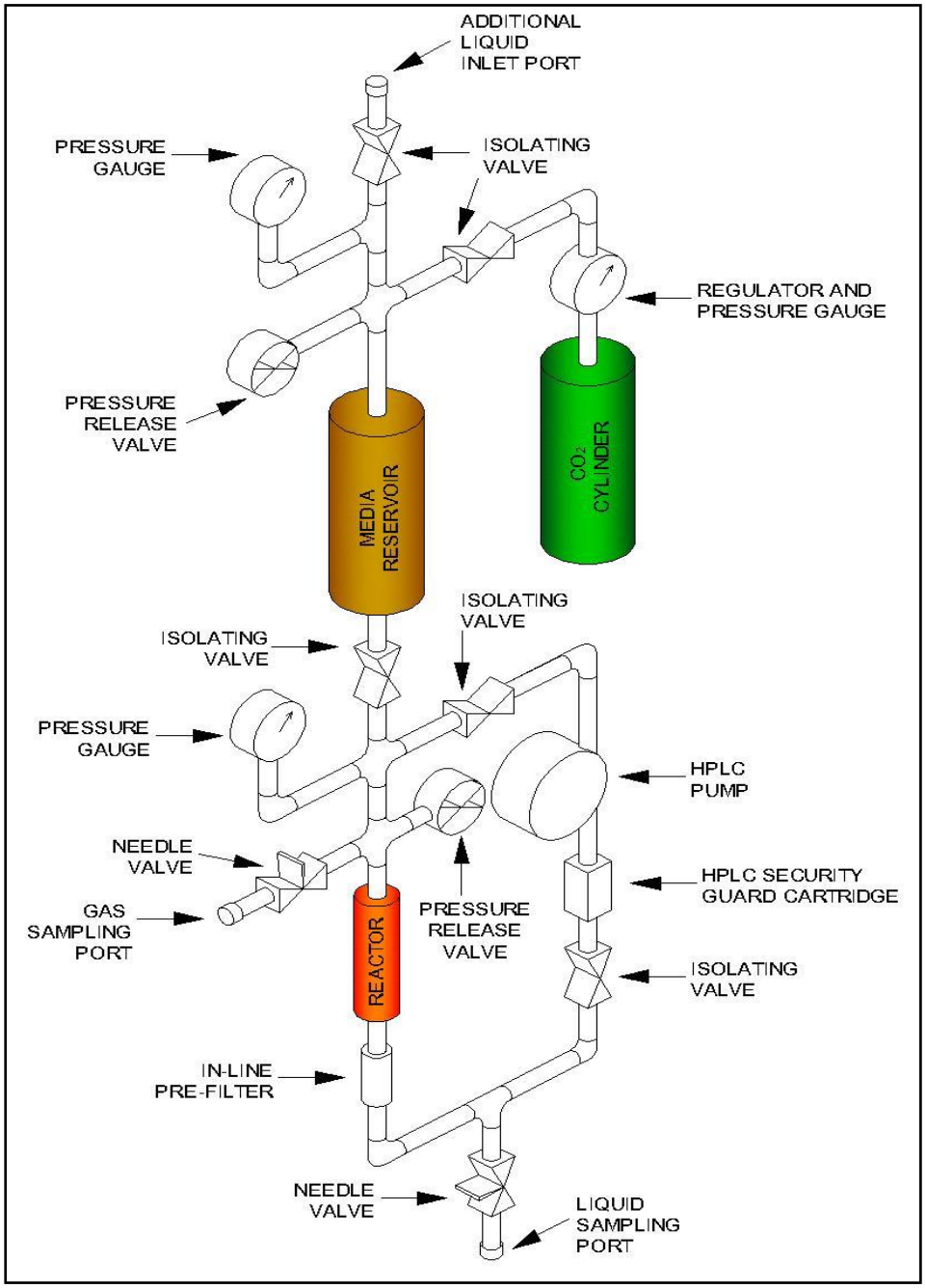

Figure 5.9: Schematic illustration of the third design of the bioreactor.

This bioreactor was constructed (Figure 5.10) and mounted inside a safety cabinet for protection. Only the HPLC pump and the CO_2 gas cylinder were outside the safety cabinet. A heating-coil was wrapped around the reactor and the media reservoir to regulate the temperature.

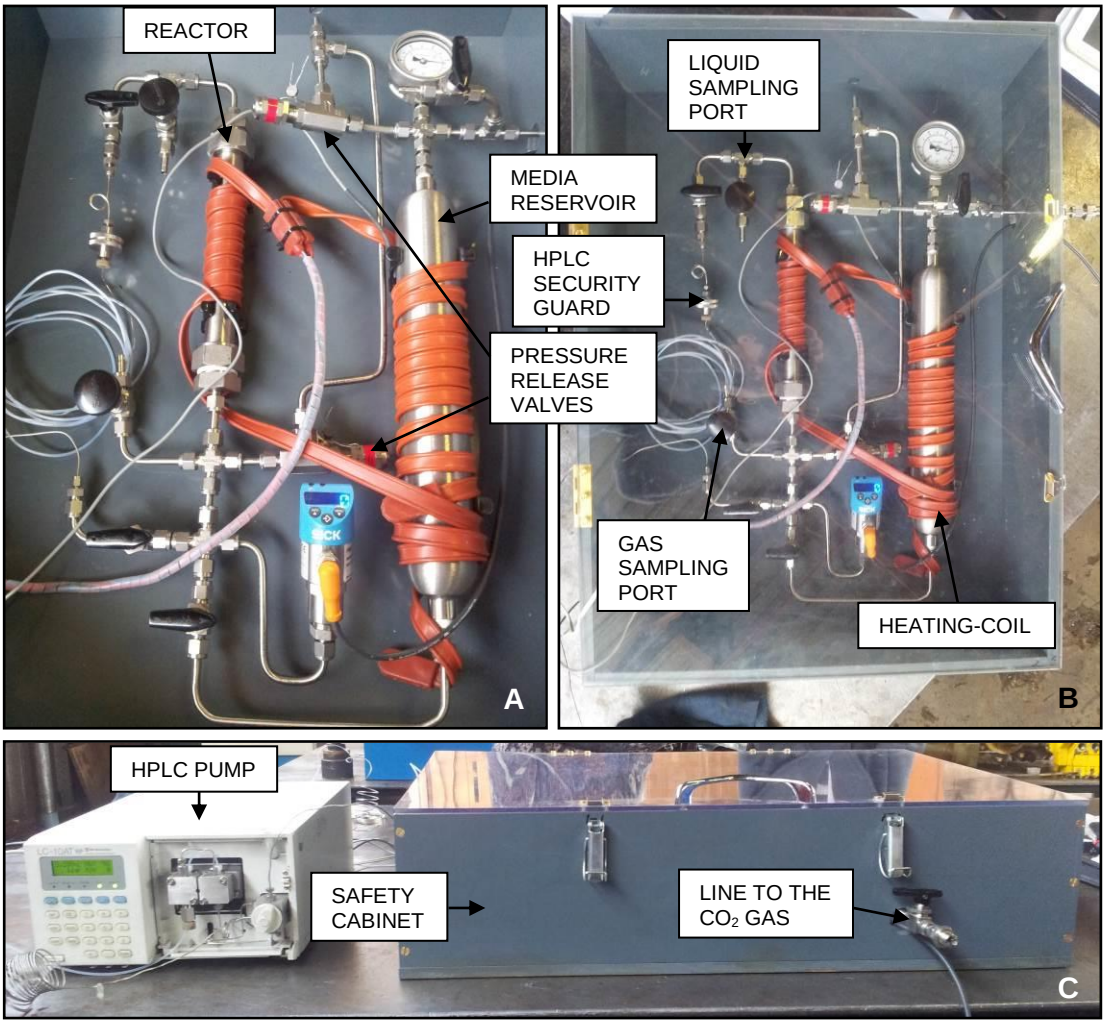

Figure 5.10: (A) The constructed bioreactor, (B) the bioreactor inside the safety cabinet, and (C) the HPLC pump connected to the bioreactor, with the line to the CO_2 gas cylinder, visible outside of the safety cabinet.

Unfortunately, with this design, a rapid drop in pressure with large increments were obtained, especially during each sampling, thus resulting in the CO_2 not being in the supercritical condition. A pressure shock on the microorganisms that were introduced each time a sample was withdrawn had to be considered. Also, the system would have

been under subcritical CO_2 conditions for extended periods of time, since the HPLC pump was not able to restore the pressure rapidly enough. The HPLC pump was also able to maintain the pressure for only short periods of time, since the inlet of the pump needs to be under low pressure and therefore, the pump was not able to handle the system pressure (≥80 bar) on the inlet. The heating-coil around the reactor and media reservoir alone was also not sufficient enough to regulate the temperature.

For the next design (Figure 5.11 and Figure 5.12), the media reservoir was replaced to a variable media reservoir, attached to a piston pressure regulator. In this design, the CO_2 was no longer used to introduce the medium into the reactor, but through the piston pressure regulator connected to a hydraulic pump (Jackco®). This piston regulator was connected to a pressure gauge, to ensure that it is always under the desired pressure and circulation still occurred through the HPLC pump. However, an adjustable pressure valve was included in the system before the HPLC pump. This valve was set to open at the operating pressure to allow small amounts of liquid to pass through each time the valve opened. This meant that everything before the adjustable pressure valve was under the high operating pressure and between the valve and the HPLC pump the liquid could be maintained under atmospheric pressure. After the HPLC pump, the high operating pressure was restored.

Several techniques, described in the literature, are used to obtain the desired temperature in the high pressure reactors, including thermistors (Bernhardt *et al*., 1987), water baths (Jannasch *et al*., 1996), and drying ovens/incubators (Miller *et al*., 1988; Takai *et al*., 2008). For this design, the heating-coil was replaced with a temperature controlled fan inside the safety cabinet and connected to an uninterruptible power supply (UPS), converting the safety cabinet into an incubator. All the openings in the safety cabinet were sealed and the temperature was verified with a thermometer.

The idea behind this system was that each time a sample was collected, the pressurized piston regulator immediately thrusts down on the variable media reservoir to keep the system under the correct pressure. The hydraulic pump was then used to restore the pressure in the piston pressure regulator. This piston regulator was designed to ensure that the oil from the pump only enters the piston regulator and never come in contact with the reactor. However, to achieve this, the collection of the sample and the

pressurizing of the piston pressure regulator had to occur simultaneously. Even though the two actions were manually carried out at the same time, the drop in pressure during sampling was faster than restoring the pressure with the hydraulic pump. This resulted in a double pressure shock on the microorganisms, once during sampling and again during re-establishing of the pressure.

The HPLC pump was only able to maintain the pressure for short periods of time, especially since gas bubble which entered the pump, prevented it from operating continuously. Gas bubbles formed each time when the pressure changed through the adjustable pressure valve to atmospheric pressure. To compensate, a small reservoir using a sterile serum vial, was included as a gas trap, just before the HPLC pump (Figure 5.12). However, a head space formed inside the reservoir from all the gas in the system. This increased the pressure on the small reservoir until it was too high for the inlet of the HPLC pump to handle. If the serum vial was to be replaced each time the pressure was too high, it would have meant that each time the reservoir was removed, a certain amount of the gas inside the system were removed as well. Sauer *et al*., (2012), included an empty HPLC column between their reactor and HPLC pump which served as a gas trap to prevent the entry of gas bubbles into the pump. They mounted the column vertically and the medium was flowing from the top to the bottom, trapping the gas bubbles at the top.

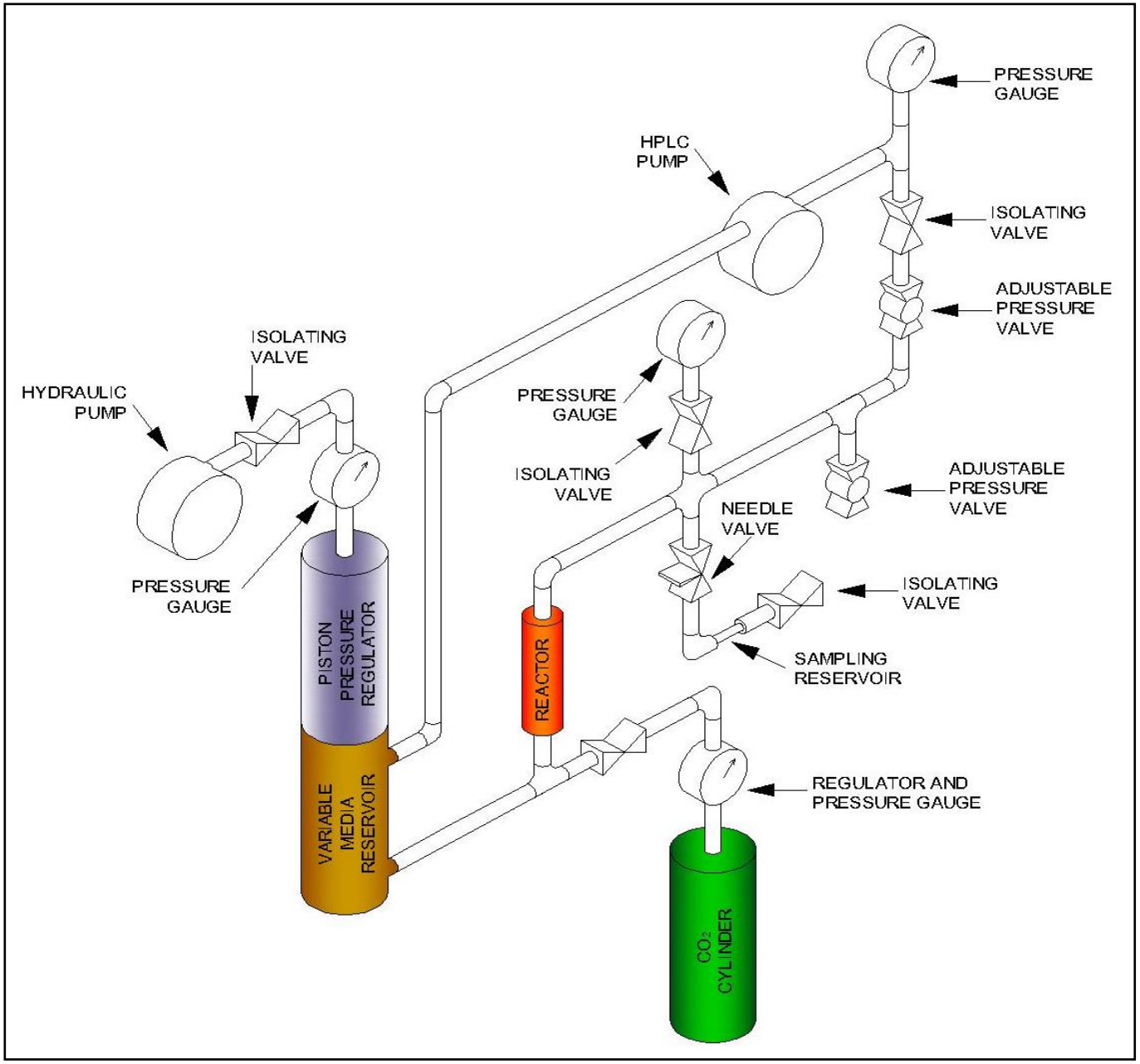

Figure 5.11: Schematic illustration of the fourth design of the bioreactor.

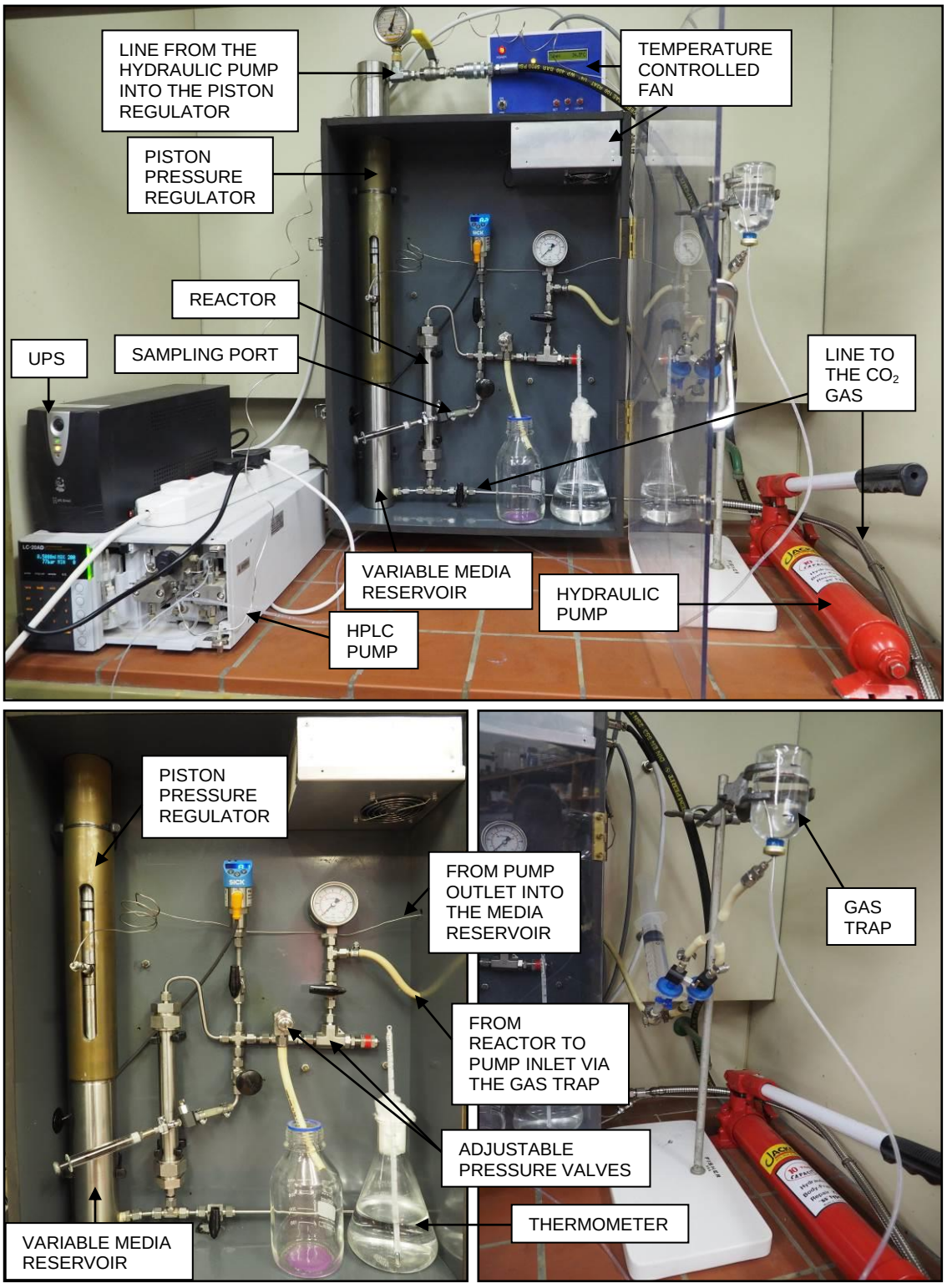

Figure 5.12: The bioreactor, constructed from the fourth design.

Even though a design like the one from Sauer *et al*., (2012), could have possibly solved the problem, it was decided to completely remove the HPLC pump from the system in the fifth design (Figure 5.13 and Figure 5.15). Thus, to ensure circulation of the liquid through the system, a second variable media reservoir, attached to a piston pressure regulator, was included. The double piston regulators worked in opposite directions via three-way valves and operated similar to a syringe pump. The hydraulic pump from the fourth design was replaced with nitrogen gas. The advantage in using the gas is that the pressure is immediately restored after a sample has been withdrawn, since the nitrogen gas cylinder was kept open at all times and the regulator was set to the desired pressure. Several non-return valves were included in the system to ensure that the circulation always occurred in one direction.

This system should ensure that the liquid, from the media reservoir, was inserted into the system with a peristaltic pump and sterile Masterflex® Norprene tubing (Cole-Parmer®). Due to the presence of non-return valves, the liquid entered the system from below the reactor until the entire system, including both the variable media reservoirs, were filled with the media. The CO_2 gas was then used to saturate the system, also from below the reactor, and to give the initial pressure (~55 bar). Since the CO_2 gas cylinders are not under enough pressure to reach ≥80 bar, the rest of the pressure was added with the piston regulators and nitrogen gas. To reach the desired pressure, the first piston pressure regulator was pressurized, while the second piston pressure regulator was set to release pressure via the pressure release valve. This meant that the three-way valve from the first piston regulator was opened between the nitrogen gas cylinder and the piston regulator which allowed the nitrogen to enter and adjust the first variable media reservoir, while the three-way valve from the second piston regulator was opened between the piston regulator and the pressure release valve to allow the nitrogen inside the piston regulator to escape. The same principle was applied to the variable media reservoirs through the opening of the three-way valves, allowing the first media reservoir to empty its contents into the system using the piston pressure regulator, while the second media reservoir was filled with liquid from the system, pushing up on the piston pressure regulator.

The moment the first media reservoir was empty, all four the three-way valves were switched to ensure that the same process was repeated just in the opposite direction.

Even though the flow direction was altered between the two media reservoirs, the flow through the reactor was always in the same direction and was controlled with the addition of the non-return valves. The flow speed of the system was controlled by opening and closing the pressure release valve until the desired flow was reached. As an additional control, a control valve was included in the system and isolating valves were added throughout the system to ensure that any part of the system can be removed, if faulty, without disturbing the pressure of the reactor itself.

Pressure gauges were connected to the reactor, the variable media reservoirs and the piston pressure regulators to ensure that the entire system was under the desired pressure at all times. As a safety measurement, an adjustable pressure valve was included in the system which was always set to release at a pressure of 5 bar higher than the operating pressure. To enable sampling, a liquid sampling port was connected to the adjustable pressure valve to allow samples to be taken in a controlled manner. The piston regulator that was under pressure, ensured that the operating pressure was maintained by decreasing the system volume after sampling.

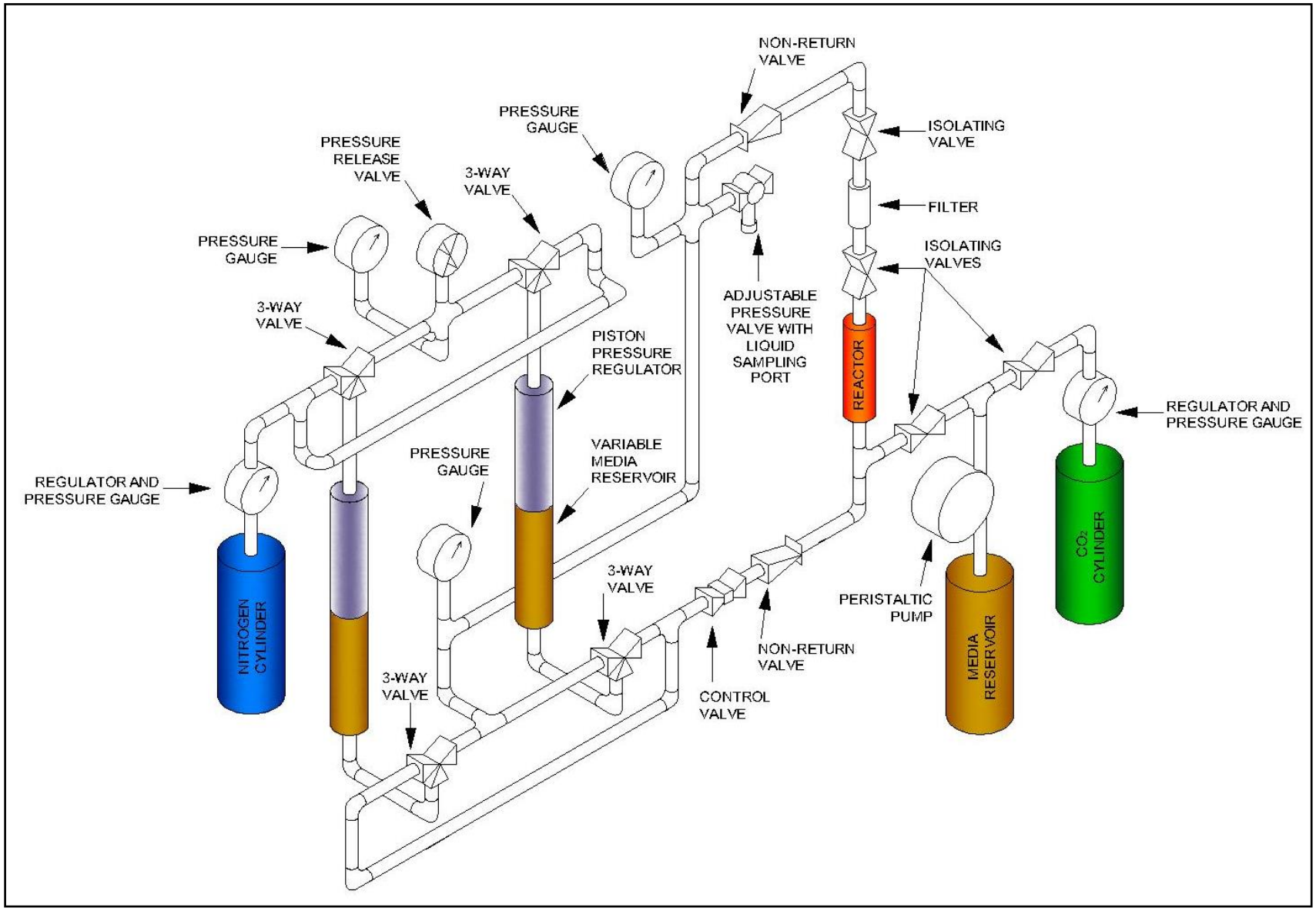

Figure 5.13: Schematic illustration of the fifth design of the bioreactor.

For the final design (Figure 5.14 and Figure 5.15), small adjustments were made, but the mode of operation stayed the same as discussed in design five. The filter added after the reactor was removed, since blockage occurred. The flow speed was still too fast, even though it was regulated with the control valve and the pressure release valve. Therefore, a flow restrictor was included in the system using 1/16 inch stainless steel tubing. This was added after the adjustable pressure valve with the sampling port and was connected via a three-way valve to ensure that the flow restrictor could be isolated when it was not needed. A liquid inlet port was added between the two variable media reservoirs to allow for any additional liquid to be introduced into the system by isolating one of the media reservoirs and releasing its pressure. The liquid can then be introduced into the media reservoir at atmospheric pressure. The media reservoir was pressurized again before opening to the system, thus the pressure on the reactor itself was never disturbed. Both the nitrogen and the CO_2 gas lines were equipped with valves that isolated them and could be used to evacuate or purge the lines to allow them to be removed from the system without being under pressure. All gas cylinders were connected to the bioreactor using high pressure, safety tubing.

The bioreactor was designed to be able to operate under high pressures and temperatures and can be used for both static and circulating experiments. The bioreactor had a total system volume of ~400 ml.

Except for the Swagelok® components and all the pumps used, everything on the bioreactors was custom-made by the Department of Instrumentation at the UFS (Bloemfontein, RSA), the Department of Electronics at the UFS (Bloemfontein, RSA) and Earthmoving Repair Services (Bloemfontein, RSA).

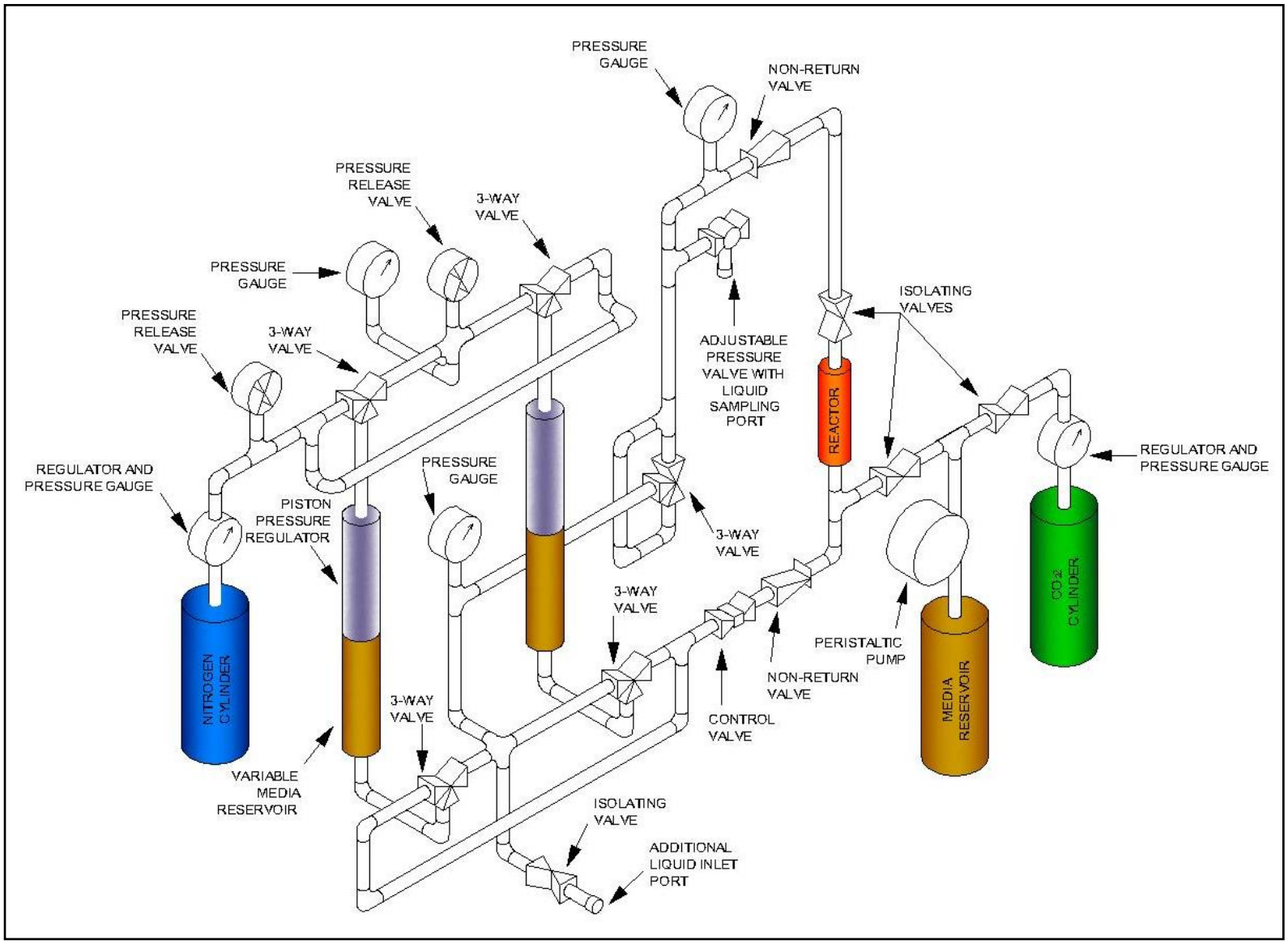

Figure 5.14: Schematic illustration of the sixth design of the bioreactor.

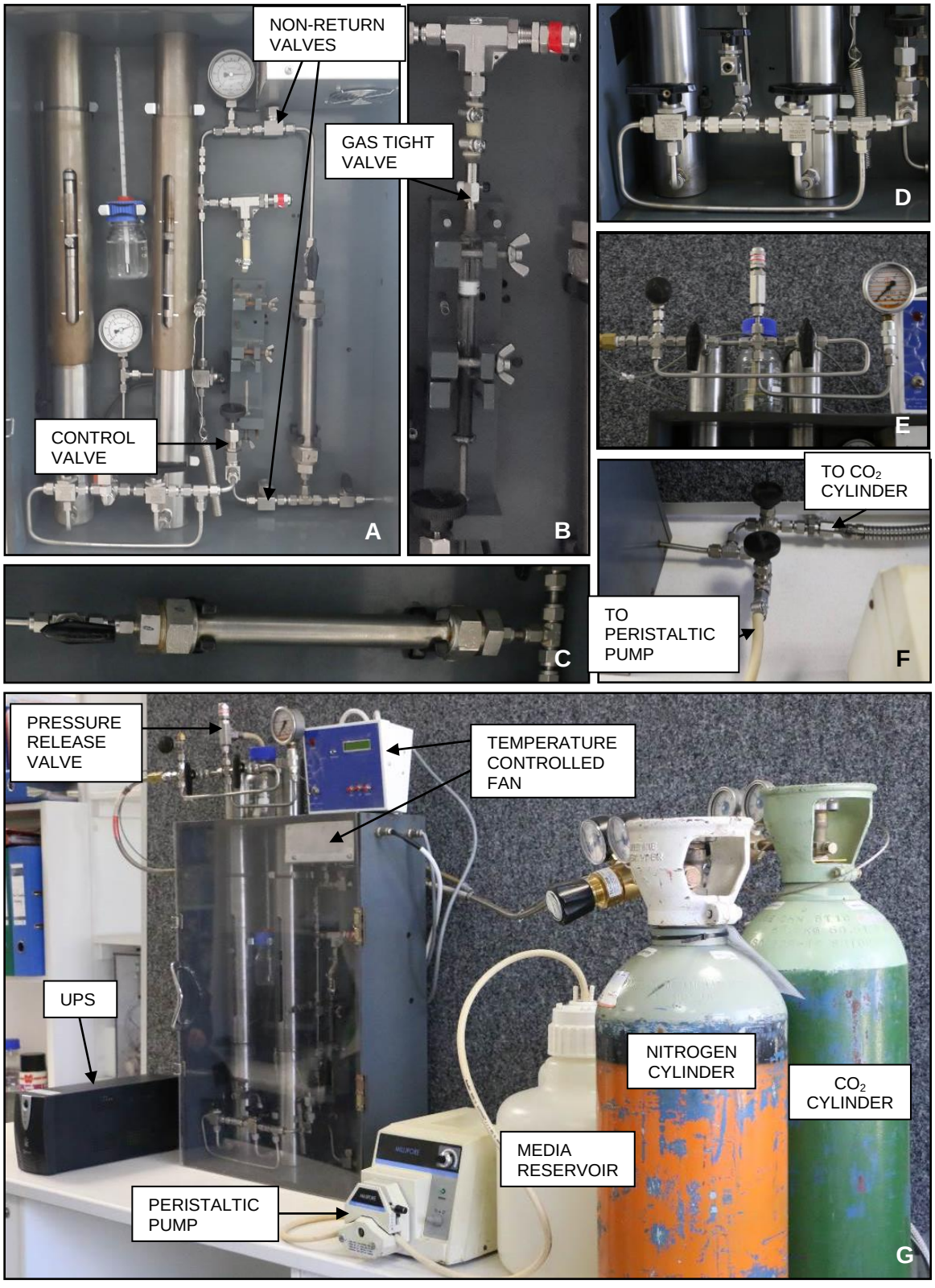

Figure 5.15: (A) The bioreactor, constructed from the fifth and sixth designs, (B) a gas tight syringe connected to the sampling port, (C) the reactor, (D) the three-way valves regulating the variable media reservoirs, (E) the three-way valves regulating the piston pressure regulators, (F) the connection to the CO_2 gas cylinder and the media reservoir through the peristaltic pump, and (G) the bioreactor as a whole.

5.3.2.2 Operational Procedures

All connections were secured to ensure a leak free system. The bioreactor was then washed overnight with 10% (v/v) HCl to remove any organic contaminants and impurities (Rotzsche, 1991), by slow circulation through the entire system. This was followed by an overnight sterilizing step, by slowly circulating 10% (v/v) commercial bleach through the system. The system was then rinsed with Nano-pure water, until all traces of the bleach was removed.

The reactor was removed from the system and packed with the rock matrix under sterile conditions in a laminar flow cabinet (Labotec®), where after the reactor was again connected to the system. The temperature controlled fan was switched on and the system was allowed to reach the operating temperature, where after the desired medium, containing the inoculum was added to the reactor until the entire system was filled using a peristaltic pump and sterile Masterflex® Norprene tubing (Cole-Parmer®). This liquid was added by bypassing the flow restrictor. CO_2 gas was then used to saturate the system and to add the initial pressure, by opening the regulator in the CO_2 gas cylinder to its maximum. The piston pressure regulators were then pressurized with the nitrogen gas, by setting the regulator on the nitrogen gas cylinder to the desired operating pressure. The three-way valves were opened to allow circulation through the flow restrictor. The CO_2 gas line was removed from the system, as well as the line used to fill the reactor from the media reservoir. Whenever fresh media had to be introduced into the system, the latter line was attached to an additional liquid inlet port between the two variable media reservoirs. One of the media reservoirs was isolated from the system and evacuated to atmospheric pressure. The fresh liquid was added into the media reservoir using the peristaltic pump, where after the media reservoir was pressurized and opened to be part of the system.

To obtain a sample, a sterilized, gas-tight glass syringe (Hamilton) was connected to the sampling port via a gas-tight valve. The pressure valve was opened to allow liquid to slowly enter into the syringe, where after the gas tight valve connected to the syringe was closed to ensure no gas escapes from the syringe. In this way, samples were taken in a controlled manner without losing system pressure or altering any of the conditions. The syringe was removed from the system and the collected sample was injected into a sterile, gas-tight vial.

To end the run, all valves in the system were closed to isolate the reactor, followed by closing the nitrogen gas cylinder. The pressure on the system was slowly released by opening the pressure release valve of the piston regulators. This was done for both the variable media reservoirs. The liquid was pumped from the system using the peristaltic pump and collected in sterile containers to be used for analyses. The reactor was removed from the system and opened under sterile conditions, where the rock was removed for analyses.

Throughout preparation and operation of the bioreactor, leak tests were constantly done to ensure a system free from any gas leakages. The final pressure in the system was always controlled with the regulator on the nitrogen gas cylinder and the flow speed was regulated by connecting a tube to the pressure release valve from the piston regulators. This tube was inserted into water to allow the visualization of bubbles that formed as the nitrogen gas was released. The pressure release valve was adjusted to obtain the desired flow speed.

5.4 CONCLUSIONS

Various authors have reported on different systems which have been used to study the effects of higher pressures on the genetic, metabolic, biochemical, and physiological aspects of microorganisms and these systems have been designed to fit the specific conditions and requirements of each experiment. The reactors used in this research were successfully designed to be versatile and corrosion resistant and were able to operate under higher pressures and temperatures, to mimic CCS conditions within the laboratory. Sampling from the bioreactor was possible, without disturbing any of the reactor conditions.

Even though the bioreactor functioned very well after the sixth design, enhancements can still be made to improve the functionality of the bioreactor. Since the three-way valves had to be switched manually each time one of the variable media reservoirs were empty, it meant that the bioreactor had to be monitored continuously to ensure constant circulation. To prevent this, one might consider the use of automatic valves for the switching.

The material used in constructing the reactors were made out of corrosion-free stainless steel, but any potential corrosion and metal leakage from the bioreactor should be considered. Thus, Nelson *et al*., (1992), had the interior of their reactor plated with 24-karat gold. To prevent the gold coating from flaking and peeling off under high pressures and mechanical stresses, they first added an undercoat of electroless nickel below the gold. This enabled better adhesion of the gold and increased the mechanical strength of the coating. Sauer *et al*., (2012), only used inert materials such as polyvinylidene fluoride (PVDF), perfluoro-elastomers (FFKM), or gold during the construction of their bioreactor, to prevent corrosion.

On another note, the design only allowed for a total reactor volume of 84.86 cm^3 which was a very limited sample to be used for comprehensive analyses and should therefore be considered to adapt the reactor to bigger volumes.

5.5 REFERENCES

- **Abe, F. and Horikoshi, K.** (2001). The Biotechnological Potential of Piezophiles. *Trends Biotechnol*. **19**:102-108.

- **Abe, F., Kato, C. and Horikoshi, K.** (1999). Pressure-Regulated Metabolism in Microorganisms. *Trends Microbiol*. **7**:447-453.

- **Arakawa, S., Nogi, Y., Sato, T., Yoshida, Y., Usami, R. and Kato, C.** (2006). Diversity of Piezophilic Microorganisms in the Closed Ocean Japan Sea. *Biosci. Biotechnol. Biochem*. **70**:749-752.

- **Bartlett, D.H., Wright, M., Yayanos, A.A. and Silverman, M.** (1989). Isolation of a Gene Regulated by Hydrostatic Pressure in a Deep-Sea Bacterium. *Nature.* **342**:572-574.

- **Berberich, J.A.** (2001). Whole Cell Biocatalysis in the Presence of Supercritical and Compressed Solvents. *PhD Thesis, University of Kentucky, Lexington*.

- **Berberich, J.A., Knutson, B.L., Strobel, H.J., Tarhan, S., Nokes, S.E. and Dawson, K.A.** (2000). Product Selectivity Shifts in *Clostridium thermocellum* in the Presence of Compressed Solvents. *Ind Eng Chem Res*. **39**:4500-4505.

- **Bernhardt, G., Jaenicke, R. and Lüdemann, H.D.** (1987). High-Pressure Equipment for Growing Methanogenic Microorganisms on Gaseous Substrates at High Temperature. *Appl. Environ. Microbiol.* **53**:1876-1879.

- **Bernhardt, G., Jaenicke, R., Ludemann, H.D., Konig, H. and Stetter, K.O.** (1988). High-Pressure Enhances the Growth Rate of the Thermophilic Archaebacterium *Methanococcus thermolithotrophicus* without Extending its Temperature Range. *Appl. Environ. Microbiol.* **54**:1258-1261.

- **Boonyaratanakornkit, B.B., Miao, L.Y. and Clark, D.S.** (2007). Transcriptional Responses of the Deep-Sea Hyperthermophile *Methanocaldococcus jannaschii* under Shifting Extremes of Temperature and Pressure. *Extremophiles*. **11**:495-503.

- **Bothun, G.D., Knutson, B.L., Berberich, J.A., Strobel, H.J. and Nokes, S.E.** (2004). Metabolic Selectivity and Growth of *Clostridium thermocellum* in Continuous Culture under Elevated Hydrostatic Pressure. *Appl Microbiol Biotechnol*. **65**:149-157.

- **Bubela, B., Labone, C.L. and Dawson, C.H.** (1987). An Apparatus for Continuous Growth of Microorganisms under Oil Reserve Conditions. *Biotechnol Bioeng*. **29**:289-291.

- **Canganella, F., Gonzalez, J.M., Yanagibayashi, M., Kato, C. and Horikoshi, K.** (1997). Pressure and Temperature Effects on Growth and Viability of the Hyperthermophilic Archaeon *Thermococcus peptonophilus*. *Arch Microbiol*. **168**:1-7.

- **Chapelle, F.H. and Lovley, D.R.** (1990). Rates of Microbial Metabolism in Deep Coastal Plain Aquifers. *Appl. Environ. Microbiol.* **56**:1865-1874.

- **Charlou, J.L., Donval, J.P., Fouquet, Y., Jean-Baptiste, P. and Holm, N.** (2002). Geochemistry of High H_2 and CH_4 Vent Fluids Issuing from Ultramafic Rocks at the Rainbow Hydrothermal Field (36°14′N, MAR). *Chem Geol.* **191**:345-359.

- **Chicoye, E., Helbert, J.R. and Rice, J.F.** (1978). Accelerated Fermentation of Lager Beer. *US Patent 4,068,005*.

- **Cloete, M.** (2010). Atlas on Geological Storage of Carbon Dioxide in South Africa. Council for Geoscience.

- **Delong, E.F. and Yayanos, A.A.** (1985). Adaptation of the Membrane Lipids of a Deep-Sea Bacterium to Changes in Hydrostatic Pressure. *Science.* **228**:1101-1103.

- **Dillow, A.K., Dehghani, F., Hrkach, J.S., Foster, N.R. and Langer, R.** (1999). Bacterial Inactivation by using Near- and Supercritical Carbon Dioxide*. Proc. Natl. Acad. Sci.* **96**:10344-10348.

- **Dixon, N.M. and Kell, D.B.** (1989). The Inhibition by CO_2 of the Growth and Metabolism of Microorganisms. *J Appl Bacteriol*. **67**:109-136.

- **Eklund, T.** (1984). The Effect of Carbon Dioxide on Bacterial Growth and on Uptake Processes in Bacterial Membrane Vesicles. *Int J Food Microbiol*. **1**:179-185.

- **Fang, J., Zhang, L. and Bazylinski, D.A.** (2010). Deep-Sea Piezosphere and Piezophiles: Geomicrobiology and Biogeochemistry. *Trends Microbiol*. **18**:413-422.

- **Hauben, K.J.A., Bartlett, D.H., Soontjens, C.C.F. and Cornelis, K.** (1997). *Escherichia coli* Mutants Resistant to Inactivation by High Hydrostatic Pressure. *Appl Environ Microbiol*. **63**:945-950.

- **Hei, D.J. and Clark, D.S.** (1994). Pressure Stabilization of Proteins from Extreme Thermophiles. *Appl. Environ. Microbiol.* **60**:932-939.

- **Hiraki, T., Sekiguchi, T., Kato, C., Hatada, Y., Maruyama, T., Abe, F. and Konishi, M.** (2012). New Type of Pressurized Cultivation Method Providing Oxygen for Piezotolerant Yeast. *Journal of Bioscience and Bioengineering*. **113(2)**:220-223.

- **Holden, J.F. and Baross, J.A.** (1995). Enhanced Thermotolerance by Hydrostatic-Pressure in the Deep-Sea Hyperthermophile *Pyrococcus* strain ES4. *FEMS Microbiol Ecol*. **18**:27-33.

- **Hong, S.I., Park, W.S. and Pyun, Y.R.** (1997). Inactivation of *Lactobacillus* sp. from Kimchi by High-Pressure Carbon Dioxide. *Food Science and Technology-Lebensmittel-Wissenschaft & Technologie.* **30**:681-685.

- http://www.sacccs.org.za/roadmap/. (2015).

- **Hutton, W.C., Elmer, W.A., Bryce, L.M., Kozlowska, E.E., Boden, S.D and Kozlowski, M.** (2001). Do the Intervertebral Disc Cells Respond to Different Levels of Hydrostatic Pressure? *Clinical Biomechanics.* **16**:728-734.

- **Jannasch, H.W., Wirsen, C.O. and Doherty, K.W.** (1996). A Pressurized Chemostat for the Study of Marine Barophilic and Oligotrophic Bacteria. *Appl Environ Microbiol*. **62**:1593-1596.

- **Jones, R.P. and Greenfield, P.F.** (1982). Effect of Carbon Dioxide on Yeast Growth and Fermentation. *Enzyme Microb Technol*. **4**:210-223.

- **Jones, W.J., Leigh, J.A., Mayer, F., Woese, C.R. and Wolfe, R.S.** (1983). *Methanococcus jannaschii* sp. nov., an Extremely Thermophilic Methanogen from a Submarine Hydrothermal Vent. *Arch Microbiol*. **136**:254-261.

- **Kaneshiro, S.M. and Clark, D.S.** (1995). Pressure Effects on the Composition and Thermal Behaviour of Lipids from the Deep-Sea Thermophile *Methanococcus jannaschii*. *J. Bacteriol.* **177**:3668-3672.

- **Kato, C.** (2006). Handling of Piezophilic Microorganisms. In Extremophiles. Methods in Microbiology, Vol. 35. *Elsevier Publishers.* 733-741.

- **Kato, C., Tamegai, H., Ikegami, A., Usami, R. and Horikoshi, K.** (1996). Open Reading Frame 3 of the Barotolerant Bacterium Strain DDS12 is Complementary with cydD in *Escherichia coli*: cydD Functions are required for Cell Stability at High-Pressure. *J. Biochem*. **120**:301-305.

- **Knutson, B.L., Strobel, H.J., Nokes, S.E., Dawson, K., Berberich, J.A. and Jones, C.R.** (1999). Effect of Pressurized Solvents on Ethanol Production by the Thermophilic Bacterium *Clostridium thermocellum*. *J Supercrit Fluids*. **16**:149-156.

- **Lamad, R.J., Lobos, J.H. and Su, T.M.** (1988). Effects of Stirring and Hydrogen on Fermentation Products of *Clostridium thermocellum*. *Appl Environ Microbiol*. **54**:1216-1221.

- **Lee, D., Heinz, V. and Knorr, D.** (2001). Biphasic Inactivation Kinetics of *Escherichia coli* in Liquid Whole Egg by High Hydrostatic Pressure Treatments. *Biotechnol Prog*. **17**:1020-1025.

- **Lin, H.M., Cao, N.J. and Chen, L.F.** (1994). Antimicrobial Effect of Pressurized Carbon-Dioxide on *Listeria monocytogenes*. *Journal of Food Science.* **59**:657-659.

- **Lovley, D.R. and Chapelle, F.H.** (1995). Deep Subsurface Microbial Processes. *Review of Geophysics*. **33(3)**:365-381.

- **Lupton, J., Lilley, M., Butterfield, D., Evans, L., Embley, R., Massoth, G., Christenson, B., Nakamura, K. and Schmidt, M.** (2008). Venting of a Separate CO_2-Rich Gas Phase from Submarine Arc Volcanoes: Examples from the Mariana and Tonga-Kermadec Arcs. *J Geophys Res.* **113**: B08S12.

- **Marteinsson, V.T., Birrien, J.L., Reysenbach, A.L., Vernet, M., Marie, D., Gambacorta, A., Messner, P., Sleytr, U.B. and Prieur, D.** (1999a). *Thermococcus barophilus* sp. nov., a New Barophilic and Hyperthermophilic Archaeon Isolated under High Hydrostatic Pressure from a Deep-Sea Hydrothermal Vent. *Int J Syst Bacteriol*. **49(Pt 2)**:351-359.

- **Marteinsson, V.T., Reysenbach, A.L., Birrien, J.L. and Prieur, D.** (1999b). A Stress Protein is Induced in the Deep-Sea Barophilic Hyperthermophile *Thermococcus barophilus* when grown under Atmospheric Pressure. *Extremophiles*. **3**:277-282.

- **McIntyre, M. and McNeil, B.** (1998). Morphogenetic and Biochemical Effects of Dissolved Carbon Dioxide on Filamentous Fungi in Submerged Cultivation. *Appl Microbiol Biotechnol*. **50**:291-298.

- **Miller, J.F., Shah, N.N., Nelson, C.M., Ludlow, J.M. and Clark, D.S.** (1988). Pressure and Temperature Effects on Growth and Methane Production of the Extreme Thermophile *Methanococcus jannaschii*. *Appl. Environ. Microbiol.* **54**:3039-3042.

- **Nelson, C.M., Schuppenhauer, M.R. and Clark, D.S.** (1991). Effects of Hyperbaric Pressure on a Deep-Sea Archaebacterium in Stainless Steel and Glass-Lined Vessels. *Applied and Environmental Microbiology.* **57(12)**:3576-3580.

- **Nelson, C.M., Schuppenhauer, M.R. and Clark, D.S.** (1992). High-Pressure, High-Temperature Bioreactor for Comparing Effects of Hyperbaric and Hydrostatic Pressure on Bacterial Growth. *Applied and Environmental Microbiology*. **58(5)**:1789-1793.

- **Orcutt, B., Samarkin, V., Boetius, A. and Joye, S.** (2008). On the Relationship between Methane Production and Oxidation by Anaerobic Methanotrophic Communities from Cold Seeps of the Gulf of Mexico. *Environ. Microbiol.* **10**:1108-1117.

- **Oulé, K.M., Dickman, M. and Arul, J.** (2010). Microbicidal Effect of Pressurized CO_2 and the Influence of Sensitizing Additives. *European Journal of Scientific Research.* **41(4)**:569-581.

- **Park, C.B. and Clark, D.S.** (2002). Rupture of the Cell Envelope by Decompression of the Deep-Sea Methanogen *Methanococcus jannaschii*. *Applied and Environmental Microbiology.* **68(3)**:1458-1463.

- **Parton, T., Elvassore, N., Bertucco, A. and Bertoloni, G.** (2007). High-Pressure CO_2 Inactivation of Food: A Multi-Batch Reactor System for Inactivation Kinetic Determination. *J. of Supercritical Fluids.* **40**:490-496.

- **Paul, K.L. and Morita, R.Y.** (1971). Effects of Hydrostatic Pressure and Temperature on the Uptake and Respiration of Amino Acids by a Facultatively Psychrophilic Marine Bacterium. *J. Bacteriol.* **108**:835-843.

- **Person, A., Seewald, J.S. and Eglinton, T.I.** (2005). Bacterial Incorporation of Relict Carbon in the Hydrothermal Environment of Guaymas Basin. *Geochim Cosmochim Acta.* **69**:5477-5486.

- **Prieur, D.** (1997). Microbiology of Deep-Sea Hydrothermal Vents. *Trends Biotechnol*. **15**:242-244.

- **Rotzsche, H.** (1991). Acid Washing. In Stationary Phases in Gas Chromatography, Vol. 48. *Elsevier Publishers.* 171. ISBN: 0444987339.

- **Sauer, P., Glombitza, C. and Kallmeyer, J.** (2012). A System for Incubations at High Gas Partial Pressure. *Frontiers in Microbiology.* **3**:25.

- **Schieche, D., Murty, M., Kermode, R. and Bhattacharyya, D.** (1997). Biohydrogenation of Fumarate using *Desulfovibrio desulfuricans*: Experimental Results and Kinetic Rate Modelling. *J Chem Tech Biotechnol*. **70**:316-322.

- **Schmid, G., Lüdemann, H.D. and Jaenicke, R.** (1978). Oxidation of Sulfhydryl Groups in Lactate Dehydrogenase under High Hydrostatic Pressure. *Eur. J. Biochem.* **86**:219-224.

- **Schulz, E., Lüdemann, H.D. and Jaenicke, R.** (1976). High-Pressure Equilibrium Studies on the Dissociation–Association of *E. coli* Ribosomes. *FEBS Lett.* **64**:40-43.

- **Seyfried, W.E.** (1979). A New Reaction Cell for Hydrothermal Solution Equipment. *Am. Mineral.* **64**:646-649.

- **Seyfried, W.E. and Janecky, D.R.** (1985). Heavy Metal and Sulfur Transport during Subcritical and Supercritical Hydrothermal Alteration of Basalt: Influence of Fluid Pressure and Basalt Composition and Crystallinity. *Geochim. Cosmochim. Acta.* **49**:2545-2560.

- **Smelt, J.P.P.M.** (1998). Recent Advances in the Microbiology of High-Pressure Processing. *Trends Food Sci Technol*. **9**:152-158.

- **Sturm, F.J., Hurwitz, S.A., Deming, J.W. and Kelly, R.M.** (1987). Growth of the Extreme Thermophile *Sulfolobus acidocaldarius* in a Hyperbaric Helium Bioreactor. *Biotechnol. Bioeng.* **29**:1066-1074.

- **Sun, M.M.C. and Clark, D.S.** (2001). Pressure Effects on Activity and Stability of Hyperthermophilic Enzymes. *Meth. Enzymol.* **334**:316-327.

- **Takai, K., Miyazaki, M., Hirayama, H., Nakagawa, S., Querellou, J. and Godfroy, A.** (2009). Isolation and Physiological Characterization of Two Novel, Piezophilic, Thermophilic Chemolithoautotrophs from a Deep-Sea Hydrothermal Vent Chimney. *Environmental Microbiology.* **11(8)**:1983-1997.

- **Takai, K., Nakamura, K., Toki, T., Tsunogai, U., Miyazaki, M., Miyazaki, J., Hirayama, H., Nakagawa, S., Nunoura, T. and Horikoshi, K.** (2008). Cell Proliferation at 122°C and Isotopically Heavy CH_4 Production by a Hyperthermophilic Methanogen under High-Pressure Cultivation. *Proc. Natl. Acad. Sci*. **105(31)**:10949-10954.

- **Vance, I. and Brink, D.E.** (1994). Propionate-Driven Sulphate-Reduction by Oil-Field Bacteria in a Pressurised Porous Rock Bioreactor. *Appl Microbiol Biotechnol.* **40**:920-925.

- **Vezzi, A., Campanaro, S., D'Angelo, M., Simonato, F., Vitulo, N., Lauro, F.M., Cestaro, A., Malacrida, G., Simionati, B., Cannata, N., Romualdi, C., Bartlett, D.H. and Valle, G.** (2005). Life at Depth: *Photobacterium profundum* Genome Sequence and Expression Analysis. *Science*. **307**:1459-1461.

- **Yanagibayashi, M., Nogi, Y., Lina, L. and Kato, C.** (1999). Changes in the Microbial Community in Japan Trench Sediment from a Depth of 6292 m during Cultivation without Decompression. *FEMS Microbiol. Lett*. **170**:271-279.

- **Yayanos, A.A.** (1986). Evolutional and Ecological Implications of the Properties of Deep-Sea Barophilic Bacteria. *Proc. Natl. Acad. Sci.* **83**:9542-9546.

- **Yayanos, A.A. and Dietz, A.S.** (1983). Death of a Hadal Deep-Sea Bacterium after Decompression. *Science*. **220**:497-498.

- **Yayanos, A.A., Dietz, A.S. and Van Boxtel, R.V.** (1982). Dependence of Reproduction Rate on Pressure as a Hallmark of Deep-Sea Bacteria. *Appl. Environ. Microbiol.* **44**:1356-1361.

- **Yayanos, A.A., Van Boxtel, R. and Dietz, A.S.** (1984). High-Pressure-Temperature Gradient Instrument: Use for Determining the Temperature and Pressure Limits of Bacterial Growth. *Appl. Environ. Microbiol.* **48**:771-776.

- **Zhang, J., Davis, T.A., Matthews M.A., Drews, M.J., LaBerge, M. and An, Y.H.** (2006). Sterilization using High-Pressure Carbon Dioxide. *Journal of Supercritical Fluids.* **38**:354-372.

- **Zhang, Y., Maignien, L., Zhao, X., Wang, F. and Boon, N.** (2011). Enrichment of a Microbial Community Performing Anaerobic Oxidation of Methane in a Continuous High-Pressure Bioreactor. *BMC Microbiology.* **11**:137.

- **Zobell, C.E. and Oppenheimer, C.H.** (1950). Some Effects of Hydrostatic Pressure on the Multiplication and Morphology of Marine Bacteria. *J. Bacteriol.* **60**:771-781.

CHAPTER 6

HIGH PRESSURE STUDIES USING THE SYRINGE INCUBATORS

6.1 INTRODUCTION

In Chapter 4 it was shown that the subsurface biome was able to stay viable and metabolically active after being subjected to various environmental changes, which included nutrient deprivation and relatively low pressure. However, as discussed in Chapter 1, geological carbon sequestration would require storage at depths of ~800 mbs which are associated with higher pressures and temperatures, thereby causing the CO_2 to be in a supercritical state (Benson & Cole, 2008; Cunningham *et al*., 2009; Cloete, 2010; Nondorf *et al*., 2011). Thus, like Mu *et al*., (2014), and other authors, an important question to address during CCS is how will the subsurface microbial biosphere respond to increased levels of CO_2?

An increase in the depth of the terrestrial subsurface results in even bigger environmental changes such as an increase in the pressure, temperature, and salinity of the water, and a possible decrease in the redox potential, pore space, and nutrient abundance (Machel & Foght, 2013; Wilkins *et al*., 2014). As a result, the microorganisms living in these environments have to be able to survive and multiply under these conditions (Wilkins *et al*., 2014), thus, living under extreme energy limiting conditions under which the microorganisms are likely to be inactive or to display exceptionally low metabolic activities (Phelps *et al*., 1994; Jørgensen & D'Hondt, 2006; Jørgensen & Boetius, 2007; Onstott *et al*., 2009).

Therefore, the subsurface biome was subjected to different conditions which the microorganisms will encounter during CCS, including high pressures and high CO_2 concentrations in both nutrient rich and nutrient deprived environments.

6.1.1 Supercritical Carbon Dioxide

At standard temperature and pressure (STP), CO_2 will behave as a gas in air, or as a solid (dry ice) when frozen. If both the temperature and pressure are increased from STP to be at or above the critical point for CO_2 (73.8 bar and 31.1°C) (Figure 6.1), it will be in a supercritical state where the CO_2 has a gas-like viscosity and the density of a liquid, but it is neither a gas nor a liquid and can therefore only be defined as a substance in a state (supercritical) above its critical temperature (Tc) and critical pressure (Pc) (Dostal *et al*., 2004; Garcia-Gonzalez *et al*., 2007; Mitchell *et al*., 2009; Cloete, 2010; Budisa & Schulze-Makuch, 2014). If CO_2 is stored at depths of ~800 mbs, the higher pressures and temperatures at these depths will result in the CO_2 being in a supercritical state and therefore, able to fill the pore spaces more efficiently, as well as decreasing the buoyancy differences when compared with *in situ* fluids (Benson & Cole, 2008). In the supercritical state, CO_2 can also dissolve more readily in water and react with cations to form stable mineral compounds (Metz *et al*., 2005; Cloete, 2010). At depths less than 800 mbs, where the pressures and temperatures are lower, the CO_2 will be in a subcritical state (liquid form), where it will be less soluble and not form a homogeneous mixture when in contact with the formation water, therefore, reactions where stable, mineral compounds are created, will be less (Metz *et al*., 2005; Cloete, 2010).

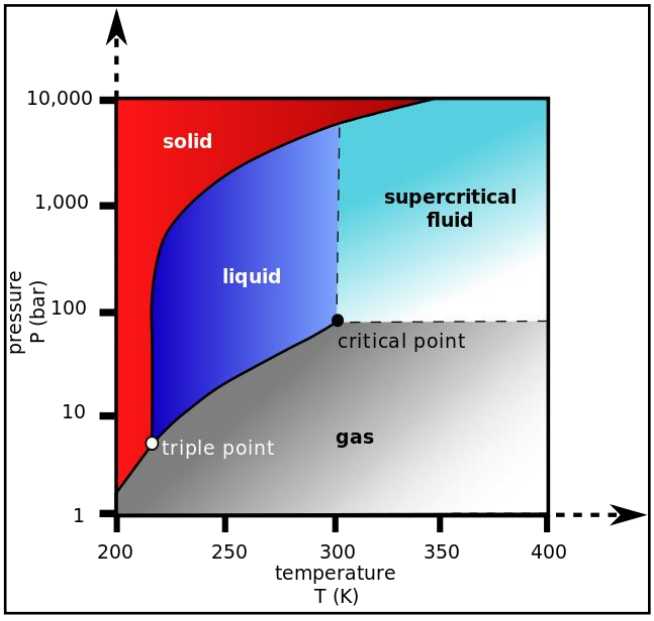

Figure 6.1: A pressure-temperature phase diagram for carbon dioxide (Taken from https://en.wikipedia.org/wiki/Supercritical_carbon_dioxide).

However, during the injection of supercritical CO_2 (sc-CO_2), the pressure in the area surrounding the injection point will increase, creating a possible upward hydrodynamic pressure gradient that can progress through the cap-rock that is responsible for trapping the CO_2 in the storage rock (Chapter 1). This can result in possible upward leakage of CO_2 through fractures near the injection wells (White *et al*., 2003; Mitchell *et al*., 2009), allowing for enhanced interaction between sc-CO_2 and the subsurface biomes.

6.1.2 Microbial Interaction with Supercritical Carbon Dioxide

The distinctive properties of sc-CO_2 under high pressures have led to it being used in a variety of fields such as the food and beverage, pharmaceutical, and biomedical industries, where it is often used as a sterilizing agent because it is non-toxic, non-flammable, and does not degrade polymers or heat-sensitive materials (Chen & Ling, 2000; Rozzi & Singh, 2002; Zhang *et al*., 2006; Glossner, 2013; Peet *et al*., 2015).

It has been found that the injection of sc-CO_2 into the deep subsurface affects the majority of microorganisms negatively, mostly due to its low viscosity and low surface tension. This results in direct physiological impacts on the subsurface microorganisms because it can quickly penetrate complex cellular material to reduce the number of viable cells (McHugh & Krukonis, 1994; Zhang *et al*., 2006; Mitchell *et al*., 2009; Basava-Reddi, 2012; Peet *et al*., 2015). This microbiocidal effect is enhanced at higher temperatures which will increase the fluidity of cellular membranes, leading to enhanced CO_2 penetration through the cell walls, as well as at higher pressures which will increase the diffusivity and solubility of sc-CO_2 (Lin *et al*., 1994; Hong *et al*., 1997; Mitchell *et al*., 2009; Basava-Reddi, 2012).

As described in the literature, the mechanism for cell deactivation through the use of sc-CO_2 under high pressures contains several steps that can take place simultaneously and in a very complex and organized manner. These steps include: 1.) solubilization of pressurized CO_2 in the external liquid phase, 2.) modification or solubilization of the cellular membranes, 3.) cell lysis due to depressurization, 4.) decreasing of the intracellular pH (pHi), 5.) inactivation of the key enzymes or inhibition of the cellular metabolism due to the lowering of the pHi, 6.) direct inhibitory effects of molecular CO_2

and HCO_3^- on metabolism, 7.) disordering of the intracellular electrolyte balance, 8.) extraction of vital components from cells and cell membranes, and 8.) interfering with protein synthesis (Garcia-Gonzalez *et al*., 2007; Basava-Reddi, 2012; Li *et al*., 2013).

Therefore, the longevity of geological carbon sequestration does not only depend on the trapping mechanisms (solubility, mineral, and physical), but also on the interaction between the subsurface microorganisms that contribute to biogeochemical cycling in the injection formations, and the sequestered CO_2 (Glossner, 2013).

6.2 AIMS OF THIS CHAPTER

The main aims of this chapter were to:

- Evaluate the subsurface biome from the Star Diamonds mine in an environment that mimics geological CCS.
- Study the potential survival and possible growth of the subsurface biome under high pressures and high CO_2 concentrations in both nutrient rich and nutrient deprived environments.

6.3 MATERIALS AND METHODS

For all the high pressure experiments throughout this chapter, the syringe incubators, as described in Section 5.3.1, were used. The syringes used for all experiments were sterilized and prepared as discussed in Section 5.3.1.2. All graphs were constructed by plotting the mean and error values from two independent studies.

6.3.1 Cultivation Conditions and Analyses for *Eubacterium limosum*

To study the growth of *E. limosum* under various pressures, PYG medium was prepared anaerobically using fissure water as discussed in Section 4.3.1. The 5 ml syringes were prepared by adding 2 ml of the PYG medium containing a 10% (v/v) inoculum of *E. limosum* (Figure 6.2A), followed by adding 3 ml of a gas mixture, containing 80% H_2 and 20% CO_2 (v/v) (Figure 6.2B) as discussed in Section 4.3.3. The 25 ml syringes were prepared by adding 4 ml of the PYG medium containing the 10% inoculum (Figure 6.2C), followed by adding 6 ml of the gas mixture (Figure 6.2D).

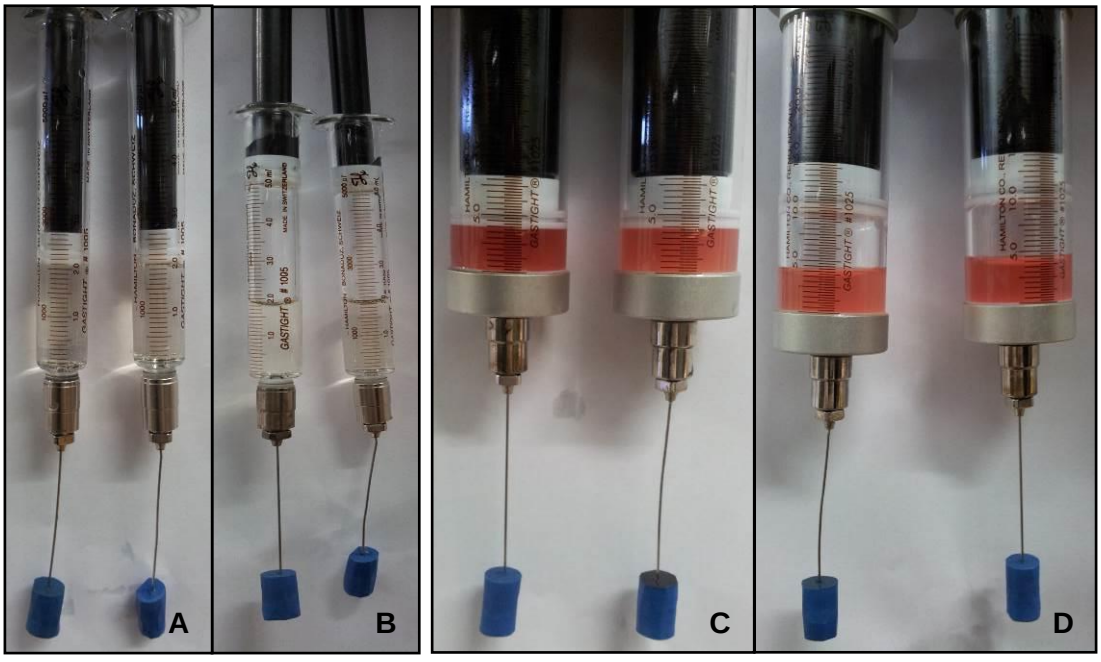

Figure 6.2: The prepared syringes for (A) 5 ml without gas, (B) 5 ml with gas, (C) 25 ml without gas, and (D) 25 ml with gas. (The LB medium is displayed in the yellow colour and the PYG medium in the red).

The syringes were transferred into heated incubators and pressurized as discussed in Section 5.3.1.3, until the desired pressure was reached. The pressurized syringes were then incubated at 35°C for 48 hours where after it was depressurized and the culture was analysed. For each syringe that was incubated for 48 hours, a duplicate set was prepared and pressurized, but immediately depressurized again. This was used as the time zero analyses. Negative controls, containing no cells, were also prepared for each pressure tested.

The pressure range tested was from 10 – 100 bar, with 10 bar increments.

Final growth yields were analysed after each syringe was sacrificed, by measuring the OD at 600 nm using a Spectronic® Genesys™ 5 spectrophotometer (Spectronic Instruments). Adenosine triphosphate (ATP) measurements were done using the CellTiter-Glo® Luminescent Cell Viability Assay (Promega) according to the manufacturer's instructions, with a Glomax® Multi+ Detection System (Promega). For additional confirmation of microorganism viability, the LIVE/DEAD® BacLight™ Bacterial Viability Kit (Molecular Probes, Inc., Invitrogen, Promega) was used as discussed in Section 3.3.6.8.2.

To study the growth of *E. limosum* under various gas concentrations, syringes were prepared with the PYG medium containing a 10% (v/v) inoculum of *E. limosum*. The desired gas mixtures were prepared using the procedure explained in Section 4.3.3 and added to each syringe. The syringes were transferred to the prepared incubators and pressurized to 80 bar, to ensure that the CO_2 is in the supercritical state. For each syringe, a duplicate set was prepared that was pressurized to only 70 bar, to ensure that the CO_2 is in the subcritical state. In this way, the influence of supercritical CO_2 could be evaluated under the same conditions as subcritical CO_2. The pressurized syringes were incubated and analysed as described previously. Time zero analyses and negative controls were again prepared for each test. Over a period of time, care was taken to consider any temperature fluxes, thus the incubators were constantly monitored to ensure growth took place under the correct pressure.

The gas range tested were different combinations of a H_2:CO_2 ratio and included 80%:20% (v/v), 50%:50% (v/v), 20%:80% (v/v), and 0%:100% (v/v).

To study the growth of *E. limosum* in both nutrient rich and nutrient deprived environments, syringes were again prepared with the desired medium containing a 10% (v/v) inoculum of *E. limosum*. Media used were prepared anaerobically and included PYG (Section 4.3.1), FW (Section 4.3.3), a minimal medium (0.2 $g.L^{-1}$ KH_2PO_4, 0.25 $g.L^{-1}$ NH_4Cl, 1 $g.L^{-1}$ NaCl, 0.4 $g.L^{-1}$ $MgCl_2$, 0.5 $g.L^{-1}$ KCl, 0.1 $g.L^{-1}$ $CaCl_2$, 0.2 $g.L^{-1}$ MOPS, 0.1 $g.L^{-1}$ yeast extract, 1 $ml.L^{-1}$ vitamin solution, 1 $ml.L^{-1}$ trace element solution, pH 7) with the addition of glucose (2 $g.L^{-1}$) (MM + Glc), and a minimal medium without the addition of glucose (MM - Glc). All media contained 0.5 $g.L^{-1}$ cysteine-$HCl.H_2O$ and 1 $mg.L^{-1}$ resazurin and the PYG and MM were prepared using fissure water. The gas, containing 0% H_2 and 100% CO_2 (v/v), was added as described previously and the syringes were pressurized to 80 bar, for supercritical CO_2 conditions and to 70 bar, for subcritical CO_2 conditions. The pressurized syringes were incubated and analysed as described previously and time zero analyses and negative controls were again prepared for each test.

6.3.2 Cultivation Conditions and Analyses for the Subsurface Biome

The growth of the subsurface biome was studied using the same pressures, gas concentrations and media compositions that were used for the cultivation of *E. limosum* as discussed in Section 4.3.3. The only differences were that general LB medium (Section 4.3.4) was used and not the PYG medium and the 10% (v/v) inoculums were made using the fissure water, containing the TFF concentrated subsurface biome (Section 3.3.6.3). Time zero analyses and negative controls were prepared for each parameter and the cultures from all the syringes were analysed for growth and viability as discussed in Section 4.3.3.

6.3.3 Experimental Layout for the Cultivation of *Eubacterium limosum* and the Subsurface Biome

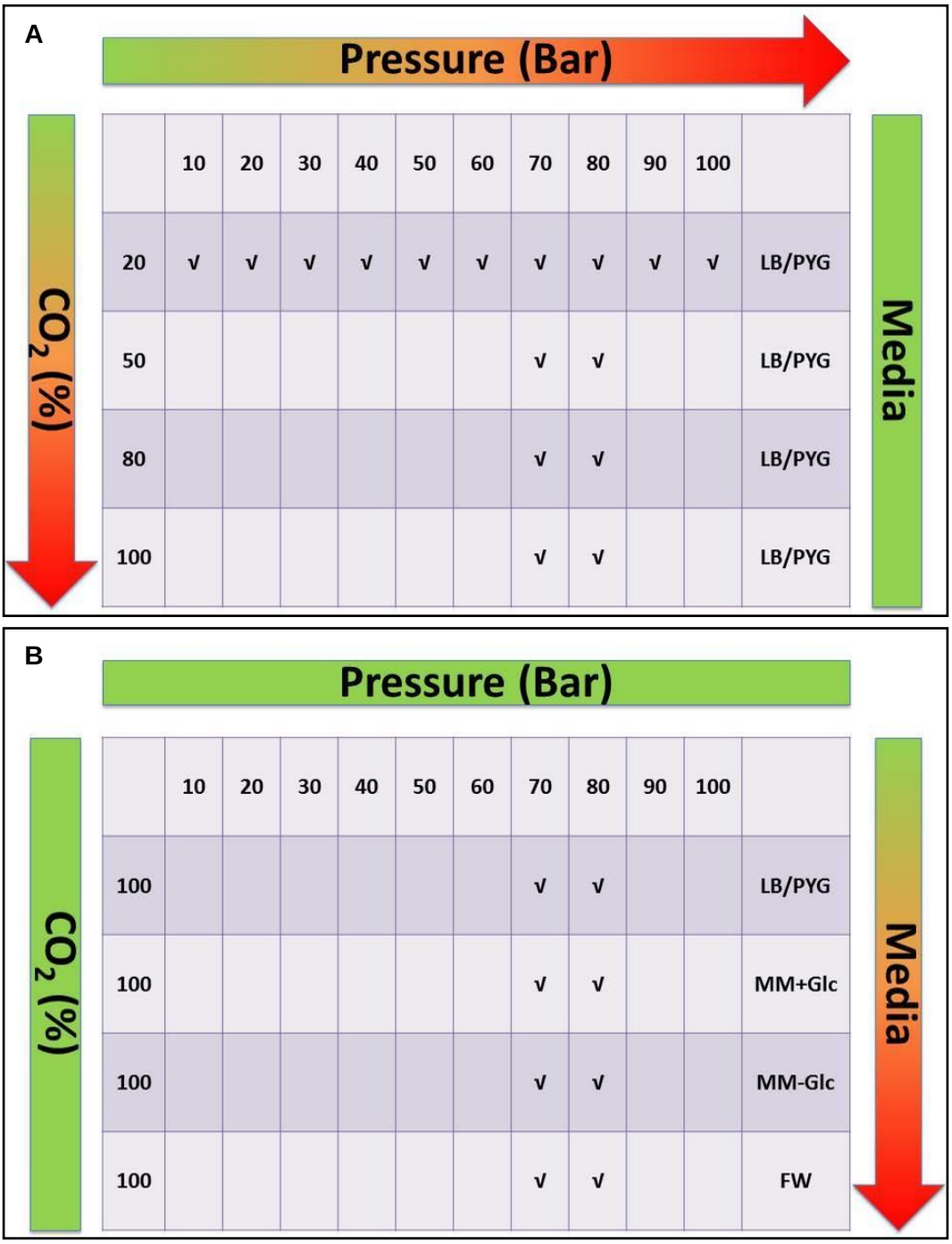

Figure 6.3: A summary of the experimental layout for the cultivation of *E. limosum* and the subsurface biome under increasing pressure and (A) different gas concentrations, with (B) different media compositions.

6.4 RESULTS AND DISCUSSIONS

6.4.1 Cultivation and Analyses of *Eubacterium limosum*

Optical density was used to analyse the growth of *E. limosum* after sacrificing the syringe experiments incubated under different pressures (Figure 6.4), different CO_2 concentrations (Figure 6.5), and different media compositions (Figure 6.6) as discussed in Section 4.3.3.

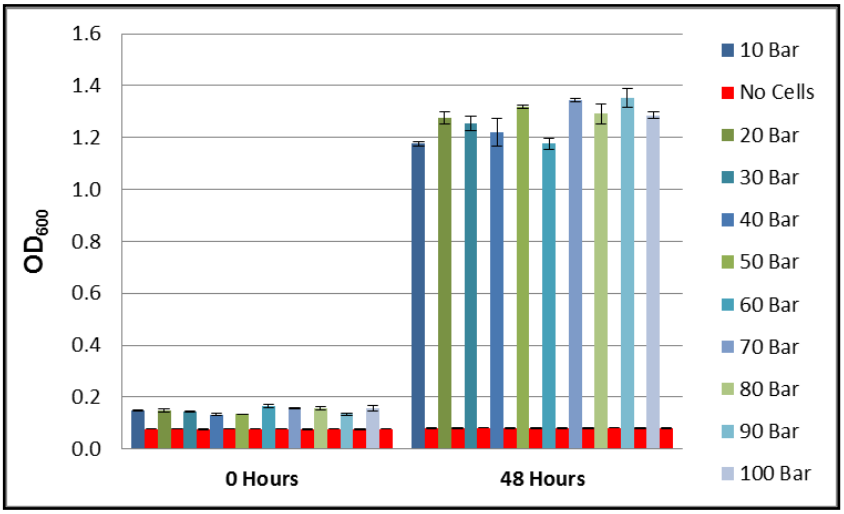

Figure 6.4: The growth of *E. limosum* after 48 hours in PYG medium, under various high pressures and 20% CO_2.

The increase in biomass yield obtained for *E. limosum* after 48 hours of growth indicated that the ability of *E. limosum* to grow under pressure was not influenced by the increasing pressure, even up to 100 bar.

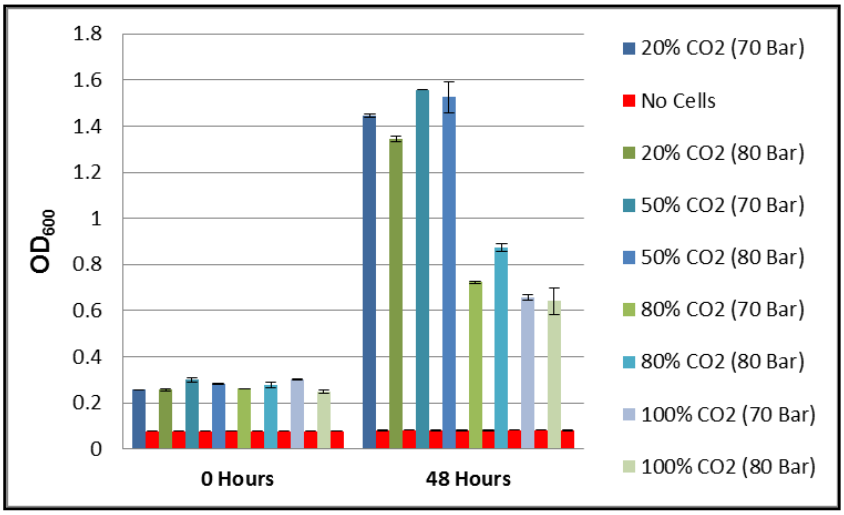

Figure 6.5: The growth of *E. limosum* after 48 hours in PYG medium, under various gas concentrations at 70 and 80 bar.

The biomass yields obtained for 80% and 100% CO_2 were much lower than those for 20% and 50% CO_2. This indicates that even though *E. limosum* was able to grow under all the gas concentrations tested, the increase in the CO_2 concentrations (with a decrease in the H_2) did influence growth. Growth was also similar for both the supercritical and the subcritical conditions, indicating that the supercritical state of the CO_2 did not affect the growth adversely when compared with the subcritical state. Considering Figure 6.4, the only parameters which changed is lowering the H_2, while increasing the CO_2, which should now reflect in the metabolic activity and thus affected the growth.

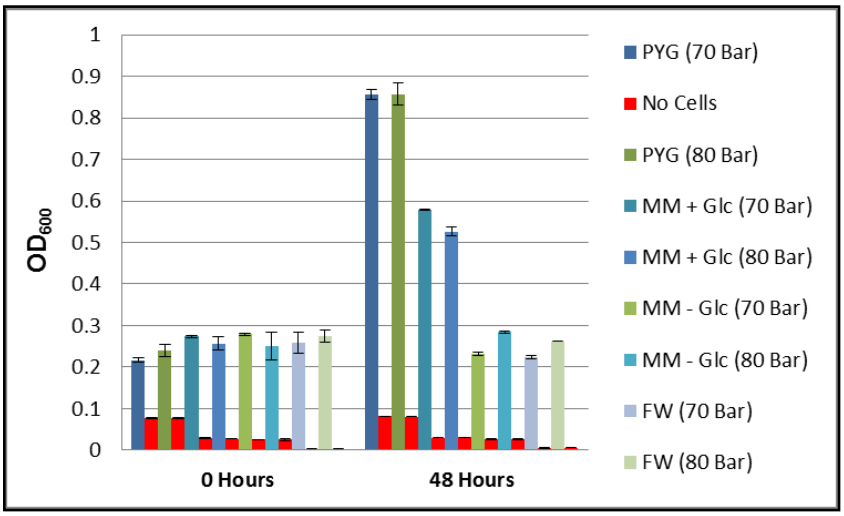

Figure 6.6: The growth of *E. limosum* after 48 hours in various media compositions, under 100% CO_2 at 70 and 80 bar.

For the different media compositions, it can be seen that an increase in the biomass yields were obtained for the PYG and MM + Glc media. However, no increase in the yields were obtained when *E. limosum* was grown in the nutrient deprived MM – Glc medium and when only fissure water was used. This indicated that when an additional carbon source was added to the medium, *E. limosum* was able to grow. However, when no additional carbon source was added, *E. limosum* was not able to use CO_2 as the sole carbon source to produce biomass when growing under >70 bar in 100% CO_2. In the literature it has been described that *E. limosum* has the ability to grow under pressures above 1 atm (1.01325 bar) when using CO as the sole carbon or energy source (Genthner & Bryant, 1982). However, when CO_2 was used as the sole carbon source, H_2 was additionally added as the energy source (Genthner *et al*., 1981; Genthner & Bryant,

1982; Loubière & Lindley, 1991; Lelait & Grivet, 1996; Roh *et al*., 2011). In other experiments, glucose, methanol, or acetate was added to improve growth (Genthner *et al*., 1981; Loubière & Lindley). Therefore, this is the first report where it was shown that *E. limosum* can grow beyond 2 bar, surprisingly even up to 100 bar using CO_2 as the sole carbon and energy source.

E. limosum has the ability to fix CO and CO_2 through the use of the Wood–Ljungdahl pathway [also known as the reductive acetyl coenzyme A (Acetyl-CoA) pathway] (Loubière & Lindley, 1991; Roh *et al*., 2011). According to Chivian *et al*., (2008), the application of the Wood–Ljungdahl pathway may have the added benefit of Na^+ export to aid in maintaining the Na^+ gradient utilized by the Na^+ antiporters and symporters. This includes the Na^+/H^+ antiporter that could aid in driving ATP synthase (H^+-dependent). Even though growth was low or minimal under certain conditions, the ATP measurements still displayed positive values for the cultures from all the syringe experiments. Therefore, one would expect that when *E. limosum* was not able to produce biomass under specific conditions, it could stay viable, but with limited metabolic activity. As additional confirmation that *E. limosum* stayed viable, live/dead stains (Section 3.3.6.10.2) were conducted for the different pressures (Figure 6.7), CO_2 concentrations (Figure 6.8), and media compositions (Figure 6.9).

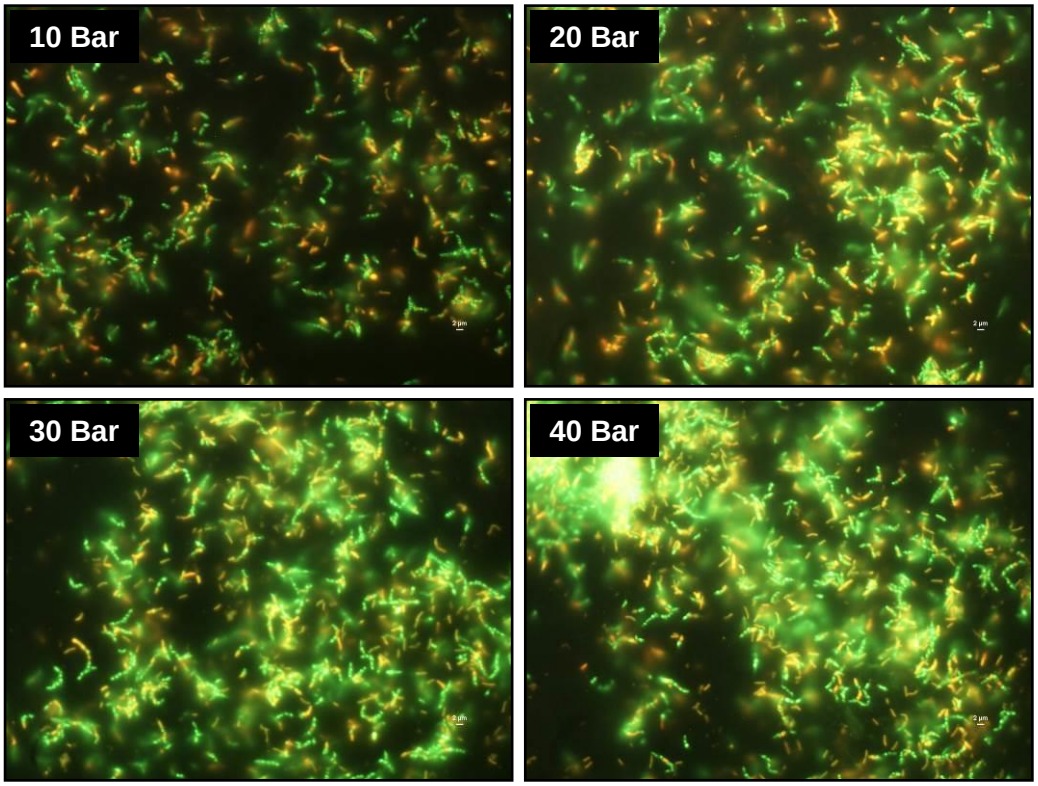

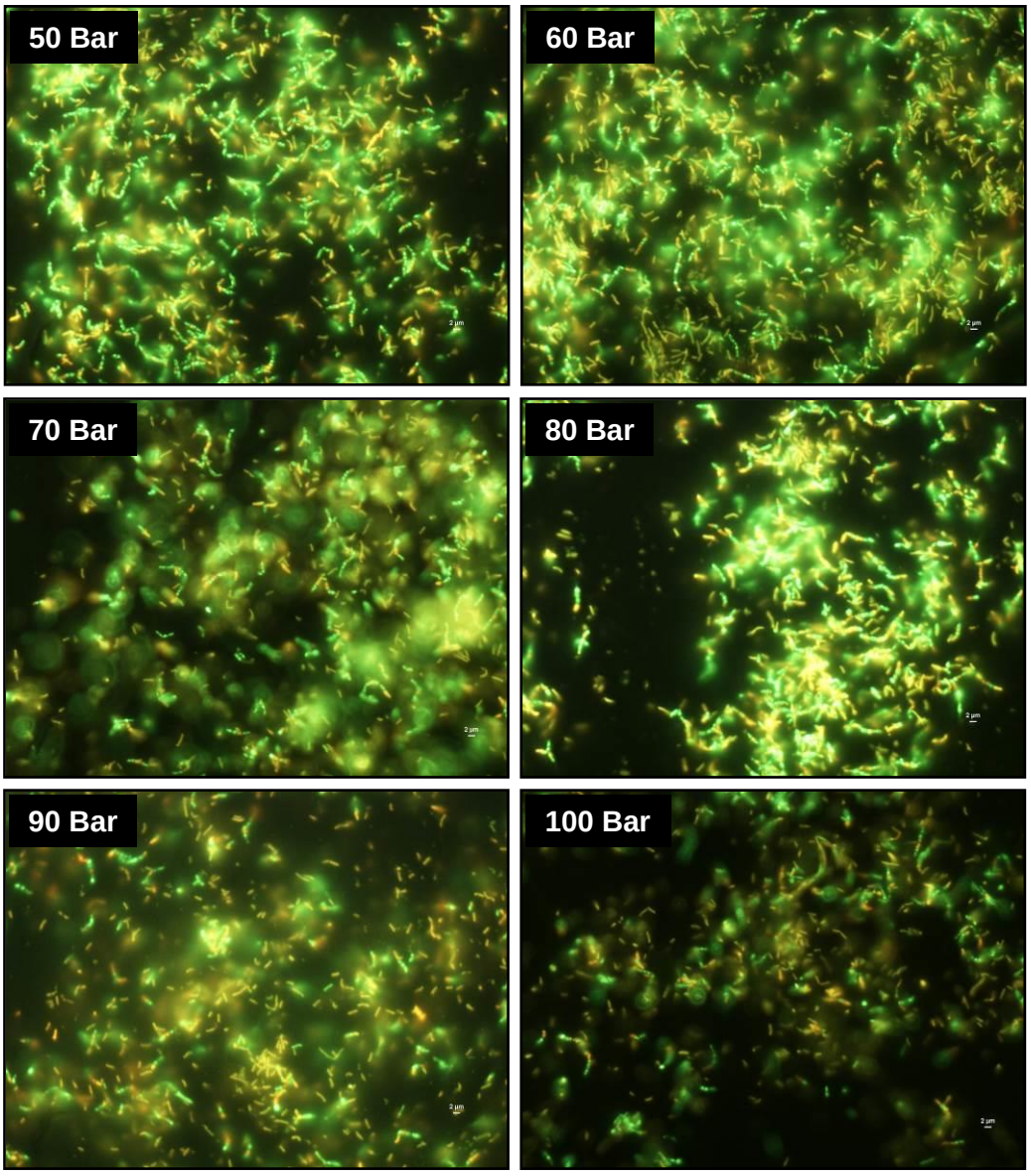

Figure 6.7: Live/Dead stain images of *E. limosum* after 48 hours in PYG medium, under various high pressures and 20% CO_2. All scale bars are equal to 2 µm.

The live/dead stains images confirmed that even though some of the cells died, many *E. limosum* cells were still alive after being subjected to pressures up to 100 bar.

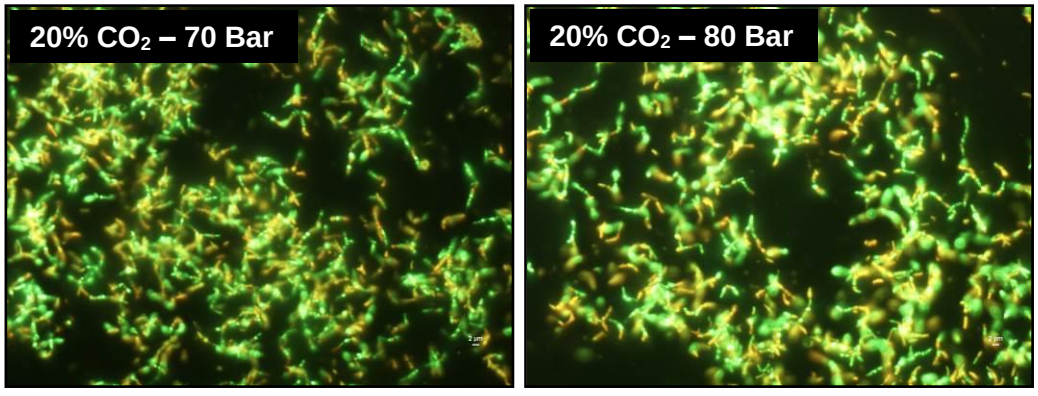

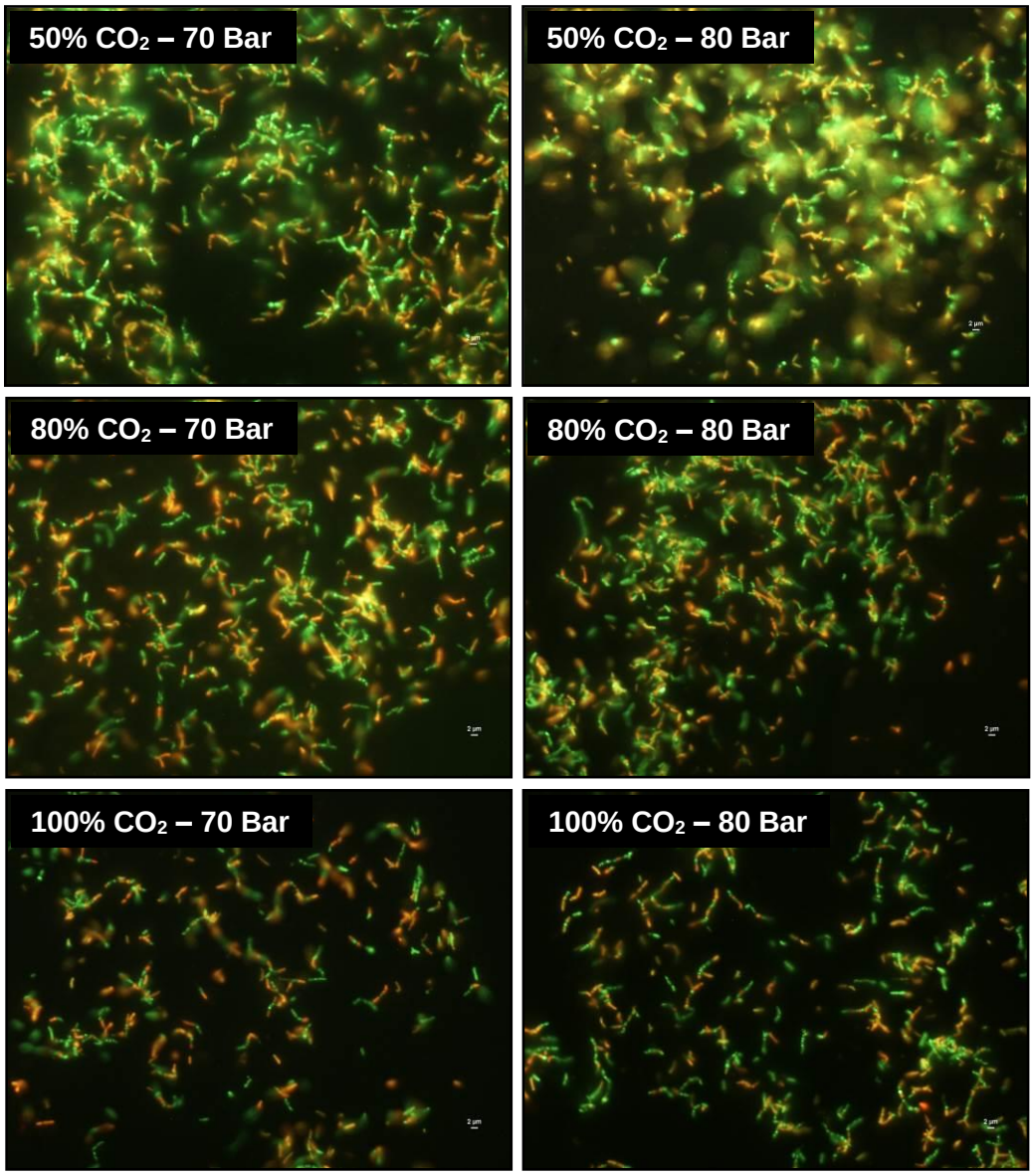

Figure 6.8: Live/Dead stain images of *E. limosum* after 48 hours in PYG medium, under various gas concentrations at 70 and 80 bar. All scale bars are equal to 2 µm.

Figure 6.8 and Figure 6.9 indicate live/dead stain activity after growth under different gas concentrations and different media compositions, respectively.

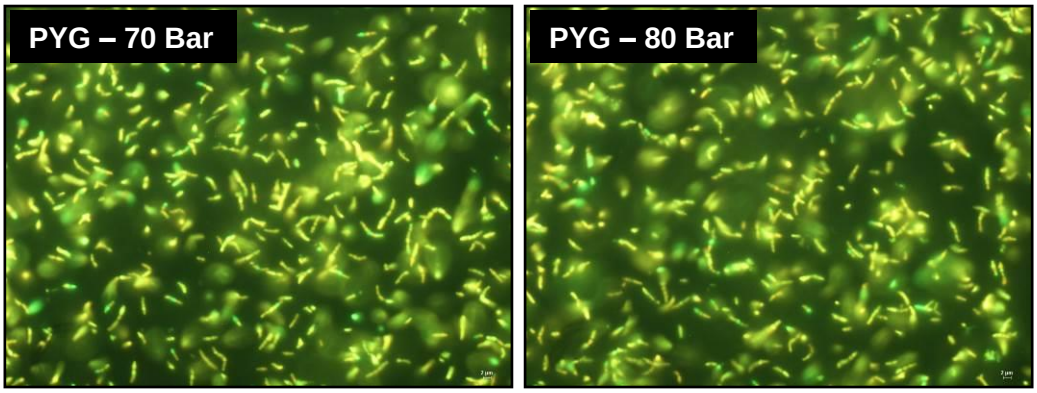

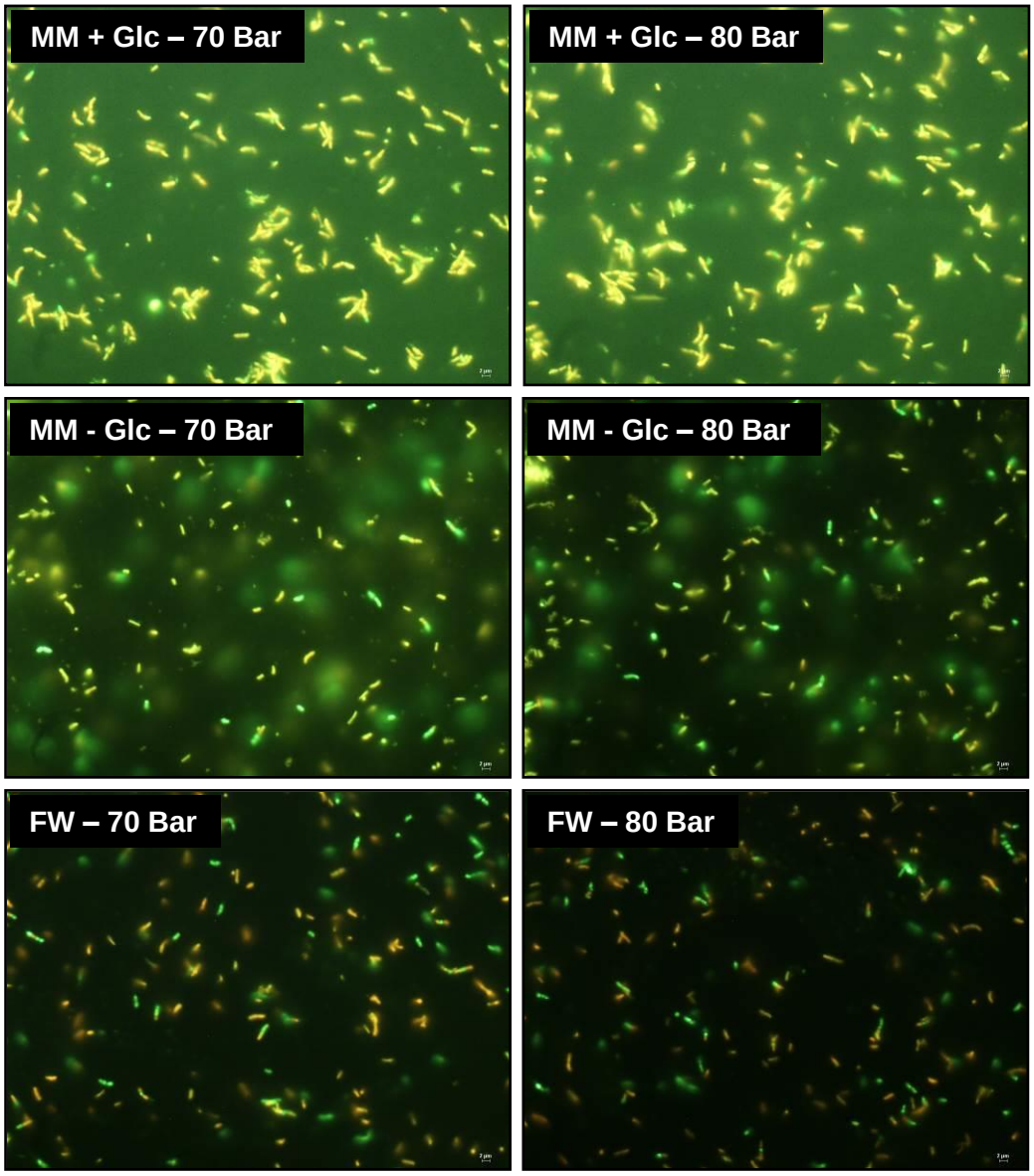

Figure 6.9: Live/Dead stain images of *E. limosum* after 48 hours in various media compositions, under 100% CO_2 at 70 and 80 bar. All scale bars are equal to 2 µm.

6.4.2 Cultivation and Analyses of the Subsurface Biome

Growth of the subsurface biome was analysed by optical density after sacrificing the syringe experiments incubated under different pressures (Figure 6.10), different CO_2 concentrations (Figure 6.11), and different media compositions (Figure 6.12) as discussed in Section 4.3.4.

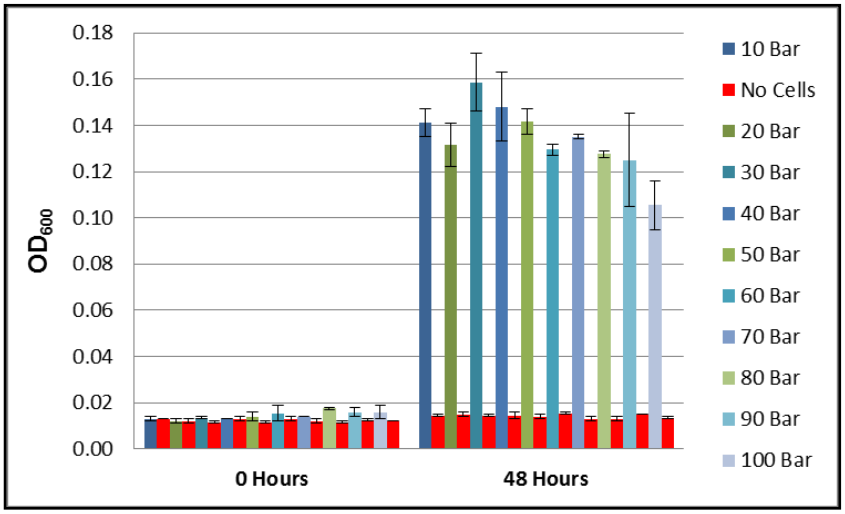

Figure 6.10: The growth of the subsurface biome after 48 hours in LB medium, under various high pressures and 20% CO_2.

An increase in the biomass yields was obtained for the subsurface biome after 48 hours of growth under all the different pressures tested. This indicated that even though the yields obtained were very low, the biome was able to proliferate under pressures up to 100 bar.

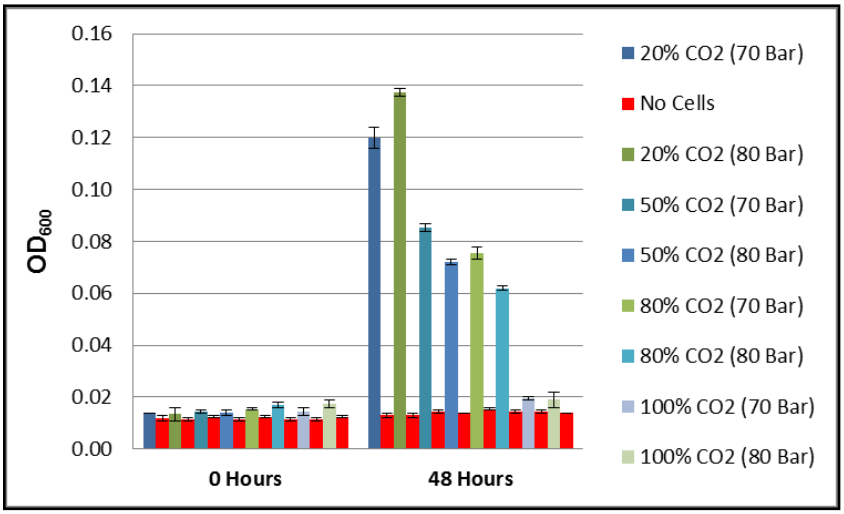

Figure 6.11: The growth of the subsurface biome after 48 hours in LB medium, under various gas concentrations at 70 and 80 bar.

The biomass yields obtained for the different gas concentrations decreased as the CO_2 concentration increased. At 100% CO_2, the biomass yields were almost negligible,

indicating that there was little to no growth after 48 hours. Growth was similar for both the supercritical and the subcritical conditions. As discussed for *E. limosum*, the lowering of the H_2 is reflected in the metabolic activity and thus affected growth.

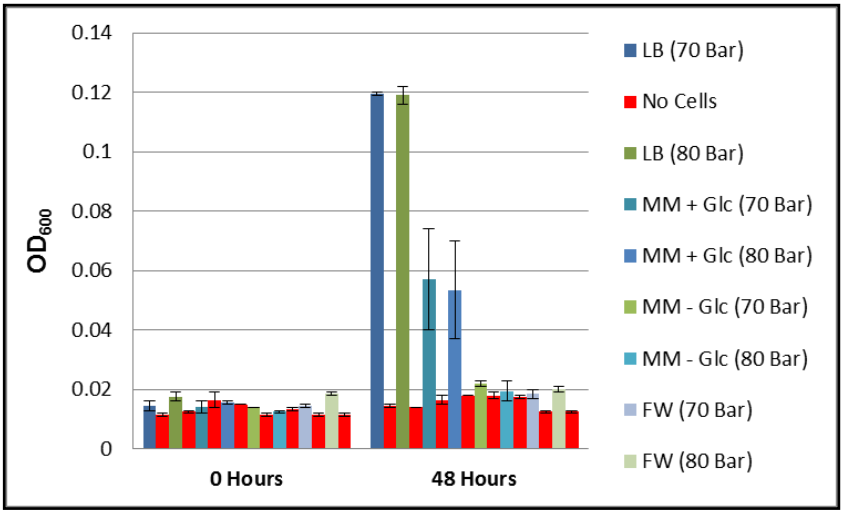

Figure 6.12: The growth of the subsurface biome after 48 hours in various media compositions, under 100% CO_2 at 70 and 80 bar.

Studies of the subsurface biome in the different media compositions indicated that growth only occurred when the medium contained an additional carbon source. Under nutrient limited conditions, almost no increase in the biomass yield was obtained. However, even though minimal growth was observed under all these conditions, the ATP measurements were still positive for the biome from all the syringe experiments. The Wood–Ljungdahl pathway occurs in the Archaeal methanogens and acetate-producing Bacteria such as *Clostridium* (Matschiavelli *et al*., 2012). As shown in Chapter 3, both these types of microorganisms are present in the subsurface biome, therefore, one would expect that the Wood–Ljungdahl pathway may aid in driving ATP synthase.

Live/dead stains (Section 3.3.6.10.2) were conducted for the different pressures (Figure 6.13), CO_2 concentrations (Figure 6.14) and media compositions (Figure 6.15), to confirm that the biome was still viable. The images shown were selected to also indicate the various morphologies present in the biome.

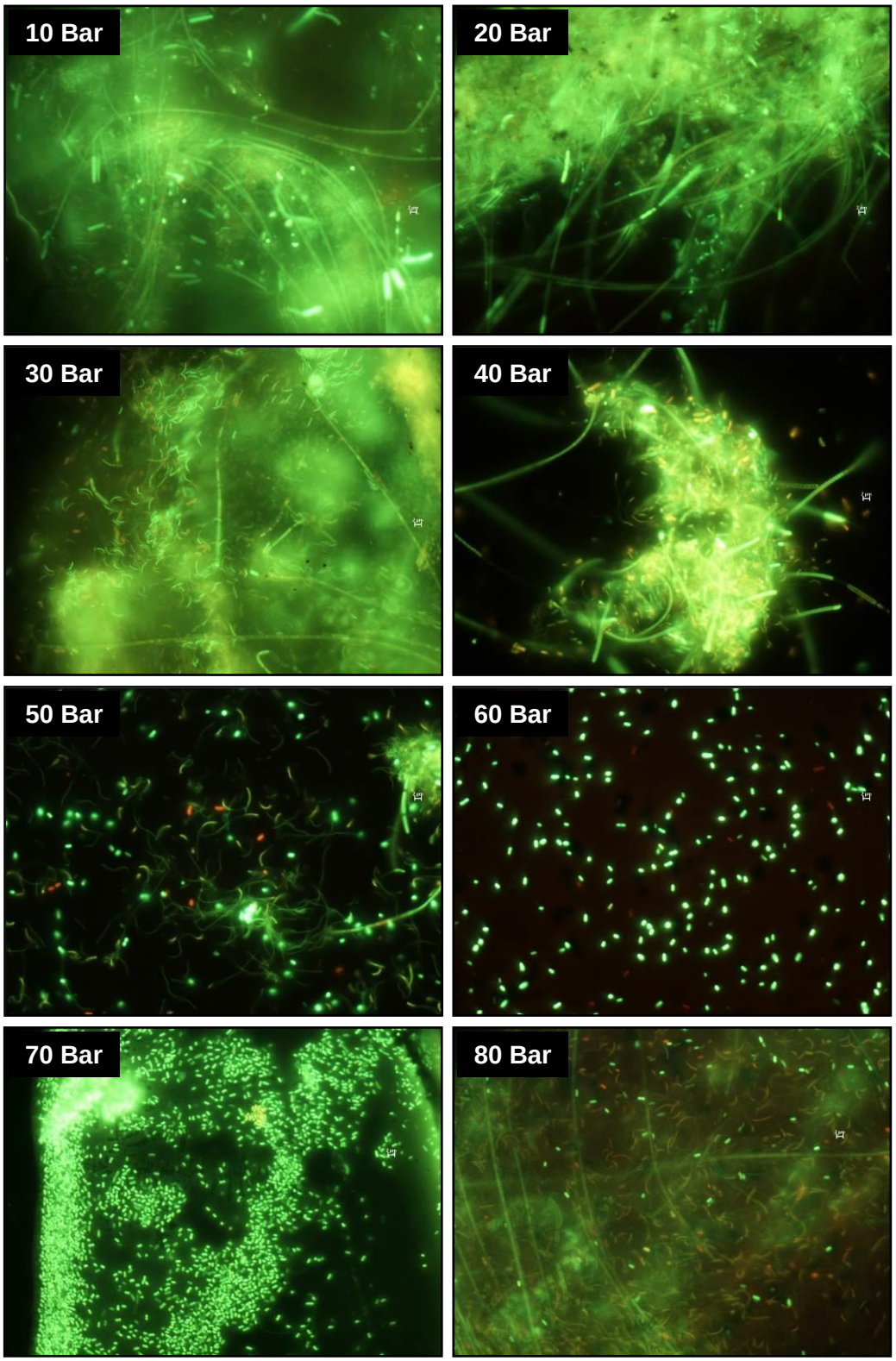
10 Bar
20 Bar
30 Bar
40 Bar
50 Bar
60 Bar
70 Bar
80 Bar

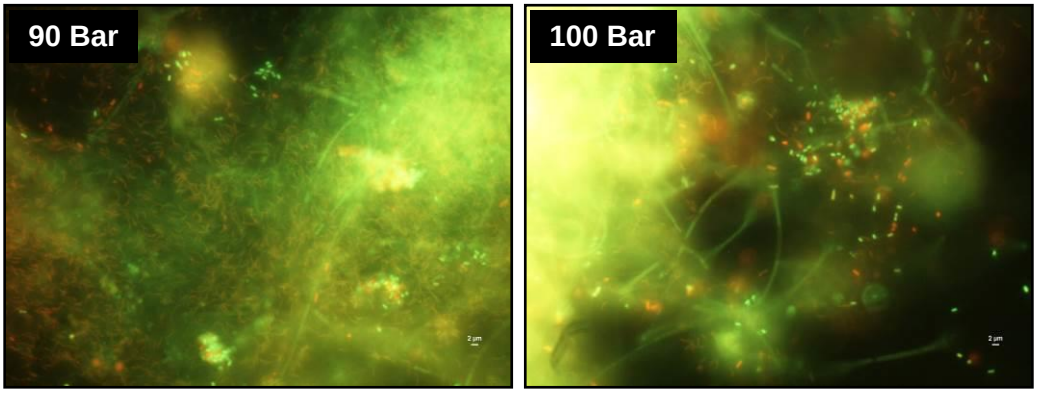

Figure 6.13: Live/Dead stain images of the subsurface biome after 48 hours in LB medium, under various high pressures and 20% CO_2. All scale bars are equal to 2 µm.

These images confirmed that the microorganisms were still mostly alive, even after 48 hours under pressures up to 100 bar. It was also found that as discussed in Section 3.4.3.3, the microorganisms formed biofilm-like structures through accumulation of cells, possibly as a stress response to protect against the conditions they were subjected to (Mitchell *et al*., 2009).

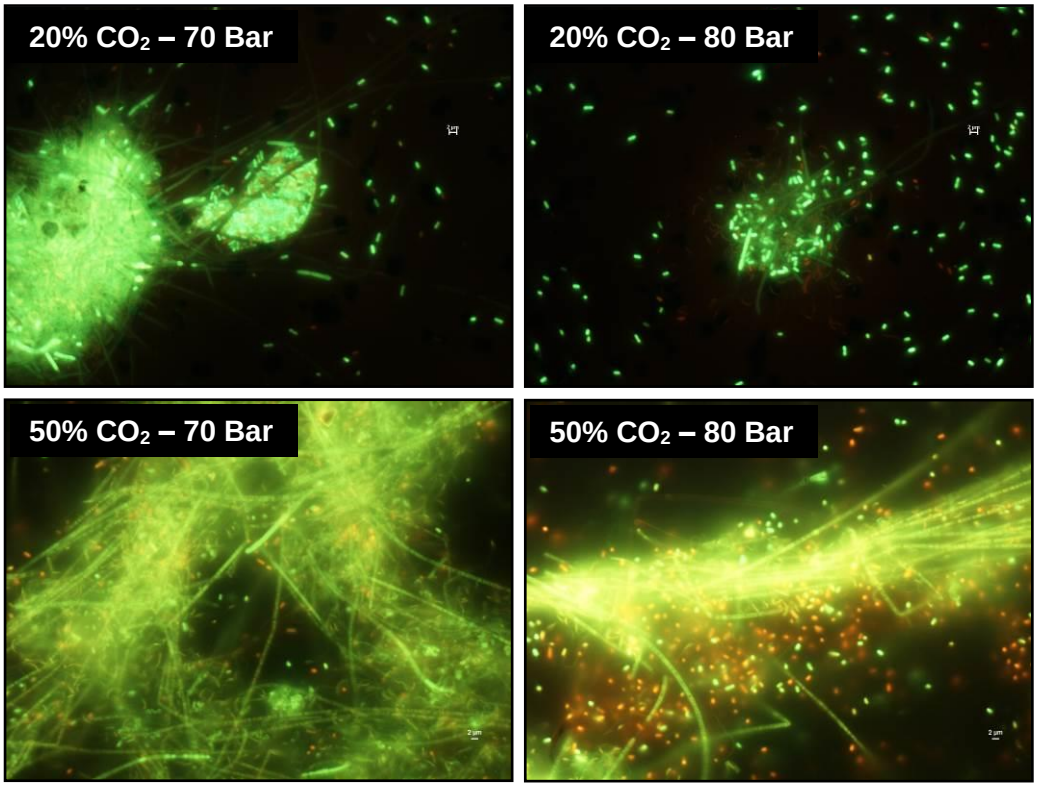

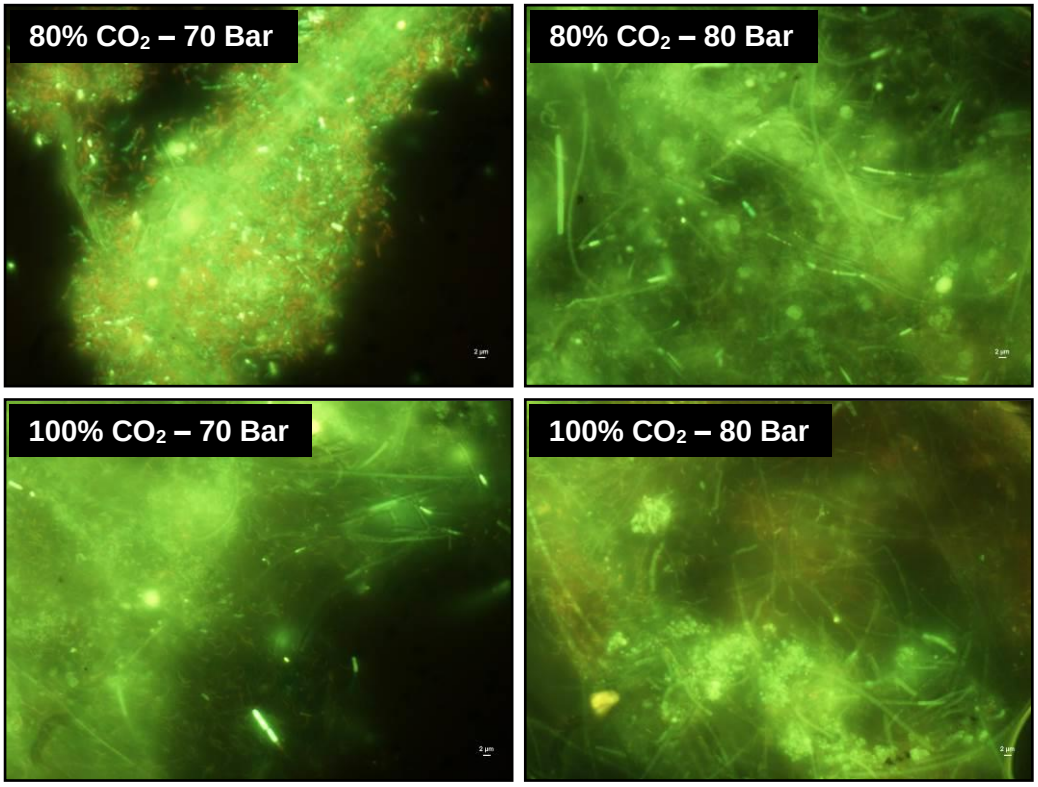

Figure 6.14: Live/Dead stain images of the subsurface biome after 48 hours in LB medium, under various gas concentrations at 70 and 80 bar. All scale bars are equal to 2 µm.

Figure 6.14 and Figure 6.15 indicate live/dead stain activity after growth under different gas concentrations and different media compositions, respectively.

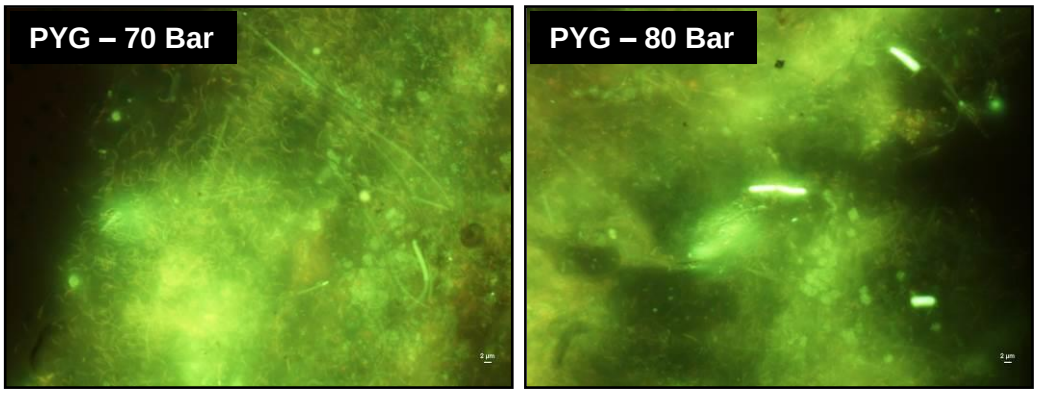

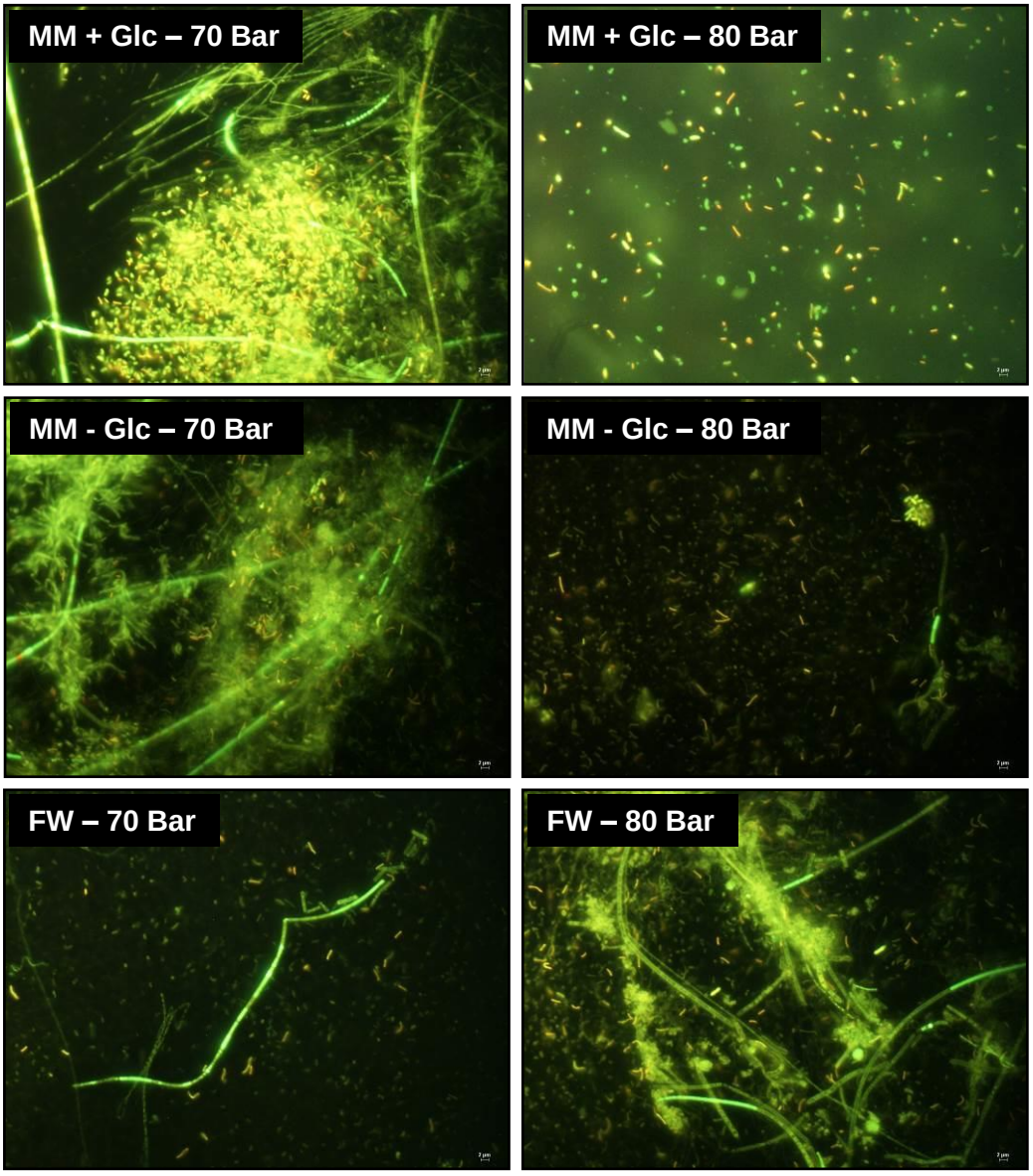

Figure 6.15: Live/Dead stain images of the subsurface biome after 48 hours in various media compositions, under 100% CO_2 at 70 and 80 bar. All scale bars are equal to 2 µm.

6.5 CONCLUSIONS

Supercritical CO_2 generally impacts the majority of microorganisms in a negative manner (McHugh & Krukonis, 1994; Zhang *et al*., 2006; Mitchell *et al*., 2009; Basava-Reddi, 2012; Peet *et al*., 2015). However, in this study it was found that even though the microorganisms were not able to grow, they still remained alive under all the conditions tested, thus the subsurface biome from the Star Diamonds could successfully be evaluated in an environment that mimics geological CCS. In the literature, several Firmicutes, especially *Bacillus* species have been described that were resistant to sc-CO_2 and were able to grow in pressurized bioreactors containing sc-CO_2 (Peet *et al*., 2015; Peet & Thompson, 2015). It has also been reported that native microorganisms that were present at CO_2 injection sites, were able to survive sc-CO_2 conditions (Colwell *et al*., 2011). Diversity studies of the subsurface biome (Chapter 3) indicate that several Firmicutes, including *Bacillus* species were present in the biome, therefore, linking these observations to microorganisms from the subsurface biome that were able to tolerate and survive the sc-CO_2 conditions.

When studies were done on the CO_2 stress response of three model organisms (*Shewanella oneidensis* MR-1, *Geobacillus stearothermophilus*, and *Methanothermobacter thermoautotrophicus*), it was shown that biofilm formation and cell wall thickness may be two very important factors in resisting sc-CO_2 toxicity, since the presence of a biofilm can create a reactive barrier that reduces the rate of CO_2 diffusion into the cytoplasmic membranes and facilitate conversion of CO_2 into long-term stable carbonate phases (Gerlach *et al*., 2011; Santillan *et al*., 2011; Basava-Reddi, 2012).

The live/dead images show that the biome formed biofilm-like structures through the accumulation of cells. Since the biofilm can offer structural support, protection from physical, chemical, and biological stresses, optimal location relative to substrates required for metabolic function, and symbiotic benefits in multi-species communities (Watnick & Kolter, 2000; Costerton & Stewart, 2001; Stoodley *et al*., 2002; Mitchell *et al*., 2009; Lewandowski & Beyenal, 2013), it is possible that the microorganisms were able to protect themselves from any stresses created by the sc-CO_2 conditions by forming these biofilm-like structures. Additionally, biofilms can cause large changes in porosity and permeability of porous media including sandstone, but it can also act as a hydraulic

barrier to prevent the flux of CO_2, making them potentially useful for preventing leakage of sc-CO_2 from the injection sites (Mitchell *et al*., 2009).

It has also been found that during nutrient starvation the vitamin, nutrient, and energy requirements of the microorganisms can no longer be fulfilled, resulting in cells that will separate themselves from the biofilm in order to find other microenvironments that have these requirements (Hunt *et al*., 2004; Thormann *et al*., 2005; Thormann *et al*., 2006; Mitchell *et al*., 2009). In order to sustain the integrity of the biofilm over time, constant feeding with sufficient nutrient and energy sources are required (Mitchell *et al*., 2009). When the microorganisms were subjected to the nutrient deprived media, they were not able to produce biomass, indicating that they were most likely not able to form sufficient biofilms to protect themselves against sc-CO_2 and as a result they used their energy to stay alive, rather than to produce biomass.

The Gram-staining properties of the microorganisms will also influence their ability to resist sc-CO_2 toxicity, since Gram-positive microorganisms are more resilient towards sc-CO_2 than Gram-negative microorganisms due to the high peptidoglycan content in their cell walls, making them less permeable (Cheftel, 1995; Zhang *et al*., 2006; Mitchell *et al*., 2009). In Chapter 4 it was shown that *E. limosum* is a Gram-positive rod (Song & Cho, 2015), and should therefore have better resistance towards sc-CO_2, explaining why they were able to stay alive under the sc-CO_2 conditions. The subsurface biome contained both Gram-positive and Gram-negative microorganisms (Chapter 4), therefore, microorganisms will be present that are more resilient towards sc-CO_2 than others, indicating that the community will most likely change during CCS.

6.6 REFERENCES

- **Basava-Reddi, L.** (2012). Microbial Effects on CO_2 Storage. IEAGHG Report.

- **Benson, S.M. and Cole, D.R.** (2008). CO_2 Sequestration in Deep Sedimentary Formations. *Elements*. **4**:325-331.

- **Budisa, N. and Schulze-Makuch, D.** (2014). Supercritical Carbon Dioxide and Its Potential as a Life-Sustaining Solvent in a Planetary Environment. *Life*. **4**:331-340.

- **Cheftel, J.C.** (1995). Review: High-Pressure, Microbial Inactivation and Food Preservation. *Food Sci. Technol. Int*. **1**:75-90.

- **Chen, Y.T. and Ling, Y.C.** (2000). An Overview of Supercritical Fluid Extraction in Chinese Herbal Medicine: From Preparation to Analysis. *J. Food Drug Anal.* **8**:235-247.

- **Chivian, D., Brodie, E.L., Alm, E.J., Culley, D.E., Dehal, P.S., DeSantis, T.Z., Gihring, T.M., Lapidus, A., Lin, L., Lowry, S.R., Moser, D.P., Richardson, P.M., Southam, G., Wanger, G., Pratt, L.M., Andersen, G.L., Hazen, T.C., Brockman, F.J., Arkin, A.P. and Onstott, T.C.** (2008). Environmental Genomics Reveals a Single-Species Ecosystem Deep Within Earth. *Science*. **322**:275-278.

- **Cloete, M.** (2010). Atlas on Geological Storage of Carbon Dioxide in South Africa. Council for Geoscience.

- **Colwell, F.S., Lavalleur, H., Verba, C., O'Connor, W. and Fisk, M.R.** (2011). Microbiological Characterization of a Basaltic System Targeted for Geological Sequestration of Carbon. *American Geophysical Union, Fall Meeting, Abstract #B51J-0543.*

- **Costerton, J.W. and Stewart, P.S.** (2001). Battling Biofilms - the War is Against Bacterial Colonies that Cause some of the most Tenacious Infections known. The

Weapon is Knowledge of the Enemy's Communication System. *Scientific American.* **285**:74-81.

- **Cunningham, A.B., Gerlach, R., Spangler, L. and Mitchell, A.C.** (2009). Microbially Enhanced Geologic Containment of Sequestered Supercritical CO_2. *Energy Procedia*. **1**:3245-3252.

- **Dostal, V., Driscoll, M.J. and Hejzlar, P.** (2004). A Supercritical Carbon Dioxide Cycle for Next Generation Nuclear Reactors. *Advanced Nuclear Power Technology Program*.

- **Garcia-Gonzalez, L., Geeraerd, A.H., Spilimbergo, S., Elst, K., Van Ginneken, L., Debevere, J., Van Impe, J.F. and Devlieghere, F.** (2007). High-Pressure Carbon Dioxide Inactivation of Microorganisms in Foods: The Past, the Present and the Future. *International Journal of Food Microbiology*. **117**:1-28.

- **Genthner, B.R. and Bryant, M.P.** (1982). Growth of *Eubacterium limosum* with Carbon Monoxide as the Energy Source. *Applied and Environmental Microbiology*. **43(1)**:70-74.

- **Genthner, B.R., Davis, C.L. and Bryant, M.P.** (1981). Features of Rumen and Sewage Sludge Strains of Eubacterium limosum, a Methanol- and H_2-CO_2-Utilizing Species. *Applied and Environmental Microbiology*. **42(1)**:12-19.

- **Gerlach, R., Mitchell, A.C., Ebigbo, A., Phillips, A. and Cunningham, A.B.** (2011). Potential of Microbes to Increase Geologic CO_2 Storage Security. *American Geophysical Union, Fall Meeting, Abstract #B51J-0547.*

- **Glossner, A.** (2013). Terminal Microbial Metabolisms in the Deep Subsurface under Conditions Relevant to CO2 Sequestration and Enhancing Methanogenesis from Coal. *PhD Thesis, Colorado School of Mines*.

- **Hong, S.I., Park, W.S. and Pyun, Y.R.** (1997). Inactivation of *Lactobacillus* sp. from Kimchi by High-Pressure Carbon Dioxide. *Food Science and Technology-Lebensmittel-Wissenschaft & Technologie.* **30**:681-685.

- https://en.wikipedia.org/wiki/Supercritical_carbon_dioxide.

- **Hunt, S.M., Werner, E.M., Huang, B.C., Hamilton, M.A. and Stewart, P.S.** (2004). Hypothesis for the Role of Nutrient Starvation in Biofilm Detachment. *Applied and Environmental Microbiology*. **70**:7418-7425.

- **Jørgensen, B.B and Boetius, A.** (2007). Feast and Famine – Microbial Life in the Deep-Sea Bed. *Nature Reviews Microbiology*. **5**:770-781.

- **Jørgensen, B.B. and D'Hondt, S.** (2006). ECOLOGY: A Starving Majority Deep Beneath the Seafloor. *Science*. **314**:932-934.

- **Lelait, M. and Grivet, J.P.** (1996). Carbon Metabolism in *Eubacterium limosum*: a ^{13}C NMR Study. *Anaerobe*. **2**:181-189.

- **Lewandowski, Z. and Beyenal, H.** (2013). Fundamentals of Biofilm Research. (2nd ed.). *CRC Press*. ISBN: 9781466559592.

- **Li, J., Wang, A., Zhu, F., Xu, R. and Hu, X.S.** (2013). Membrane Damage Induced by Supercritical Carbon Dioxide in *Rhodotorula mucilaginosa*. *Indian J Microbiol*. **53(3)**:352-358.

- **Lin, H.M., Cao, N.J. and Chen, L.F.** (1994). Antimicrobial Effect of Pressurized Carbon-Dioxide on *Listeria monocytogenes*. *Journal of Food Science.* **59**:657-659.

- **Loubière, P. and Lindley, N.D.** (1991). The use of Acetate as an Additional Co-Substrate Improves Methylotrophic Growth of the Acetogenic Anaerobe *Eubacterium limosum* when CO_2 Fixation is Rate-Limiting. *Journal of General Microbiology*. **137**:2247-2251.

- **Machel, H.G. and Foght, J.** (2013). Products and Depth Limits of Microbial Activity in Petroliferous Subsurface Settings. In: Microbial Sediments. *Springer Science & Business Media Publishers*. ISBN: 9783662040362.

- **Matschiavelli, N., Oelgeschlager, E., Cocchiararo, B., Finke, J. and Rother, M.** (2012). Function and Regulation of Isoforms of Carbon Monoxide Dehydrogenase/Acetyl-CoA Synthase in *Methanosarcina acetivorans*. *Journal of Bacteriology*. **194(19)**:5377-5387.

- **McHugh, M.A. and Krukonis, V.J.** (1994). Supercritical Fluid Extraction: Principles and Practice. *Butterworth–Heinemann Publishers.* (2nd ed.).

- **Metz, B., Davidson, O., De Coninck, H., Loos, M and Meyer, L.** (2005). Carbon Dioxide Capture and Storage - Intergovernmental Panel on Climate Change (IPCC) Special Report. *Cambridge University Press*. ISBN: 9780521866439.

- **Mitchell, A.C., Phillips, A.J., Hiebert, R., Gerlach, R., Spangler, L.H. and Cunningham, A.B.** (2009). Biofilm Enhanced Geologic Sequestration of Supercritical CO_2. *International Journal of Greenhouse Gas Control*. **3**:90-99.

- **Mu, A., Boreham, C., Leong, H.X., Haese, R.R. and Moreau, J.W.** (2014). Changes in the Deep Subsurface Microbial Biosphere Resulting from a Field-Scale CO_2 Geosequestration Experiment. *Frontiers in Microbiology*. **5**:209.

- **Nondorf, L., Gutierrez, M. and Plymate, T.G.** (2011). Modelling Carbon Sequestration Geochemical Reactions for a Proposed Site in Springfield, Missouri. *Environmental Geosciences*. **18**:91-99.

- **Onstott, T.C., Colwell, F.S., Kieft, T.L., Murdoch, L. and Phelps, T.J.** (2009). New Horizons for Deep Subsurface Microbiology. *Microbe Magazine.* **4(11)**:499–505.

- **Peet, K.C. and Thompson, J.R.** (2015). Draft Genome Sequences of Supercritical CO_2-Tolerant Bacteria *Bacillus subterraneus* MITOT1 and *Bacillus cereus* MIT0214. *Genome Announcements*. **3(2)**:e00140-15.

- **Peet, K.C., Freedman, A.J.E., Hernandez, H.H., Britto, V., Boreham, C., Ajo-Franklin, J.B. and Thompson, J.R.** (2015). Microbial Growth under Supercritical CO_2. *Appl Environ Microbiol.* **81(8)**:2881-2892.

- **Phelps, T.J., Murphy, E.M., Pfiffner, S.M. and White, D.C.** (1994). Comparison between Geochemical and Biological Estimates of Subsurface Microbial Activities. *Microb. Ecol*. **28**:335-349.

- **Roh, H., Ko, H., Kim, D., Choi, D.G., Park, S., Kim, S., Chang, I.S. and Choi, I.** (2011). Complete Genome Sequence of a Carbon Monoxide-Utilizing Acetogen, *Eubacterium limosum* KIST612. *Journal of Bacteriology*. **193(1)**:307-308.

- **Rozzi, N.L. and Singh, R.K.** (2002). Supercritical Fluids and the Food Industry. *Comp. Rev. Food Sci. Food Safety.* **1**:33-44.

- **Santillan, E.F.U., Franks, M.A., Omelon, C.R. and Bennett, P.** (2011). Microbes under Pressure: A Comparison of CO_2 Stress Responses on Three Model Organisms and their Implications for Geologic Carbon Sequestration. *American Geophysical Union, Fall Meeting, Abstract #B51J-0552*.

- **Song, Y. and Cho, B.** (2015). Draft Genome Sequence of Chemolithoautotrophic Acetogenic Butanol-Producing *Eubacterium limosum* ATCC 8486. *Genome Announcements*. **3(1)**:e01564-14.

- **Stoodley, P., Sauer, K., Davies, D.G. and Costerton, J,W.** (2002). Biofilms as Complex Differentiated Communities. *Annual Review of Microbiology*. **56**:187-209.

- **Thormann, K.M., Duttler, S., Saville, R.M., Hyodo, M., Shukla, S., Hayakawa, Y. and Spormann, A.M.** (2006). Control of Formation and Cellular Detachment from

Shewanella oneidensis MR-1 Biofilms by Cyclic di-GMP. *Journal of Bacteriology*. **188**:2681-2691.

- **Thormann, K.M., Saville, R.M., Shukla, S. and Spormann, A.M.** (2005). Induction of Rapid Detachment in *Shewanella oneidensis* MR-1 Biofilms. *Journal of Bacteriology*. **187**:1014-1021.

- **Watnick, P and Kolter, R.** (2000). Biofilm, City of Microbes. *Journal of Bacteriology*. **182**:2675-2679.

- **White, C.M., Strazisar, B.R., Granite, E.J., Hoffman, J.S. and Pennline, H.W.** (2003). Separation and Capture of CO_2 from Large Stationary Sources and Sequestration in Geological Formations - Coalbeds and Deep Saline Aquifers. *Journal of the Air & Waste Management Association.* **53**:645-715.

- **Wilkins, M.J., Daly, R.A., Mouser, P.J., Trexler, R., Sharma, S., Cole, D.R., Wrighton, K.C., Biddle, J.F., Denis, E.H., Fredrickson, J.K., Kieft, T.L., Onstott, T.C., Peterson, L., Pfiffner, S.M., Phelps, T.J. and Schrenk, M.O.** (2014). Trends and Future Challenges in Sampling the Deep Terrestrial Biosphere. *Frontiers in Microbiology*. **5**:481.

- **Zhang, J., Davis, T.A., Matthews M.A., Drews, M.J., LaBerge, M. and An, Y.H.** (2006). Sterilization using High-Pressure Carbon Dioxide. *Journal of Supercritical Fluids.* **38**:354-372.

CHAPTER 7

CARBON SEQUESTRATION SIMULATIONS OF THE SUBSURFACE BIOME USING A CONTINUOUS HIGH PRESSURE BIOREACTOR

7.1 INTRODUCTION

Before CO_2 can be stored on a scale that can make a difference in global climate change, the longevity of sequestering CO_2 in the storage formation must be addressed. The temperatures and pressures required for the injection of sc-CO_2 can affect the composition and metabolic activity and in turn, the metabolic cycling of a wide variety of microorganisms and could thus potentially have an impact on CO_2 injection, migration, and storage longevity (Morozova *et al*., 2010; Glossner, 2013). Various studies on subsurface microbial communities have revealed that the more important metabolic groups, dominating the deep subsurface, are sulphate reduction, iron reduction, fermentation, and methanogenesis (Takai *et al*., 2001; Kotelnikova, 2002; Baker *et al*., 2003; Newberry *et al*., 2004; Onstott, 2005; Webster *et al*., 2006; Fry *et al*., 2008; Basso *et al*., 2009; Morozova *et al*., 2010; Ragon *et al*., 2013), thus, the presence of sc-CO_2 can affect the metabolism of both heterotrophic microorganisms, which play a major role in carbon cycling, as well as the chemolithoautotrophic microorganisms which are able to use CO_2 as a sole carbon and energy source (Chapelle *et al*., 2002; Morozova *et al*., 2010; Hubert *et al.,* 2011; Bordenave *et al*., 2012).

As discussed in Chapter 6, sc-CO_2 has been shown to be harmful to several microorganisms, but has less of an effect on biofilm-forming microorganisms. Mitchell *et al*., (2008) and Mitchell *et al*., (2009), have studied the effect of sc-CO_2 on biofilm microorganisms in Berea sandstone and unconsolidated sand. They found that biofilm-forming microorganisms increased the permeability of the Berea sandstone, but the sc-CO_2 had a negligible effect on their biofilm formation, confirming that sc-CO_2 may not completely sterilize geological environments when the microorganisms are attached to

rock surfaces. However, these studies were done with pure cultures and not much is known about the effects of sc-CO_2 on mixed microbial communities, especially those found in the subsurface environments considered for CCS (Morozova *et al*., 2010; Glossner, 2013).

Other than temperature, pressure, and the presence of sc-CO_2, factors such as changes in pH and salinity, occurring due to the sequestration of CO_2, may also significantly influence subsurface microbial communities (Morozova *et al*., 2010; Krüger *et al*., 2011; Santillan *et al*., 2013). Thus, it becomes extremely important to characterize the diversity of the deep subsurface, before, during, and after injection of CO_2 since the interaction of the subsurface microbial communities within the storage rock could be responsible for significant changes in the structure and chemical composition of the rock formations and as a result, can influence the porosity and permeability of the storage reservoir and leakage of the CO_2 (Morozova *et al*., 2010; Krüger *et al*., 2011; Santillan *et al*., 2013). This leakage can affect the quality of the ground water through acidification of the water, resulting in the mobilization of metals to toxic concentrations, which can influence the native microbial communities (Krüger *et al*., 2011).

7.2 AIMS OF THIS CHAPTER

The main aims of this chapter were to:

- Evaluate the potential impact of CO_2 sequestration on the subsurface microbial communities through bench-scale simulations of these interactions using a continuous high pressure bioreactor.
- Determine the impact on the diversity within the selected biome and define possible CO_2 fixation pathways that the subsurface biome might use during CCS interaction.

7.3 MATERIALS AND METHODS

For all the high pressure experiments in this phase, the bioreactor described in the final design (Section 5.3.2), was used. The bioreactor was sterilized and prepared as discussed in Section 5.3.2.2. Unless otherwise specified, the fissure water containing the subsurface biome was from the Nalgene Carboy bottle that contained large amounts of cells after collection on the massive filter as discussed in Section 3.3.6.4. Crushed sandstone, prepared as discussed in Section 3.3.5, was used as the rock matrix inside the bioreactor.

7.3.1 Adhesion Studies

Adhesion studies were carried out to determine the amount of time needed for the microorganisms from the subsurface biome to adhere to the crushed rock before the reactor was circulated. This was done by filling 20 ml syringes with the crushed sandstone. The syringes were wrapped in foil and sterilized. After sterilization, the syringes were filled with fissure water containing the subsurface biome and covered at both ends with parafilm (Lasec) (Figure 7.1).

Figure 7.1: The prepared syringes, used for the adhesion studies.

At each specified time interval, triplicate syringes were sacrificed by draining the syringe and collecting the liquid in a sterile 15 ml falcon tube. To determine if the microorganisms adhered to the rock, live/dead stains using the LIVE/DEAD® BacLight™

Bacterial Viability Kit (Molecular Probes, Inc., Invitrogen, Promega) (Section 3.3.6.8.2), and ATP measurements using the CellTiter-Glo® Luminescent Cell Viability Assay (Promega) were done according to the manufacturer's instructions. This was repeated at various time intervals, until no cells were released and the corresponding ATP values were negative, ensuring complete adhesion of the microorganisms. The time of complete adhesion was determined to be 24 hours, but the adhesion studies were continued for 48 hours, to confirm that the microorganisms remained attached to the sandstone particles.

7.3.2 Carbon Sequestration Simulations with the Subsurface Biome

The sterilized bioreactor was packed with the crushed sandstone, where after the fissure water, containing the subsurface biome was added to the bioreactor until the entire volume was filled as discussed in Section 5.3.2.2. This was left to stand for 24 hours, as determined by the adhesion studies (Section 7.3.1), in order for the microorganisms to adhere to the rock. CO_2 gas was then added to saturate the system and to achieve the initial pressure (~50 bar). The final pressure of ≥80 bar, to allow the CO_2 to be in a supercritical state, was achieved and maintained by pressurizing the piston pressure regulators with the nitrogen gas and the valves were opened to allow circulation as discussed in Section 5.3.2.2. No additional carbon and energy sources were added, to simulate the subsurface CO_2 storage conditions. The temperature was maintained at 35°C and the reactor was allowed to run for six weeks.

During the six weeks, 1 ml samples were taken at various time intervals for continual analyses to determine if any metabolic cycling occurred inside the bioreactor under CCS conditions. As discussed in Section 5.4, the bioreactor design only allowed for a total system volume of ~400 ml, therefore, only limited samples could be withdrawn and thus analyses were restricted. Sampling was done with a gas tight syringe as discussed in Section 5.3.2.2. Half of the liquid sample (500 µl), as well as any gas that might have formed inside the syringe headspace was immediately added to a sterile 15 ml serum vial, which was sealed with a blue chlorobutyl stopper (Bellco Glass Inc.) and crimp sealed with an aluminium cap. This was used to test the gas composition, especially the CO_2 usage using a GC-2010 Plus capillary gas chromatograph (GC), coupled to a

Barrier Discharge Ionization (BID) detector (Shimadzu). A micropacked ShinCarbon ST 80/100 column (Restek®), with an inner diameter of 0.53 mm and 2 m in length, was used. Gas samples were introduced into the system by means of a manual injection valve fitted with a 20 µL loop. The injector port temperature was 80°C in the splitless mode and the carrier gas was helium (99.9999%). The initial oven temperature was 40°C held for 2 minutes and then raised at 20°C/minute to 140°C. Detection was carried out with a BID detector set a 280°C and with a plasma gas flow of 80 $ml.min^{-1}$. Instrument control, data collection, and data processing were carried out with Shimadzu LabSolutions software (V.5.57). For the other 500 µl of the sample, 100 µl was inoculated into a sterile Hungate tube containing 5 ml LB medium (Section 4.3.4) and incubated at 35°C, as a visual test, to determine of the microorganisms inside the bioreactor were still viable. The remaining 400 µl was first used to measure the pH, where after it was sonicated for 10 minutes, to allow breakage of the cell walls of the microorganisms in order to detect any intracellular product formation. The cell suspension was centrifuged (20 000 *x g,* 10 minutes, 4°C) using an Allegra™ 25R centrifuge (Beckman Coulter™) and the supernatant was added to a high performance liquid chromatograph (HPLC) vial to be used for the detection of any saccharide or acid formation. HPLC analyses were carried out on a system consisting of an isocratic pump, an auto sampler, and a photodiode array detector (Finnegan Surveyor). Analytes were separated on an Aminex HPX-87H (7.8 x 300 mm) ion exchange column (Bio-Rad Laboratories, Inc.), maintained at 65°C. Elution was performed with 5 mM sulphuric acid at a flow rate of 0.5 $ml.min^{-1}$. Organic acids were detected at 202 and 276 nm and saccharides were detected with a 2414 Refractive Index detector (RID) (Waters) connected in series. RID cell temperature was 40°C and data recording and analyses were carried out with the Clarity software package (DataApex).

Analyses were also done on samples that were taken from the fissure water before it was inserted into the bioreactor, from the bioreactor after adhesion occurred, but before the addition of the CO_2 gas, as well as immediately after the addition of the CO_2 gas.

After the six weeks, circulation of the bioreactor was stopped and microbial diversity analyses using DGGE (Section 3.3.6.6), as well as geochemical analyses were conducted on the remaining liquid. Cations were measured using an ICP Optima 3000 DV (PerkinElmer Inc.), and anions were analysed using an IC DX-120 (Dionex).

Geochemical analyses were done at the Institute for Ground Water Studies (IGS) at the UFS (Bloemfontein, RSA). The composition of the sandstone was analysed with XRF (Section 3.3.5.2) at the Department of Geology at the UFS (Bloemfontein, RSA). The microbial diversity in the bioreactor was visualized using SEM, with EDS analyses (Section 3.3.6.8.4) at the Centre for Microscopy at the UFS (Bloemfontein, RSA).

The bioreactor study was repeated using the same conditions as before, except the CO_2 gas used to saturate the system was labelled with the ^{13}C isotope ($^{13}CO_2$) and consisted of 99 atom % ^{13}C, with <3 atom % ^{18}O (Sigma-Aldrich®). This was done to detect possible incorporation of the ^{13}C in the DNA using Nuclear Magnetic Resonance (NMR) to indicate metabolic fixation of the CO_2 by the microorganisms. Unfortunately, this technique required high biomass concentrations and since this could not be obtained under the CCS conditions and current bioreactor conditions, as indicated in Chapters 4 and 6, it was not possible to carry out analyses using NMR. In the subsurface, the microorganisms are constantly in contact with a fresh fissure water supply, thus, in order to better simulate the subsurface CCS conditions, additional fissure water was added to the reactor every second day, to ensure that any nutrients from the fissure water did not become depleted.

After six weeks, microbial diversity assessments using targeted rRNA gene sequencing, was done on the Ion Torrent PGM™ as discussed in Section 3.3.6.7. Sequencing was done at the CAF, Stellenbosch University (Stellenbosch, RSA).

7.3.3 Bioreactor Control Experiments

As discussed in Chapter 5, the material used in constructing the bioreactor was made out of corrosion-free stainless steel, but any potential corrosion and metal leakage from the bioreactor was considered. Thus; to determine the degree to which metals would leach from the reactor itself, if at all, several negative control experiments were done. All these experiments were carried out in the absence of the subsurface biome. Control experiments continued for two weeks under specific conditions, as indicated in Table 7.1.

Table 7.1: Conditions for the bioreactor control experiments.

Component	A1	A2	B1	B2	B3
Fissure water	+	+	+	+	+
Sandstone	-	-	+	+	+
CO_2	-	+	-	-	+
Pressure (Bar)	0	80	0	80	80

Legend: + = component was added to the reactor, - = component was not added to the reactor.

After the two weeks, the water chemistry and sandstone composition was analysed for each control as discussed in Section 7.3.2. These analyses were compared with fissure water and sandstone that was not in contact with the bioreactor.

7.3.4 Whole Transcriptome Sequencing using Ion Torrent Proton™

The diversity studies in Chapter 3 indicated that carbon fixing microorganisms are present in the subsurface biome. Thus, in order to define possible CO_2 fixation pathways that these microorganisms might follow if they survive the CCS conditions, whole transcriptome sequencing was done on the subsurface biome.

7.3.4.1 Total RNA Isolation

Total ribonucleic acid (RNA) was isolated from the massive filters (Section 3.3.6.4), the PVC cartridges (Section 3.3.6.5), and the second bioreactor (Section 7.3.2) using two different methods. The first method was according to the procedures of Lau *et al*., (2014) as discussed in Section 3.3.6.7.1, but by adding rDNase (Macherey-Nagel) to the re-suspended pellets. The second method used was with the NucleoSpin® RNA kit (Macherey-Nagel) according to the manufacturer's instructions. The primers and standards used were as recommended by the manufacturer.

7.3.4.2 RNA Sequencing and Analyses

The RNA was used for RNA sequence analyses using the Ion Torrent Proton™ platform (Life Technologies™), by constructing a whole transcriptome library from the RNA for up

to 200-base-read sequencing according to the manufacturer's instructions. The main steps in constructing the library included hybridizing and ligating the RNA, reverse transcription (RT) to make complementary DNA (cDNA), purification and amplification of the cDNA, purification of the amplified cDNA, and assessment of the yield and size distribution of the amplified cDNA. The template was prepared from the whole transcriptome library and sequenced using the Ion PI™ Hi-Q™ OT2 200 Kit (Thermo Fisher Scientific) according to the manufacturer's instructions. Sequencing reactions were done with the Ion Torrent Proton™ (Life Technologies™) at the CAF, Stellenbosch University (Stellenbosch, RSA). The data was analysed with MG-RAST using the default settings (Meyer *et al*., 2008).

7.4 RESULTS AND DISCUSSIONS

7.4.1 Carbon Sequestration Simulations with the Subsurface Biome

Immediately after the addition of the CO_2 gas, a drop in the pH was observed (Table 7.2) due to the formation of carbonic acid as the CO_2 dissolves in the water (Fierer & Jackson, 2006; Mu *et al*., 2014). The presence of sc-CO_2 or carbonic acid can lead to reactions with the minerals in the storage formations, resulting in dissolved ions which could in turn lead to mineral dissolution or precipitation. This could influence the ionic strength and the distribution of bioavailable terminal electron acceptors such as Fe(III), affecting microbial metabolism in the subsurface (McMahon & Chapelle, 1991; Cozzarelli *et al*., 1994; Banfield *et al*., 1999; Rogers & Bennett, 2004), but also the geochemistry and mineralogy of the storage rock, changing its porosity, and leading to possible acetogenesis and methanogenesis (Ragsdale, 2004; Gadd, 2010; Sato *et al*., 2013). However, other than this initial drop, no dramatic changes in the pH were observed during the six weeks. This potentially indicated that products such as acetate, which would have caused a further decrease in the pH, or carbonates, which would have caused an increase in the pH, were not formed in amounts significant enough to cause a shift in the pH.

Table 7.2: pH and growth measurements obtained of the bioreactor during the six weeks.

Sample name	Date	pH	Growth obtained
Fissure water	27/11/2014	7.44	+
Before the addition of CO_2	28/11/2014	7.29	+
After the addition of CO_2	28/11/2014	5.43	+
S1	02/12/2014	5.48	+
S2	05/12/2014	5.53	+
S3	09/12/2014	5.63	+
S4	17/12/2014	5.63	+
S5	20/12/2014	5.56	+
S6	24/12/2014	5.57	+
S7	29/12/2014	5.58	+
S8	03/01/2015	5.61	+

Legend: + = growth was obtained for the sample.

The pH measurements for the second bioreactor followed the same trends from 23/01/2015 until 05/03/2015. However, the pH was not measured under pressure and is

therefore just a possible indication of a trend that was followed, not an actual statement of the supercritical conditions inside the bioreactor.

It is known that changes in environmental parameters such as a decrease in the pH, could affect the microorganisms and their cellular and biochemical functions, influencing their activity and composition (Booth *et al*., 2002; Morozova *et al*., 2010; Basava-Reddi, 2012), but it can also allow growth, and thus dominance of acid tolerant species (Fierer & Jackson, 2006). Therefore, each time the pH was measured, the sample was also inoculated for growth as discussed in Section 7.3.2. It was found that even though no further changes in the pH were observed, the microorganisms remained viable, even after six weeks subjected to CCS conditions, since they were able to grow when revived in the LB medium. But the effect which the CO_2 has on pH could influence the microbial communities present in the subsurface biomes. Since the diversity studies in Chapter 3 revealed that both the methanogens and the acetogens such as *Clostridium*, are present within the subsurface biome, this might potentially lead to methanogenesis, however, according to Basava-Reddi, (2012), the extent to which the decreased pH will affect the microbial communities, depends on the microorganisms present, the geology and mineralogy of the storage rock, as well as the chemistry of the water. Thus, product formation such as acetate and methane, could be an indication of potential methanogenesis.

The GC results (Figure 7.2) indicated that after six weeks, no major differences were observed in the compositional gas analyses and that the formation of methane was not detected. It is however possible that since the reactor was over saturated with CO_2, the GC analyses were not sensitive enough to detect changes, indicating minor usage thereof. Since results were constant during the six weeks, analyses for the rest of the samples are not shown. As discussed in Section 7.3.2, the sample used for the GC analyses was immediately added to a sterile 15 ml serum vial. This vial was not evacuated before injection; therefore, prominent N_2 and O_2 peaks were detected in the analyses.

The HPLC results also did not yield any products after six weeks subjected to CCS conditions, with no real differences observed for the formation of acetate and formate, also no saccharides such as glucose were detected.

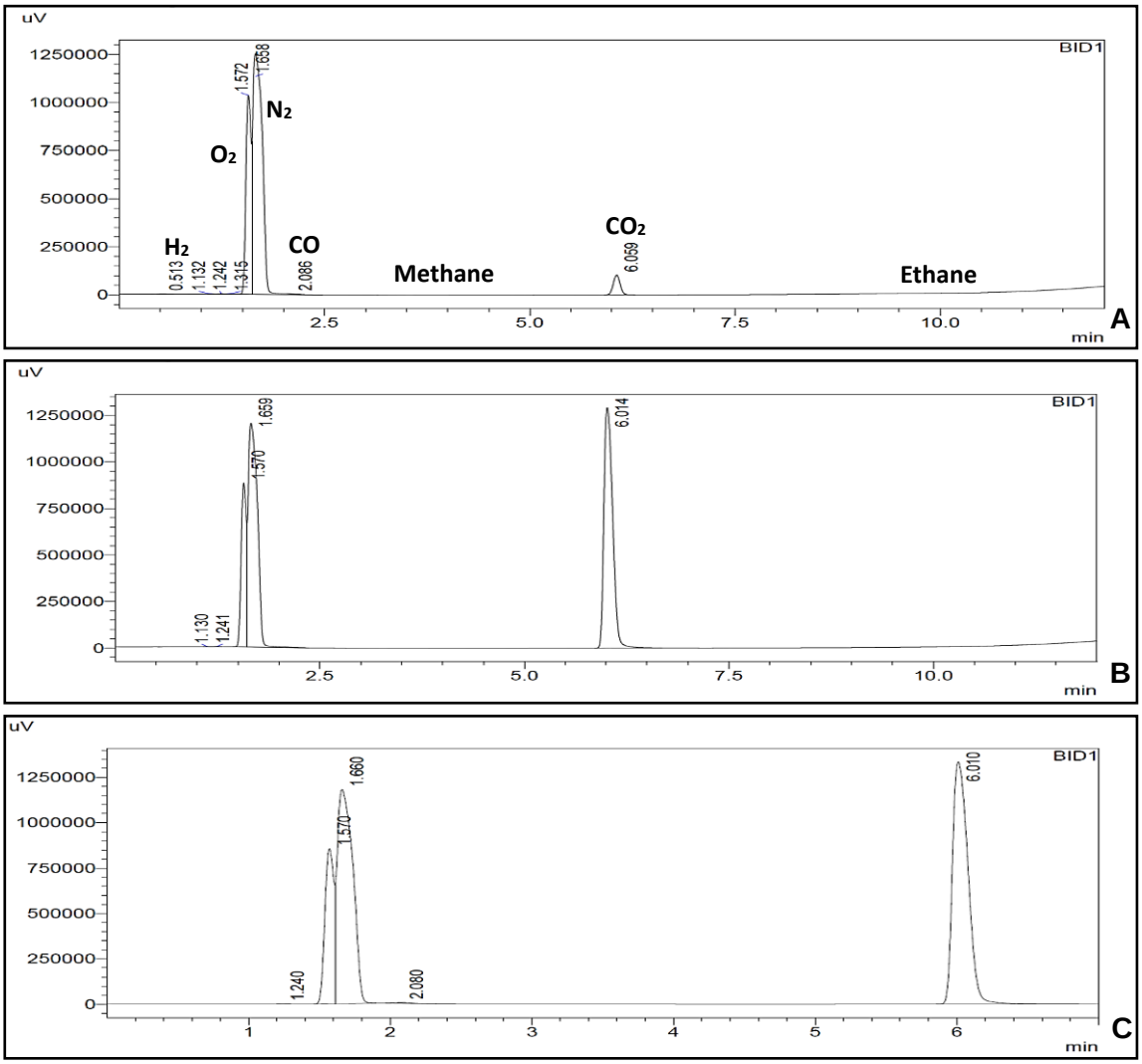

Figure 7.2: GC analyses of (A) fissure water, before the addition of CO_2, (B) after the addition of CO_2, and (C) S8 - after 6 weeks.

7.4.2 Geochemical Analyses

Geochemical analyses of the bioreactor water were conducted as discussed in Section 7.3.2, and the data is displayed in Table 7.3. When the geochemical results from the bioreactor water were compared with the geochemical analyses of the fissure water (Section 3.4.1.2), it can be seen that in general the composition remained relatively constant, indicating that the bioreactor water and the fissure water stayed geochemically very similar (Figure 7.3), except for the increase in aluminium, iron, and M-alkalinity in the bioreactor water after six weeks (Figure 7.4).

Table 7.3: Geochemical analyses of the bioreactor.

Analyses:	Bioreactor
pH	5.6
EC (mS.m^{-1})	461
TDS (mg.L^{-1})	2832
P-Alkalinity (mg.L^{-1})	0
M-Alkalinity (mg.L^{-1}	425
Calcium Hardness (mg.L^{-1})	239
Magnesium Hardness (mg.L^{-1})	39
Total Hardness (mg.L^{-1})	279
Aluminium as Al (mg.L^{-1})	2731.5
Barium as Ba (mg.L^{-1})	0.516
Bromide as Br (mg.L^{-1})	7.30
Cadmium as Cd (mg.L^{-1})	<0.002
Calcium as Ca (mg.L^{-1})	95.7
Chloride as Cl (mg.L^{-1})	1428
Cobalt as Co (mg.L^{-1})	0.213
Copper as Cu (mg.L^{-1})	<0.002
Fluoride as F (mg.L^{-1})	0.86
Iron as Fe (mg.L^{-1})	97.99
Lead as Pb (mg.L^{-1})	0.012
Magnesium as Mg (mg.L^{-1})	9.6
Manganese as Mn (mg.L^{-1})	1.51
Potassium as K (mg.L^{-1})	11
Sodium as Na (mg.L^{-1})	743.5
Sulphate as SO_4 (mg.L^{-1})	14.12
Zinc as Zn (mg.L^{-1})	2.90

Legend: EC = electrical conductivity, TDS = total dissolved solids, P-Alkalinity = phenolphthalein alkalinity, M-Alkalinity = total alkalinity.

The P-alkalinity was zero, thus the M-alkalinity represents bicarbonate, indicating possible formation of bicarbonate inside the bioreactor. Microorganisms can execute carboxylation and decarboxylation reactions, interconverting inorganic and organic carbon, and is extremely important in the biogeochemical cycle of carbon, since each of these reactions are responsible for a global flux of at least 10 Pmol of carbon per year (Raven, 2006; Ramanan *et al*., 2009). Depending on the enzyme involved, the carboxylases use either CO_2 or HCO_3^-. Carbonate precipitation can be achieved by an enzymatic reaction with both CO_2 and HCO_3^-. This enzyme, known as carbonic anhydrase (CA) is a zinc metalloenzyme, found in basically every animal and plant and in certain bacteria and catalyses the conversion of CO_2 to HCO_3^- (hydration) and the reverse reaction (bicarbonate dehydration). CA is amongst the fastest catalytic enzymes known (turnover values close to one million bicarbonate molecules per second) and is usually stable, even up to 85°C (Zaihua, 2001; Lane *et al*., 2005; Raven, 2006; Ramanan *et al*., 2009).

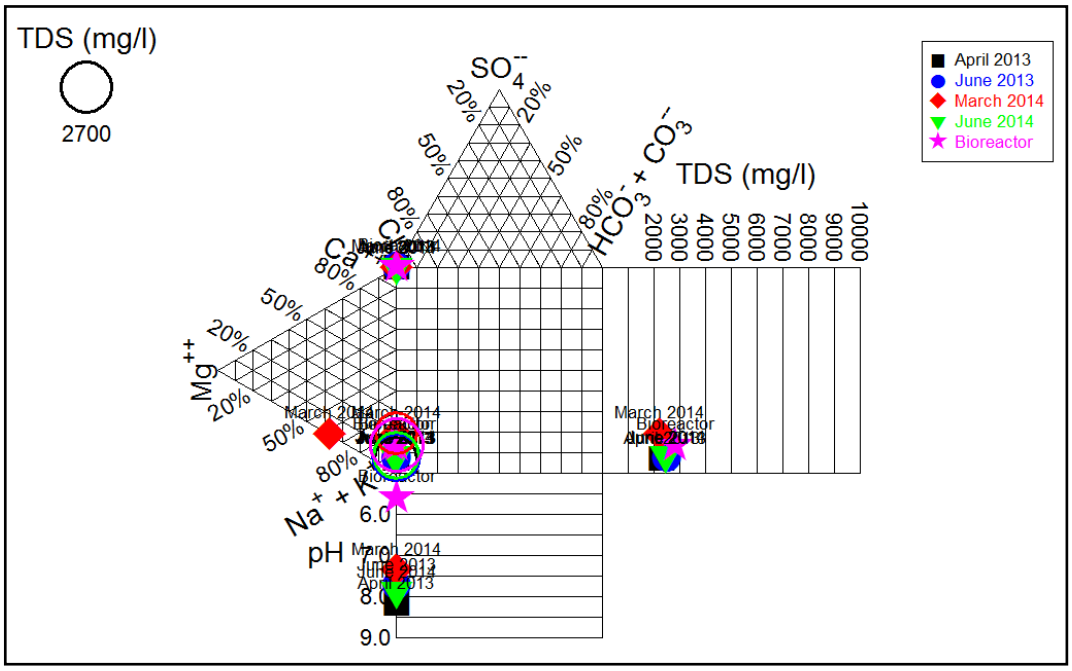

Figure 7.3: A Durov diagram of the geochemical analyses of the fissure water and the bioreactor water after six weeks.

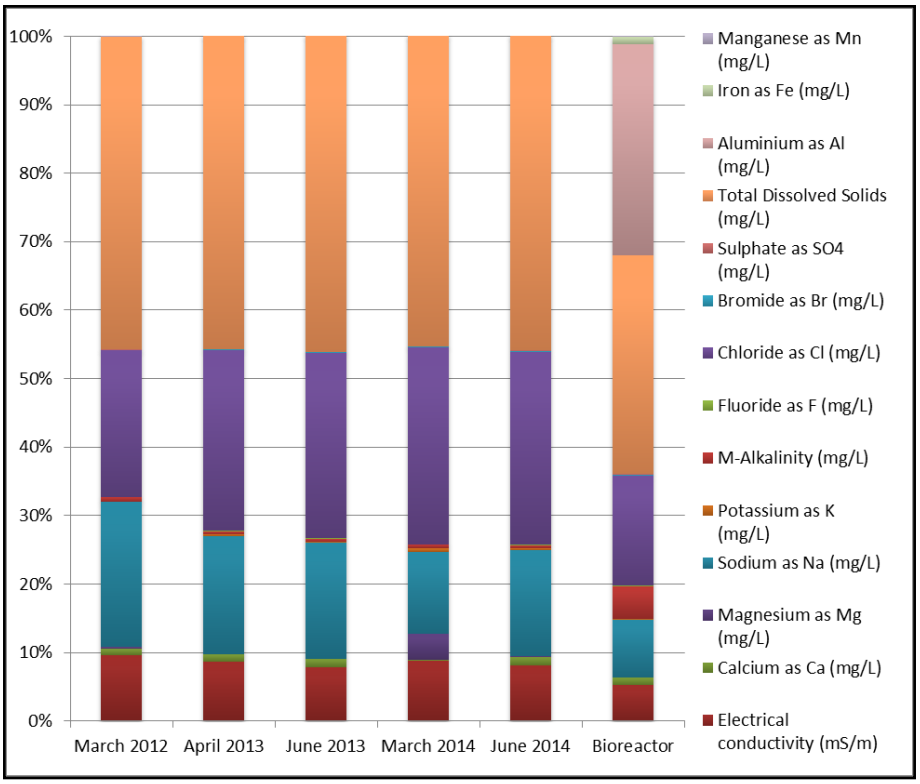

Figure 7.4: Comparisons of the geochemical analyses for the bioreactor with the fissure water. The bioreactor displayed an increase in the aluminium, the iron and the M-alkalinity.

7.4.3 X-Ray Fluorescence Analyses

Major-element XRF analyses (Section 3.3.5.2) of the sandstone from the bioreactor was conducted after six weeks and compared with the XRF analyses of the sandstone before it was inserted into the bioreactor (Section 3.4.2). Results of this comparison are shown in Table 7.4.

Table 7.4: Major-element XRF analyses of the sandstone before and after six weeks inside the bioreactor.

Analyses:	Sandstone	Bioreactor Sandstone
Al_2O_3 (%)	20.81	18.76
Fe_2O_3 (%)	1.065	0.89
CaO (%)	0.064	0.15
MgO (%)	0.17	0.49
MnO (%)	0.012	0.01
Na_2O (%)	0	0.45
K_2O (%)	2.64	2.63
P_2O_5 (%)	0.039	0.04
TiO_2 (%)	1.103	1.01
SiO_2 (%)	74.01	70.15
LOI (%)	0.087	5.42
Total (%)	100	100

Small increases were observed in the bioreactor sandstone for sodium, magnesium, iron, and calcium. But the most important difference obtained was the decrease in the aluminium after six weeks in the bioreactor, indicating that the increase in the aluminium detected in the bioreactor water with the geochemical analyses was due to the aluminium leaching from the sandstone under CCS conditions, most probably from kaolinite.

Microorganisms are constantly interacting with inorganic ions. These ions can be important for their biological functions or can have inhibitory effects on their growth such as aluminium - the most abundant metal in the Earth's crust in the form of oxides and silicates (Piña & Cervantes, 1996). It has been shown in the literature that the presence of aluminium can result in toxic effects on several microorganisms (Driscoll, 1985; Meyer *et al*., 1994; Hervieux *et al*., 2002; Mecteau *et al*., 2002; Amonette *et al*., 2003; Illmer & Erlebach, 2003), usually through binding to the cell wall, causing a decrease in the permeability (Bradley & Parker, 1968; Johnson, 1988). Other mechanisms include: 1.) replacing divalent metal complexes such as magnesium and calcium in the cells and

their membranes (Amonette *et al*., 2003), 2.) inactivating enzymes (Illmer & Erlebach, 2003), 3.) osmoregulative disorder (Illmer & Erlebach, 2003), 4.) altering lipid-protein interactions and modifying transport activity (Suhayda & Haug, 1986; Zambenedetti *et al*., 1994), or 5.) complexing with ATP, DNA, and phosphates, resulting in a deficiency of the phosphate (Haug, 1984; Pettersson *et al*., 1985; Wood, 1995). Yaganza *et al*., (2004), showed that bacterial mortality rates were high, with damaged cell membranes, after exposure to 0.2 M aluminium, for 10 minutes, but at concentrations of 0.1 M and 0.05 M, membrane damage did not occur. Guida *et al*., (1991), found that growth of *E. coli* in the presence of aluminium was inhibited at 0.9 mM (pH 5.4) and at 2.25 mM (pH 6.6) and the toxicity of the aluminium increased when iron was removed from the medium, suggesting that the uptake of aluminium involves the iron transport systems (Davis *et al*., 1971). Thus, the toxic effects which aluminium can have on microorganisms, depends on the pH, the concentration of the aluminium, the time of exposure, as well as the presence of other metals.

Aluminium usually adsorbs to mineral surfaces and when the pH is close to neutral, hydroxide complexes are formed which are insoluble, making the bioavailability of aluminium in soils and its concentrations in water very low (Piña & Cervantes, 1996). However, a decrease in the pH of soil and water, through acid rain, incorrect agricultural procedures, or disposal of industrial, mining, and domestic wastes, can result in the aluminium being solubilized and released from its natural reservoirs (Foy *et al*., 1978; Keyser & Munns, 1979; Ganrot, 1986; Martin, 1986; Macdonald & Martin, 1988; Myrold & Nason, 1992; Gagen *et al*., 1993; Stenson *et al*., 1993; Rogers & Bennett, 2004).

After six weeks inside the bioreactor, the aluminium concentration increased to 0.1 M, at a pH of 5.6. This increase in the aluminium concentration was most likely due to the acidic and pressurized environment created by the CCS conditions, which allowed the metals to leach from the sandstone (Piña & Cervantes, 1996). Therefore, the effect of the subsurface microorganisms should be characterized. The subsurface biome was grown in LB medium containing various aluminium concentrations (0.005 M – 0.5 M) at both pH 7.0 and 5.6, and the OD was measured over time as discussed in Section 4.3.3. The pH did not influence the tolerance to aluminium and 0.2 M was the maximum aluminium concentration allowing growth. Higher concentrations resulted in detrimental effects on the subsurface biome. The μ_{max} for each concentration was calculated as

discussed in Section 4.3 and it was observed that an increase in the aluminium concentration showed a marked decrease in the μ_{max}. The control experiment without aluminium, showed a μ_{max} of 0.152 h^{-1}. As representative values, the 0.08 M aluminium concentration test also resulted in a μ_{max} of 0.152 h^{-1}, the 0.1 M had a μ_{max} of 0.120 h^{-1}, the 0.2 M had a μ_{max} of 0.066 h^{-1}, and the 0.5 M had a μ_{max} of 0.011 h^{-1}. Therefore, the 0.1 M aluminium which the biome will encounter in the bioreactor, will slow its growth rate significantly. To determine the true effect that the aluminium might have under CCS conditions on the subsurface biome over time, the aluminium concentrations should be followed continuously inside the bioreactor during the experiments.

7.4.4 Bioreactor Control Experiments

To confirm that the soluble aluminium and iron detected in the water from the bioreactor leached from the rock under acidic and higher pressure conditions, and not from the reactor material, negative control experiments were done as discussed in Section 7.3.3. Results for the geochemical analyses of the water are shown in Table 7.5. Parameters with values always below the detection limits are not shown.

Table 7.5: Geochemical analyses for the fissure water and the control experiments.

Analyses:	FW	A1	A2	B1	B2	B3
pH	7.38	7.31	5.67	7.36	7.31	5.63
EC (mS/m)	444	450	424	450	424	429
TDS (mg/L)	2210	2220	2210	2230	2200	2210
Aluminium as Al (mg/L)	0.06	0.08	0.07	0.21	1.98	1.4
Boron as B (mg/L)	2.85	2.89	2.6	2.93	3.08	3.06
Barium as Ba (mg/L)	0.77	0.78	0.73	0.32	0.27	0.24
Calcium as Ca (mg/L)	56.6	56.6	53.2	49.2	55.4	51.7
Iron as Fe (mg/L)	<0.05	<0.05	<0.05	0.05	10.4	0.28
Potassium as K (mg/L)	8.6	8.9	7.8	11.4	12.1	12.0
Lithium as Li (mg/L)	0.73	0.8	0.7	0.98	1.08	1.09
Magnesium as Mg (mg/L)	1.40	1.40	1.4	5.20	6.70	5.9
Manganese as Mn (mg/L)	<0.05	<0.05	0.11	0.25	0.66	0.25
Sodium as Na (mg/L)	715.5	749.0	715.3	704.9	770.3	802.6
Nickel as Ni (mg/L)	<0.05	<0.05	<0.05	0.31	1.83	0.36
Silicon as Si (mg/L)	8.15	8.29	7.41	8.19	14.01	10.64
Strontium as Sr (mg/L)	3.55	3.54	3.33	2.94	3.26	3.08
Zinc as Zn (mg/L)	<0.05	<0.05	0.07	0.38	2.20	0.2
Chloride as Cl (mg/L)	1856.4	1781.8	1754.1	1809.6	1428.5	1881.4

Legend: FW = fissure water, EC = electrical conductivity, TDS = total dissolved solids.

When the controls were compared with the FW, a drop in pH was again observed, but only for the controls containing CO_2 (A2 and B3), under 80 bar pressure. In A1, no

noticeable changes were observed, thus the bioreactor itself did not contribute to the increase in the metal concentrations, even though pressure was applied (A2), no increase in the metals was observed. The B-series controls that contained sandstone, especially when pressure was added (B2 and B3), demonstrated that metals can be released from the sandstone.

The XRF results of the sandstone (Table 7.6), confirmed that the aluminium and iron leached from the sandstone. This should be considered during carbon sequestration, and especially the influence it will have on the composition and cycling of the subsurface microbial communities.

Table 7.6: XRF analyses for the sandstone and the control experiments.

Analyses:	Sandstone	B1	B2	B3
Al_2O_3 (%)	20.81	18.2	18.2	18.4
Fe_2O_3 (%)	1.065	0.9	0.9	0.8
CaO (%)	0.064	0.1	0.1	0.1
MgO (%)	0.17	0.4	0.5	0.4
MnO (%)	0.012	0	0	0
Na_2O (%)	0	1.8	1.9	1.8
K_2O (%)	2.64	2.6	2.6	2.6
P_2O_5 (%)	0.039	0	0	0
TiO_2 (%)	1.103	0.8	0.8	0.7
SiO_2 (%)	74.01	71.0	70.6	70.0
LOI (%)	0.087	4.2	4.3	5.0
Total (%)	100	100	100	100

7.4.5 Microbial Diversity Assessments using Denaturing Gradient Gel Electrophoresis

7.4.5.1 Genomic DNA Isolation and Polymerase Chain Reaction

Genomic DNA was isolated from the contents of the second bioreactor after six weeks (Section 3.3.6.6.1) and used to amplify the Archaeal 16S (~600 bp) (Figure 7.5B), Bacterial 16S (~1500 bp) (Figure 7.5C), and Eukaryal 18S (~1700 bp) (Figure 7.5D) rRNA gene fragments as discussed in Section 3.3.6.6.2. Reactions were done in triplicate.

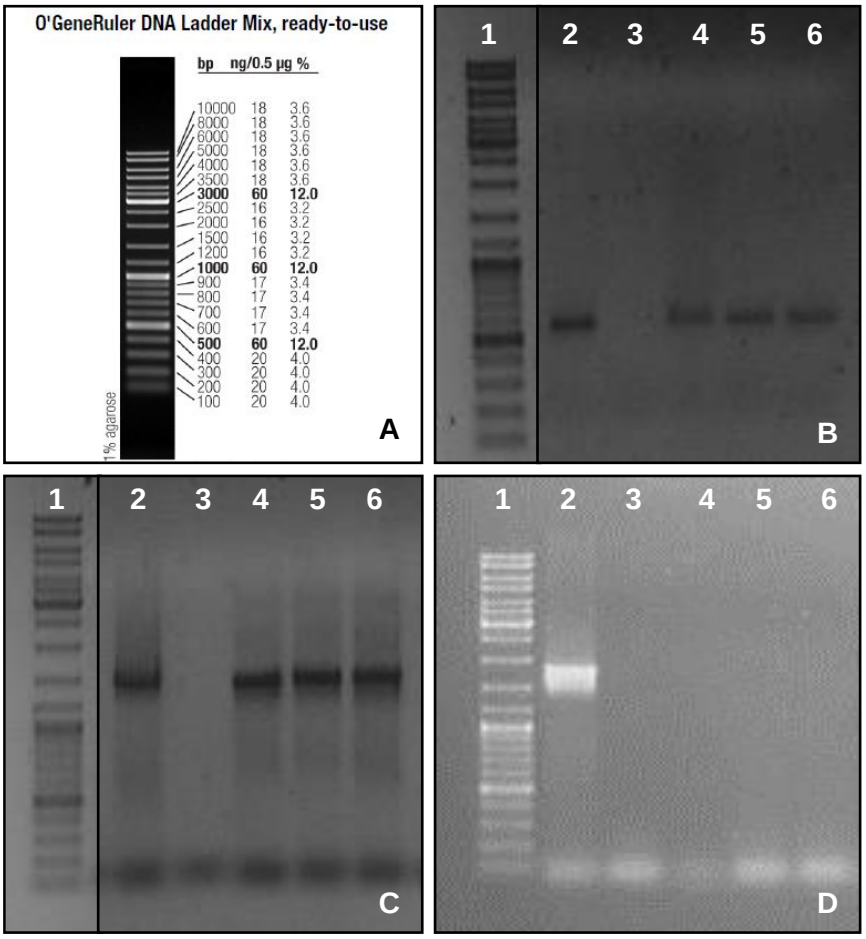

Figure 7.5: (A) The O'GeneRuler™ DNA Ladder Mix (Thermo Scientific) used to determine the size of the amplicons, with the amplified rRNA gene fragments for (B) Archaea, (C) Bacteria, and (D) Eukarya. In lane 1, the O'GeneRuler™ DNA Ladder Mix is shown. Lanes 2 and 3 contain the positive and negative controls, respectively. Lanes 4 – 6 contain the amplicons from the bioreactor.

Amplicons were obtained for the Archaeal and Bacterial domains, but not for the Eukarya, confirming the statement made in Section 4.4.5.3, that the Eukarya will most likely not be able to survive and adapt to CCS conditions and therefore will probably not play a major role, if any, in carbon cycling in the subsurface.

7.4.5.2 Nested Polymerase Chain Reaction

The purified PCR products were used to amplify the V3/V4 hypervariable regions for Archaea (~600 bp) (Figure 7.6B) and Bacteria (~600 bp) (Figure 7.6C) using a nested

DGGE PCR as discussed in Section 3.3.6.6.3. Amplicons were obtained for the V3/V4 hypervariable regions from all the samples.

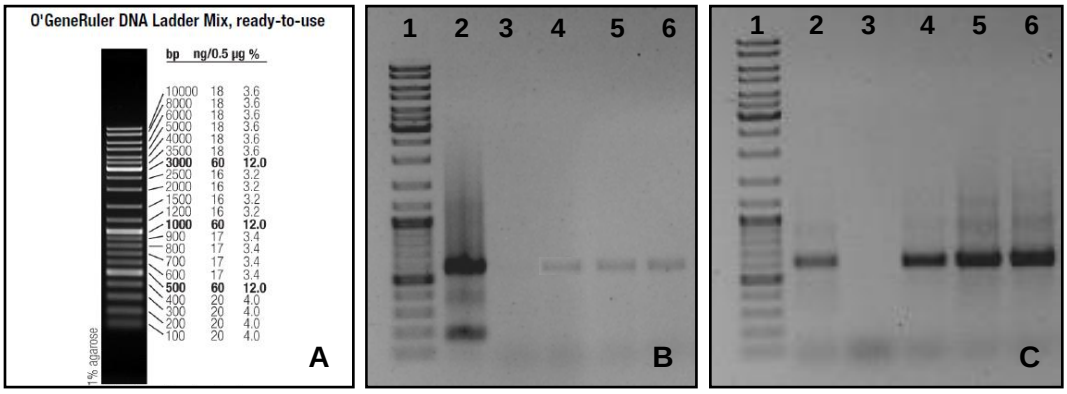

Figure 7.6: (A) The O'GeneRuler™ DNA Ladder Mix (Thermo Scientific) used to determine the size of the amplicons with the amplified V3/V4 hypervariable regions for (B) Archaea and (C) Bacteria. In lane 1, the O'GeneRuler™ DNA Ladder Mix is shown. Lanes 2 and 3 contain the positive and negative controls, respectively. Lanes 4 – 6 contain the amplicons from the bioreactor.

7.4.5.3 Denaturing Gradient Gel Electrophoresis, Sanger Sequencing and Analyses

The DGGE PCR products were used to construct a preliminary diversity profile for Archaea (Figure 7.7A) and Bacteria (Figure 7.7B) as discussed in Section 3.3.6.6.4.

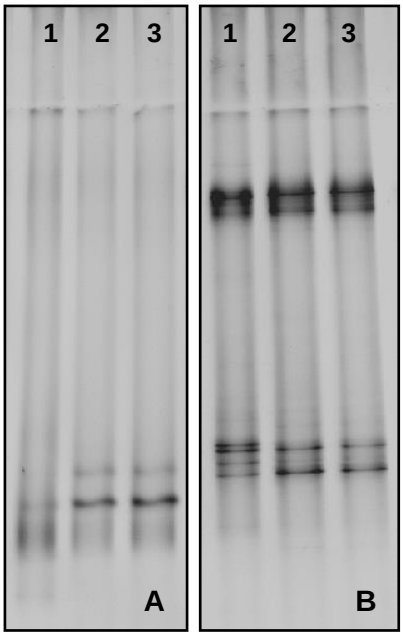

Figure 7.7: DGGE diversity profiles of (A) Archaea and (B) Bacteria.

The DGGE profiles obtained for the Archaea and the Bacteria after six weeks under CCS conditions inside the bioreactor, was different than what was initially obtained for the subsurface biome (Section 3.4.3.1.3), probably confirming that carbon sequestration will influence the diversity of the subsurface biome.

Sequencing and analyses were conducted on selected DGGE bands as discussed in Sections 3.3.6.6.5 and 3.3.6.6.6. The analysed sequences indicated that the Bacteria were still dominated by the Proteobacteria phylum, mainly consisting of the Beta- and Gammaproteobacteria classes. This was followed by the Firmicutes phylum, consisting of the Clostridia class, the Bacteriodetes phylum, containing the Actinobacteria, Flavobacteria, and Sphingobacteriia classes, and the Deinococci class of the Deinococcus-Thermus phylum which is highly resistant to environmental hazards (Brooks & Murray, 1981; Albuquerque *et al*., 2005; Ekman *et al*., 2011). The Archaea only contained the Euryarchaeota phylum, consisting of the Methanobacteria and the Halobacteria classes. This confirmed that an overall decrease in the diversity was seen after exposure to CCS conditions.

7.4.6 Microbial Diversity Assessments using Targeted rRNA Gene Sequencing

Targeted rRNA gene sequencing was done using the Ion Torrent PGM™ as discussed in Section 3.3.6.7. Extending the DGGE results, it can be seen that even though a substantial decrease in the overall diversity was observed (Figure 7.8) the Proteobacteria, especially the Betaproteobacteria, remained the dominant group, but the Firmicutes and the Bacteroidetes were also present (Figure 7.9). In Chapter 6 it was discussed that Gram-positive microorganisms are more resilient towards sc-CO_2 than Gram-negative microorganisms due to the high peptidoglycan content in their cell walls, making them less permeable (Cheftel, 1995; Zhang *et al*., 2006; Mitchell *et al*., 2009). However, most of the orders present in the bioreactor were from the Gram-negative group, most probably indicating the importance of biofilm formation of the subsurface microorganisms in order to protect themselves from the stressful conditions they will be subjected to during carbon sequestration.

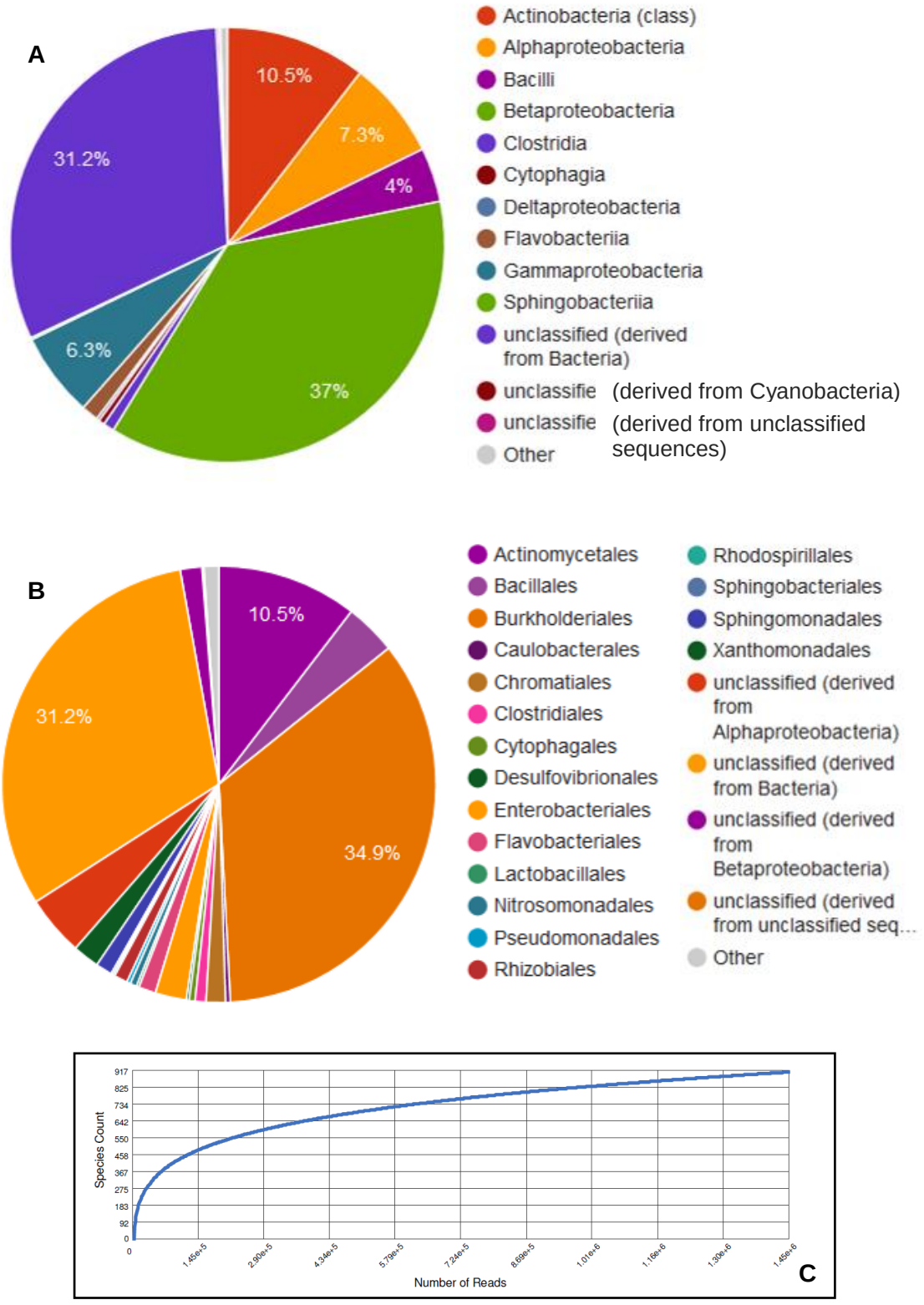

Figure 7.8: MG-RAST taxonomic hits distribution of the diversity in the subsurface biome for (A) class and (B) order, with (C) a rarefaction curve indicating the annotated species richness.

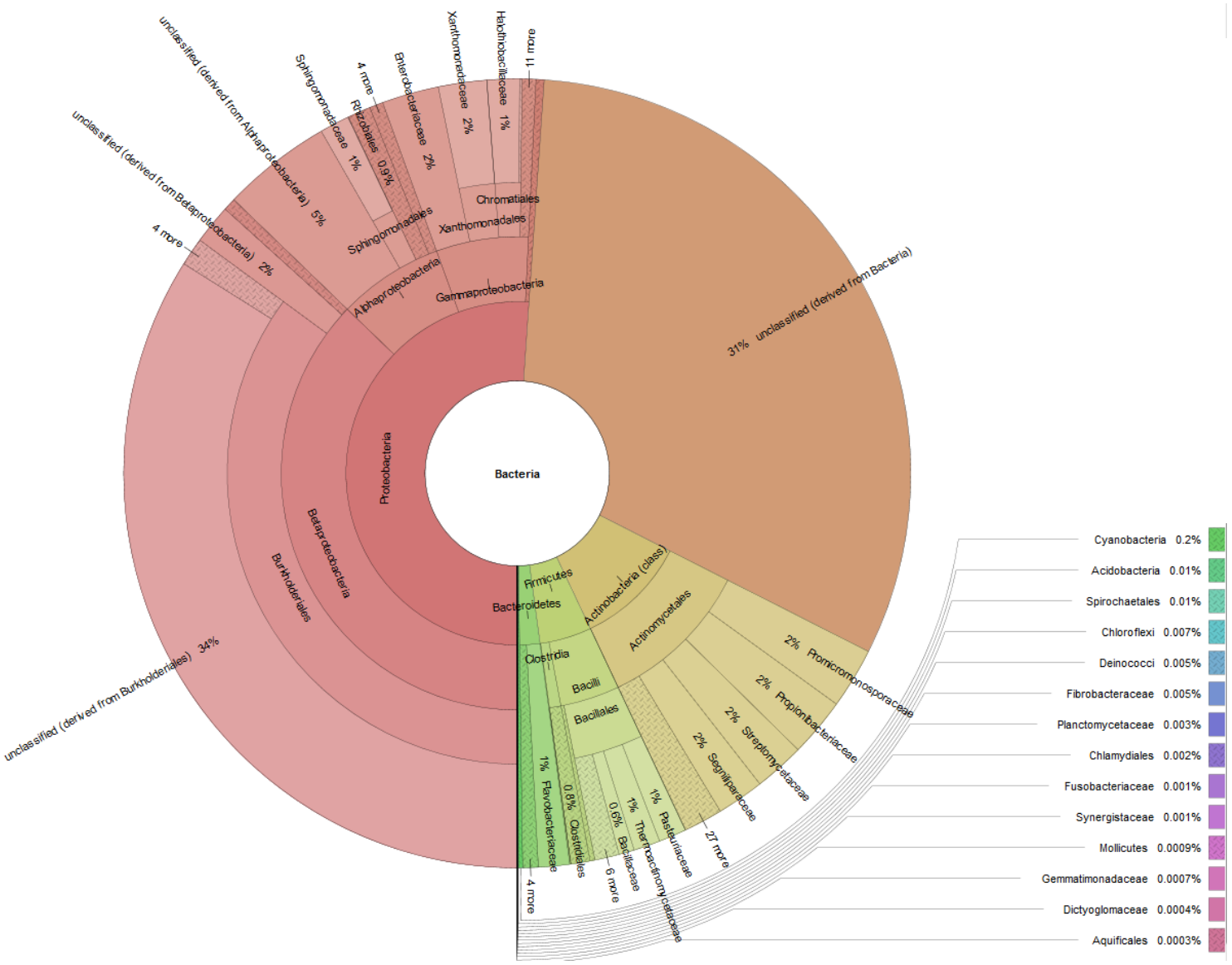

Figure 7.9: MG-RAST Krona diagram of the Bacteria at order level.

7.4.7 Microbial Diversity Assessments using Visual Methods

7.4.7.1 Scanning Electron Microscopy

Scanning electron microscopy was conducted as discussed in Section 3.3.6.8.4. Images were falsely coloured using Adobe® Photoshop (V.CS5) and EDS analyses confirmed that the biofilm was indeed biological material. These images suggest that even though there was a substantial decrease in diversity, the biome was still composed of diverse microorganisms with varying morphology and distinctive structures (Figure 7.10).

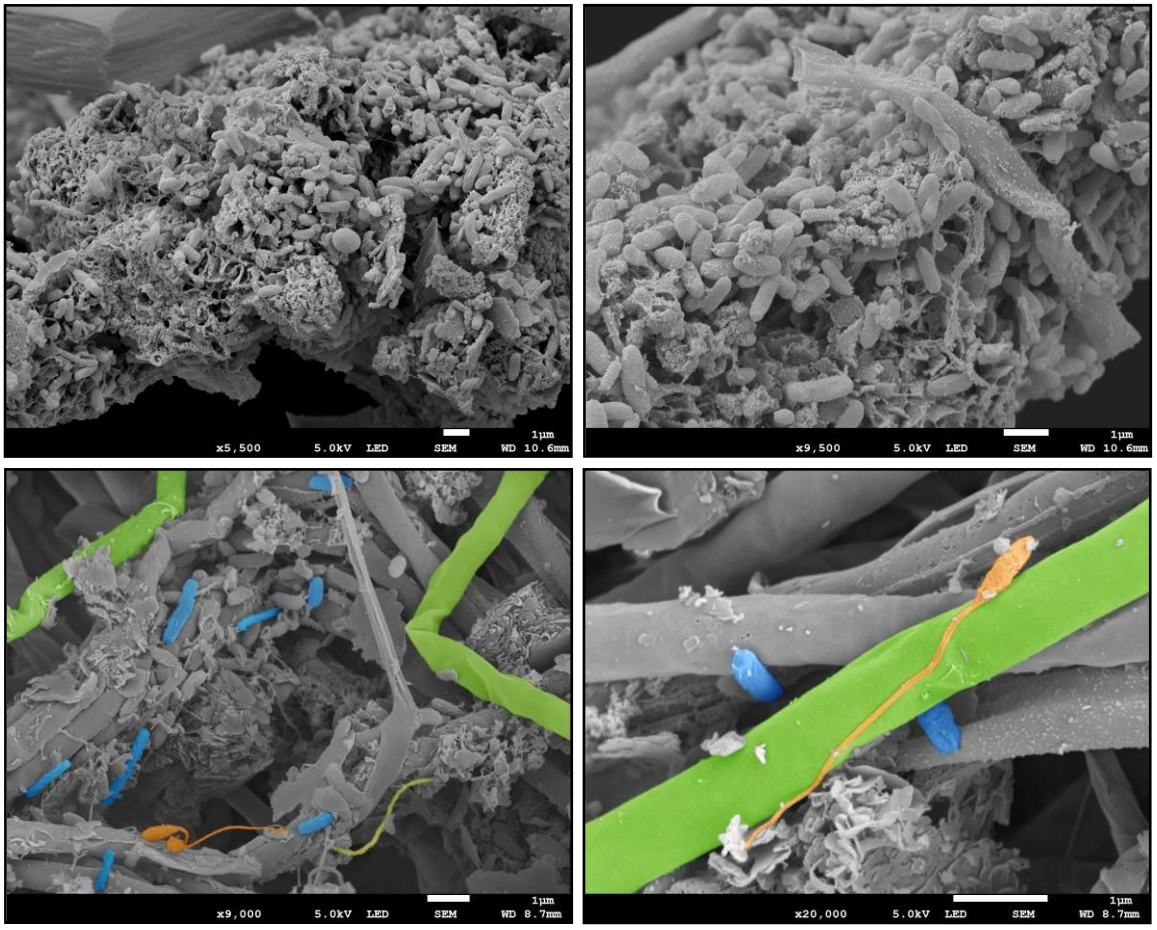

Figure 7.10: Scanning electron microscopy images of the biome after being subjected to CCS conditions. Scale bars are equal 1 µm.

However, several tube-like structures (Figure 7.11) were now found to be present which were not prominent in the subsurface biome from the Star Diamonds mine. The formation of these structures could possibly be biofilm formation which takes place under

high pressures. Also, more hyphae-like structures were observed, however, the hyphae appeared to be damaged, likely due to the presence of sc-CO_2, the metals, or high pressure. This suggests that, even though the microorganisms can protect themselves from these conditions to an extent, it may have detrimental effects on the subsurface biome.

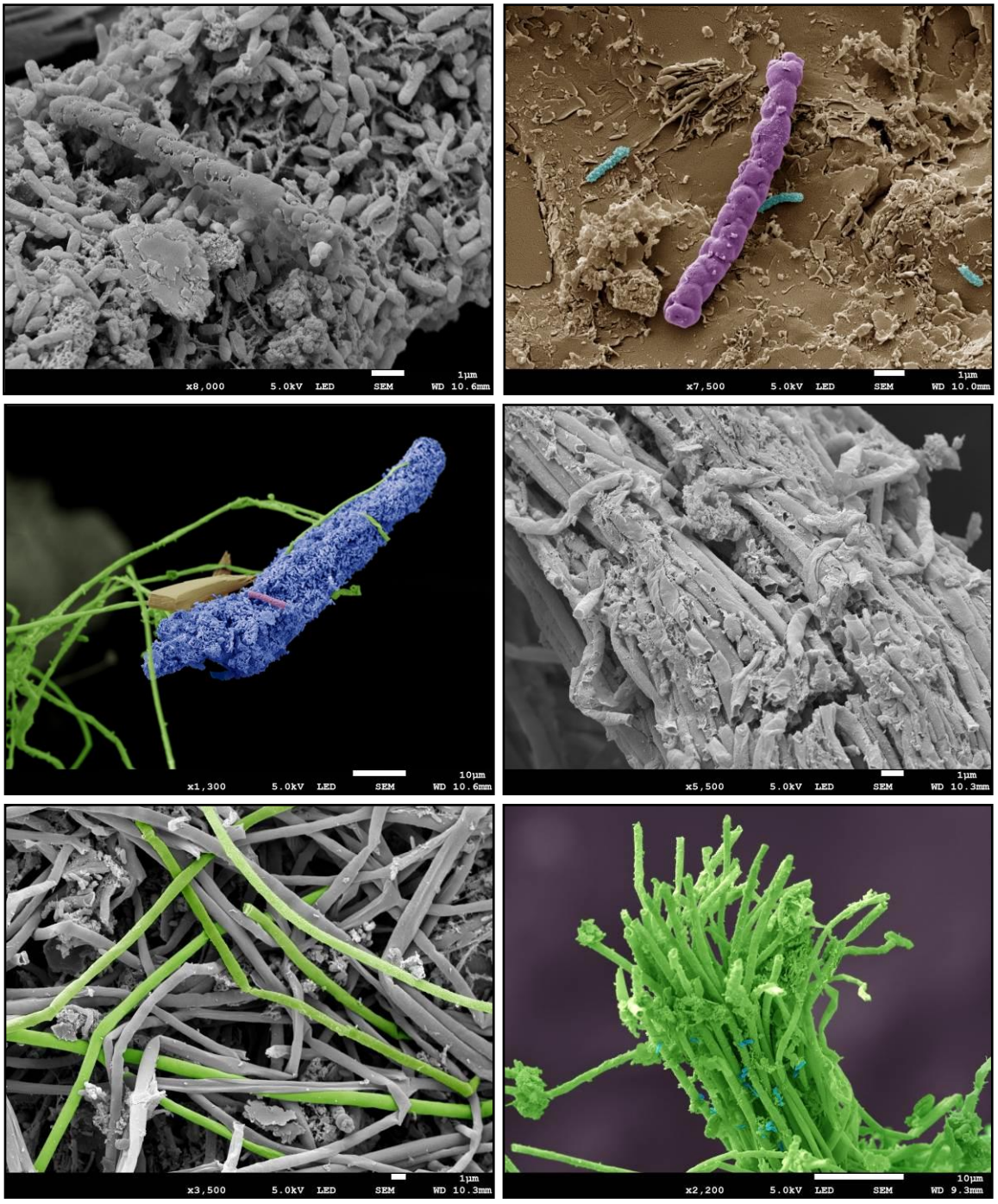

Figure 7.11: Scanning electron microscopy images, indicating the tube-like and hyphae-like structures. Scale bars are equal to either 1 µm or 10 µm.

EDS analyses also detected the presence of aluminium precipitation (Figure 7.12), most likely from the interaction with metals leached from the sandstone. Spectrum 40 is shown as a representative sample.

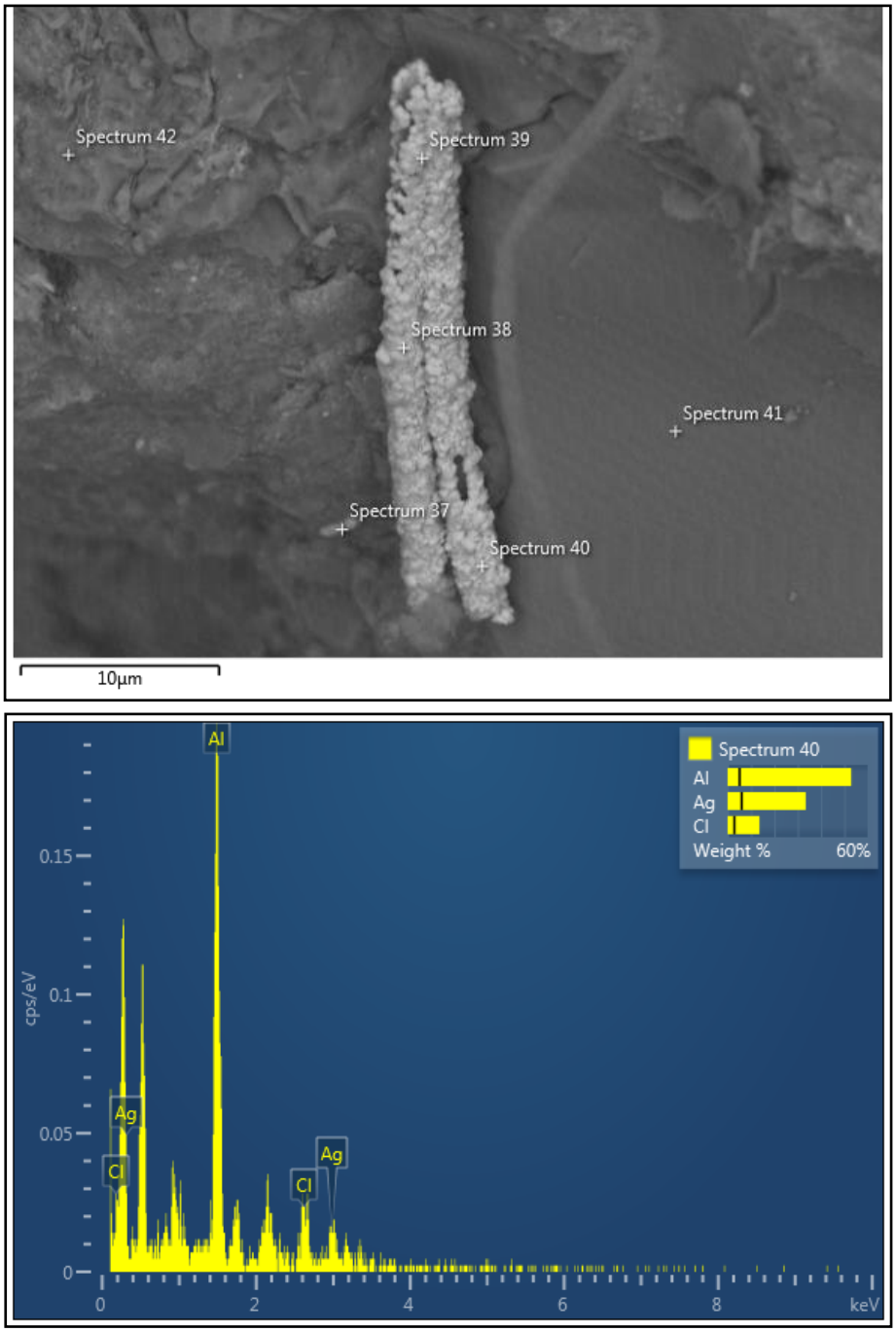

Figure 7.12: EDS analyses, confirming the presence of aluminium precipitation.

7.4.8 Whole Transcriptome Sequencing using Ion Torrent Proton™

Total RNA was isolated from the massive filters, the PVC cartridges, and the second bioreactor for whole transcriptome sequencing as discussed in Section 7.3.4. Unfortunately, not enough biomass could be obtained under the bioreactor conditions to allow proper RNA isolation. The RNA that was obtained from the bioreactor was of poor quality and could not be used for sequencing.

From the diversity studies on the subsurface biome (Chapter 3), it was found that microorganisms with various metabolisms were present (Section 3.4.3.2), and included the methanogens that can fix CO_2, several sulphate-reducing bacteria, including the Desulfobacterales, Desulfovibrionales, and Syntrophobacterales orders, microorganisms known to fix nitrogen such as the Cyanobacteria and Chlorobi phyla, as well as the Pseudomonadales, Rhizobiales, and Actinomycetales orders.

Possible pathways that these microorganisms might follow during carbon sequestration can be divided into two general groups, as described in Bar-Even *et al*., (2012). The first group contains pathways such as the reductive acetyl-CoA pathway, also known as the Wood–Ljungdahl pathway, which directly utilize reduced C1 compounds (Figure 7.14) (Bar-Even *et al*., 2012).

With the reductive acetyl-CoA pathway, the CO_2 is reduced to produce CO using CO dehydrogenase. The CO combines with a methyl group to produce acetyl-CoA, via acetyl-CoA synthase (Figure 7.13) (Ljungdahl & Wood, 1965; Ragsdale, 2006; Lindahl, 2009; Ljungdahl, 2009) and occurs in acetate-producing Bacteria such as *Clostridium*, and the Archaea such as the methanogens (Matschiavelli *et al*., 2012). Thus, this may lead to the production of acetate and finally methane if hydrogen is available. Both of these groups have been found to be present in the subsurface biome, as well as after the bioreactor conditions.

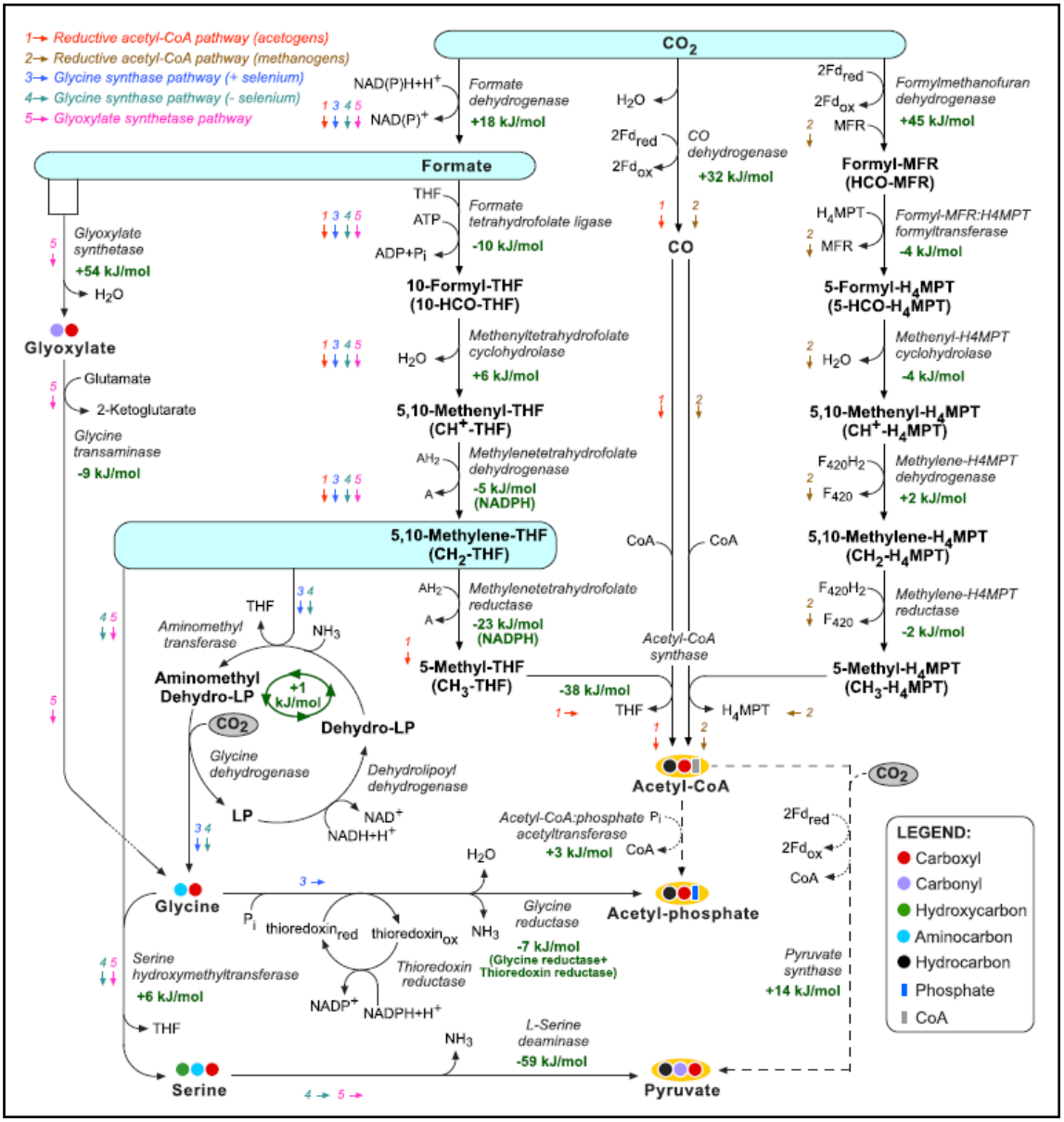

Figure 7.13: The C1 carbon fixation pathways cycles [Taken from Bar-Even *et al*., (2012)].

The second group contains pathways such as the reductive TCA cycle, also known as the reverse Krebs cycle, through which CO_2 is integrated into the carbon backbone of other metabolites, thus, reduced C1 compounds are not part of the pathway (Figure 7.13) (Bar-Even *et al*., 2012).

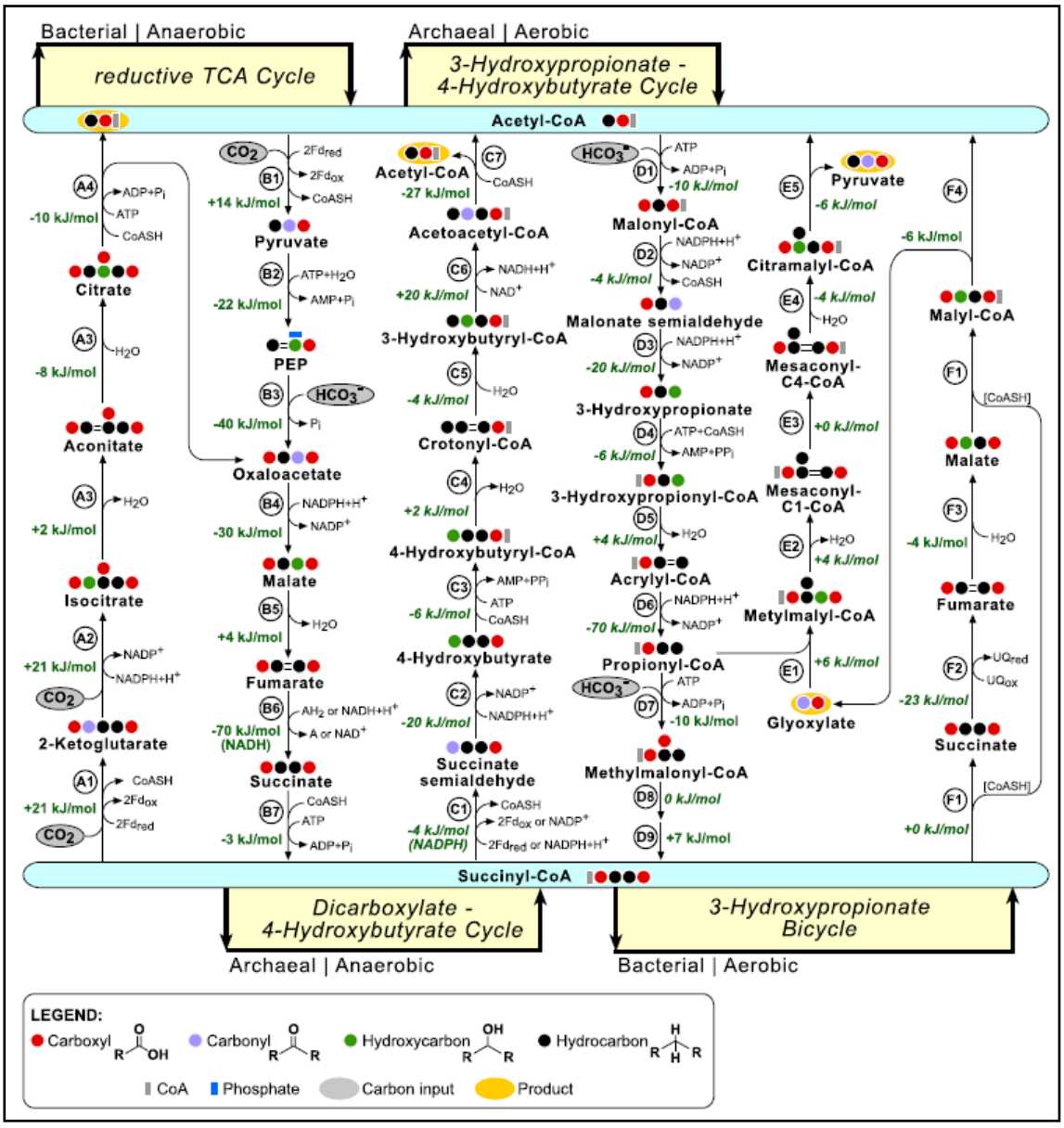

Figure 7.14: The acetyl-CoA-succinyl-CoA carbon fixation cycles [Taken from Bar-Even *et al*., (2012)].

The Calvin cycle, which is responsible for the fixation of most of the carbon in the biosphere, can be used to fix CO_2 in order to produce glyceraldehyde-3-phosphate (G3P) which can be used to synthesize hexose sugars such as glucose, the main nutrient source for heterotrophic microorganisms (Berg *et al*., 2002).

Results from the whole transcriptome sequencing of the subsurface biome confirmed that sulphur metabolism, nitrogen metabolism, and CO_2 fixation are present (Figure 7.15). For the CO_2 fixation metabolism (Figure 7.16), it was found that gene products from the Calvin cycle were present, in particular, ribulose-1,5-biphosphate carboxylase/oxygenase (RuBisCO). RuBisCO is the predominant enzyme in carbon fixation and the rate limiting enzyme in the Calvin Cycle and is a carbonic anhydrase (Feller *et al*., 2008; Yeates *et al*., 2008), therefore, the production of bicarbonates are possible (Zaihua, 2001; Lane *et al*., 2005; Raven, 2006; Ramanan *et al*., 2009). The carboxysomes also contain the RuBisCO enzyme. Some of the more important enzymes involved in the C1 carbon fixation pathways present in the subsurface biome, included formate dehydrogenase, CO dehydrogenase, and acetyl-CoA synthase. The acetogens, present within the subsurface biome, as well as after the bioreactor conditions, can reduce CO_2 to formate using formate dehydrogenase (Yamamoto *et al*., 1983; Ljungdahl, 1986). The acetogens can also synthesize CO from CO_2 using ferredoxin as the electron donor and they can use acetyl-CoA synthase to generate acetyl-CoA (Drake *et al*., 2006; Ragsdale, 2008). Other gene products involved in central carbohydrate metabolism such as the gene products for hydroxyacylglutathione hydrolase, were also present. Thus, one might anticipate that the subsurface biome should be able to produce formate, acetate, methane, and bicarbonates under CCS conditions.

The diversity studies on the bioreactor indicated that the Desulfovibrionales order, which have the ability to metabolize sulphate, was present. Within the transcriptome data, sulphur metabolism was confirmed to be present, involving gene products such as sulphite reductase (alpha and beta subunits), including the dissimilatory sulphite reductase alpha subunit (*dsrA*) and gamma subunit (*dsrC*), as well as the adenylylsulphate reductase (APSR) beta subunit.

The bioreactor diversity also indicated that the Pseudomonadales, Rhizobiales, and Actinomycetales orders, which have the ability to fix nitrogen, were present. Transcriptome data confirmed that nitrogen metabolism was present, containing gene products such as the nitrate reductase catalytic subunit, the periplasmic nitrate reductase precursor, and 2-nitropropane dioxygenase.

For the methanogenic Archaea, the heterodisulphide reductase (HDR) which catalyses the reversible reduction of the heterodisulphide (CoM-S-S-CoB) of the methanogenic thiol-coenzymes such as coenzyme M (CoM-SH) and coenzyme B (CoB-SH) (Hedderich *et al*., 2005), were all present in the transcriptome, thus the survival of these groups could eventually have a possible effect on methane production.

Several gene products involved in chemotaxis, regulation, and cell signaling were also detected such as the methyl-accepting chemotaxis protein (MCP), the aerotaxis receptor (Aer), and the signaling proteins CheY, CheZ, and CheV. Other gene products of interest found included the Fe/S oxidoreductases, involved in stress response and oxidative stress, the methyltransferases, Zn-dependent hydrolase/oxidoreductases, aldehyde ferredoxin oxidoreductases, Quinone oxidoreductases, ferredoxin, and GTPase – a putative metal chaperone involved in zinc homeostasis.

Even though full pathways were not identified from the sequence analyses (Figure 7.17), several gene products were detected that are indicative of suspected active cycling in subsurface metabolisms, also found by Lau *et al*., (2014) and could allow the subsurface biome to deal with CCS conditions.

Figure 7.15: MG-RAST Krona diagram of the functional category hits distribution of the subsurface biome.

Figure 7.16: MG-RAST Krona diagram of CO_2 fixation in the subsurface biome.

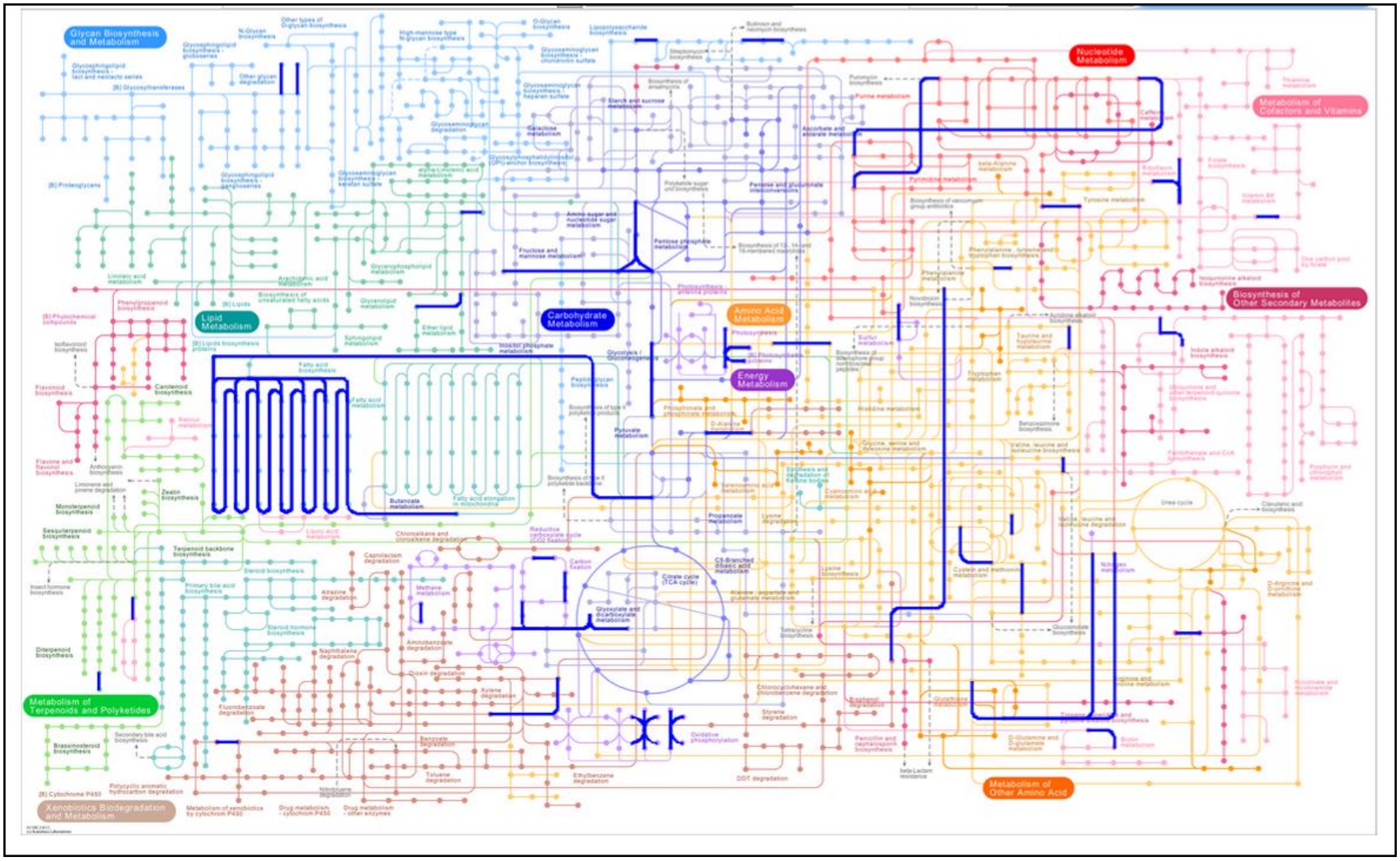

Figure 7.17: MG-RAST KeggMapper. The genes present within the subsurface biome are shown in the blue highlighted lines.

7.5 CONCLUSIONS

According to the literature (Morozova *et al*., 2010; Basava-Reddi, 2012; Mu *et al*., 2014), the injection of sc-CO_2 could cause a substantial decrease in the diversity in the subsurface, but ultimately the surviving microorganisms might be able to adapt and utilize the CO_2. Using the continuous high pressure bioreactor, it was found that indeed a significant decrease in the diversity was observed however, several microorganisms were able to survive the CCS conditions likely due to their ability to form biofilms which protected them from these stressful conditions. It is known that microorganisms living in the extreme conditions of the deep subsurface environments display limited growth with exceptionally low metabolic activities and turnover times (Phelps *et al*., 1994; Teske, 2005; Jørgensen & D'Hondt, 2006; Jørgensen & Boetius, 2007; Onstott *et al*., 2009), therefore it was not unexpected that typical metabolic products were not observed during/after the six weeks of circulation under CCS conditions, even though these microorganisms remained viable.

As expected, groups from the Bacteria and Archaea were able to survive the CCS conditions, but no Eukarya could be detected after six weeks. For the Archaea, only the Euryarchaeota phylum, consisting of the Methanobacteria and the Halobacteria classes, could be detected. The Bacteria remained the dominant domain, with the Proteobacteria still the main phylum present, similar to what has been found in the subsurface biome. The Firmicutes and the Bacteriodetes were also detected.

In the acidic and high pressure environment created by the CCS conditions, metals, especially aluminium and iron, leached from the sandstone. This resulted in even more stressful conditions for the subsurface biome thus, restricting the already limited growth even further. This phenomenon should be considered before employing carbon sequestration, especially the influence it will have on the composition and cycling of the subsurface microbial communities. These extreme conditions limited successful RNA extractions and ultimately transcriptome analyses of the diversity, but data obtained for the subsurface biome indicated that gene products from sulphur metabolism, nitrogen metabolism, and carbon metabolism were present. The diversity within the bioreactor confirmed that microorganisms utilizing these metabolisms were present, and thus

specific cycling can be anticipated from the subsurface biome. If an active biome is exposed to CCS conditions they should be able to produce formate, acetate, methane, and bicarbonates. Thus this project effectively demonstrated new considerations in terms of diversity, geological changes, as well as metabolic cycling that should be considered before implementing CCS technology.

7.6 REFERENCES

- **Albuquerque, L., Simões, C., Nobre, M.F., Pino, N.M., Battista, J.R., Silva, M.T., Rainey, F.A. and da Costa, M.S.** (2005). *Truepera radiovictrix* gen. nov., sp. nov., a New Radiation Resistant Species and the Proposal of Trueperaceae fam. nov. *Int FEMS Microbiology Letters*. **247**:161-169.

- **Amonette, J.E., Russell, C.K., Carosino, K.A., Robinson, N.L. and Ho, J.T.** (2003). Toxicity of Al to *Desulfovibrio desulfuricans*. *Appl. Environ. Microbiol*. **69**:4057-4066.

- **Baker, B.J., Moser, D.P., MacGregor, B.J., Fishbain, S., Wagner, M., Fry, N.K., Jackson, B., Spoelstra, N., Loos, S., Takai, K., Sherwood Lollar, B., Fredrickson, J.K., Balkwill, D., Onstott, T.C., Wimpee, C.F. and Stahl, D.A.** (2003). Related Assemblages of Sulphate Reducing Bacteria Associated with Ultra Deep Gold Mines of South Africa and Deep Basalt Aaquifers of Washington State. *Environ Microbiol*. **5(4)**:267–277.

- **Banfield, J.F., Barker, W.W., Welch, S.A. and Taunton, A.** (1999). Biological Impact on Mineral Dissolution: Application of the Lichen Model to Understanding Mineral Weathering in the Rhizosphere. *Proc. Natl. Acad. Sci*. **96**:3404-3411.

- **Bar-Even, A., Noor, E. and Milo, R.** (2012). A Survey of Carbon Fixation Pathways through a Quantitative Lens. *Journal of Experimental Botany*. **63(6)**:2325-2342.

- **Basava-Reddi, L.** (2012). Microbial Effects on CO_2 Storage. IEAGHG Report.

- **Basso, O., Lascourreges, J.F., Le Borgne, F., Le Goff, C. and Margot, M.** (2009). Characterization by Culture and Molecular Analysis of the Microbial Diversity of a Deep Subsurface Gas Storage Aquifer. *Res. Microbiol*. **160**:107–116.

- **Berg, J.M., Tymoczko, J.L. and Stryer, L.** (2002). Biochemistry (5^{th} ed.). *WH Freeman Publishers*. ISBN: 0716730510.

- **Booth, I.R., Cash, P. and O'Byrne, C.O.** (2002). Sensing and Adapting to Acid Stress. *Antonie van Leeuwenhoek.* **81**:33-42.

- **Bordenave, S., Chatterjee, I. and Voordouw, G.** (2012). Microbial Community Structure and Microbial Activities Related to CO_2 Storage Capacities of a Salt Cavern. *Int. Biodeterior. Biodegrad.* **81**:82-87.

- **Bradley, T.J. and Parker, M.S.** (1968). Binding of Aluminium Ions by *Staphylococcus aureus* 893. *Experientia*. **24**:1175-1176.

- **Brooks, B.W. and Murray, R.G.E.** (1981). Nomenclature for *Micrococcus radiodurans* and other Radiation-Resistant Cocci: Deinococcaceae fam. nov. and *Deinococcus* gen. nov., Including Five Species. *Int. J. Syst. Bacteriol*. **31(3)**:353-360.

- **Chapelle, F.H., O'Neill, K., Bradley, P.M., Methé, B.A., Ciufo, S.A., Knobel, L.L. and Lovley, D.R.** (2002). A Hydrogen-Based Subsurface Microbial Community Dominated by Methanogens. *Nature*. **415**:312-315.

- **Cheftel, J.C.** (1995). Review: High-Pressure, Microbial Inactivation and Food Preservation. *Food Sci. Technol. Int*. **1**:75-90.

- **Cozzarelli, I.M., Baedecker, M.J., Eganhouse, R.P. and Goerlitz, D.F.** (1994). The Geochemical Evolution of Low-Molecular-Weight Organic Acids Derived from the Degradation of Petroleum Contaminants in Groundwater. *Geochim. Cosmochim. Acta.* **58**:863-877.

- **Davis, W.B., McCauley, M.J. and Byers, B.R.** (1971). Iron Requirements and Aluminum Sensitivity of Hydroxamic Requiring Strain of *Bacillus meyaterium*. *J Bacteriol*. **105**:589-594.

- **Drake, H.L., Kirsten, K. and Matthies, C.** (2006). Acetogenic Prokaryotes. In The Prokaryotes. *Springer Publishers*. 354-442.

- **Driscoll, C.T.** (1985). Aluminium in Acidic Surface Waters: Chemistry, Transport and Effects. *Environ Health Perspect*. **63**:93-104.

- **Ekman, J.V., Raulio, M., Busse, H.J., Fewer, D.P. and Salkinoja-Salonen, M.** (2011). Deinobacterium chartae gen. nov., sp. nov., an Extremely Radiation Resistant Biofilm-Forming Bacterium Isolated from a Finnish Paper Mill. *Int J Syst Evol Microbiol*. **61(3)**:540-548.

- **Feller, U., Anders, I. and Mae, T.** (2008). Rubiscolytics: Fate of Rubisco After its Enzymatic Function in a Cell is Terminated. *J. Exp. Bot*. **59(7)**:1615-1624.

- **Fierer, N. and Jackson, R.B.** (2006). The Diversity and Biogeography of soil Bacterial Communities. *Proc. Natl. Acad. Sci.* **103**:626-631.

- **Foy, C.D., Chaney, R.L. and Shite, M.C.** (1978). The Physiology of Metal Toxicity in Plants. *Annu Rev Plant Physiol*. **29**:1259-1261.

- **Fry, J.C., Parkes, R.J., Cragg, B.A., Weightman, A.J. and Webster, G.** (2008). Prokaryotic Biodiversity and Activity in the Deep Subseafloor Biosphere. *FEMS Microbiol.Ecol*. **66**:181-196.

- **Gadd, G.M.** (2010). Metals, Minerals and Microbes: Geomicrobiology and Bioremediation. *Microbiology.* **156**:609-643.

- **Gagen, C.J., Sharpe, W.E. and Carline, R.F.** (1993). Mortality of Brook Trout, Mottled Sculpins and Slimy Sculpins during Acidic Episodes. *Trans Am Fish Soc*. **122**:616-628.

- **Ganrot, P.O.** (1986). Metabolism and Possible Health Effects of Aluminium. *J Environ Health Perspect*. **65**:363-441.

- **Glossner, A.** (2013). Terminal Microbial Metabolisms in the Deep Subsurface under Conditions Relevant to CO_2 Sequestration and Enhancing Methanogenesis from Coal. *PhD Thesis, Colorado School of Mines*.

- **Guida, L., Saidi, Z., Hughes, M.N. and Poole, R.K.** (1991). Aluminium Toxicity and Binding to *Escherichia coli*. *Arch Microbiol*. **156**:507-512.

- **Haug, A.** (1984). Molecular Aspects of Aluminium Toxicity. *Crit. Rev. Plant Sci*. **1**:345-373.

- **Hedderich, R., Hamann, N. and Bennati, M.** (2005). Heterodisulfide Reductase from Methanogenic Archaea: a New Catalytic Role for an Iron-Sulfur Cluster. *Biological Chemistry*. **386(10)**:961-970.

- **Hervieux, V., Yaganza, E.S., Arul, J. and Tweddell, R.J.** (2002). Effect of Organic and Inorganic Salts on the Development of *Helminthosporium solani*, the Causal Agent of Potato Silver Scurf. *Plant Dis*. **86**:1014-1018.

- **Hubert, C.R., Oldenburg, T.B., Fustic, M., Gray, N.D., Larter, S.R., Penn, K., Rowan, A.K., Seshadri, R., Sherry, A., Swainsbury, R., Voordouw, G., Voordouw, J.K. and Head, I.M.** (2011). Massive Dominance of Epsilonproteobacteria in Formation Waters from a Canadian Oil Sands Reservoir Containing Severely Biodegraded Oil. *Environ. Microbiol*. **14(2)**:387-404.

- **Illmer, P. and Erlebach, C.** (2003). Influence of Al on growth, cell size and content of intracellular water of *Arthrobacter* sp. PI/1-95. *Antonie Van Leeuwenhoek*. **84(3)**:239-246.

- **Johnson, A.C.** (1988). The mechanism of aluminium toxicity to *Rhizobium*. *PhD Thesis, University of Reading*.

- **Jørgensen, B.B and Boetius, A.** (2007). Feast and Famine – Microbial Life in the Deep-Sea Bed. *Nature Reviews Microbiology*. **5**:770-781.

- **Jørgensen, B.B. and D'Hondt, S.** (2006). ECOLOGY: A Starving Majority Deep Beneath the Seafloor. *Science*. **314**:932-934.

- **Keyser, H.H. and Munns, D.N.** (1979). Tolerance of Rhizobia to Acidity, Aluminium and Phosphate. *Soil Sci Soc Am J*. **43**:519-523.

- **Kotelnikova, S.** (2002). Microbial Production and Oxidation of Methane in Deep Subsurface. *Earth-Sci. Rev*. **58**:367–395.

- **Krüger, M., Jones, D., Frerichs, J., Oppermann, B.I., West, J., Coombs, P., Green, K., Barlow, T., Lister, R., Shaw, R., Strutt, M. and Möller, I.** (2011). Effects of Elevated CO_2 Concentrations on the Vegetation and Microbial Populations at a Terrestrial CO_2 Vent at Laacher See, Germany. *Int J Greenh Gas Contl*. **5(4)**:1093-1098.

- **Lane, T.W., Saito, M.A., George, G.N., Pickering, I.J., Prince, R.C. and Morel, F.M.M.** (2005). The First Cadmium Enzyme – Carbonic Anhydrase 2 from the Marine Diatom *Thalassiosira weissflogii*. *Science Highlight.*

- **Lau, M.C.Y., Cameron, C., Magnabosco, C., Brown, C.T., Schilkey, F., Grim, S., Hendrickson, S., Pullin, M., Sherwood Lollar, B., van Heerden, E., Kieft, T.L. and Onstott, T.C.** (2014). Phylogeny and Phylogeography of Functional Genes Shared Among Seven Terrestrial Subsurface Metagenomes Reveal N-Cycling and Microbial Evolutionary Relationships. *Front. Microbiol*. **5**:531.

- **Lindahl, P.A.** (2009). Nickel-Carbon Bonds in Acetyl-Coenzyme Synthases/Carbon Monoxide Dehydrogenases. *Met Ions Life Sci*. **6**:133-150.

- **Ljungdahl, L. and Wood, H.G.** (1965). Incorporation of C^{14} from Carbon Dioxide into Sugar Phosphates, Carboxylic Acids, and Amino Acids by *Clostridium thermoaceticum*. *J. Bacteriol*. **89(4)**:1055-1064.

- **Ljungdahl, L.G.** (1986). The Autotrophic Pathway of Acetate Synthesis in Acetogenic Bacteria. *Annu. Rev. Microbiol*. **40**:415-450.

- **Ljungdahl, L.G.** (2009). A Life with Acetogens, Thermophiles, and Cellulolytic Anaerobes. *Annu. Rev. Microbiol*. **63**:1-25.

- **Macdonald, T.L. and Martin, R.B.** (1988). Aluminium Ion in Biological Systems. *Trends Biochem Sci*. **13(1)**:15-19.

- **Martin, R.B.** (1986). The Chemistry of Aluminium as Related to Biology and Medicine. *Clin Chem*. **32**:1797-1806.

- **Matschiavelli, N., Oelgeschlager, E., Cocchiararo, B., Finke, J. and Rother, M.** (2012). Function and Regulation of Isoforms of Carbon Monoxide Dehydrogenase/Acetyl-CoA Synthase in *Methanosarcina acetivorans*. *J. Bacteriol*. **194(19)**:5377-5387.

- **McMahon, P.B. and Chapelle, F.H.** (1991). Microbial Production of Organic Acids in Aquitard Sediments and its Role in Aquifer Geochemistry. *Nature.* **349**:233-235.

- **Mecteau, M.R., Arul, J. and Tweddell, R.J.** (2002). Effect of Organic and Inorganic Salts on the Growth and Development of *Fusarium sambucinum*, a Causal Agent of Potato Dry Rot. *Mycol. Res*. **106**:688-696.

- **Meyer, F., Paarmann, D., D'Souza, M., Olson, R., Glass, E.M., Kubal, M., Paczian, T., Rodriguez, A., Stevens, R., Wilke, A., Wilkening, J. and Edwards, R.A.** (2008). The Metagenomics RAST Server – A Public Resource for the Automatic Phylogenetic and Functional Analysis of Metagenomes. *BMC Bioinformatics*. **9**:386.

- **Meyer, J.R., Shew, H.D. and Harrison, U.J.** (1994). Inhibition of Germination and Growth of *Thielaviopsis basicola* by Aluminium. *Phytopathology*. **84**:598-602.

- **Mitchell, A.C., Phillips, A.J., Hamilton, M.A., Gerlach, R., Hollis, W.K. and Kaszuba, J.P.** (2008). Resilience of Planktonic and Biofilm Cultures to Supercritical CO_2. *J. Supercrit.Fluids*. **47**:318-325.

- **Mitchell, A.C., Phillips, A.J., Hiebert, R., Gerlach, R., Spangler, L.H. and Cunningham, A.B.** (2009). Biofilm Enhanced Geologic Sequestration of Supercritical CO_2. *International Journal of Greenhouse Gas Control*. **3**:90-99.

- **Morozova, D., Wandrey, M., Alawi, M., Zimmer, M., Vieth, A., Zettlitzer, M and Würdemann, H.** (2010). Monitoring of the Microbial Community Composition in Saline Aquifers during CO_2 Storage by Fluorescence *in situ* Hybridisation. *International Journal of Greenhouse Gas Control*. **4**:981-989.

- **Mu, A., Boreham, C., Leong, H.X., Haese, R.R. and Moreau, J.W.** (2014). Changes in the Deep Subsurface Microbial Biosphere Resulting from a Field-Scale CO_2 Geosequestration Experiment. *Frontiers in Microbiology*. **5**:209.

- **Myrold, D.D. and Nason, G.E.** (1992). Effect of Acid Rain on Soil Microbial Processes. In: Mitchell R, ed. Environmental Microbioloy. *Wiley-Liss Publishers*. 59-81.

- **Newberry, C.J., Webster, G., Cragg, B.A., Parkes, R.J., Weightman, A.J. and Fry, J.C.** (2004). Diversity of Prokaryotes and Methanogenesis in Deep Subsurface Sediments from the Nankai Trough, Ocean Drilling Program Leg 190. *Environ.Microbiol*. **6**:274-287.

- **Onstott, T.C.** (2005). Impact of CO_2 Injections on Deep Subsurface Microbial Ecosystems and Potential Ramifications for the Surface Biosphere. Chapter 30 in Carbon Dioxide Capture for Storage in Deep Geologic Formations – Results from the CO_2 Capture Project, Geological Storage of Carbon Dioxide with Monitoring and Verification. *Elsevier Publishing*. **2**:1217-1250. ISBN: 0080445705.

- **Onstott, T.C., Colwell, F.S., Kieft, T.L., Murdoch, L. and Phelps, T.J.** (2009). New Horizons for Deep Subsurface Microbiology. *Microbe Magazine.* **4(11)**:499–505.

- **Pettersson, A., Kunst, L., Bergman, B. and Roomans, G.M.** (1985). Accumulation of Aluminium by *Anabaena cylindrica* into Polyphosphate Granules and Cell Walls: an X-Ray Energy-Dispersive Microanalysis Study. *J. Gen. Microbiol*. **131**:2545-2548.

- **Phelps, T.J., Murphy, E.M., Pfiffner, S.M. and White, D.C.** (1994). Comparison between Geochemical and Biological Estimates of Subsurface Microbial Activities. *Microb. Ecol*. **28**:335-349.

- **Piña, R.G. and Cervantes, C.** (1996). Mini Review: Microbial Interactions with Aluminium. *BioMetals*. **9**:311-316.

- **Ragon, M., Van Driessche, A.E.S., García-Ruíz, J.M., Moreira, D. and López-García, P.** (2013). Microbial Diversity in the Deep-Subsurface Hydrothermal Aquifer Feeding the Giant Gypsum Crystal-Bearing Naica Mine, Mexico. *Frontiers in Microbiology*. **4**:37.

- **Ragsdale, S.W.** (2004). Life with Carbon Monoxide. *Crit. Rev. Biochem. Mol. Biol*. **39**:165-195.

- **Ragsdale, S.W.** (2006). Metals and Their Scaffolds to Promote Difficult Enzymatic Reactions. *Chem. Rev*. **106**:3317-3337.

- **Ragsdale, S.W.** (2008). Enzymology of the Wood-Ljungdahl Pathway of Acetogenesis. *Ann N Y Acad Sci*. **1125**:129-136.

- **Ramanan, R., Kannan, K., Sivanesan, S.D., Mudliar, S., Kaur, S., Tripathi, A.K. and Chakrabarti, T.** (2009). Bio-sequestration of Carbon Dioxide using Carbonic Anhydrase Enzyme Purified from *Citrobacter freundii*. *World J Microbiol Biotechnol*. **25**:981-987.

- **Raven, J.A.** (2006). Sensing Inorganic Carbon: CO_2 and HCO_3^-. *Biochem Journal.* **396**:5-7.

- **Rogers, J.R. and Bennett, P.C.** (2004). Mineral Stimulation of Subsurface Microorganisms: Release of Limiting Nutrients from Silicates. *Chemical Geology*. **203**:91-108.

- **Santillan, E.U., Kirk, M.F., Altman, S.J. and Bennett, P.C.** (2013). Mineral Influence on Microbial Survival during Carbon Sequestration. *Geomicrobiology Journal*. **30(7)**:578-592.

- **Sato, K., Kawaguchi, H. and Kobayashi, H.** (2013). Energy Conversion and Management. *Energy Convers. Manage*. **66**:343-350.

- **Stenson, J.A.E., Svensson, J.E. and Cronberg, G.** (1993). Changes and Interactions in the Pelargic Community in Acidified Lakes in Sweden. *Ambio*. **22**:277-282.

- **Suhayda, C.G. and Haug, A.** (1986). Organic Acids Reduce Aluminium Toxicity in Maize Root Membranes. *Physiologia Plantarum*. **68**:189-195.

- **Takai, K., Moser, D., DeFlaun, M., Onstott, T.C. and Fredrickson, J.K.** (2001). Archaeal Diversity in Waters from Deep South African Gold Mines. *Applied and Environmental Biology.* **67(12)**:5750-5760.

- **Teske, A.P.** (2005). The Deep Subsurface Biosphere is Alive and Well. *Trends Microbiol.* **13(9)**:402-404.

- **Webster, G., Parkes, R.J., Cragg, B.A., Newberry, C.J., Weightman, A.J. and Fry, J.C.** (2006). Prokaryotic Community Composition and Biogeochemical Processes in Deep Subseafloor Sediments from the Peru Margin. *FEMS Microbiol. Ecol*. **58**:65-85.

- **Wood, M.** (1995). A mechanism of Aluminium Toxicity to Soil Bacteria and Possible Ecological Implications. *Plant Soil*. **171**:63-69.

- **Yaganza, E., Rioux, D., Simard, M. Arul, J. and Tweddell, R.J.** (2004). Ultrastructural Alterations of *Erwinia carotovora* subsp. *atroseptica* caused by Treatment with Aluminum Chloride and Sodium Metabisulfite. *Appl Environ Microb*. **70(11)**:6800-6808.

- **Yamamoto, I., Saiki, T., Liu, S.M. and Ljungdahl, L.G.** (1983). Purification and Properties of NADP-Dependent Formate Dehydrogenase from *Clostridium thermoaceticum*, a Tungsten-Selenium-Iron Protein. *J Biol Chem*. **258**:1826-1832.

- **Yeates, T.O., Kerfeld, C.A., Heinhorst, S., Cannon, G.C. and Shively, J.M.** (2008). Protein-Based Organelles in Bacteria: Carboxysomes and Related Microcompartments. *Nature Reviews Microbiology*. **6(9)**:681-691.

- **Zaihua, L.** (2001). Role of Carbonic Anhydrase as an Activator in Carbonate Rock Dissolution and its Implication for Atmospheric CO_2 Sink. *Acta Geologica Sinica.* **75**:275-278.

- **Zambenedetti, P., Tisato, F., Corain, B. and Zatta, P.F.** (1994). Reactivity of AI(III) with Membrane Phospholipids: a NMR Approach. *BioMetals*. **7**:244-252.

- **Zhang, J., Davis, T.A., Matthews, M.A., Drews, M.J., LaBerge, M. and An, Y.H.** (2006). Sterilization using High-Pressure Carbon Dioxide. *Journal of Supercritical Fluids.* **38**:354-372.

CHAPTER 8

FINAL CONCLUSIONS

Since the beginning of industrialization in the early 1800's, a significant amount of greenhouse gases, especially CO_2, have been emitted into the atmosphere, mainly through human activities such as the burning of fossil fuels. The rise in population levels around the world has increased the energy demand and subsequent greenhouse gas emmissions. These activities are the main contributor to the increase in average temperatures worldwide, resulting in a global climate change problem. Therefore, carbon resources have to be managed more effectively in order to limit CO_2 emissions. Current technologies include storing anthropogenic CO_2 in geological formations. This might be a possible solution to mitigate the CO_2 emissions on a scale that can stabilize the atmospheric greenhouse gases and make an impact on climate change. This study has illustrated that if these activities continue unmonitored, problems may occur as a result from the sequestered CO_2.

Studies have revealed that South Africa has the potential for storing CO_2 in geological formations and that of the more than 400 million tonnes of annual carbon dioxide emissions in South Africa ~60% can be sequestered. However, it is well-established that the deep subsurface environment is a diverse and geologically complex domain, containing a considerable percentage of the Earth's biomass in the form of microorganisms. The deep terrestrial biosphere in South Africa is dominated by radiogenic noble gases and crustal-derived carbon sources, with microbial metabolisms dominated by methanogenesis, sulphate reduction, and fermentation. Therefore, the hydrological, microbiological, and geochemical processes of these subsurface microbial communities could result in natural chemical fluxes, influencing the quality of the water.

In order to survive these extreme environments with high pressures and temperatures, limited nutrient and energy sources, metal toxicity, as well as radioactive processes, the subsurface microbial communities had to evolve various mechanisms to adapt. In the process of adaptation, microorganisms can also change their surrounding environment in order to provide the necessary nutrients. As a result, the survival of microorganisms depends mainly on their ecological and metabolic capabilities. These subsurface microbial activities could potentially play a critical role in the cycling of carbon. Microbial metabolism under these conditions can substantially change the structure and chemical composition of rock formations, and potentially lead to changes in the porosity and permeability of the storage reservoir, resulting in leakage of the CO_2, or even methane, since the CO_2 may be fixed into organic matter by chemoautotrophs and converted into methane by the methanogens.

This study evaluated subsurface microbial diversity from an environment of similar geological strata and depth as the sites proposed for carbon sequestration in South Africa. The biogeochemistry of the fissure water from the Star Diamonds mine in the Karoo sandstone was characterized over time. The fissure water was geochemically very similar over time, with a calculated conventional radiocarbon age of 24 320 (~131) years BP. Radiolysis of water could not be observed, possibly an indication that influx from older water sources are not relevant for this time period. Isotopic signatures revealed a possible mixing of thermogenic and biogenic gases, with positional and isotopic characteristics that could be consistent with production by methanogens utilizing the CO_2 reduction pathway.

The microbial diversity assessments confirmed that all three domains of life were present in the subsurface biome from the study site. The Bacterial domain was dominated by the Proteobacteria phylum, mainly consisted of Alpha-, Beta-, and Gammaproteobacteria classes but it also contained the Firmicutes, with the Bacilli and Clostridia classes. The Archaeal domain was dominated by the methanogens and halobacteria from the Euryarchaeota phylum, but also contained the Crenarchaeota. Chemolithoautotrophic microorganisms, as well as microorganisms with heterotrophic metabolisms were present in the subsurface biome and included the methanogens, which can fix CO_2, sulphate-reducing bacteria, and microorganisms known to fix nitrogen. For the Eukaryal

domain, the main phyla present were Arthropoda, Streptophyta, Nematoda, Apicomplexa and Chlorophyta.

When the subsurface biome was subjected to low pressure, in both nutrient rich and nutrient deprived environments, high biomass yields could be obtained for the nutrient rich conditions. However, for the nutrient deprived conditions, consisting of fissure water alone, exponential growth did not occur; the fissure water was not able to provide all the necessary nutrients for optimum growth. Changes in diversity can occur when subsurface biomes are exposed to different nutritional environments, as well as different physiological growth conditions. This was confirmed through diversity studies after the subsurface biome was grown under the various growth conditions. Although exponential growth did not occur under all the conditions tested, the microorganisms remained viable and metabolically active. Due to the extreme conditions of the deep subsurface environments, most of these microorganisms encounter energy limiting conditions, making them likely to be inactive or to display very low levels of metabolic activity. Microbial viability may ultimately prove to be a more important parameter than specific diversity changes or biomass yields for carbon cycling studies in the deep subsurface.

To study the subsurface biome under conditions similar to what they could encounter during carbon sequestration, specifically designed bioreactors were used that were able to operate under higher pressures and temperatures. Under these conditions, the addition of CO_2 resulted in it being in a supercritical state. Supercritical CO_2 generally has harmful impacts on the majority of the microorganisms. However, throughout this research it was found that even though the microorganisms were not able to proliferate under these harsh conditions, they remained alive, even under 100 bar pressure, in the presence of 100% CO_2 and in a nutrient deprived environment. This allowed for successful evaluations of the subsurface biome in an environment that mimics geological carbon sequestration. The presence of biofilm formations have been observed throughout these evaluations and could be the most important protection mechanisms used by microbial communities to survive the stress created by the presence of supercritical CO_2.

The presence of supercritical CO_2 could cause a substantial decrease in the diversity of the deep subsurface, but ultimately the surviving microorganisms might be able to adapt

and utilize the CO_2. To evaluate the influence of geological carbon sequestration on the subsurface microbial diversity and metabolic carbon cycling, a continuous high pressure bioreactor, specifically designed for this research, was used. These studies confirmed that a significant decrease in the diversity was indeed observed, but several microorganisms were able to survive these carbon sequestration conditions, most likely due to their ability to form biofilms.

Even though several microorganisms remained viable, expected metabolic products were not observed during/after six weeks of circulation in the bioreactor, likely due to extremely low metabolic activities under carbon sequestration conditions. A substantial decrease in the diversity was observed after the six weeks of carbon sequestration conditions and as expected, groups from the Bacteria and Archaea were able to survive these conditions, but no Eukarya could be detected. The Bacteria remained the dominant domain, with the Proteobacteria the main phylum present, similar to what has been found in the subsurface biome. Firmicutes and Bacteriodetes were also detected. For the Archaea only the Euryarchaeota phylum, consisting of the Methanobacteria and the Halobacteria classes were observed.

Transcriptome data obtained for the subsurface biome indicated that gene products from sulphur metabolism, nitrogen metabolism, and carbon metabolism were present and diversity analyses of the bioreactor confirmed that microorganisms, utilizing these metabolisms, were present. Thus, specific metabolic cycling can be expected from the subsurface biome, resulting in the production of formate, acetate, methane, and bicarbonates. The acidic and high pressure environment created by the carbon sequestration conditions allowed for significant leaching of metals from the sandstone, especially aluminium and iron. This increased the stress on the subsurface biome, limiting their already slow growth even further. This occurrence is of great importance and should be considered during carbon sequestration, since the influence it will have on the subsurface microbial communities could result in substantial impacts on the carbon cycling occurring in the deep subsurface.

Ultimately, this project effectively demonstrated new considerations in terms of diversity, geological changes, and metabolic cycling that should also be considered during the planning and implementation of the carbon sequestration technology.

SUMMARY

Climate change is a reality and is a consequence of too high levels of greenhouse gases being emitted into the atmosphere, especially CO_2. This is happening mainly due to the burning of fossil fuels, but other human or industrial activities are also contributing. These additional emissions are responsible for the greenhouse effect, resulting in an increase in the global average temperature of the Earth's atmosphere. Industrialization and the rise in population levels around the world has increased the demand for energy and by meeting that demand more emissions are being released into the atmosphere and are responsible for an atmospheric increase of CO_2 from 280 ppm around 1850 to 400 ppm today. This is creating long term, harmful conditions on the Earth, influencing the economy, the ecology, and human health. As an attempt to manage the carbon resources more efficiently, South Africa will be storing anthropogenic CO_2 in geological formations.

Within these deep subsurface environments, considered for carbon sequestration, highly diverse microbial communities can be found and the metabolic activities of these microorganisms are closely tied to the geochemical and mineralogical processes occurring within the subsurface. Therefore, to determine possible influences that the CO_2 could have on the diversity and metabolic carbon cycling of these subsurface microorganisms, consideration was given to the interaction between the sequestered CO_2 and the subsurface biome, as well as the geological environments. In order to possibly understand how these subsurface biomes will operate *in situ*, the biogeochemistry for a study site, similar to proposed sites for carbon sequestration in South Africa, was characterized comprehensively. The subsurface biome from the study site, used for this research, was found to contain microorganisms belonging to the Archaeal, the Bacterial, and the Eukaryal domains, but was dominated by the Bacteria, specifically the Proteobacteria. A specifically designed, continuous high pressure bioreactor was used to evaluate the influence of the stored CO_2 on the subsurface microbial diversity and metabolic carbon cycling, by mimicking carbon sequestration conditions.

Due to the extreme conditions of the deep subsurface, most of these microorganisms have to grow and survive in extreme energy limiting conditions, making them likely to be inactive or to display exceptionally low metabolic activities. Even though this research indicated that in most of the conditions tested the microorganisms were not able to multiply or to produce detectable amounts of expected metabolic products; they surprisingly remained viable. The most likely reason for this was due to the presence of biofilm formations which the microorganisms used as a possible protection mechanism towards resisting the harsh conditions they were subjected to. Ultimately, this indicated that viability might be more important, than specific diversity changes or biomass yields for carbon cycling studies in the deep subsurface.

A considerable decrease in the diversity was observed after the biome was subjected to carbon sequestration conditions. Only groups from the Bacteria and Archaea were able to survive these conditions, but no Eukarya could be detected. Transcriptome data obtained for the subsurface biome indicated that gene products from sulphur metabolism, nitrogen metabolism, and carbon metabolism were present and diversity analyses of the bioreactor confirmed that microorganisms, utilizing these metabolisms, remained viable after six weeks under carbon sequestration conditions. These conditions, mainly due to the acidic environment created by the dissolved CO_2, allowed for significant leaching of metals from the sandstone, especially aluminium and iron, creating more stressful conditions, thus restricting the growth of the subsurface biome even more. This could result in substantial impacts on the carbon cycling occurring in the deep subsurface, and should therefore be considered during carbon sequestration.

Key words: climate change; carbon sequestration; geological storage; deep subsurface; metabolic carbon cycling; CO_2 fixation; high pressure bioreactors; aluminium toxicity.

OPSOMMING

Klimaatsverandering is ‘n werklikheid en is die gevolg van te hoë vlakke van kweekhuisgasse, veral CO_2, wat in die atmosfeer uitgestraal word. Dit gebeur hoofsaaklik as gevolg van die verbranding van fossielbrandstof, maar ander menslike en industriële aktiwiteite lewer ook ‘n bydrae. Hierdie addisionele uitstralings is verantwoordelik vir die kweekhuiseffek en dit veroorsaak gevolglik ‘n toename in die totale gemiddelde temperatuur van die aarde se atmosfeer. As gevolg van industrialisering en die die toename in die bevolkingsaanwas, het die vraag na energie verhoog en om in hierdie aanvraag te voorsien, word meer uitstralings in die atmosfeer gedoen, wat dus verantwoordelik is vir ‘n toename van atmosferiese CO_2 van 280 dpm rondom 1850 tot 400 dpm vandag. Dit veroorsaak langtermyn skadelike toestande op die aarde wat weer ‘n invloed het op die ekonomie, die ekologie, en ook menslike gesondheid. Suid Afrika beplan om antropogenetiese CO_2 in geologiese formasies te stoor, in ‘n poging om die koolstof voorrade meer doeltreffend te bestuur.

Binne in hierdie diep ondergrondse omgewings, wat oorweeg word vir koolstofberging, word hoë mikrobiese bevolkings gevind en die metabolise aktiwiteite van hierdie mikroorganismes is baie nou verbind aan die geochemiese en mineralogiese prosesse wat in die ondergrondse omgewing plaasvind. Die interaksie tussen die opgeruimde CO_2 en die ondergrondse bioom, asook die geologiese omgewings was ondersoek, om te bepaal wat die gevolglike invloed mag wees wat die CO_2 op die mikrobiese diversiteit en metabolise koolstofsiklus mag hê. Om te probeer verstaan hoe hierdie ondergrondse bioom *in situ* funksioneer, was die biogeochemie vir ‘n studieterrein, soortgelyk aan die voorgestelde omgewings vir koolstofberging in Suid Afrika, volledig ondersoek. Dit was bevind dat die ondergrondse bioom van hierdie studieterrein mikroorganismes vanuit die Archaea, die Bakterieë, en die Eukariote bevat, maar was oorheers deur die Bakterieë, veral die Proteobakterieë. Koolstofbergingstoestande is nageboots deur die gebruik van ‘n spesiaal ontwerpte, deurlopende hoëdruk bioreaktor, om die invloed wat die gestoorde CO_2 op die ondergrondse mikrobiese diversiteit en metabolise koolstofsiklus het, te evalueer.

As gevolg van die uiterste toestande in die diep ondergrondse omgewing, moet die oorgrote meerderheid van hierdie mikroorganismes groei en oorleef in besondere energie beperkende toestande, wat veroorsaak dat hulle onaktief is, of besondere lae metaboliese aktiwiteite vertoon. Alhoewel hierdie studie aangedui het dat in die meeste van die toestande wat getoets is, die mikroorganismes nie in staat was om te vermeerder nie, of selfs waarneembare hoeveelhede van verwagte metabolise produkte te genereer nie, het hulle verbasend lewensvatbaar gebly. Die mees aanvaarbare verklaring hiervoor is dat die mikroorganismes biofilm gevorm het, wat hulle kon gebruik het as ‘n moontlike beskermingsmeganisme teen die uiterste toestande waaraan hulle blootgestel is. Dit dui uiteindelik daarop dat lewensvatbaarheid moontlik belangriker is as die spesifieke veranderinge in die diversiteit of die biomassa opbrengste, wanneer studies op die ondergrondse koolstofsiklus gedoen word.

‘n Merkbare afname in diversiteit was waarneembaar nadat die bioom blootgestel was aan koolstofbergingstoestande. Slegs groepe vanuit die Bakterieë en die Archaea was in staat om hierdie toestande te oorleef, terwyl geen Eukariote opgespoor kon word nie. Die transkriptoom data, wat verkry is vir die ondergrondse bioom, het aangedui dat geenprodukte van swaelmetabolisme, stikstofmetabolisme, en koolstofmetabolisme teenwoordig was en verskeie ontledings van die bioreaktor het bevestig dat mikroorganismes, wat gebruik maak van hierdie metabolismes, steeds lewensvatbaar was na ses weke onder koolstofbergingstoestande. Hierdie toestande, hoofsaaklik as gevolg van die suuromgewing wat deur die opgeloste CO_2 geskep is, veroorsaak dat loging van metale uit die sandsteen, veral aluminium en yster, plaasvind, wat op hul beurt verdere stresvolle toestande veroorsaak en die groei van die ondergrondse bioom nog verder beperk. Dit kan ‘n baie groot invloed uitoefen op die ondergrondse koolstofsiklus en behoort gevolglik oorweeg te word tydens koolstofberging.

Sleutelwoorde: klimaatsverandering; koolstofberging; geologiese berging; diep ondergrond; metabolise koolstofsiklus; CO_2 fiksasie; hoëdruk bioreaktors; aluminium toksiteit.